	ESA Climate Change Initiative (CCI)	Page 1
	Product Validation and Intercomparison Report (PVIR)	
	for the Essential Climate Variable (ECV) Greenhouse Gases (GHG)	Version 5.0 Final
		9 Feb 2017

ESA Climate Change Initiative (CCI)

Product Validation and Intercomparison Report (PVIR)

for the Essential Climate Variable (ECV)

Greenhouse Gases (GHG)


for data set

Climate Research Data Package No. 4 (CRDP#4)

Written by:

GHG-CCI VALidation Team (VALT) and Earth Observation Science Team (EOST):

Michael Buchwitz (lead author, IUP-UB), Bart Dils (BIRA), Hartmut Boesch (Univ. Leicester), Dominik Brunner (Empa), André Butz (KIT/DLR), Cyril Crevoisier (LMD), Robert Detmers (SRON), Christian Frankenberg (JPL/CalTech), Otto Hasekamp (SRON), William Hewson (Univ. Leicester), Alexandra Laeng (KIT), Stefan Noël (IUP-UB), Justus Notholt (IUP-UB), Robert Parker (Univ. Leicester), Maximilian Reuter (IUP-UB), Oliver Schneising (IUP-UB), Peter Somkuti (Univ. Leicester), Anu-Maija Sundström (Empa), Evelyn De Wachter (BIRA)

	ESA Climate Change Initiative (CCI)	Page 2
	Product Validation and Intercomparison Report (PVIR)	
	for the Essential Climate Variable (ECV) Greenhouse Gases (GHG)	Version 5.0 Final
		9 Feb 2017

Change log:

Version Nr.	Date	Status	Reason for change
Draft 1 of version 5.0	15. Nov. 2016	Initial draft for team members	Generate new version 5.0 (based on final version 4.0).
Draft 2 of version 5.0	2. Feb. 2017	2 nd draft for team members	To integrate inputs from all team members.
Version 5.0	9. Feb. 2017	As submitted	To integrate inputs from team members and to consider GCOS-200 requirements.




	ESA Climate Change Initiative (CCI)	Page 3
	Product Validation and Intercomparison Report (PVIR)	
	for the Essential Climate Variable (ECV) Greenhouse Gases (GHG)	Version 5.0 Final
		9 Feb 2017

Table of Contents


1	Executive Summary	6
2	Satellite data sets to be validated: CRDP#4.....	15
3	Validation of CRDP#4 ECA products using TCCON	18
3.1	Overview.....	18
3.1.1	Methodology	18
3.2	Results.....	23
3.2.1	SCIAMACHY XCO ₂	24
3.2.2	GOSAT XCO ₂	29
3.2.3	EMMA XCO ₂	34
3.2.4	SCIAMACHY XCH ₄	41
3.2.5	GOSAT XCH ₄	46
3.2.6	GLINT XCO ₂	54
3.2.7	GLINT XCH ₄	59
3.2.8	Overall Results	67
3.3	Summary and conclusions TCCON validation of ECA products.....	70
3.3.1	SCIAMACHY XCO ₂	73
3.3.2	GOSAT XCO ₂	75
3.3.3	EMMA XCO ₂	77
3.3.4	SCIAMACHY XCH ₄	79
3.3.5	GOSAT XCH ₄	81
3.3.6	EMMA XCH ₄	83
4	Validation of ECA products using NDACC (no update)	84
5	Verification using ground-based in-situ measurements (no update)	84
6	Retrieval team assessments of CRDP#4	85
6.1	Assessment of XCO ₂ data products	85

	ESA Climate Change Initiative (CCI)	Page 4
	Product Validation and Intercomparison Report (PVIR)	
	for the Essential Climate Variable (ECV) Greenhouse Gases (GHG)	Version 5.0 Final
		9 Feb 2017

6.1.1	Assessment of SCIAMACHY BESD (and WFMD) XCO ₂	85
6.1.2	Assessment of SCIAMACHY WFMD XCO ₂	96
6.1.3	Assessment of GOSAT OCFP XCO ₂	103
6.1.4	Assessment of GOSAT SRFP (RemoTeC) XCO ₂	109
6.1.5	Assessment of SCIAMACHY/GOSAT EMMA XCO ₂	116
6.2	Assessment of XCH ₄ data products.....	130
6.2.1	Assessment of SCIAMACHY WFMD XCH ₄	130
6.2.2	Assessment of SCIAMACHY IMAP XCH ₄	137
6.2.3	Assessment of GOSAT OCPR XCH ₄	143
6.2.4	Assessment of GOSAT SRFP (RemoTeC) XCH ₄	149
6.2.5	Assessment of GOSAT SRPR (RemoTeC) XCH ₄	155
6.2.6	Assessment of GOSAT OCFP XCH ₄	162
6.3	Assessment of ACA products.....	168
6.3.1	Assessment of CO2_AIR_NLIS (no update)	168
6.3.2	Assessment of CO2_IAS_NLIS.....	168
6.3.3	Assessment of CO2_ACE_CLSR (no update)	170
6.3.4	Assessment of CO2_SCI_ONPD (no update).....	170
6.3.5	Assessment of CH4_IAS_NLIS.....	172
6.3.6	Assessment of CH4_SCI_ONPD (no update)	175
6.3.7	Assessment of CH4_MIP_IMK.....	177
6.3.8	Assessment of CH4_IAS_ASMT	180
6.4	Consistency of XCO ₂ data products	185
6.5	Consistency of XCH ₄ data products	191
6.5.1	Assessment results from IUP-UB.....	191
6.5.2	Assessment results from SRON.....	198

	ESA Climate Change Initiative (CCI)	Page 5
	Product Validation and Intercomparison Report (PVIR)	
	for the Essential Climate Variable (ECV) Greenhouse Gases (GHG)	Version 5.0 Final
		9 Feb 2017

7	QA/QC: TCCON comparisons.....	205
7.1	XCO ₂ QA/QC comparison results.....	212
7.2	XCH ₄ QA/QC comparison results.....	215
8	Assessment of aerosol induced biases	218
8.1	Introduction	218
8.2	Data and methods.....	219
8.2.1	Data.....	219
8.2.2	Collocation of the data	221
8.2.3	Multiple linear regression model.....	226
8.3	Results.....	228
8.3.1	Quality of the filtering for highly scattering aerosol scenes.....	228
8.3.2	Regression of XCO ₂ bias against AERONET aerosol observations.....	230
8.3.3	AOD differences between the TCCON and satellite XCO ₂ pixel locations ...	233
8.3.4	Regression of XCO ₂ bias against satellite aerosol observations.....	235
8.4	Summary	240
9	References	243
10	Acronyms and Abbreviations.....	250
11	Acknowledgements.....	253

	ESA Climate Change Initiative (CCI)	Page 6
	Product Validation and Intercomparison Report (PVIR)	
	for the Essential Climate Variable (ECV) Greenhouse Gases (GHG)	Version 5.0 Final
		9 Feb 2017

1 Executive Summary

This document is the Product Validation and Intercomparison Report (PVIR), which is a deliverable of the ESA project GHG-CCI (<http://www.esa-ghg-cci.org/>).

This document describes the validation of the second Climate Research Data Package (CRDP#4) generated by GHG-CCI during the third year (March 2016 – February 2017) of Phase 2 of the GHG-CCI project.

The GHG-CCI project is one of several projects of ESA's Climate Change Initiative (CCI). The aim of GHG-CCI is to deliver the Essential Climate Variable (ECV) Greenhouse Gases (GHG) in line with the "Systematic observation requirements for satellite-based products for climate" as defined by GCOS (Global Climate Observing System): "Distribution of greenhouse gases, such as CO₂ and CH₄, of sufficient quality to estimate regional sources and sinks".


The focus of this document is to describe the validation of the GHG-CCI core data products generated with GHG-CCI ECV Core Algorithms (ECAs). These products are near-surface-sensitive column-averaged dry air mole fractions (mixing ratios) of atmospheric CO₂ and CH₄, i.e., XCO₂ (in ppm) and XCH₄ (in ppb), as retrieved from SCIAMACHY on ENVISAT (nadir mode) and TANSO-FTS onboard GOSAT. These products are the core products generated within GHG-CCI as they are sensitive to near-surface atmospheric CO₂ and CH₄ concentration variations and therefore contain information on regional surface sources and sinks, which can be extracted using surface flux inverse modelling. The XCO₂ and XCH₄ atmospheric (Level 2) data products have primarily been validated by comparisons with Total Carbon Column Observation Network (TCCON) ground-based XCO₂ and XCH₄ observations. Additional results based on, e.g., model comparisons and satellite product inter-comparisons, are also reported in this document.

Within GHG-CCI also additional satellite-derived data products are generated and assessed with respect to their quality. These products are retrieved with Additional Constraints Algorithms (ACAs). The ACA products are sensitive to CO₂ and CH₄ variations in higher atmospheric levels, i.e., levels above the planetary boundary layer. They are retrieved from IASI, MIPAS, SCIAMACHY solar occultation mode and ACE-FTS. For some of these products (e.g., IASI CO₂ and IASI and MIPAS CH₄) updates have been generated for CRDP#4 and a new IASI CH₄ product has been added.

The TCCON validation of the ECA core products is summarized in **Tab. S-1** for the XCO₂ products and in **Tab. S-2** for the XCH₄ products.

Tab. S-1 summarizes the results from the XCO₂ validation based on the application of several independent assessment methods:

Tab. S-1, column "Details (section)": VAL indicates the comparison results of the GHG-CCI validation team (VALT), DP are the validation results from the Data Provider (DP), EMMA denotes the validation done in the framework of the EMMA ensemble median algorithm activities and QA/QC are the results from the Quality Assurance / Quality Control (QA/QC) activities. In brackets the corresponding section numbers are given, where the underlying details are presented.


	ESA Climate Change Initiative (CCI)		Page 7
	Product Validation and Intercomparison Report (PVIR)		
	for the Essential Climate Variable (ECV) Greenhouse Gases (GHG)		Version 5.0 Final
			9 Feb 2017

Tab. S-1, column “Random error”: Estimate of the random error or single measurement precision. Green numbers in **Tab. S-1** (and **Tab. S-2**, see below) indicate that at least the corresponding Threshold (T) user requirement as defined in the GHG-CCI User Requirements Document **/URD GHG-CCI v2.1/** has been met (but not necessarily the more demanding Breakthrough (B) or Goal (G) requirements).

As can be seen from **Tab. S-1**, the required XCO₂ single measurement precision (random error) is achieved for all products. The precision is typically ~2 ppm (except for CO2_SCI_WFMD: ~2.7 ppm). The various assessment methods give quite similar results indicating that the single observation random error estimates are robust.

Tab. S-1, column “Systematic error”: As can be seen from **Tab. S-1**, the XCO₂ systematic error (“relative accuracy”) is 0.5 ppm +/- a few 0.1 ppm. For several products and several assessment methods errors as low as 0.4 ppm or even 0.3 ppm are reported, which is essentially the uncertainty of the TCCON reference data (0.4 ppm, 1-sigma). The **/URD GHG-CCI v2.1/** threshold requirement is 0.5 ppm. It is therefore likely, that the URD threshold requirement has been met for all products with the exception of CO2_SCI_WFMD, where the systematic error is somewhat larger than 0.5 ppm. What one can say with confidence is that the achieved (relative) accuracy (at the TCCON validation sites) is at least close to the URD threshold requirement. The GCOS (target=goal) requirement for “uncertainty” is 0.5 ppm (1-sigma; note that GCOS specifies the uncertainty requirement as 1 ppm (95%, i.e., approx. 2-sigma)) **/GCOS-200/**. It is assumed here that the “GCOS uncertainty requirement” for product “tropospheric CO₂ column” corresponds to the URD (relative) accuracy requirement for XCO₂ (but not to the random error requirement or to the root-sum-square of random and systematic errors). As shown in **Tab. S-1**, the achieved performance is close to the required GCOS target performance for all XCO₂ products at the TCCON validation sites.

Tab. S-1, column “Stability”: For the XCO₂ products the stability in terms of a long-term drift (linear trend) is very high: better than 0.2 ppm/year (with the exception of one analysis method (EMMA) as applied to two products). This means that for all products the **/URD GHG-CCI v2.1/** goal requirement (< 0.2 ppm/year) is likely met for linear trend / drift as indicated by several independent assessment methods. The **/GCOS-200/** target requirement is 0.15 ppm/year (1.5 ppm per decade), i.e., more demanding. As shown in **Tab. S-1**, the required GCOS target stability performance is likely met for all products for long-term (linear) drift. For stability interpreted as year-to-year bias variations the situation is less clear. Unclear or no significant year-to-year bias variations have been found by several assessment methods except for the validation (VAL) team assessments. “Not significant” means that the obtained values for year-to-year instability are so uncertain, that their numerical value should not be compared with the user requirement (these values are marked with a star in brackets) or that it is at least unclear if the obtained numerical value is meaningful or not (these values are marked with a question mark in brackets). According to the VAL assessment significant values have been obtained for year-to-year instability, which are around 0.3 ppm/year for the individual sensor Level 2 products and better than 0.2 ppm/year for the merged Level 2 EMMA products. What can be concluded from **Tab. S-1** is that it is very likely that at least the URD threshold requirement of < 0.5 ppm/year has been met for year-to-year bias variations and possibly even the breakthrough requirement of < 0.3 ppm/year. The very demanding GCOS target requirement of < 0.15 ppm/year has however likely not been met for year-to-year bias variations.

	ESA Climate Change Initiative (CCI)	Page 8
	Product Validation and Intercomparison Report (PVIR)	
	for the Essential Climate Variable (ECV) Greenhouse Gases (GHG)	Version 5.0 Final
		9 Feb 2017


Tab. S-2 summarizes the results from the XCH₄ validation based on the application of several independent assessment methods:

The structure of this table is identical to **Tab. S-1** (see above).

Tab. S-2, column “Random error”: As can be seen from **Tab. S-2**, the required XCH₄ single measurement precision (random error) is achieved for all GOSAT products, not however for the SCIAMACHY products after October 2005. Note that the SCIAMACHY data quality suffers from detector degradation after October 2005 and that the reported validation values are dominated by this “degraded” time period, due to the non-availability of most TCCON sites before October 2005. For WFMD and IMAP an estimate of the pre-October 2005 precision is given in brackets (32 ppb for both products). The precision is typically around 14 ppb (+/- a few ppb) for GOSAT. For SCIAMACHY the precision is in the range 32 – 80 ppb depending on time period, assessment method and product. The various assessment methods give quite similar results indicating that the single observation random error estimates are robust.

Tab. S-2, column “Systematic error”: As can be seen from **Tab. S-2**, the XCH₄ systematic error (“relative accuracy”) is 3 ppb +/- approx. 2 ppb for all GOSAT products, which is essentially the uncertainty of the TCCON reference data (3.5 ppb, 1-sigma). The **/URD GHG-CCI v2.1/** threshold requirement is 10 ppb. The URD threshold requirement has therefore been met for all GOSAT products and likely also the breakthrough requirement of < 5 ppb. For the SCIAMACHY products this is not the case. Here **Tab. S-2** shows that the achieved performance is close to the URD threshold performance of 10 ppb. The GCOS (target=goal) requirement for “uncertainty” is 5 ppb (1-sigma; note that GCOS specifies the uncertainty requirement as 10 ppb (95%, i.e., approx. 2-sigma)) **/GCOS-200/**. It is assumed here that the “GCOS uncertainty requirement” for product “tropospheric CH₄ column” corresponds to the URD (relative) accuracy requirement for XCH₄ (but not to the random error requirement or to the root-sum-square of random and systematic errors). As shown in **Tab. S-2**, the achieved performance is close to the required GCOS target performance for all GOSAT XCH₄ products at the TCCON validation sites. For SCIAMACHY the achieved performance is approximately a factor of 2 worse compared to the GCOS target requirement.

Tab. S-2, column “Stability”: For the XCH₄ products the stability in terms of a long-term drift (linear trend) is very high: better than 1-2 ppb/year. This means that for all products the **/URD GHG-CCI v2.1/** breakthrough requirement (< 2 ppb/year) has likely been met for linear trend / drift as indicated by several independent assessment methods. The **/GCOS-200/** target requirement is 0.7 ppb/year, i.e., more demanding. As shown in **Tab. S-2**, the achieved performance for long-term drift as required by GCOS has been met for some GOSAT and the EMMA product, but not for all products. For stability interpreted as year-to-year bias variations the situation is less clear. Unclear or no significant year-to-year bias variations have been found by several assessment methods except for the validation (VAL) team assessments. “Not significant” means that the obtained values for year-to-year instability are so uncertain, that their numerical value should not be compared with the user requirement (these values are marked with a star in brackets) or that it is at least unclear if the obtained numerical value is meaningful or not (these values are marked with a question mark in brackets). According to the VAL assessment significant values have been obtained for year-to-year bias variability, which are around 1.6 ppb/year for the individual sensor Level 2 GOSAT products (exception: OCFP: 4.3 ppb/year; for the SCIAMACHY products < 4.3 ppb/year has been achieved) and for the merged Level 2 EMMA product. What can be concluded from **Tab. S-2** is that it is very likely that at least the URD threshold requirement of < 3 ppm/year has been met for year-to-

	ESA Climate Change Initiative (CCI)	Page 9
	Product Validation and Intercomparison Report (PVIR)	
	for the Essential Climate Variable (ECV) Greenhouse Gases (GHG)	Version 5.0 Final
		9 Feb 2017

year bias variations and possibly even the breakthrough requirement of < 2 ppb/year. The very demanding GCOS target requirement of < 0.7 ppb/year has however very likely not been met for year-to-year bias variations.


As already explained above, the satellite errors as listed in **Tabs. S-1 – S-2** are differences relative to TCCON and the numerical values listed in these tables have been computed assuming that TCCON is error-free, i.e., here we do not consider (ignore) the TCCON network uncertainty, which is 0.4 ppm for XCO_2 and 3.5 ppb for XCH_4 (both values are 1-sigma). Considering this effectively implies that algorithms, which reach a relative accuracy of 0.7 ppm for XCO_2 or 11.3 ppb for XCH_4 , may well have passed the threshold relative accuracy user requirement of 0.5 ppm and 10 ppb, respectively (see also **/PVIRv2 CRDP#1/**). Furthermore, also the estimated statistical parameters are inherent uncertain (see Sections 3.3.5 and 3.4 of PVIRv2 **/PVIRv2 CRDP#1/**). On the other hand, TCCON is not fully representative for all conditions (e.g., tropics, deserts). For example, it has been shown in **/Buchwitz et al., 2013/** and **/Reuter et al., 2013/** that the difference of the various assessed satellite products remote from TCCON may be somewhat larger during certain time periods and regions as the TCCON comparison suggests.

Overall it can be concluded that the summary values listed in **Tabs. S-1 – S-2** are robust estimates for the overall quality of the satellite data products, especially w.r.t. random error and (relative) accuracy (as the different assessment methods result in quite similar overall figures of merit as listed in **Tabs. S-1 – S-2**).

As explained, the validation results shown in **Tabs. S-1 – S-2** are strictly speaking valid only at the TCCON validation sites and it is expected that the data quality may differ for conditions not covered by these sites (e.g., for high albedo scenes such as deserts and in particular for desert dust storm conditions). We therefore recommend to use the data products with care if they are to be used for challenging applications. In particular we recommend to make use of the fact that for each product type (e.g., “ XCO_2 ” and even for “ XCO_2 from a single satellite”) more than one product exists which has been generated with a different algorithm. User can take advantage of this to verify the robustness of their findings. It is also recommended to contact the corresponding retrieval team expert prior to using the data for a given application or at a later stage of the analysis process, when first results are available for discussion.

For the ECA products, **Table S-3** shows as an overall summary a comparison of GHG-CCI CRDP#4 XCO_2 and XCH_4 product characteristics with GCOS requirements **/GCOS-154/** and GHG-CCI Climate Research Group (CRG) user requirements **/URD GHG-CCI v2.1/**.

Finally, it has also been investigated in detail if XCO_2 biases can be explained by aerosol-related error (see the very detailed assessment given in Sect. 8). Based on the results obtained in this study, both with AERONET and satellite-based data, it can be concluded that aerosols have only a minor effect on the XCO_2 bias at the existing TCCON stations. However, it would be desirable to have TCCON observations also at locations with higher aerosol loading, so that any aerosol effects could be investigated more rigorously.


	ESA Climate Change Initiative (CCI)	Page 10
	Product Validation and Intercomparison Report (PVIR)	
	for the Essential Climate Variable (ECV) Greenhouse Gases (GHG)	Version 5.0 Final
		9 Feb 2017

GHG-CCI: Estimates of achieved data quality (#): CRDP#4 XCO ₂						
Sensor	Algorithm	Random error [ppm]	Systematic error [ppm]	Stability [ppm/year]		Details (section)
				Long-term drift	Year-to-year	
SCIAMACHY on ENVISAT	BESD v02.01.02	1.9	0.37 - 0.56	-0.03 +/- 0.06 (*)	0.32 +/- 0.08	VAL (Sect. 3)
		1.9	0.38 - 0.40	-0.13 +/- 0.28 (?)	0.34 (?)	DP (6.1.1)
		2.0	0.39 - 0.43	-0.02 +/- 0.33 (?)	0.23 (?)	EMMA (6.1.5)
		1.9	0.4 - 0.8	-0.01 +/- 0.08 (*)	1.68 +/- 2.03 (*)	QA/QC (7.1)
SCIAMACHY on ENVISAT	WFMD V4.0	2.7	0.57 - 0.71	-0.03 +/- 0.10 (*)	0.31 +/- 0.11	VAL (3)
		2.6	0.48 - 0.52	[0.00, 0.04] (?)	0.21 (?)	DP (6.1.2)
		2.9	0.60 - 0.75	0.14 +/- 0.21 (?)	0.46 (?)	DP (6.1.1)
		3.0	0.60 - 0.63	0.23 +/- 0.42 (?)	0.33 (?)	EMMA (6.1.5)
		2.7	0.5 - 1.0	-0.04 +/- 0.09 (*)	1.86 +/- 2.41 (*)	QA/QC (7.1)
TANSO on GOSAT	OCFP v7.0 (UoL-FP)	1.8	0.36 - 0.58	-0.07 +/- 0.07 (*)	0.29 +/- 0.06	VAL (3)
		1.9	0.47	0.11 (?)	0.9 (?)	DP (6.1.3)
		1.8	0.36 - 0.42	-0.15 +/- 0.11 (?)	0.23 (?)	EMMA (6.1.5)
		1.7	0.3 - 0.5	-0.09 +/- 0.08	1.48 +/- 2.06 (*)	QA/QC (7.1)
TANSO on GOSAT	SRFP v2.3.8 (RemoTeC)	2.0	0.36 - 0.51	0.02 +/- 0.04 (*)	0.27 +/- 0.12	VAL (3)
		1.9	0.43	-0.05 +/- 0.12 (*)	0.34 +/- 0.12	DP (6.1.4)
		2.1	0.28 - 0.48	0.00 +/- 0.16 (?)	0.24 (?)	EMMA (6.1.5)
		1.9	0.4 - 0.5	-0.06 +/- 0.11 (*)	1.30 +/- 2.11 (*)	QA/QC (7.1)
SCIAMACHY & GOSAT	EMMA v2.2a	2.0	0.37 - 0.45	0.08 +/- 0.22 (*)	0.18 +/- 0.12	VAL (3)
		2.4	0.47 - 0.54	-0.30 +/- 0.64 (?)	0.25 (?)	EMMA (6.1.5)
SCIAMACHY & GOSAT	EMMA v2.2b	1.7	0.29 - 0.38	-0.08 +/- 0.20 (*)	0.16 +/- 0.11	VAL (3)
		1.8	0.32 - 0.40	-0.13 +/- 0.42 (?)	0.20 (?)	EMMA (6.1.5)
TANSO on GOSAT	EMMA v2.2c	1.7	0.30 - 0.39	-0.14 +/- 0.20 (*)	0.16 +/- 0.12	VAL (3)
		1.8	0.24 - 0.44	-0.04 +/- 0.16 (?)	0.26 (?)	EMMA (6.1.5)
Required	G / B / T	< 1 / 3 / 8	< 0.2 / 0.3 / 0.5	< 0.2 / 0.3 / 0.5		/URD GHG-CCI v2.1/
Required	Target	< 0.5 ppm (uncertainty; 1-sigma)		< 0.15 ppm/year		/GCOS-200/
(#) As estimated (mostly) by comparison with ground-based TCCON observations neglecting TCCON accuracy (1-sigma) of 0.4 ppm (*) NOT significant; (?) Significance unclear Green numbers: at least URDv2.1 threshold requirement met; single values random and systematic errors are 1-sigma						

Table S-1: Summary of the estimated quality of the satellite-derived GHG-CCI CRDP#4 XCO₂ data products obtained via comparisons with ground-based TCCON XCO₂ retrievals using several independent assessment methods. Please see main text for details.

GHG-CCI: Estimates of achieved data quality (#): CRDP#4 XCH ₄						
Sensor	Algorithm	Random error [ppb]	Systematic error [ppb]	Stability [ppb/year]		Details (section)
				Long-term drift	Year-to-year	
SCIAMACHY on ENVISAT	WFMD V4.0	76 79 (32 §) 80	8.8 – 10.1 5 – 8 12 – 16	-1.1 +/- 1.2 (*) [0.03, 0.04] (?) 1.6 +/- 3.8 (*)	4.2 +/- 1.3 2.2 (?) 26 +/- 68 (*)	VAL (Sect. 3) DP (6.2.1) QA/QC (7.2)
SCIAMACHY on ENVISAT	IMAP v7.2	45 50 (32 §) 47	8.8 – 9.0 < 10 11 – 12	0.7 +/- 0.8 (*) (*) 1.0 +/- 2.7 (*)	3.3 +/- 1.3 (?) 19 +/- 44 (*)	VAL (3) DP (6.2.2) QA/QC (7.2)
TANSO on GOSAT	OCPR v7.0 (UoL-PR)	14 14 12	4.1 – 4.3 3.9 3 – 4	-0.3 +/- 0.5 (*) 0.06 (?) -0.2 +/- 0.9 (*)	1.5 +/- 0.5 6.1 (?) 8 +/- 11 (*)	VAL (3) DP (6.2.3) QA/QC (7.2)
TANSO on GOSAT	SRFP v2.3.8 (RemoTeC)	14 14 13	4.8 – 5.1 3.4 3 – 4	-0.5 +/- 0.6 (*) -0.8 +/- 1 (*) -0.4 +/- 1.0 (*)	1.6 +/- 0.5 5 +/- 2 9 +/- 15 (*)	VAL (3) DP (6.2.4) QA/QC (7.2)
TANSO on GOSAT	SRPR v2.3.8 (RemoTeC)	14 15 13	3.8 – 4.8 3.7 2 – 5	-0.6 +/- 0.7 (*) -0.8 +/- 2 (*) -0.9 +/- 0.9	1.6 +/- 0.6 6 +/- 2 9 +/- 11 (*)	VAL (3) DP (6.2.5) QA/QC (7.2)
TANSO on GOSAT	OCFP v2.02 (UoL-FP)	15 15 13	4.7 – 4.8 3.6 5	1.5 +/- 1.0 (?) 0.4 (?) 1.2 +/- 0.8	4.3 +/- 0.9 11.4 (?) 16 +/- 14	VAL (3) DP (6.2.6) QA/QC (7.2)
TANSO GOSAT	EMMA v1.2	13	4.0 – 4.4	-0.4 +/- 0.7 (*)	1.2 +/- 0.5	VAL (3)
Required	G / B / T	< 9 / 17 / 34	< 1 / 5 / 10	< 1 / 2 / 3		/URD GHG-CCI v2.1/
Requires	Target	< 5 ppb (uncertainty; 1-sigma)		< 0.7 ppb/year		/GCOS-200/
(#) As estimated (mostly) by comparison with ground-based TCCON observations neglecting TCCON accuracy (1-sigma) of 3.5 ppb (§) Before Nov. 2005; (*) NOT significant; (?) Significance unclear Green numbers: at least URDv2.1 threshold requirement met; single values random and systematic errors are 1-sigma						

Table S-2: Summary of the estimated quality of the satellite-derived GHG-CCI CRDP#4 XCH₄ data products obtained via comparisons with ground-based TCCON XCH₄ retrievals using several independent assessment methods. Please see main text for details.

	ESA Climate Change Initiative (CCI)	Page 12
	Product Validation and Intercomparison Report (PVIR)	
	for the Essential Climate Variable (ECV) Greenhouse Gases (GHG)	Version 5.0 Final
		9 Feb 2017

GHG-CCI CRDP#4: Comparison with GCOS Requirements

Variable ^(*)	Resolution	Accuracy	Stability
XCO ₂	Temporal: GCOS: 4 hours Achieved: Days No existing nor any planned mission meets the GCOS temporal resolution requirement. Spatial: GCOS: 5-10 km Achieved ^(§) : 10 km (§) for GOSAT. SCIAMACHY: 30x60 km ² . URD: SCIAMACHY and GOSAT are useful to generate the ECV GHG. Note: GCOS requirements are target (maximum) requirements but URD requirements listed here are threshold (minimum) requirements.	GCOS ^(§) : < 0.5 ppm URD ^(#) : < 0.5 ppm Achieved ^(#) : 0.3-0.7 ppm ^(?) (§) GCOS uncertainty (1-sigma) (?) Depending on sensor, product, time period and assessment method	GCOS: < 0.15 ppm/yr URD: < 0.5 ppm/yr Achieved: Trend/drift: < 0.2 ppm/yr ⁽⁺⁾ Year-to-year: < 0.35 ppm/yr ⁽⁺⁾ (+) No significant instability found
XCH ₄		GCOS ^(§) : < 5 ppb URD ^(#) : < 10 ppb Achieved ^(#) : 3-10 ppb ^(?)	GCOS: < 0.7 ppb/yr URD: < 3 ppb/yr Achieved: Trend/drift: < 1-2 ppb/yr ⁽⁺⁾ Year-to-year: < 2-5 ppb/yr ⁽⁻⁾ (-) Depending on sensor, assessment method and product; VAL assessment: < 2 ppb/yr for GOSAT except for OCFP (4.3 ppb/yr); SCIAMACHY: < 4.3 ppb/yr
		(#) Relative accuracy (i.e., excluding a possible constant global offset) Estimated by comparison with TCCON ground-based observations; TCCON accuracy (1-sigma): 0.4 ppm for XCO ₂ and 3.5 ppb for XCH ₄	

(*) Requirements for column-averaged mole fractions (= air column normalized vertical GHG columns) as required by URD; it is assumed here that this corresponds to GCOS variables „Tropospheric CO₂ column“ and „Tropospheric CH₄ column“


References: Requirements for ECV Greenhouse Gases (GHG):

- GCOS-200: „The Global Observing System for Climate: Implementation Needs“
- URD: “GHG-CCI User Requirements Document”, v2.1

Definition: ECV GHG (GCOS-154):

- Product A.8.1: Retrievals of CO₂ and CH₄ of sufficient quality to estimate regional sources and sinks

Table S-3: Comparison of GHG-CCI CRDP#4 ECA product characteristics with GCOS requirements /**GCOS-200**/ and GHG-CCI Climate Research Group (CRG) user requirements /**URD GHG-CCI v2.1**/.


	ESA Climate Change Initiative (CCI)	Page 13
	Product Validation and Intercomparison Report (PVIR)	
	for the Essential Climate Variable (ECV) Greenhouse Gases (GHG)	Version 5.0 Final
		9 Feb 2017

The ACA products assessments can be summarized as follows:

CO₂_SCI_ONPD (see **Sect. 6.3.4**): Note that this product has not been updated for CRDP#4, i.e., the analysis presented in this document is identical with the one as given in the previous version of this document. The SCIAMACHY solar occultation ONPD algorithm stratospheric CO₂ profile retrievals (V4.5.2) have been compared with collocated CarbonTracker (CT2013) data provided by NOAA. The SCIAMACHY ONPD CO₂ has compared to CarbonTracker on average no significant bias. However, there is a pronounced oscillation with altitude visible in the mean difference between SCIAMACHY and CT2013. The amplitude of this oscillation is about 10 ppm (3%). This oscillation is currently considered to be the most limiting factor for the accuracy of the SCIAMACHY ONPD CO₂ product. The mean error of the SCIAMACHY CO₂ product is about 4 ppm (1%) at 17 km, increasing to about 16 ppm (4%) at 45 km.

CH₄_SCI_ONPD (see **Sect. 6.3.6**): Note that this product has not been updated for CRDP#4, i.e., the analysis presented in this document is identical with the one as given in the previous version of this document. The SCIAMACHY solar occultation ONPD algorithm stratospheric methane profile retrievals (V4.5.2) have been compared with collocated ACE-FTS data V3 (as used for CO₂ (see above for CO₂_SCI_ONPD)). Overall, the two data sets agree within about 5-10%, which is within the expected accuracy of the products. The differences show a small oscillation with altitude, which might be related to the onion peeling approach. The estimated error of the SCIAMACHY CH₄ product is about 0.05 ppm (50 ppb) below 35 km (smaller than the standard deviation of the difference between the two data sets) and increasing for altitudes above. Especially from 20 to 40 km the correlation between SCIAMACHY and ACE-FTS methane is high, reaching about 0.95 between 30 and 35 km. A similar comparison has been performed with MIPAS methane data provided by KIT. Collocation criteria are 800 km / 9h maximum distance. Only closest collocations have been used. The average agreement between SCIAMACHY and MIPAS is almost perfect above 25 km. Below this altitude, the deviation between SCIAMACHY and MIPAS data increases with decreasing altitude, reaching about -0.2 ppmv (10–15%) at 17 km. This negative bias of SCIAMACHY towards MIPAS is in line with the about 0.2 ppmv positive bias of MIPAS in this altitude range. The correlation between MIPAS and SCIAMACHY methane is somewhat lower than for SCIAMACHY vs. ACE-FTS, which is related to the different effective collocation criteria, especially the larger time differences between the MIPAS limb measurements and the SCIAMACHY occultation measurements. Improved MIPAS/ENVISAT limb stratospheric profiles (product CH₄_MIP_IMK) have also been generated for CRDP#4.

MD products: Mid-tropospheric columns of CO₂ and CH₄ from IASI (products CO₂_IAS_NLIS and CH₄_IAS_NLIS) have been updated for CRDP#4 and the products are available via the GHG-CCI website. These products have been generated using the NLIS algorithm developed and used by LMD, France. Quality assessments for these products have been carried out for the two IASI products as shown in this document. Comparisons with aircraft measurements yield a difference of 0.57 ± 0.99 ppm for CO₂ and 3.0 ± 15.0 ppb, respectively. Comparisons with AirCore balloon 0-30 km profiles yield a difference of -2.0 ± 7.9 ppb for CH₄. Stratospheric CO₂ profiles have been retrieved from ACE-FTS. This product (CO₂_ACE_CLSR) has been updated for CRDP#2 (and is available from the GHG-CCI website. No update is foreseen until relevant spectroscopy studies concerning the N₂ continuum and the CO₂ absorption in the 4µm band are undertaken. LMD AIRS mid-tropospheric CO₂ retrievals (product

	ESA Climate Change Initiative (CCI)		Page 14
	Product Validation and Intercomparison Report (PVIR)		
	for the Essential Climate Variable (ECV) Greenhouse Gases (GHG)		Version 5.0 Final
			9 Feb 2017


CO2_AIR_NLIS) have been generated for CRDP#1 during GHG-CCI Phase 1. The corresponding data set and related documentation is available from the GHG-CCI website (-> CRDP (Data)) but it is not planned to update this data set within the ongoing GHG-CCI Phase 2 project due to channel failures.

For IASI a new methane product is available, which was not part of previous CRDPs: the BIRA product CH4_IAS_ASMT (see Sect. 6.3.8). The CH4_IAS_ASMT product provides CH₄ profiles, together with averaging kernels which give information on the vertical sensitivity of the retrieved profile. Overall 1 independent piece of information is retrieved, with a good sensitivity in the altitude range 4-17 km. The CH4_IAS_ASMT product has been validated with co-located ground-based NDACC FTIR observations. Overall, a small negative bias of the CH4_IAS_ASMT product between -0.28 and 2.27% has been found with the exception of 3 NDACC stations, which show a positive bias. The standard deviation of the difference lies in the range 1.40 to 3.65%. Very good correlations are found for 7 out of the 13 NDACC stations with correlation coefficients between 0.73 and 0.96. Particularly for the 3 high-latitude stations we find a very good correlation, as well as for the 2 high-quality mid-latitude stations Jungfraujoch and Zugspitze. Poorer correlations are found for the stations Bremen, La Reunion, Mauna Loa and Toronto with correlation coefficients in the range 0.4-0.5.

For MIPAS CH₄ profiles these versions have been assessed: V5H_CH4_21 (full resolution period, FR), V5R CH4_224 and V5R CH4_225 (reduced resolution period, RR). The assessments are based on comparisons with collocated methane profiles from ACE-FTS, HALOE and SCIAMACHY. Generally, a good agreement has been found. In the lower part of the profiles, a positive bias of the order of 0.1 to 0.2 ppmv has been found. This bias is lower than that of the previous data versions V5H_CH4_20 (FR), V5R CH4_222 (RR) and V5R CH4_223 (RR). The latter two versions (for RR) have been validated by Laeng et al. (2015). The reduction of the bias of the new versions for RR is of the order of 0.08 to 0.15 ppmv. The comparison of the different MIPAS measurement periods FR and RR suggest, that the RR data leads to slightly higher volume mixing ratios.

Data access:

The CRDP#4 data products presented and discussed in this document are (freely) publicly available via the GHG-CCI website. For data access please see: <http://www.esa-ghg-cci.org/> -> CRDP (Data); (direct link: <http://www.esa-ghg-cci.org/?q=node/106>).

	ESA Climate Change Initiative (CCI) Product Validation and Intercomparison Report (PVIR) for the Essential Climate Variable (ECV) Greenhouse Gases (GHG)	Page 15
		Version 5.0 Final
		9 Feb 2017

2 Satellite data sets to be validated: CRDP#4


The focus of this document is to present and discuss the results of the validation and inter-comparison activities which have been carried out during the second year of Phase 2 of the GHG-CCI project (March 2016 - February 2017). The validated data set is the 4th version of the GHG-CCI Climate Research Data Package (CRDP#4).

Focus is on the validation of the GHG-CCI XCO₂ and XCH₄ satellite-derived core data products generated with ECV Core Algorithms (ECAs) by comparison with Total Carbon Column Observing Network (TCCON) ground based XCO₂ and XCH₄ retrievals. **Table 2.1** presents an overview about the GHG-CCI CRDP#4 ECA algorithms and corresponding data products.

As can be seen from **Table 2.1**, more than one algorithm exists to generate a certain product (e.g., XCO₂ from SCIAMACHY). Where possible, a baseline algorithm and corresponding baseline product has been defined, which is the GHG-CCI recommended product for users who only would like to use one product. The main purpose of the alternative products is to permit ensemble assessments (important, e.g., to verify the robustness of scientific results obtained using the baseline product) and “to challenge the baseline”. As can also be seen, not for all products a single baseline algorithm has been defined yet.

In addition, other ECA data products have been generated using the ensemble algorithm EMMA /**Reuter et al., 2013**/. This algorithm is not a “retrieval algorithm” as the other ECA algorithm but uses existing SCIAMACHY and GOSAT Level 2 products as input to generate merged SCIAMACHY and GOSAT Level 2 product. Input products are the GHG-CCI products but also non-European products (e.g., the GOSAT XCO₂ products generated at NIES, Japan, and the NASA ACOS product).

Table 2.2 shows the temporal coverage of the GHG-CCI CRDP#4 ECA products, which are available from the GHG-CCI website and which have been validated as described in this document.


	ESA Climate Change Initiative (CCI)	Page 16
	Product Validation and Intercomparison Report (PVIR)	
	for the Essential Climate Variable (ECV) Greenhouse Gases (GHG)	Version 5.0 Final
		9 Feb 2017

GHG-CCI CRDP#4: ECV Core Algorithm (ECA) Products				
Algorithm / Product ID (version)	Product	Sensor Satellite	Algorithm Institute	Comment (Reference)
CO2_SCI_BESD (v02.01.02)	XCO ₂	SCIAMACHY ENVISAT	BESD IUP	SCIAMACHY XCO ₂ baseline product (Reuter et al., 2011)
CO2_SCI_WFMD (v4.0)	XCO ₂	SCIAMACHY ENVISAT	WFM-DOAS IUP	SCIAMACHY XCO ₂ alternative product (Schneising et al., 2011)
CO2_GOS_OCFP (v7.0)	XCO ₂	TANSO GOSAT	UoL-FP UoL	GOSAT XCO ₂ baseline product (Cogan et al., 2012)
CO2_GOS_SRF (v2.3.8)	XCO ₂	TANSO GOSAT	RemoTeC SRON/KIT	GOSAT XCO ₂ alternative product (Butz et al., 2011)
CO2_EMMA (v2.2)	XCO ₂	Merged SCIA and GOSAT	EMMA IUP (lead)	Ensemble product (Reuter et al., 2013)
CH4_SCI_WFMD (v4.0)	XCH ₄	SCIAMACHY ENVISAT	WFM-DOAS IUP	SCIAMACHY XCH ₄ proxy product (baseline not yet decided) (Schneising et al., 2011)
CH4_SCI_IMAP (v7.2)	XCH ₄	SCIAMACHY ENVISAT	IMAP SRON/JPL	SCIAMACHY XCH ₄ proxy product (baseline not yet decided) (Frankenberg et al., 2011)
CH4_GOS_OCFP (v7.0)	XCH ₄	TANSO GOSAT	UoL-PR UoL	GOSAT XCH ₄ proxy baseline product (Parker et al., 2011)
CH4_GOS_SRF (v2.3.8)	XCH ₄	TANSO GOSAT	RemoTeC SRON/KIT	GOSAT XCH ₄ proxy alternative product (Butz et al., 2010)
CH4_GOS_SRF (v2.3.8)	XCH ₄	TANSO GOSAT	RemoTeC SRON/KIT	GOSAT XCH ₄ full physics baseline product (Butz et al., 2011)
CH4_GOS_OCFP (v2.02)	XCH ₄	TANSO GOSAT	UoL-PR UoL	GOSAT XCH ₄ full physics alternative product (Parker et al., 2011)
CH4_EMMA (v1.2)	XCO ₂	TANSO GOSAT	EMMA IUP (lead)	Ensemble product (Reuter et al., 2013)
Details (temporal coverage, etc.): http://www.esa-ghg-cci.org -> CRDP (Data)				

Tables 2.1: Overview GHG-CCI core data products of the Climate Research Data Package No. 4 (CRDP#4).

GHG-CCI Climate Research Data Package (CRDP#4)																
Product ID	Product (Level 2, mixing ratios)	Years processed														
		2002	03	04	05	06	07	08	09	10	11	12	13	14	15	
ECV Core Algorithm (ECA) Products																
XCO2_SCIA	XCO ₂															
XCH4_SCIA	XCH ₄															
XCO2_GOSAT	XCO ₂															
XCH4_GOSAT	XCH ₄															
Details please see GHG-CCI Data Products Main Website: http://www.esa-ghg-cci.org/sites/default/files/documents/public/documents/GHG-CCI_DATA.html																

Table 2.2: Overview temporal coverage of the GHG-CCI CRDP#4 ECA products.

	ESA Climate Change Initiative (CCI)	Page 17
	Product Validation and Intercomparison Report (PVIR)	
	for the Essential Climate Variable (ECV) Greenhouse Gases (GHG)	Version 5.0 Final
		9 Feb 2017

In addition to the GHG-CCI core products a number of Additional Constraints Algorithms (ACA) and corresponding data products are further developed within GHG-CCI. An overview about these products is shown in **Table 2.3**.


GHG-CCI CRDP#4: Additional Constraints Algorithm (ACA) Products				
Algorithm / Product ID	Product	Sensor	Algorithm / Institute	Reference
CO2_IAS_NLIS	Mid/upper tropospheric column	IASI	NLIS / LMD	<i>Crevoisier et al., 2009</i>
CO2_ACE_CLRS	Upper trop. / stratospheric profile	ACE-FTS	CLRS / LMD	<i>Foucher et al., 2009</i>
CH4_IAS_NLIS	Upper trop. / stratospheric profile	IASI	NLIS / LMD	<i>Crevoisier et al., 2013</i>
CH4_MIP_IMK	Upper trop. / stratospheric profile	MIPAS	MIPAS / KIT-IMK	<i>Laeng et al., 2015</i>
CH4_SCI_ONPD	Stratospheric profile	SCIAMACHY	ONPD / IUP	<i>Noël et al., 2016</i>
CO2_SCI_ONPD	Stratospheric profile	SCIAMACHY	ONPD / IUP	<i>Noël et al., 2016</i>
CH4_IAS_ASMT	Profile	IASI	ASMT / BIRA	<i>Wachter et al.</i>
Details (temporal coverage, etc.): http://www.esa-ghg-cci.org -> CRDP (Data)				

Table 2.3: Overview GHG-CCI ACA products.

These data products set including documentation are available from the GHG-CCI website: <http://www.esa-ghg-cci.org/> -> CRDP (Data); (direct link: <http://www.esa-ghg-cci.org/?q=node/106>).

Direkt link to GHG-CCI „Main products website“:

http://www.esa-ghg-cci.org/sites/default/files/documents/public/documents/GHG-CCI_DATA.html

	ESA Climate Change Initiative (CCI)	Page 18
	Product Validation and Intercomparison Report (PVIR)	
	for the Essential Climate Variable (ECV) Greenhouse Gases (GHG)	Version 5.0 Final
		9 Feb 2017

3 Validation of CRDP#4 ECA products using TCCON

3.1 Overview


In this section the analysis performed by the GHG-CCI Validation Team (VALT) is described, in which the CRDP#4 ECA products have been compared with ground-based remote sensing data from the TCCON network (using TCCON version GGG2014R1). This version deals with the laser sampling error which plagued version GGG2012 and for which posteriori corrections had to be applied. Note that the TCCON dataset still contains some strong outliers which either indicate a not-yet-perfect error flag routine and/or strong ‘local’ events. Given that these outliers pertain to both spikes and sinks in the time series, the first is more likely. Therefore, we put all TCCON data through an additional filter, where we first fit the time series using the curve-fitting routines described by **/Thoning et al. 1989/**, after which an interquartile range filter is applied to the residuals. Typically, one flags data that are more than 1.5 times the IQR (difference between upper and lower quartile) above or below the upper or lower quartile respectively. Here we have flagged data that are beyond 4 times the IQR. In selecting the TCCON stations we have only taken sites which have amassed a longer than 1 year time series. Furthermore, Tsukuba and Pasadena/JPL have been excluded because they feature very strong biases (probably, being highly urban, related to non-ideal representativity with regards to their surrounding area). Both stations however are included in our analysis of Glint measurements given the limited number of coastal stations. Also included in the glint analysis is the Izaña station which is located at 2370 m a.s.l.. The satellite measurements that are collocated with this particular station undergo an additional correction based on the retrievals’ a priori profile and the surface pressure measured at the TCCON site. Given potential remaining biases in these stations, we focus our Glint analysis on the relative Glint vs land differences and not the absolute values.

With respect to the CRDP#3 analysis (detailed in **/PVIRv4/**) we have changed the collocation methodology from a mid-tropospheric temperature/emission based method to one based on CTM model (from CAMS) output. As mentioned above, we also include the analysis of glint measurements (using a different set of TCCON stations) and we have expanded the section on stability requirements. In most regards this work is a continuation of the first CRDP VALT analysis described in the **/PVIRv3/** and **/PVIRv4/** documents.

A detailed description of the methodology is given in section 3.1.1, while the most relevant obtained Figures of Merit (FoM) and example timeseries are shown in **Sect. 3.2** and a summary of the results is outlined in **Sect. 3.3**.

3.1.1 Methodology

Prior to the comparison with TCCON data (stations listed in **Tab. 3.1.1.1** for the normal and **Tab 3.1.1.2** for the glint analysis), the retrieval algorithm data have been corrected for their different a-priori profiles. According to **/Rodgers 2000/**, one can correct for the different a-

	ESA Climate Change Initiative (CCI)	Page 19
	Product Validation and Intercomparison Report (PVIR)	
	for the Essential Climate Variable (ECV) Greenhouse Gases (GHG)	Version 5.0 Final
		9 Feb 2017

priori profiles used in the TCCON and satellite retrieval algorithms. Here we have opted to use the TCCON a-priori as the common a-priori profile for all measurements. Using **/Rodgers 2000/**:

$$x_{cor} = x + \frac{1}{m_0} \sum_l m^l (A^l - 1) (ap_x^l - ap_T^l) \quad (3.1.1.1)$$


In which x_{cor} and x are the a-priori-corrected and original column-averaged dry air mole fractions, l is the vertical layer index, m^l corresponds with the mass of dry air in layer l , which is directly derived from $\Delta p^l/g^l$. Here Δp^l is the dry air pressure difference over layer l and g the gravitational constant. m_0 is the sum of m^l over all layers. A^l corresponds with the satellite algorithm's column averaging kernel, while ap_x and ap_T are the original and TCCON a-priori dry-air mole fractions respectively. It must be noted that this correction is fairly limited, and does not impact the conclusions reached in any significant way.

After the a-priori-correction, all available time series have been trimmed so as to work, in each given comparison round (of which there are 5), with data that have matching temporal coverage.

The comparison rounds are SCIAMACHY XCO₂ (BESD and WFMD), GOSAT XCO₂ (OCFP and SRFP, Full Physics algorithms), EMMA GOSAT XCO₂ (3 versions of the EMMA algorithm, EMMAv2.2a, v2.2b and v2.2c and OCFP and SRFP using the common EMMA overlap time. Note that in the output EMMAv2.2a is listed as EMMA, v2.2b as EMMB and V2.2c as EMMC, SCIAMACHY XCH₄ (IMAP and WFMD), GOSAT XCH₄ (OCFP, OCP, SRFP, SRPR and EMMA). In the last round, we include EMMA even though it has a much shorter timeseries. We did run a comparison in which the regular GOSAT algorithms were trimmed to the EMMA timeseries, but we do not explicitly show the results as they were very similar to the full timeseries.

To match satellite with TCCON data we used the following procedure. First we select all satellite data within 30° longitude and 10° latitude of a TCCON site. Then, for each satellite point, we select all TCCON measurements which meet the following conditions: the measurements needed to be taken within 3 days of the satellite measurement and be performed during the same time of day (within 2 hours). Furthermore, the difference between the total column mole fractions, derived from the CAMS model output, interpolated to the satellites' coordinates and those interpolated to the TCCON's coordinates cannot exceed 0.25 ppm (for XCO₂) and 5 ppb for XCH₄ respectively. All TCCON measurements that fall within these criteria are then averaged, producing a single Satellite-TCCON pair. Note that we not use the model for any correction nor do we need the model to be correct in an absolute sense. We rely on its capability of capturing relative differences within the pre-selected (+-30° lon, +-10° lat, 3 days) frame. We are also aware that the real variability can exceed the model predicted one due to the limited resolution of the model output. Nevertheless, any collocation method is bound to introduce biases and we feel that this method provides the best compromise between minimising this potential error and yielding enough data for our analysis.

From these data-pairs we derived various statistical parameters, the so-called Figures of Merit or FoM. In the Figures and Tables in chapter 3, N corresponds with the number of

	ESA Climate Change Initiative (CCI)	Page 20
	Product Validation and Intercomparison Report (PVIR)	
	for the Essential Climate Variable (ECV) Greenhouse Gases (GHG)	Version 5.0 Final
		9 Feb 2017

collocated data pairs, R is the Pearson's r correlation coefficient, Bias stands for the average satellite-FTS difference as in:

$$\text{Bias} = \text{mean}(X_{\text{sat}} - X_{\text{FTS}}) \quad (3.1.1.2)$$

While the scatter corresponds with the standard deviation of said difference as in:

$$\text{Scatter} = \text{std}(X_{\text{sat}} - X_{\text{FTS}}) \quad (3.1.1.3)$$

All these parameters have been calculated using the individual data pairs, including R (different from PVIRv2). The example time series plots however show daily averages.

Other FoM are the Relative accuracy (RA), Seasonality (Seas) and Seasonal Relative Accuracy (SRA). We define RA as the standard deviation on the overall biases (derived from individual data) obtained at each station. The "Seasonal Relative Accuracy" (SRA), differs from the relative accuracy in that it uses the seasonal bias means at each station, instead of the overall biases obtained at each station, it is thus the standard deviation over all station seasonal bias results. The seasonal bias results are constructed from all data pairs which fall within the months of January till March (JFM), April till June (AMJ), July till September (JAS) or October till December (OND), regardless of the year the measurements are taken. Some stations feature only limited data during certain seasons, which sometimes results in erratic (seasonal) bias results. To avoid the inclusion of these results into the RA and SRA calculation, we do not include those results which are derived from less than 10 individual data points or have a standard error (σ/\sqrt{N}) which exceeds the threshold Relative Accuracy requirements (0.5 ppm XCO₂, 10 ppb XCH₄). RA and SRA are also derived from a common dataset, thus if one algorithm in the validation round fails to meet the quality requirements for station x and season y, the corresponding bias result is also excluded from the SRA and RA calculation of its competitor. If no data is excluded, the RA is the standard deviation of 13 station bias results, while the SRA is the standard deviation over 52 (13x4) seasonal bias results, in case temporal overlap between satellite and TCCON permits it.

The Seasonality (Seas) is the standard deviation of the 4 overall (using all data pairs over all stations) seasonal biases, and yields some information on how the seasonal cycle is captured in conjunction with the seasonal time series figures of which several examples are shown in the following sections, as well as the fit results, particularly the amplitude results discussed later.



Product Validation and Intercomparison Report (PVIR)

for the Essential Climate Variable (ECV)
Greenhouse Gases (GHG)

Version 5.0
Final

9 Feb 2017

TCCON stations					
Name	Lat(°)	Lon(°)	Alt(m)	Time covered	N
Sodankyla (SOD)	67.37	26.63	179	05/2009-05/2016	115613
Bialystok(BIA)	53.23	23.03	183	03/2009-08/2015	91202
Bremen(BRE)	49.10	8.44	110	01/2007-08/2015	30804
Karlsruhe (KAR)	49.10	8.44	110	04/2010-08/2015	16821
Orleans (ORL)	47.96	2.11	132	08/2009-08/2015	65227
Garmisch (GAR)	47.48	11.06	744	07/2007-08/2015	67029
Park Falls (PAR)	45.94	-90.27	442	06/2004-05/2016	271820
Lamont (LAM)	36.60	-97.49	320	07/2008-05/2016	399400
Saga (SAG)	33.24	130.29	7	07/2011-02/2016	47702
Darwin (DAR)	-12.42	130.89	30	08/2005-08/2015	299326
Reunion(REU)	-20.9	55.49	87	09/2011-05/2016	89719
Wollongong (WOL)	-34.41	150.88	30	06/2008-08/2015	124508
Lauder (LAU)	-45.05	169.68	370	06/2004-03/2016	416908

Table 3.1.1.1: List of TCCON stations, their location, the coverage of their dataset and number of data (N).


TCCON stations(glint)					
Name	Lat(°)	Lon(°)	Alt(m)	Time covered	N
Tsukuba (TSU)	36.05	140.12	31	08/2011-08/2015	72635
JPL Pasadena(JPL)	53.23	23.03	183	03/2009-08/2015	91202
Saga (SAG)	33.24	130.29	7	07/2011-02/2016	47702
Izana (IZA)	49.10	8.44	110	04/2010-08/2015	16821
Ascension (ASC)	47.96	2.11	132	08/2009-08/2015	65227
Darwin (DAR)	-12.42	130.89	30	08/2005-08/2015	299326
Reunion(REU)	-20.9	55.49	87	09/2011-05/2016	89719
Wollongong (WOL)	-34.41	150.88	30	06/2008-08/2015	124508
Lauder (LAU)	-45.05	169.68	370	06/2004-03/2016	416908

Table 3.1.1.2: List of TCCON stations, their location, the coverage of their dataset and number of data (N) used for the glint data quality assessment.

We also calculate the average variability of the FTIR measurements within the collocation timeframe for error analysis purposes, the so called TCCON_error.

In order to determine if the reported uncertainties on the algorithm are correct (Sat_error), we compare these uncertainties with the Scatter, taking into account the above mentioned variability of the TCCON data itself as in

$$\text{Scatter} = \sqrt{\text{Sat_error}^2 + \text{TCCON_error}^2} \quad (3.1.1.4)$$

	ESA Climate Change Initiative (CCI)	Page 22
	Product Validation and Intercomparison Report (PVIR)	
	for the Essential Climate Variable (ECV) Greenhouse Gases (GHG)	Version 5.0 Final
		9 Feb 2017


To verify the stability of the algorithm over time we fit a linear trend and seasonal cycle through the daily averaged satellite-TCCON difference timeseries:

$$X = i + s \cdot t + A \cdot \sin(2\pi \cdot (t + ph)) \quad (3.1.15)$$

Here, X represents the satellite minus TCCON difference, i the intercept, s the slope which corresponds with the linear drift, A the amplitude of the seasonal cycle and ph the phase shift. The overall stability of an algorithm is determined by the weighted average of all linear drift (s) results over all stations. The weights are determined by $1/(s_err)^2$, where s_err is the standard deviation on the s fit result. In practice this eliminates any significant contribution to said stability from stations with limited timeseries such as Reunion and Saga. Likewise the uncertainty of this stability corresponds with the 95% confidence interval for the weighted mean. The results of these fits are reported in **Tables 3.2.x.2**.

While the slope yields information on any potential drift, the amplitude in the above fit results gives us information on the potential mismatch between Satellite and TCCON seasonal cycles. Ideally there should be no difference between these cycles which would yield an amplitude=0 in the bias timeseries. The bias amplitude can either be the result of a phase shift between satellite and TCCON cycles or a difference in Amplitude. Therefore the above equation is also fitted on the TCCON and satellite data itself, whereby the slope 's' now corresponds with the actual observed growthrate in stead of the seasonal drift and A and ph are the actual TCCON or Satellite seasonal cycle components. To assess these results we focus on the overall Northern and Southern Hemisphere data, where we show these timeseries and their fit using a **/Thoning et al 1989/** approach. We also show the long term trend fit through the bias timeseries.

To further assess the stability we calculate the standard deviation and range (maximum difference) of all the yearly averages in the bias timeseries. This yields information on the stability of the bias, which is not captured by a steady drift. To calculate this **/year-to-year variability and range/** or YtY_std and YtY_range for a particular station, we, for a given starting point in the timeseries, cut the timeseries in yearly portions. Then we calculate the median for all yearly sections and the corresponding standard deviation and range for this particular set of medians. We repeat this for different starting points in the timeseries until all combinations of yearly medians are obtained and thus for a given station we have acquired a set of standard deviations and ranges. From this set of standard deviations for one particular station the mean standard deviation and range can be draw as well as its 95% confidence band on the mean using the approach outlined in **/Oliphant T.E. 2006/**. The overall mean and confidence band of said station means is then derived from the (13) station values yielding the overall year to years standard deviation and year to year range (YtY std and YtY range).

	ESA Climate Change Initiative (CCI)	Page 23
	Product Validation and Intercomparison Report (PVIR)	
	for the Essential Climate Variable (ECV) Greenhouse Gases (GHG)	Version 5.0 Final
		9 Feb 2017

3.2 Results

In this section we list the most relevant FoM and several example time series for each of the validation rounds. Note that the timeseries shown in the figures have not yet been trimmed so as to exactly overlap with the timespan of its competitors. Hence the bias and scatter results in the figures may differ from those in the tables.

In each section we show

- 1) A table listing all Bias, Scatter, R and N results as well as the RA, Seas and SRA FoM.
- 2) An overview plot showing Bias, Scatter, R and N per TCCON station.
- 3) Example timeseries (not trimmed to the same timeframe).
- 4) An overview table listing the Slope, Amplitude and their respective 95% confidence intervals obtained from a seasonal fit through the Sat-TCCON difference timeseries as well as the derived Stability.
- 5) Northern and Southern Hemisphere timeseries (trimmed) of the satellite and TCCON data with their respective seasonal fit results.
- 6) Northern and Southern Hemisphere timeseries of the algorithm-TCCON Bias and its respective long-term trend fit.



ESA Climate Change Initiative (CCI)

**Product Validation and
Intercomparison Report (PVIR)**

for the Essential Climate Variable (ECV)
Greenhouse Gases (GHG)

Page 24

Version 5.0
Final

9 Feb 2017

3.2.1 SCIAMACHY XCO₂

SCIAMACHY XCO ₂ results								
Station	BESD				WFMD			
	Bias	Scatter	R	N	Bias	Scatter	R	N
SOD	0.67	2.38	0.84	3264	-0.04	3.47	0.71	4828
BIA	-0.28	2.00	0.86	11305	0.52	2.96	0.71	25656
BRE	-0.42	1.97	0.87	10666	-0.07	3.00	0.76	21730
KAR	0.05	2.23	0.74	7883	0.65	3.09	0.64	17196
ORL	-0.22	2.02	0.88	6234	0.50	2.94	0.76	11438
GAR	-0.24	2.17	0.90	19047	-0.07	3.01	0.81	35652
PAR	-0.08	1.95	0.95	55214	0.03	2.77	0.90	142357
LAM	-0.11	1.85	0.88	48285	-0.05	2.71	0.78	110456
SAG	-0.61	2.03	0.73	1313	-0.32	3.95	0.38	2276
DAR	0.07	1.73	0.89	41459	-1.29	1.90	0.86	69313
REU	-0.52	1.46	0.34	678	-1.28	2.69	0.20	2488
WOL	0.49	1.90	0.72	53449	-0.15	2.07	0.66	87627
LAU	0.34	2.11	0.89	3293	-0.05	2.80	0.80	5371
N-H	-0.13	1.99	0.92	163211	0.06	2.85	0.87	371589
S-H	0.30	1.85	0.88	98879	-0.64	2.12	0.85	164799
All	0.03	1.95	0.91	262090	-0.15	2.67	0.87	536388
RA	0.37				0.57			
Seas	0.17				0.15			
SRA	0.56				0.71			

Table 3.2.1.1: BESD and WFMD XCO₂ validation results for all individual stations and using all data combined (ALL). All units apart from R and N are in ppm. NH and SH are the results obtained from all Northern and Southern Hemisphere data pairs. Seasonality (Seas) and Seasonal Relative accuracy are drawn from the seasonal FoM bias results (not shown).

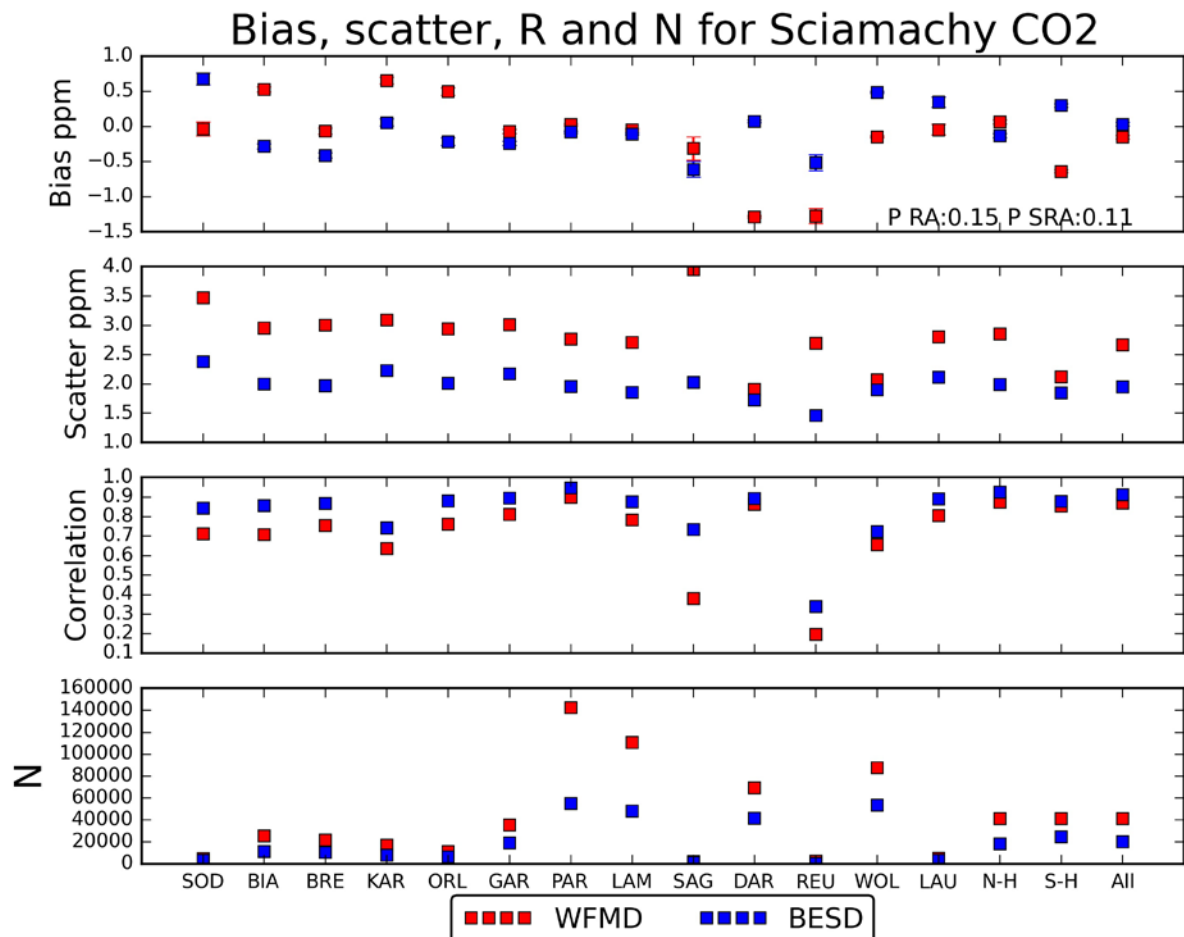


Figure 3.2.1.1: BESD and WFMD XCO₂ validation results for all individual stations, Northern and Southern hemisphere (NH and SH respectively) and using all data combined (All). All units apart from R and N are in ppm. a) Bias, b) scatter, c) correlation and d) number of datapairs. Note that for N “NH”, “SH” and “All” correspond with the average number per station.



ESA Climate Change Initiative (CCI)

Product Validation and Intercomparison Report (PVIR)

for the Essential Climate Variable (ECV)
Greenhouse Gases (GHG)

Page 26

Version 5.0
Final

9 Feb 2017

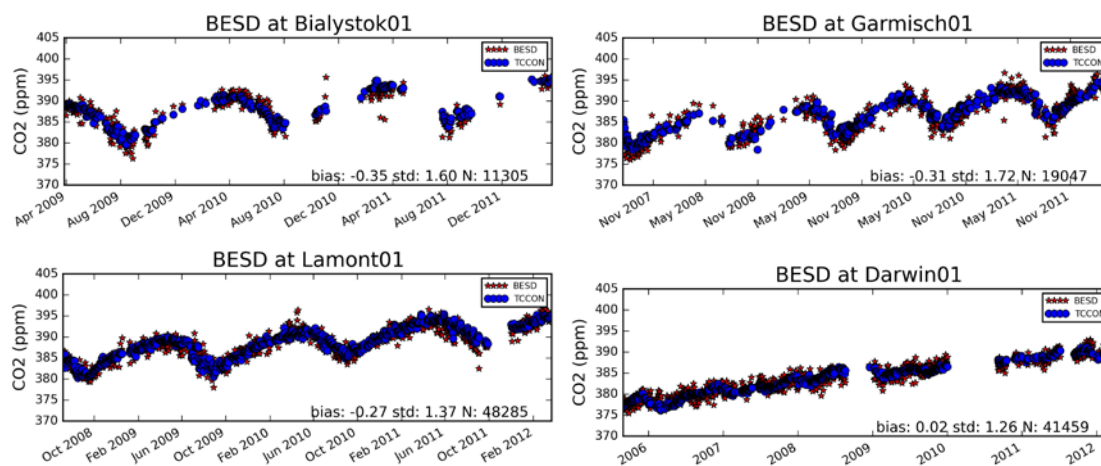


Figure 3.2.1.2: Example timeseries of daily averaged BESD and FTIR XCO₂ data.

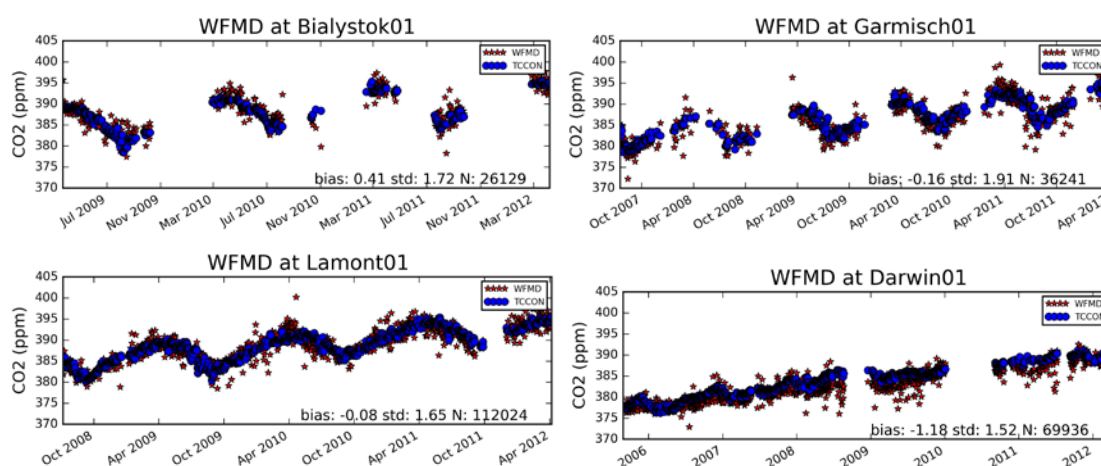


Figure 3.2.1.3: Example timeseries of daily averaged WFMD and FTIR XCO₂ data.



ESA Climate Change Initiative (CCI)

**Product Validation and
Intercomparison Report (PVIR)**

for the Essential Climate Variable (ECV)
Greenhouse Gases (GHG)

Page 27

Version 5.0
Final

9 Feb 2017

SCIAMACHY XCO ₂ fit results								
Station	BESD				WFMD			
	Slope	Slope err	Ampli	Ampli err	slope	Slope err	Ampli	Ampli err
SOD	0.05	-0.27	3.42	-4.14	0.58	-0.36	3.06	-4.82
BIA	-0.13	-0.20	0.52	-0.71	0.17	-0.20	0.30	-0.11
BRE	0.07	-0.10	0.30	-0.63	0.28	-0.13	0.18	-0.34
KAR	0.22	-0.45	0.52	-1.06	0.22	-0.37	0.18	-0.38
ORL	0.50	-0.19	0.10	-0.61	0.35	-0.27	0.32	-1.04
GAR	0.06	-0.09	0.80	0.56	0.08	-0.10	0.79	0.48
PAR	0.08	-0.03	0.14	-0.05	0.13	-0.03	0.34	-0.58
LAM	-0.18	-0.08	0.29	0.35	-0.10	-0.09	0.50	0.46
SAG	8.90	-9.55	1.76	-9.26	33.57	-13.76	7.66	-29.57
DAR	-0.03	-0.04	0.33	-0.41	-0.15	-0.04	0.52	0.55
REU	-12.82	-15.87	3.09	6.25	-22.63	-16.94	4.63	14.86
WOL	0.00	-0.09	0.78	-0.92	-0.12	-0.09	1.09	-1.13
LAU	0.13	-0.10	0.35	-0.76	-0.03	-0.10	0.89	-1.25
N-H	0.04	-0.03	0.14	-0.25	0.12	-0.03	0.12	-0.33
S-H	0.08	-0.04	0.33	-0.50	0.08	-0.04	0.11	-0.08
All	0.05	-0.02	0.22	-0.34	0.08	-0.02	0.19	-0.34
Stability	0.03 ± 0.06 ppm/year				0.03 ± 0.10 ppm/year			

Table 3.2.1.2: BESD and WFMD XCO₂ SAT-FTS fit results for all individual stations and using all data combined (All). All units are in ppm. NH and SH are the results obtained from all Northern and Southern Hemisphere data pair. Stability is the weighted average over all station slope results, with weights=1/(slope error)². The uncertainty on the stability corresponds with the 95% confidence interval.

SCIAMACHY XCO ₂ Year to Year results								
Station	BESD				WFMD			
	YtYstd	95% err	YtY range	95% err	YtYstd	95% err	YtY range	95% err
SOD	0.26	0.05	0.52	0.10	0.20	0.04	0.40	0.07
BIA	0.27	0.02	0.54	0.04	0.13	0.02	0.25	0.04
BRE	0.26	0.02	0.67	0.06	0.38	0.02	0.96	0.05
KAR	NULL	NULL	NULL	NULL	NULL	NULL	NULL	NULL
ORL	0.23	0.03	0.46	0.07	0.12	0.02	0.24	0.04
GAR	0.39	0.02	1.02	0.07	0.28	0.01	0.71	0.02
PAR	0.28	0.00	0.82	0.01	0.36	0.00	1.11	0.01
LAM	0.22	0.01	0.50	0.01	0.28	0.01	0.62	0.01
SAG	NULL	NULL	NULL	NULL	NULL	NULL	NULL	NULL
DAR	0.40	0.01	1.09	0.02	0.55	0.00	1.62	0.01
REU	NULL	NULL	NULL	NULL	NULL	NULL	NULL	NULL
WOL	0.32	0.01	0.76	0.02	0.26	0.01	0.63	0.02
LAU	0.59	0.02	1.83	0.08	0.52	0.04	1.51	0.14
N-H	0.17	0.01	0.53	0.02	0.26	0.01	0.70	0.02
S-H	0.28	0.03	0.83	0.12	0.39	0.02	1.07	0.04
All	0.19	0.01	0.60	0.03	0.26	0.00	0.79	0.01
Mean	0.32±0.08 ppm		0.82±0.30 ppm		0.31 ± 0.11 ppm		0.80±0.35 ppm	

Table 3.2.1.3: BESD and WFMD XCO₂ SAT-FTS year-to-year stability results for all individual stations and using all data combined (All). All units are in ppm. NH and SH are the results obtained from all Northern and Southern Hemisphere data pair.



ESA Climate Change Initiative (CCI)

Product Validation and Intercomparison Report (PVIR)

for the Essential Climate Variable (ECV)
Greenhouse Gases (GHG)

Page 28

Version 5.0
Final

9 Feb 2017

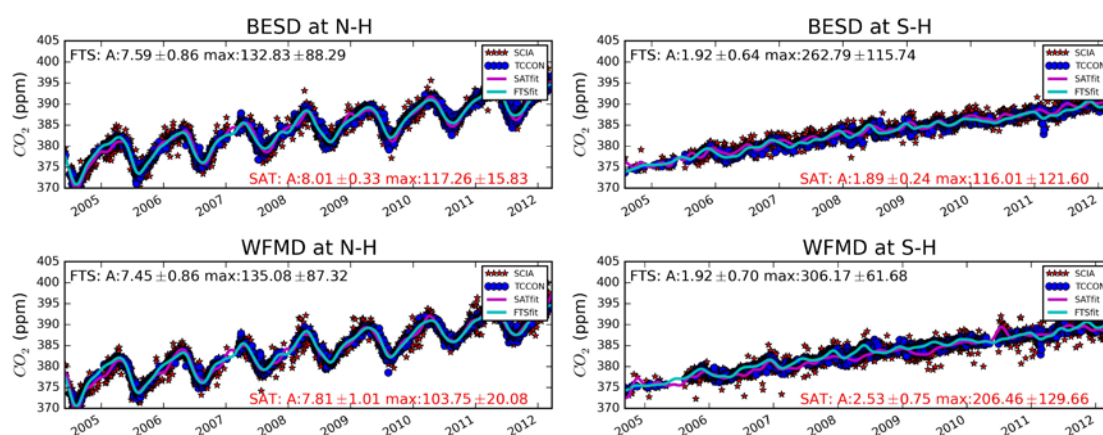


Figure 3.2.1.4: Northern and Southern Hemisphere timeseries of daily averaged BESD,WFMD and TCCON XCO_2 data, including trend and seasonal fit results.

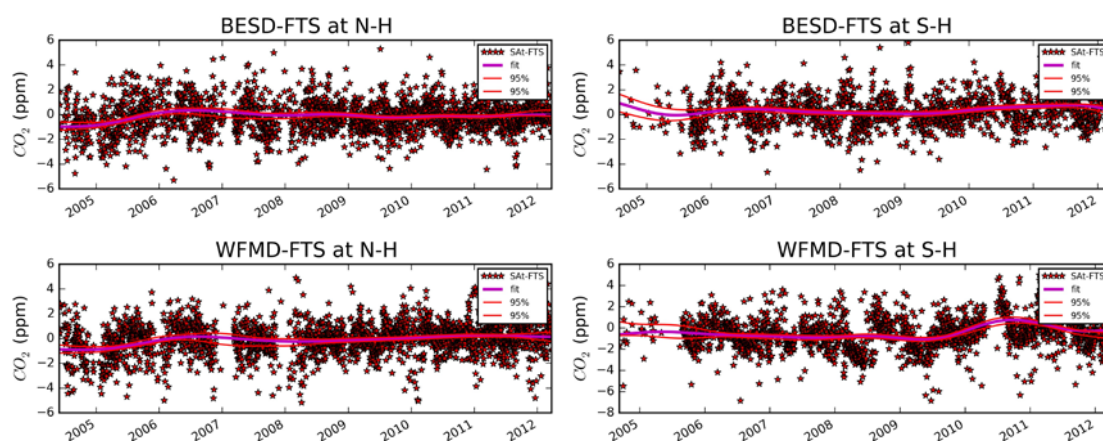


Figure 3.2.1.5: Northern and Southern Hemisphere timeseries of daily averaged BESD,WFMD - TCCON XCO_2 Bias data, including trend fit results.



3.2.2 GOSAT XCO₂

GOSAT XCO ₂ results								
Station	OCFP				SRFP			
	Bias	Scatter	R	N	Bias	Scatter	R	N
SOD	0.59	2.00	0.93	1304	0.67	2.04	0.93	1253
BIA	0.47	1.81	0.95	4453	0.11	2.04	0.93	5776
BRE	0.48	1.93	0.92	1730	0.25	2.05	0.91	2171
KAR	0.40	1.99	0.92	4345	0.28	2.18	0.91	4485
ORL	0.34	1.84	0.94	3787	0.02	2.19	0.92	3857
GAR	0.42	1.85	0.94	5587	0.05	2.12	0.92	5986
PAR	0.16	1.78	0.94	11343	-0.07	1.98	0.92	12849
LAM	-0.01	1.92	0.92	21650	-0.09	2.05	0.92	22707
SAG	-0.13	2.21	0.84	1632	0.71	2.49	0.83	1977
DAR	-0.21	1.60	0.92	6957	-0.68	1.68	0.92	9432
REU	0.51	1.77	0.86	3394	0.26	1.91	0.84	3819
WOL	-0.18	1.49	0.93	12844	-0.39	1.68	0.91	16413
LAU	1.12	1.94	0.90	1043	0.12	2.27	0.88	797
N-H	0.19	1.90	0.93	55831	0.03	2.09	0.92	61061
S-H	-0.03	1.62	0.93	24238	-0.38	1.75	0.92	30461
All	0.12	1.82	0.93	80069	-0.11	1.99	0.92	91522
RA	0.36 (0.35)				0.36 (0.41)			
Seas	0.15 (0.14)				0.24 (0.21)			
SRA	0.58 (0.52)				0.51 (0.52)			

Table 3.2.2.1: OCFP and SRFP XCO₂ validation results for all individual stations and using all data combined (ALL). All units apart from R and N are in ppm. NH and SH are the results obtained from all Northern and Southern Hemisphere data pairs. RA, Seas and SRA values in brackets correspond with the trimmed to fit EMMA timeseries results

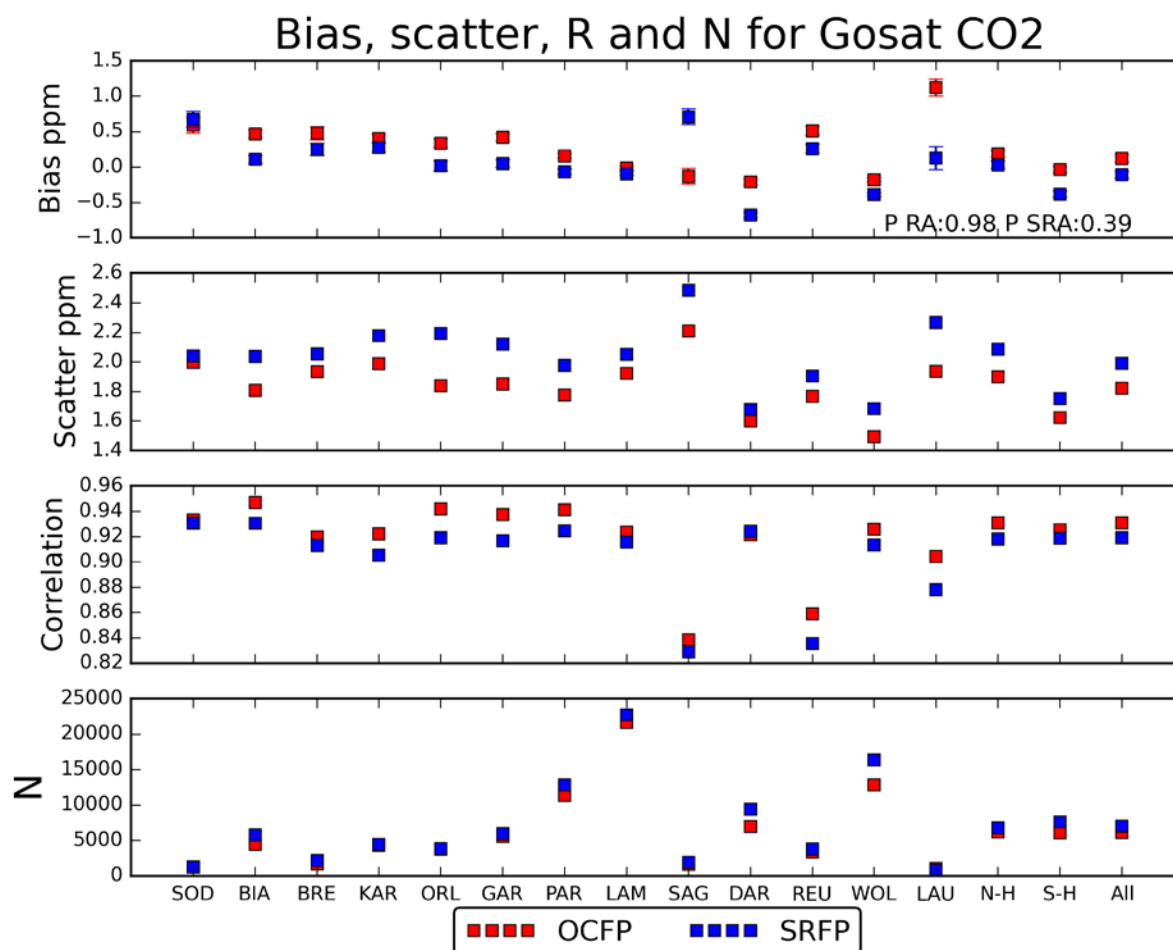


Figure 3.2.2.1: OCFP and SRFP XCO₂ validation results for all individual stations, Northern and Southern hemisphere (NH and SH respectively) and using all data combined (All). All units apart from R and N are in ppm. a) Bias, b) scatter, c) correlation (from daily averaged data) and d) number of datapairs. Note that for N “NH”, “SH” and “All” correspond with the average number per station.



ESA Climate Change Initiative (CCI)

**Product Validation and
Intercomparison Report (PVIR)**

for the Essential Climate Variable (ECV)
Greenhouse Gases (GHG)

Page 31

Version 5.0
Final

9 Feb 2017

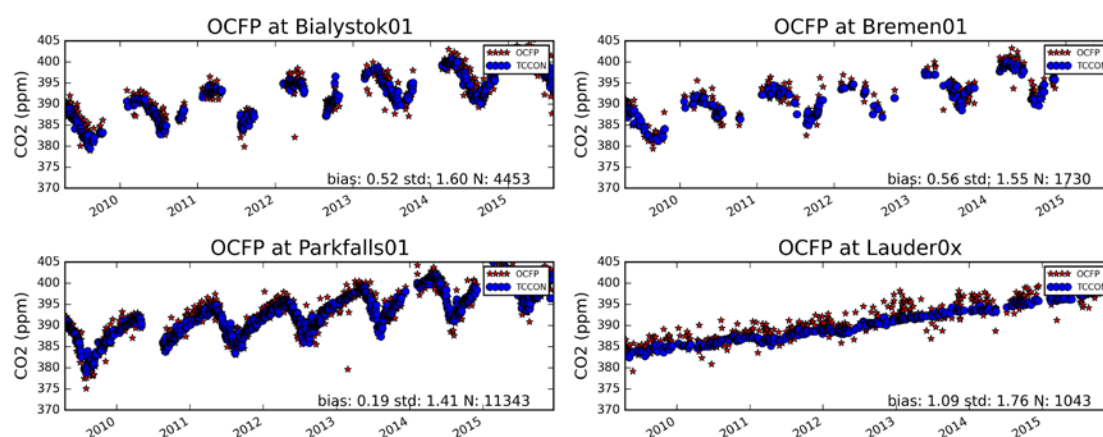


Figure 3.2.2.2: Example timeseries of daily averaged OCFP and FTIR XCO₂ data.

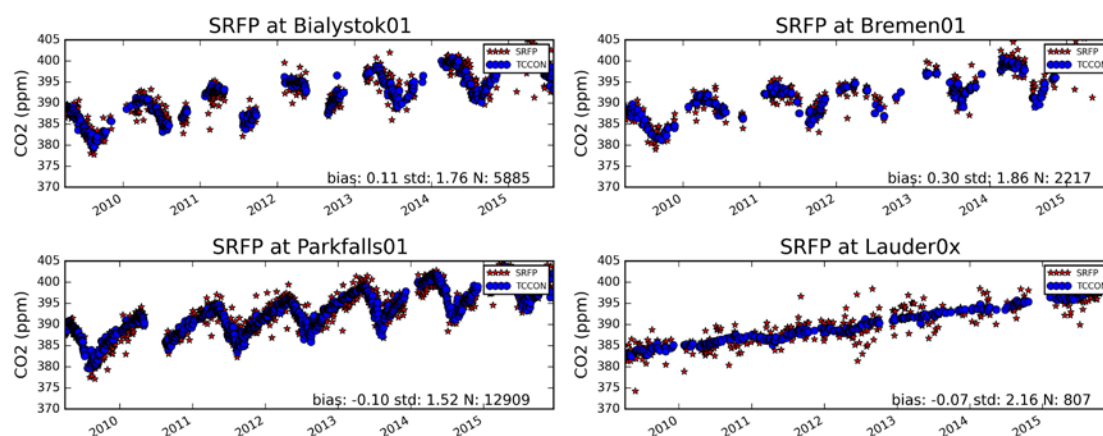


Figure 3.2.2.3: Example timeseries of daily averaged SRFP and FTIR XCO₂ data.



ESA Climate Change Initiative (CCI)

**Product Validation and
Intercomparison Report (PVIR)**

for the Essential Climate Variable (ECV)
Greenhouse Gases (GHG)

Page 32

Version 5.0
Final

9 Feb 2017

GOSAT XCO ₂ fit results								
Station	OCFP				SRFP			
	Slope	Slope err	Ampli	Ampli err	slope	Slope err	Ampli	Ampli err
SOD	-0.10	0.09	1.94	0.68	0.06	0.10	0.52	0.67
BIA	-0.11	0.05	0.70	0.22	0.05	0.06	1.03	0.21
BRE	0.02	0.08	0.26	0.21	0.12	0.09	0.64	0.29
KAR	-0.17	0.07	0.33	0.21	-0.11	0.07	0.64	0.21
ORL	-0.10	0.06	0.46	0.18	0.03	0.07	0.79	0.19
GAR	-0.09	0.05	0.08	0.15	-0.02	0.06	0.28	0.17
PAR	-0.03	0.04	0.23	0.11	0.01	0.04	0.56	0.12
LAM	-0.11	0.03	0.29	0.08	-0.01	0.03	0.44	0.09
SAG	-0.06	0.14	0.49	0.29	-0.09	0.15	0.59	0.30
DAR	-0.03	0.04	1.07	0.12	0.11	0.04	0.81	0.12
REU	0.02	0.10	0.91	0.17	-0.13	0.10	0.67	0.17
WOL	-0.04	0.03	0.23	0.09	0.06	0.03	0.16	0.09
LAU	-0.05	0.08	1.05	0.23	-0.01	0.11	0.44	0.33
N-H	-0.11	0.02	0.21	0.06	0.02	0.02	0.45	0.06
S-H	0.00	0.03	0.39	0.07	0.08	0.03	0.28	0.07
All	-0.09	0.02	0.20	0.04	0.03	0.02	0.36	0.04
Stability	-0.07 ± 0.07 ppm/year				0.02 ± 0.04 ppm/year			

Table 3.2.2.2: OCFP and SRFP XCO₂ SAT-FTS fit results for all individual stations and using all data combined (All). All units are in ppm. NH and SH are the results obtained from all Northern and Southern Hemisphere data pair. Stability is the weighted average over all station slope results, with weights=1/(slope error)². The uncertainty on the stability corresponds with the 95% confidence interval.

GOSAT XCO ₂ fit results								
Station	OCFP				SRFP			
	YtYstd	95% err	YtY range	95% err	YtYstd	95% err	YtY range	95% err
SOD	0.22	0.03	0.61	0.07	0.16	0.01	0.45	0.03
BIA	0.31	0.01	0.89	0.02	0.30	0.02	0.87	0.05
BRE	0.38	0.02	1.01	0.04	0.48	0.01	1.22	0.03
KAR	0.30	0.01	0.73	0.02	0.24	0.01	0.65	0.03
ORL	0.29	0.01	0.79	0.03	0.17	0.01	0.45	0.03
GAR	0.21	0.01	0.56	0.02	0.28	0.01	0.79	0.04
PAR	0.27	0.01	0.73	0.02	0.26	0.01	0.78	0.02
LAM	0.39	0.01	1.08	0.02	0.28	0.00	0.75	0.01
SAG	0.20	0.01	0.49	0.04	0.24	0.01	0.59	0.04
DAR	0.51	0.02	1.59	0.08	0.48	0.02	1.45	0.05
REU	0.28	0.01	0.71	0.03	0.24	0.02	0.58	0.04
WOL	0.13	0.00	0.36	0.01	0.21	0.00	0.56	0.01
LAU	0.27	0.01	0.77	0.03	0.23	0.01	0.65	0.05
N-H	0.23	0.00	0.68	0.01	0.08	0.00	0.22	0.01
S-H	0.11	0.00	0.31	0.01	0.16	0.00	0.44	0.01
All	0.18	0.00	0.56	0.00	0.06	0.00	0.16	0.00
Mean	0.29±0.06 ppm		0.79±0.19 ppm		0.27 ± 0.12 ppm		0.75±0.18 ppm	

Table 3.2.2.3: OCFP and SRFP XCO₂ SAT-FTS year-to-year stability results for all individual stations and using all data combined (All). All units are in ppm. NH and SH are the results obtained from all Northern and Southern Hemisphere data pair.



ESA Climate Change Initiative (CCI)

Product Validation and Intercomparison Report (PVIR)

for the Essential Climate Variable (ECV)
Greenhouse Gases (GHG)

Page 33

Version 5.0
Final

9 Feb 2017

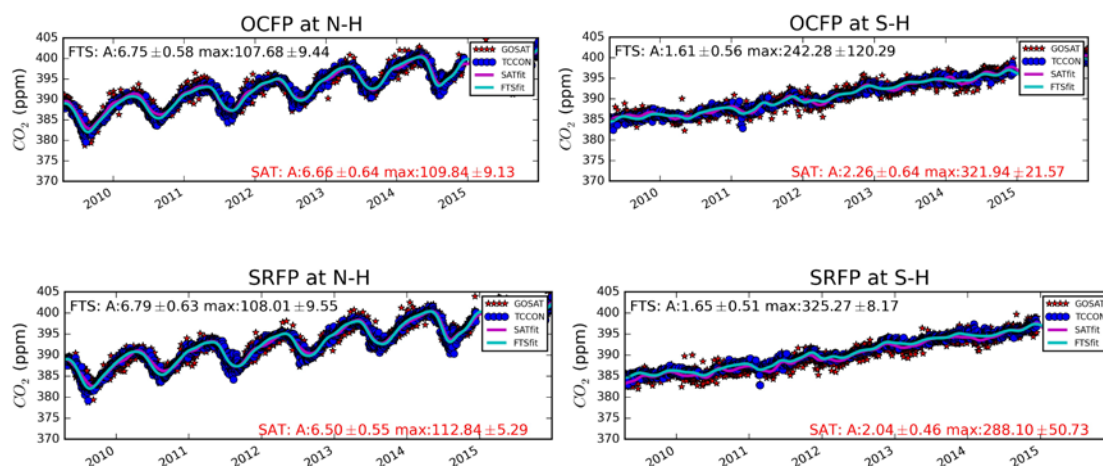


Figure 3.2.2.4: Northern and Southern Hemisphere timeseries of daily averaged SRFP, OCFP and TCCON XCO₂ data, including trend and seasonal fit results.

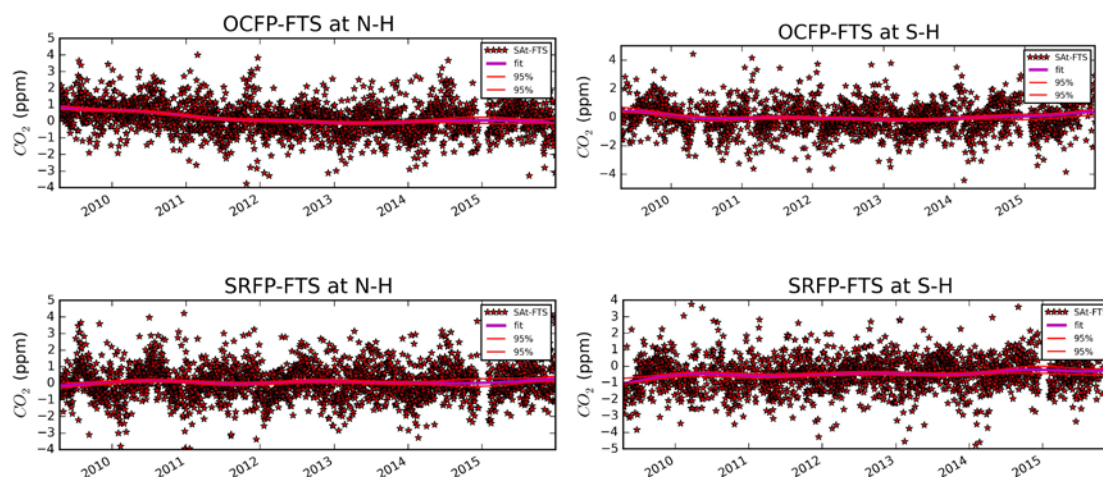


Figure 3.2.2.5: Northern and Southern Hemisphere timeseries of daily averaged SRFP, OCFP -TCCON Bias XCO₂ data, including trend fit results.



ESA Climate Change Initiative (CCI)

**Product Validation and
Intercomparison Report (PVIR)**

for the Essential Climate Variable (ECV)
Greenhouse Gases (GHG)

Page 34

Version 5.0
Final

9 Feb 2017

3.2.3 EMMA XCO₂

EMMA XCO ₂ results												
Station	EMMA				EMMB				EMMC			
	Bias	Scatter	R	N	Bias	Scatter	R	N	Bias	Scatter	R	N
SOD	0.84	2.55	0.81	654	0.87	1.96	0.88	493	0.91	1.84	0.90	464
BIA	0.90	2.54	0.80	2736	0.51	1.76	0.91	1695	0.51	1.88	0.90	1682
BRE	0.43	2.28	0.78	1383	0.43	1.81	0.87	912	0.35	1.82	0.88	894
KAR	0.88	2.24	0.72	2539	0.88	1.89	0.80	1859	0.86	1.92	0.80	1844
ORL	0.46	2.15	0.84	1956	0.40	1.83	0.89	1464	0.42	1.95	0.87	1495
GAR	0.50	2.16	0.82	4084	0.47	1.91	0.87	3378	0.55	1.88	0.87	3073
PAR	0.43	2.03	0.83	5909	0.59	1.74	0.87	4875	0.41	1.68	0.88	4618
LAM	0.41	1.93	0.83	10239	0.40	1.75	0.86	8987	0.30	1.73	0.86	8678
SAG	0.93	2.12	0.75	269	0.79	2.24	0.72	287	0.72	2.24	0.71	269
DAR	-0.50	1.67	0.66	3326	-0.15	1.33	0.77	2241	-0.22	1.36	0.77	2019
REU	0.18	1.86	0.25	159	0.21	1.34	0.32	150	0.26	1.19	0.51	121
WOL	0.37	1.68	0.61	8064	0.34	1.45	0.70	6697	0.11	1.43	0.71	6183
LAU	0.79	1.73	0.72	349	0.85	1.69	0.70	432	0.62	1.69	0.71	431
N-H	0.53	2.13	0.81	29769	0.51	1.81	0.87	23950	0.44	1.80	0.87	23017
S-H	0.14	1.73	0.62	11898	0.24	1.46	0.72	9520	0.06	1.44	0.72	8754
All	0.42	2.03	0.80	41667	0.44	1.72	0.86	33470	0.34	1.72	0.86	31771
RA	0.37				0.29				0.30			
Seas	0.11				0.11				0.12			
SRA	0.45				0.38				0.39			

Table 3.2.3.1: EMMA (v2.2a, b and c, flagged as EMMA, EMMB and EMMC) XCO₂ validation results for all individual stations and using all data combined (ALL). All units apart from R and N are in ppm. NH and SH are the results obtained from all Northern and Southern Hemisphere data pairs.

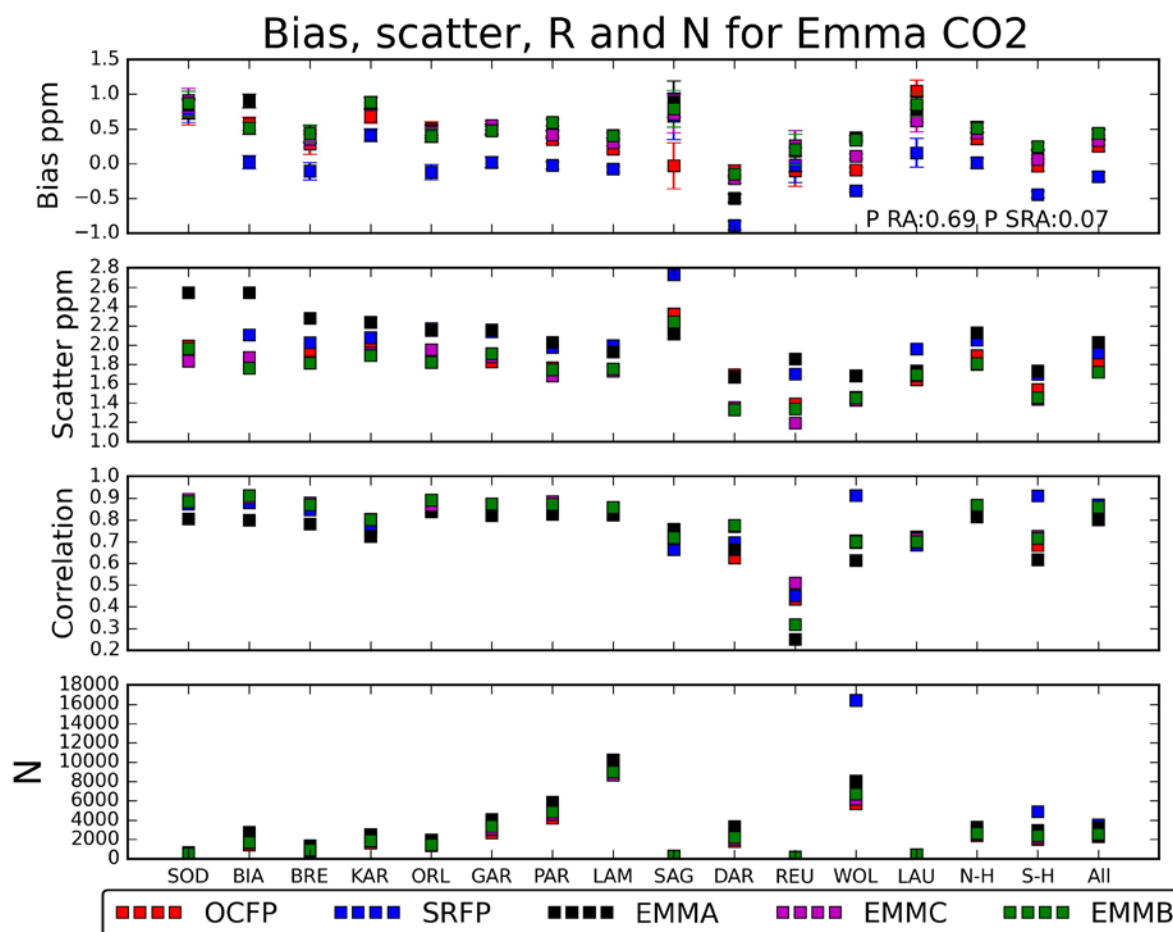


Figure 3.2.3.1: GOSAT XCO₂ validation results for 3 versions of EMMA as well as OCFP and SRFP (trimmed to match the EMMA coverage in time) for all individual stations, Northern and Southern hemisphere (NH and SH respectively) and using all data combined (All). All units apart from R and N are in ppm. a) Bias, b) scatter, c) correlation and d) number of datapairs. Note that for N “NH”, “SH” and “All” correspond with the average number per station.



ESA Climate Change Initiative (CCI)

Product Validation and Intercomparison Report (PVIR)

for the Essential Climate Variable (ECV)
Greenhouse Gases (GHG)

Page 36

Version 5.0
Final

9 Feb 2017

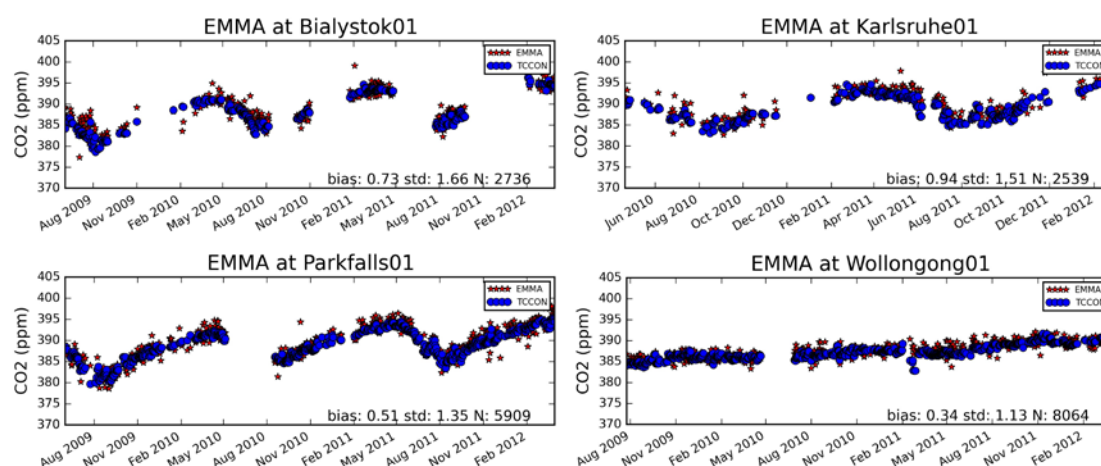


Figure 3.2.3.2: Example timeseries of daily averaged EMMAv2.2a (EMMA) and FTIR XCO₂ data.

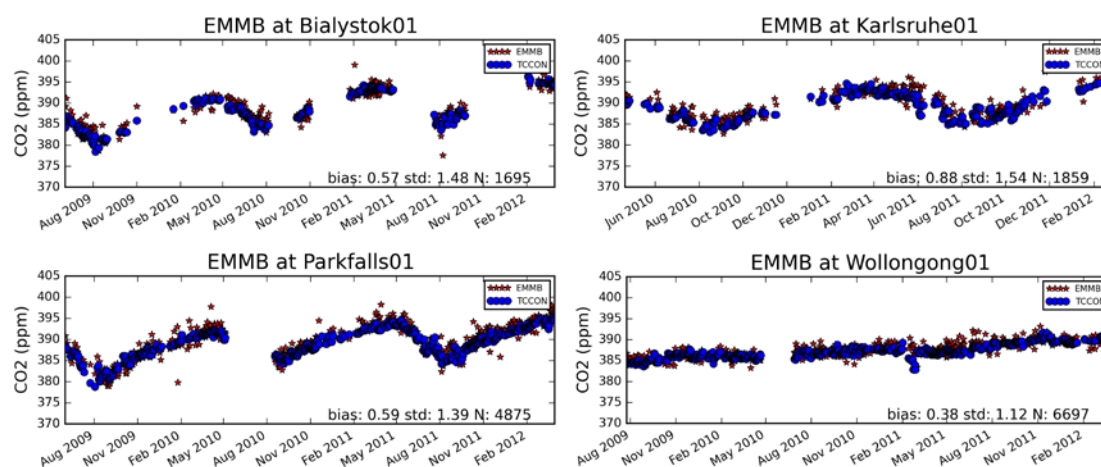


Figure 3.2.3.3: Example timeseries of daily averaged EMMAv2.2b (EMMB) and FTIR XCO₂ data.



ESA Climate Change Initiative (CCI)

**Product Validation and
Intercomparison Report (PVIR)**

for the Essential Climate Variable (ECV)
Greenhouse Gases (GHG)

Page 37

Version 5.0
Final

9 Feb 2017

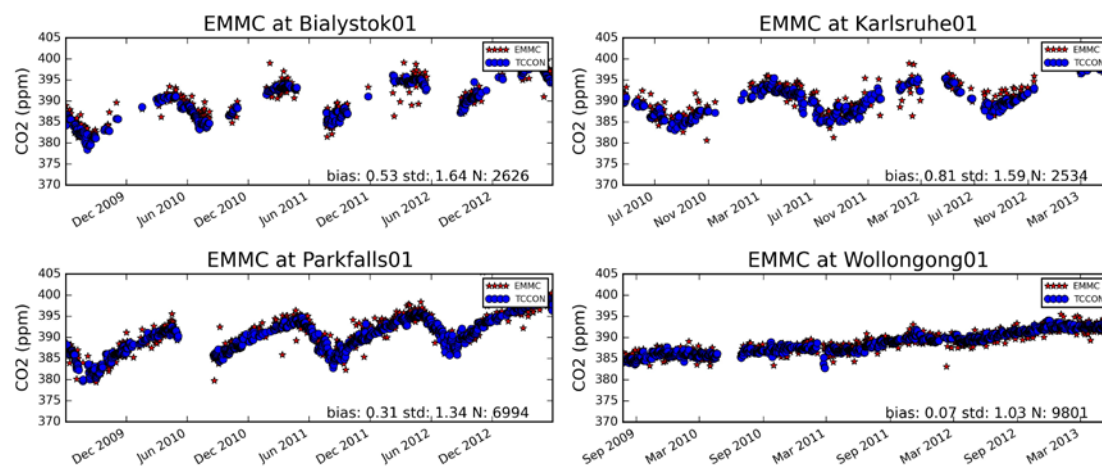


Figure 3.2.3.4: Example timeseries of daily averaged EMMAv2.2c (EMMC) and FTIR XCO₂ data.



ESA Climate Change Initiative (CCI)

**Product Validation and
Intercomparison Report (PVIR)**

for the Essential Climate Variable (ECV)
Greenhouse Gases (GHG)

Page 38

Version 5.0
Final

9 Feb 2017

EMMA XCO ₂ fit results												
	EMMA				EMMB				EMMC			
Station	Slope	Slope err	Ampli	Ampli err	Slope	Slope err	Ampli	Ampli err	Slope	Slope err	Ampli	Ampli err
SOD	-0.19	0.47	0.29	0.54	-0.30	0.45	0.83	0.61	-0.03	0.39	0.65	0.64
BIA	-0.03	0.24	0.86	0.34	-0.11	0.22	0.65	0.33	-0.35	0.24	0.54	0.33
BRE	0.05	0.35	0.54	0.49	-0.07	0.32	0.40	0.43	-0.14	0.30	0.63	0.37
KAR	0.40	0.38	0.57	0.32	0.19	0.38	0.62	0.31	-0.25	0.43	0.33	0.36
ORL	0.17	0.20	0.59	0.25	0.14	0.20	0.56	0.26	0.13	0.23	0.77	0.29
GAR	0.08	0.17	0.15	0.19	0.04	0.18	0.23	0.18	-0.09	0.18	0.19	0.22
PAR	0.24	0.13	0.09	0.15	0.21	0.13	0.08	0.15	0.21	0.13	0.03	0.15
LAM	-0.62	0.12	0.15	0.13	-0.61	0.12	0.20	0.13	-0.60	0.11	0.17	0.12
SAG	12.87	14.62	2.03	3.37	4.03	15.64	2.27	1.65	8.31	13.42	2.21	3.01
DAR	-0.28	0.15	0.58	0.18	-0.14	0.15	0.63	0.17	-0.15	0.14	0.64	0.16
REU	-18.94	26.76	4.80	5.95	-27.85	22.28	6.72	5.15	-4.85	23.15	1.07	5.39
WOL	0.01	0.11	0.37	0.14	0.05	0.11	0.40	0.13	-0.07	0.11	0.21	0.13
LAU	0.53	0.32	0.34	0.35	0.31	0.30	0.25	0.31	0.30	0.28	0.27	0.30
N-H	-0.12	0.08	0.13	0.10	-0.11	0.08	0.15	0.09	-0.18	0.07	0.20	0.08
S-H	0.02	0.10	0.07	0.11	0.06	0.09	0.10	0.11	0.00	0.09	0.09	0.11
All	-0.09	0.06	0.07	0.07	-0.07	0.04	0.08	0.04	-0.14	0.06	0.11	0.07
Stability	-0.08 ± 0.22 ppm/year				-0.08 ± 0.20 ppm/year				-0.14 ± 0.20 ppm/year			

Table 3.2.3.2: EMMAv2.2a (EMMA), EMMAv2.2b (EMMB), EMMAv2.2c (EMMC) XCO₂ SAT-FTS fit results for all individual stations and using all data combined (All). All units are in ppm. NH and SH are the results obtained from all Northern and Southern Hemisphere data pair. Stability is the weighted average over all station slope results, with weights=1/(slope error)². The uncertainty on the stability corresponds with the 95% confidence interval.

EMMA XCO ₂ fit results												
	EMMA				EMMB				EMMC			
Station	YtY std	95% err	YtY range	95% err	YtY std	95% err	YtY range	95% err	YtY std	95% err	YtY range	95% err
SOD	0.03	0.01	0.06	0.02	0.02	0.01	0.04	0.02	0.00	0.00	0.01	0.00
BIA	0.26	0.04	0.53	0.07	0.21	0.03	0.43	0.06	0.24	0.03	0.47	0.06
BRE	0.12	0.03	0.24	0.06	0.10	0.02	0.20	0.05	0.11	0.03	0.21	0.05
KAR	NULL	NULL	NULL	NULL	NULL	NULL	NULL	NULL	NULL	NULL	NULL	NULL
ORL	0.04	0.01	0.08	0.02	0.03	0.01	0.05	0.01	0.04	0.01	0.08	0.02
GAR	0.05	0.01	0.10	0.02	0.08	0.01	0.16	0.02	0.06	0.01	0.12	0.02
PAR	0.13	0.01	0.26	0.03	0.06	0.01	0.11	0.02	0.14	0.02	0.29	0.03
LAM	0.26	0.01	0.52	0.03	0.29	0.02	0.58	0.03	0.29	0.02	0.57	0.03
SAG	NULL	NULL	NULL	NULL	NULL	NULL	NULL	NULL	NULL	NULL	NULL	NULL
DAR	0.60	0.04	1.19	0.07	0.51	0.04	1.01	0.07	0.54	0.03	1.08	0.06
REU	NULL	NULL	NULL	NULL	NULL	NULL	NULL	NULL	NULL	NULL	NULL	NULL
WOL	0.10	0.01	0.20	0.02	0.12	0.01	0.24	0.02	0.09	0.01	0.17	0.02
LAU	0.23	0.05	0.47	0.10	0.18	0.04	0.35	0.09	0.13	0.03	0.26	0.06
N-H	0.08	0.00	0.16	0.01	0.07	0.01	0.15	0.01	0.11	0.01	0.21	0.01
S-H	0.07	0.01	0.13	0.01	0.05	0.01	0.10	0.01	0.06	0.00	0.12	0.01
All	0.04	0.00	0.08	0.01	0.04	0.00	0.08	0.01	0.09	0.01	0.17	0.01
Mean	0.18 ± 0.12 ppm		0.36 ± 0.25 ppm		0.16 ± 0.11 ppm		0.32 ± 0.22 ppm		0.16 ± 0.12 ppm		0.33 ± 0.23 ppm	

Table 3.2.3.3: EMMA, EMMC and EMMB XCO₂ SAT-FTS year-to-year stability results for all individual stations and using all data combined (All). All units are in ppm. NH and SH are the results obtained from all Northern and Southern Hemisphere data pair.



ESA Climate Change Initiative (CCI)

Product Validation and Intercomparison Report (PVIR)

for the Essential Climate Variable (ECV)
Greenhouse Gases (GHG)

Page 39

Version 5.0
Final

9 Feb 2017

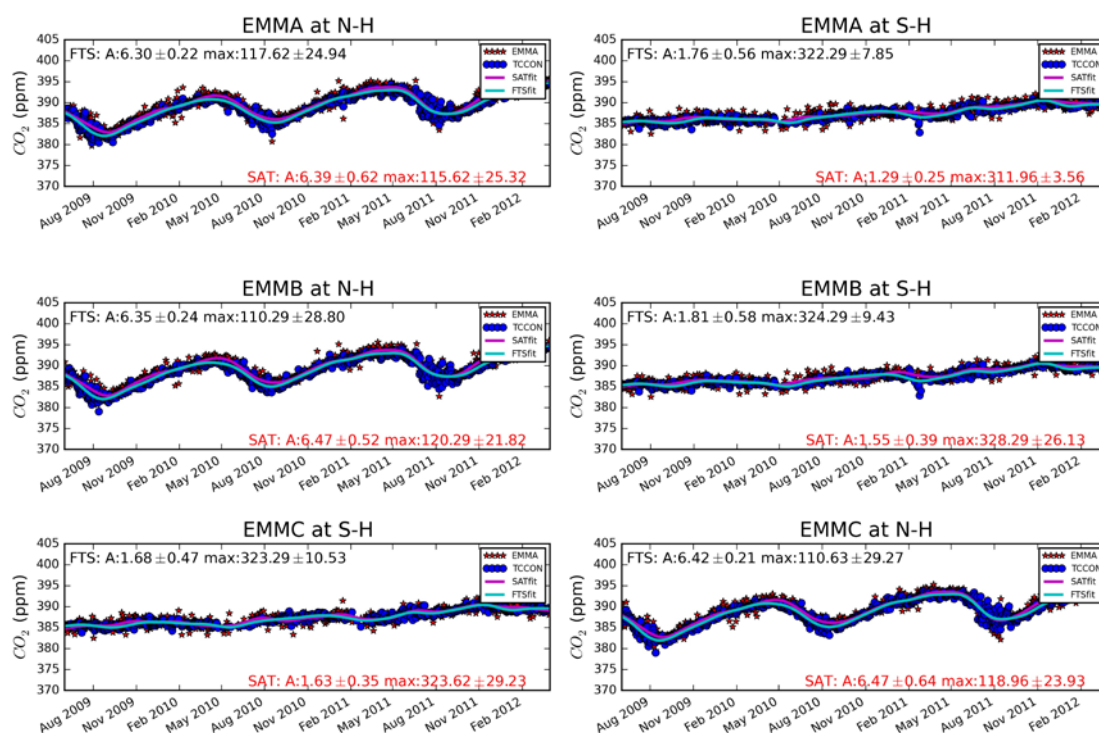


Figure 3.2.3.5: Northern and Southern Hemisphere timeseries of daily averaged EMMA, EMMB, EMMC and TCCON XCO₂ data, including trend and seasonal fit results.



ESA Climate Change Initiative (CCI)

Product Validation and Intercomparison Report (PVIR)

for the Essential Climate Variable (ECV)
Greenhouse Gases (GHG)

Page 40

Version 5.0
Final

9 Feb 2017

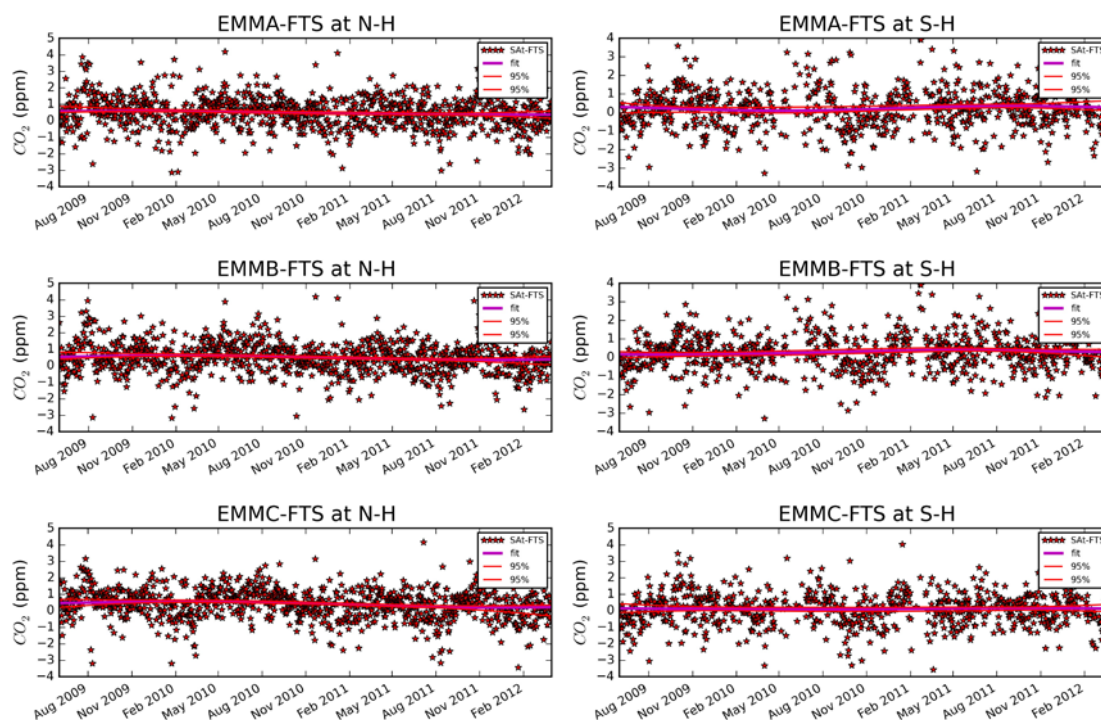


Figure 3.2.3.6: Northern and Southern Hemisphere timeseries of daily averaged EMMA, EMMB, EMMC - TCCON Bias XCO₂ data, including trend fit results.



ESA Climate Change Initiative (CCI)

**Product Validation and
Intercomparison Report (PVIR)**

for the Essential Climate Variable (ECV)
Greenhouse Gases (GHG)

Page 41

Version 5.0
Final

9 Feb 2017

3.2.4 SCIAMACHY XCH₄

SCIAMACHY XCH ₄ results								
Station	IMAP				WFMD			
	Bias	Scatter	R	N	Bias	Scatter	R	N
SOD	21.11	49.48	0.11	10747	11.66	114.37	0.01	3173
BIA	18.81	46.15	0.06	63514	13.66	85.14	0.04	33164
BRE	14.61	49.65	0.24	51351	12.00	85.70	0.05	35486
KAR	16.21	45.87	0.06	24699	-0.17	93.97	0.04	13978
ORL	16.85	45.58	0.14	22122	9.99	88.70	0.02	10811
GAR	11.08	46.75	0.20	39412	1.76	84.77	0.07	23742
PAR	12.26	44.52	0.27	295673	14.13	71.01	0.16	213838
LAM	10.31	44.69	0.18	183099	10.88	77.83	0.12	137654
SAG	-4.31	50.57	0.24	1886	-0.17	123.08	0.02	430
DAR	1.37	45.66	0.20	64895	9.37	66.44	0.11	59849
REU	6.06	37.52	0.04	6092	-9.14	98.75	0.09	2098
WOL	-6.88	38.92	0.16	63706	-11.26	68.24	0.12	66595
LAU	-0.74	49.55	0.30	6682	-7.89	76.45	0.25	5003
N-H	12.83	45.52	0.28	692503	11.82	77.63	0.15	472276
S-H	-2.25	42.84	0.27	141375	-1.85	69.11	0.16	133545
All	10.28	45.43	0.43	833878	8.81	76.04	0.27	605821
RA	8.75				8.84			
Seas	4.02				3.93			
SRA	8.99				10.07			

Table 3.2.4.1: IMAP and WFMD XCH₄ validation results for all individual stations and using all data combined (ALL). All units apart from R and N are in ppb. NH and SH are the results obtained from all Northern and Southern Hemisphere data pairs.

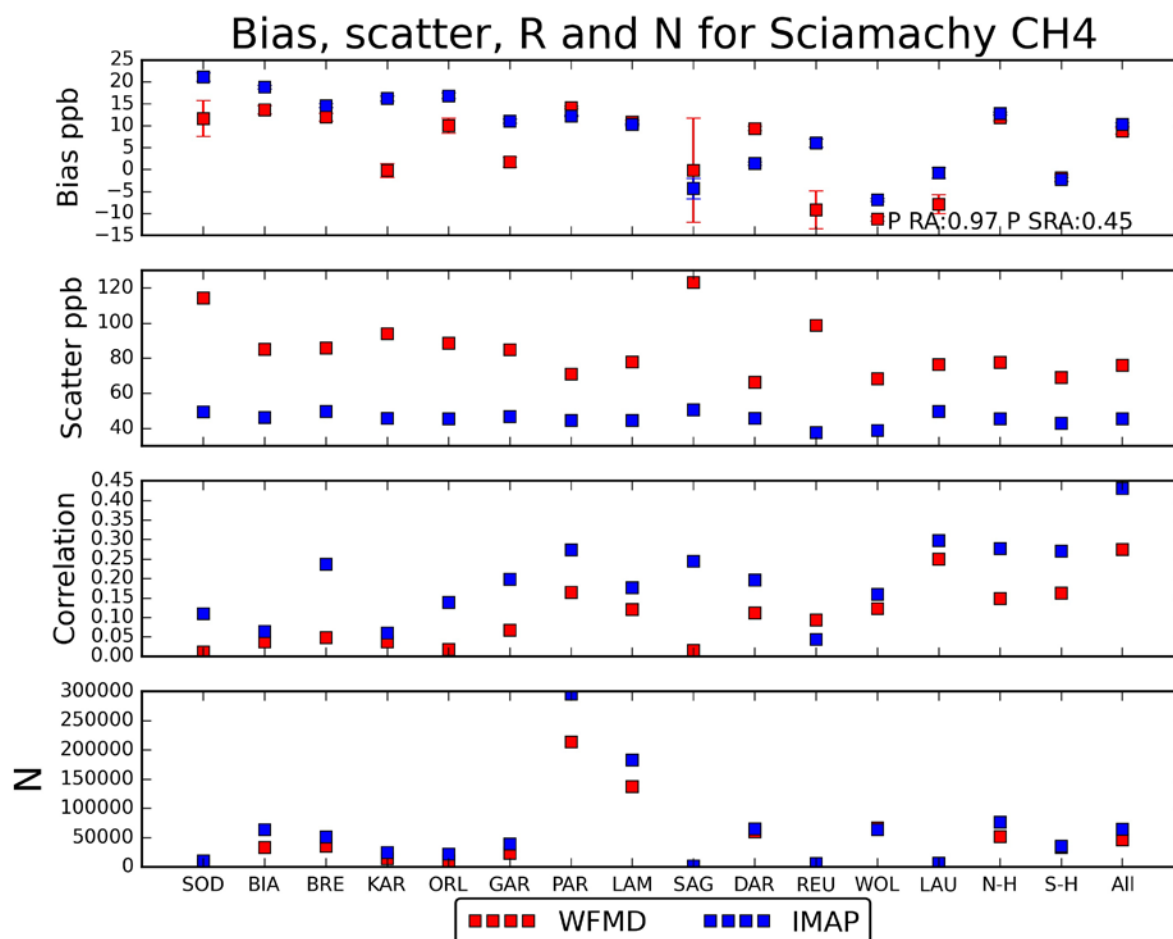


Figure 3.2.4.1: IMAP and WFMD XCH₄ validation results for all individual stations, Northern and Southern hemisphere (NH and SH respectively) and using all data combined (All). All units apart from R and N are in ppb. a) Bias, b) scatter, c) correlation and d) number of datapairs. Note that for N “NH”, “SH” and “All” correspond with the average number per station.



ESA Climate Change Initiative (CCI)

**Product Validation and
Intercomparison Report (PVIR)**

for the Essential Climate Variable (ECV)
Greenhouse Gases (GHG)

Page 43

Version 5.0
Final

9 Feb 2017

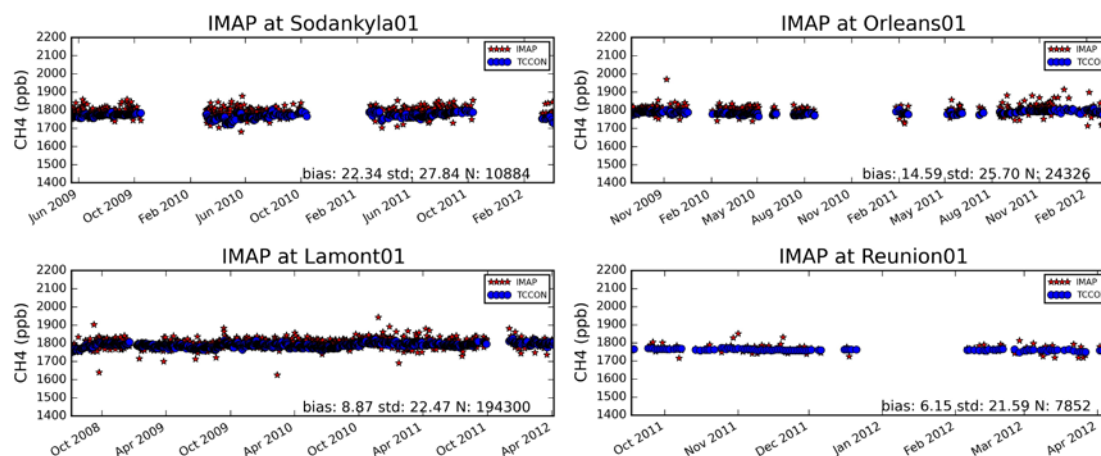


Figure 3.2.4.2: Example timeseries of daily averaged IMAP and FTIR XCH₄ data.

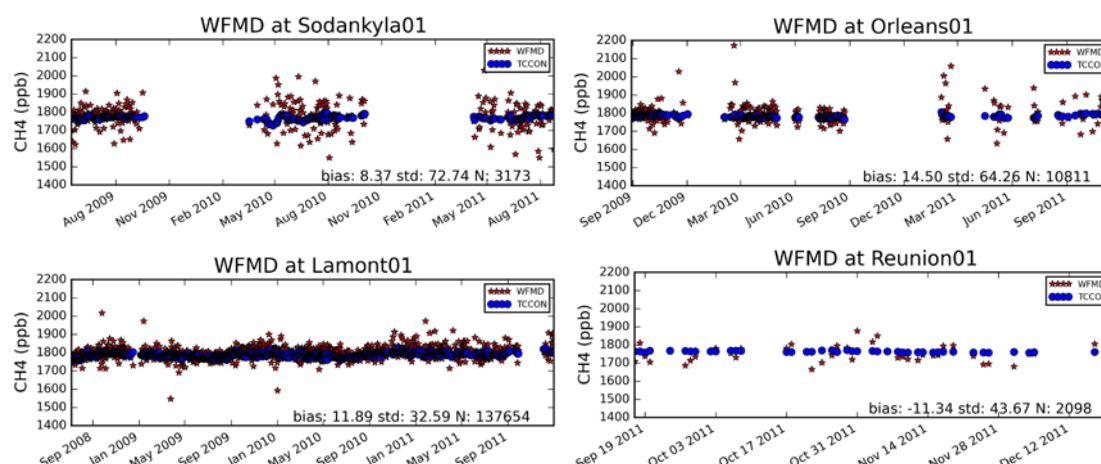


Figure 3.2.4.3: Example timeseries of daily averaged WFMD and FTIR XCH₄ data.



ESA Climate Change Initiative (CCI)

**Product Validation and
Intercomparison Report (PVIR)**

for the Essential Climate Variable (ECV)
Greenhouse Gases (GHG)

Page 44

Version 5.0
Final

9 Feb 2017

SCIAMACHY XCH ₄ fit results								
	IMAP				WFMD			
Station	Slope	Slope err	Ampli	Ampli err	slope	Slope err	Ampli	Ampli err
SOD	-2.30	3.31	6.88	3.63	-9.76	11.30	26.19	27.12
BIA	-1.47	2.50	2.71	2.40	-5.04	6.53	6.47	6.64
BRE	2.17	1.34	1.84	2.45	-1.91	3.08	2.85	8.30
KAR	-7.34	5.36	4.30	3.68	-0.44	15.76	15.52	10.19
ORL	0.97	3.48	1.75	3.62	2.24	12.54	17.81	13.00
GAR	2.21	1.49	1.12	2.79	-0.13	3.68	3.94	6.76
PAR	0.88	0.43	5.49	1.40	1.24	0.76	3.65	2.59
LAM	1.27	1.53	4.38	1.98	2.91	2.24	4.31	3.01
SAG	341.03	1056.46	48.79	192.93	2368.59	2933.54	453.79	551.15
DAR	-0.15	0.92	4.99	2.37	-0.34	1.47	7.23	3.68
REU	-752.79	2273.10	130.34	368.79	2740.69	5302.40	469.16	902.98
WOL	-2.41	2.45	6.21	3.48	5.13	2.97	3.59	3.95
LAU	-0.18	1.50	5.86	5.26	2.78	2.74	9.12	11.26
N-H	0.62	0.36	4.68	1.15	-0.14	0.67	1.89	2.15
S-H	-0.89	0.74	2.44	2.11	-2.65	1.02	3.83	2.85
All	0.10	0.39	5.20	1.21	-1.07	0.53	2.81	1.63
Stability	0.69 ± 0.77 ppb/year				1.09 ± 1.23 ppm/year			

Table 3.2.4.2: IMAP and WFMD XCH₄ SAT-FTS fit results for all individual stations and using all data combined (All). All units are in ppb. NH and SH are the results obtained from all Northern and Southern Hemisphere data pair. Stability is the weighted average over all station slope results, with weights=1/(slope error)². The uncertainty on the stability corresponds with the 95% confidence interval.

SCIA XCH ₄ fit results								
	IMAP				WFMD			
Station	YtYstd	95% err	YtY range	95% err	YtYstd	95% err	YtY range	95% err
SOD	2.16	0.23	4.33	0.45	4.60	0.80	9.19	1.61
BIA	2.42	0.23	4.85	0.46	4.13	0.31	8.25	0.62
BRE	5.53	0.14	14.56	0.36	6.11	0.20	15.74	0.56
KAR	NULL	NULL	NULL	NULL	NULL	NULL	NULL	NULL
ORL	0.73	0.14	1.46	0.27	1.36	0.31	2.72	0.62
GAR	2.09	0.15	5.20	0.41	4.80	0.29	12.65	0.83
PAR	3.13	0.05	9.10	0.18	2.78	0.11	8.48	0.32
LAM	2.76	0.17	5.95	0.38	1.98	0.13	4.48	0.31
SAG	NULL	NULL	NULL	NULL	NULL	NULL	NULL	NULL
DAR	5.58	0.14	16.06	0.45	3.45	0.10	9.43	0.27
REU	NULL	NULL	NULL	NULL	NULL	NULL	NULL	NULL
WOL	2.90	0.23	6.75	0.59	4.81	0.24	11.26	0.65
LAU	6.12	0.18	18.60	0.96	7.58	0.37	22.32	1.26
N-H	3.01	0.04	9.45	0.09	2.57	0.08	8.18	0.29
S-H	4.91	0.10	14.55	0.35	8.11	0.10	23.06	0.37
All	3.49	0.04	11.11	0.08	3.95	0.04	11.54	0.15
Mean	3.34±1.28 ppb		8.69±4.11 ppb		4.16 ± 1.34 ppb		10.54 ± 4.00 ppb	

Table 3.2.4.3: IMAP and WFMD XCO₂ SAT-FTS year-to-year stability results for all individual stations and using all data combined (All). All units are in ppm. NH and SH are the results obtained from all Northern and Southern Hemisphere data pair.



ESA Climate Change Initiative (CCI)

Product Validation and Intercomparison Report (PVIR)

for the Essential Climate Variable (ECV)
Greenhouse Gases (GHG)

Page 45

Version 5.0
Final

9 Feb 2017

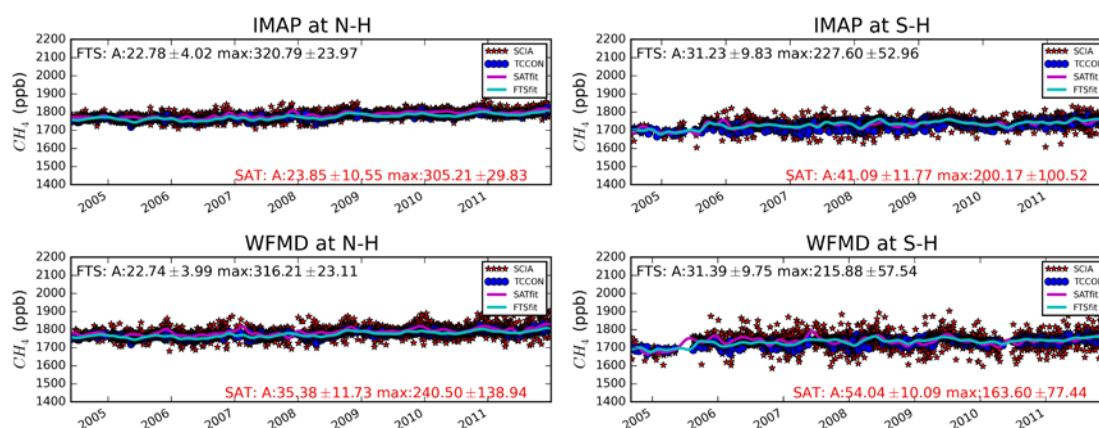


Figure 3.2.4.4: Northern and Southern Hemisphere timeseries of daily averaged IMAP, WFMD and TCCON XCH_4 data, including trend and seasonal fit results.

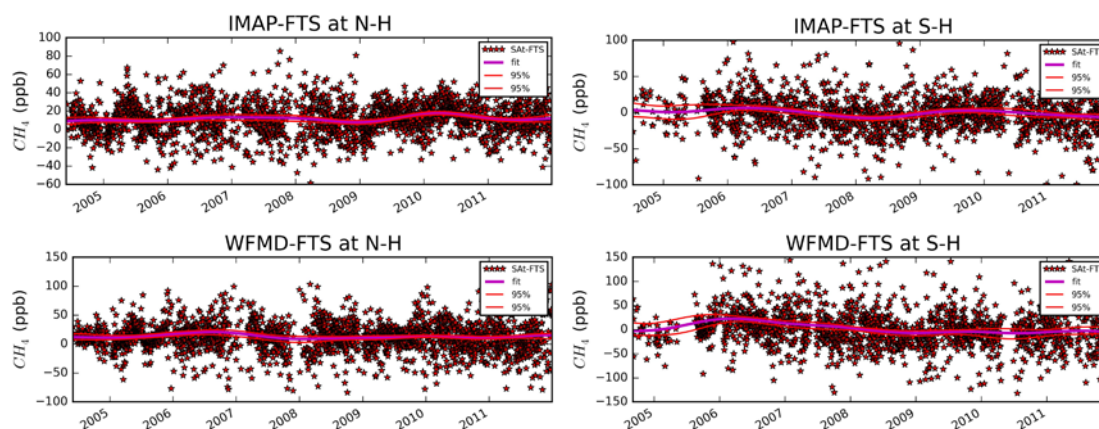


Figure 3.2.4.5: Northern and Southern Hemisphere timeseries of daily averaged IMAP, WFMD - TCCON Bias XCH_4 data, including trend fit results.



ESA Climate Change Initiative (CCI)

**Product Validation and
Intercomparison Report (PVIR)**

for the Essential Climate Variable (ECV)
Greenhouse Gases (GHG)

Page 46

Version 5.0
Final

9 Feb 2017

3.2.5 GOSAT XCH₄

GOSAT XCH ₄ results												
	OCFP				SRFP				EMMA			
Station	Bias	Scatter	R	N	Bias	Scatter	R	N	Bias	Scatter	R	N
SOD	4.64	14.28	0.77	1494	14.66	13.45	0.72	1506	7.18	13.43	0.65	3384
BIA	-1.69	14.02	0.77	6292	11.06	13.00	0.73	8197	5.74	12.86	0.61	9139
BRE	-0.67	15.02	0.71	2592	13.40	13.89	0.68	3128	6.53	13.53	0.59	3962
KAR	-3.66	14.14	0.76	5708	10.04	13.14	0.70	5990	4.69	12.80	0.61	7921
ORL	-3.94	13.74	0.75	5001	9.30	13.17	0.70	5187	3.64	12.50	0.66	7655
GAR	-8.32	14.98	0.75	3975	5.79	13.45	0.71	3682	0.08	12.96	0.64	6188
PAR	-2.34	15.29	0.76	12589	11.35	13.87	0.72	14902	6.44	13.91	0.61	20671
LAM	-10.79	15.00	0.81	23827	3.89	14.22	0.77	25835	-0.94	13.40	0.74	33749
SAG	-9.33	15.76	0.68	1573	9.09	16.16	0.65	1962	-3.24	15.40	0.57	3832
DAR	-5.51	9.94	0.82	5814	3.39	10.29	0.75	8030	0.85	10.51	0.59	11156
REU	1.54	11.10	0.72	4624	12.77	10.94	0.67	5052	2.55	10.34	0.55	6739
WOL	-12.13	13.08	0.73	10447	-3.26	11.70	0.73	14059	-6.85	10.89	0.69	17466
LAU	-3.54	13.70	0.75	647	4.89	12.26	0.77	447	1.01	10.88	0.64	1187
N-H	-6.03	15.41	0.77	63051	8.13	14.28	0.74	70389	2.66	13.85	0.69	96501
S-H	-7.15	13.08	0.84	21532	1.74	12.68	0.82	27588	-2.51	11.47	0.79	36548
All	-6.32	14.86	0.86	84583	6.33	14.14	0.87	97977	1.24	13.44	0.86	133049
RA	4.68 (4.60)				4.83 (4.76)				4.03			
Seas	1.73 (1.65)				0.94 (1.03)				1.02			
SRA	4.81(4.84)				5.11(5.18)				4.39			

GOSAT XCH ₄ results										
	OCPR				SRPR					
Station	Bias	Scatter	R	N	Bias	Scatter	R	N		
SOD	7.81	14.94	0.74	9764	9.84	15.03	0.73	12944		
BIA	5.83	13.35	0.74	26063	10.16	13.52	0.72	28509		
BRE	7.17	14.10	0.70	10455	11.29	14.23	0.68	10501		
KAR	3.94	12.90	0.73	21036	8.45	12.91	0.72	19956		
ORL	3.23	12.81	0.72	19193	7.99	12.95	0.70	18533		
GAR	-0.07	13.16	0.73	14603	4.94	13.22	0.71	13808		
PAR	5.97	14.16	0.72	46146	10.95	14.37	0.70	49652		
LAM	-1.88	13.59	0.79	62895	3.76	14.13	0.77	65914		
SAG	-1.83	15.59	0.67	8730	2.38	16.55	0.67	7835		
DAR	0.57	8.85	0.81	14000	4.18	10.71	0.73	13061		
REU	4.08	8.74	0.75	9793	10.09	8.97	0.76	10958		
WOL	-6.96	10.02	0.79	26937	-1.74	10.63	0.76	27233		
LAU	1.01	10.76	0.80	3248	7.91	11.19	0.79	2988		
N-H	2.69	14.17	0.76	218885	7.60	14.36	0.75	227652		
S-H	-2.52	10.59	0.87	53978	2.60	11.42	0.85	54240		
All	1.66	13.69	0.87	272863	6.64	13.98	0.86	281892		
RA	4.09 (4.07)				3.78 (3.93)					
Seas	1.18 (1.12)				0.95 (0.89)					
SRA	4.31 (4.29)				4.77 (4.96)					

Table 3.2.5.1: OCFP, SRFP, EMMA, OCPR, and SRPR XCH₄ validation results for all individual stations and using all data combined (ALL). All units apart from R and N are in ppb. NH and SH are the results obtained from all Northern and Southern Hemisphere data pairs. Results in Brackets are the RA, Seas and SRA results, when the data is trimmed to the EMMA timeseries

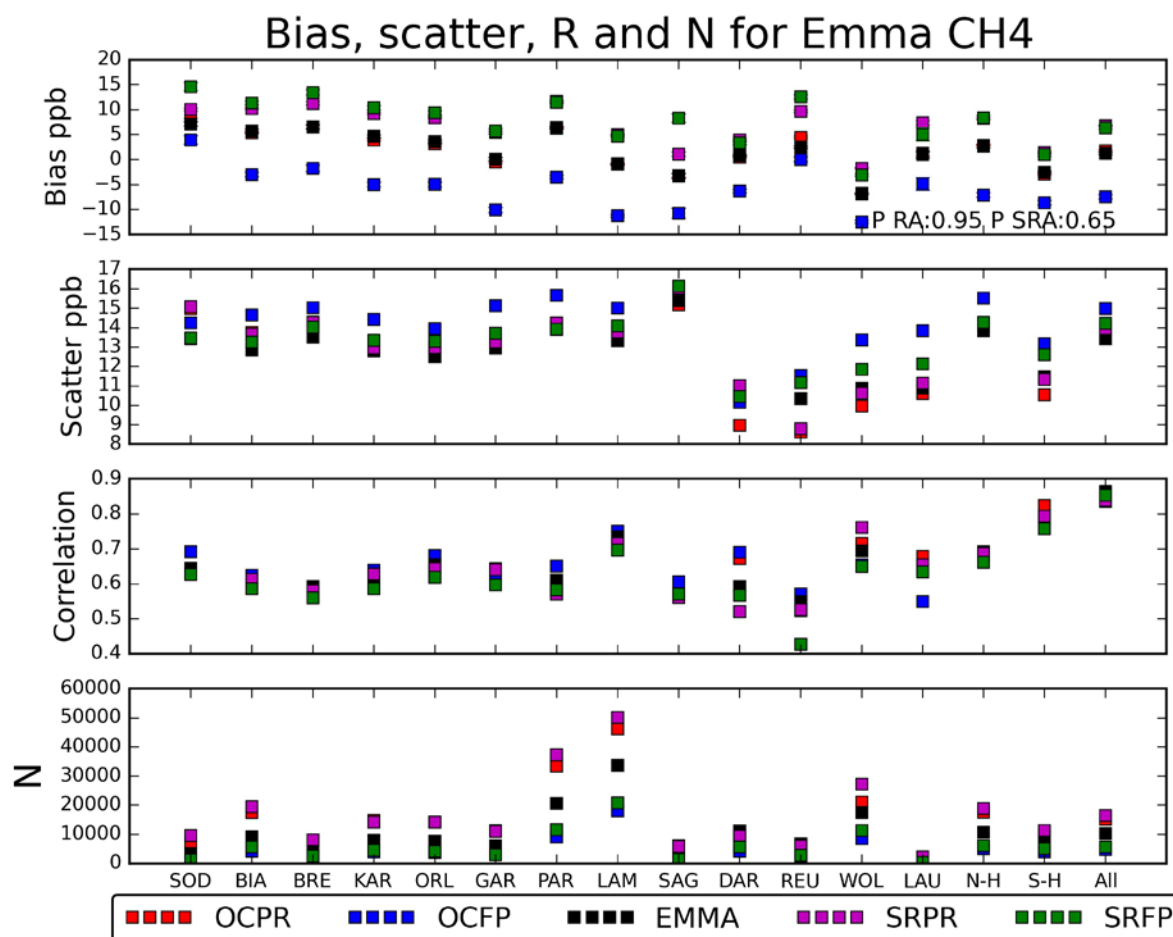


Figure 3.2.5.1: OCP, OCF, EMMA, SRP and SRF XCH₄ validation results for all individual stations, Northern and Southern hemisphere (NH and SH respectively) and using all data combined (All). All units apart from R and N are in ppm. a) Bias, b) scatter, c) correlation and d) number of datapairs. Note that NH,SH and All correspond with the average number per station.

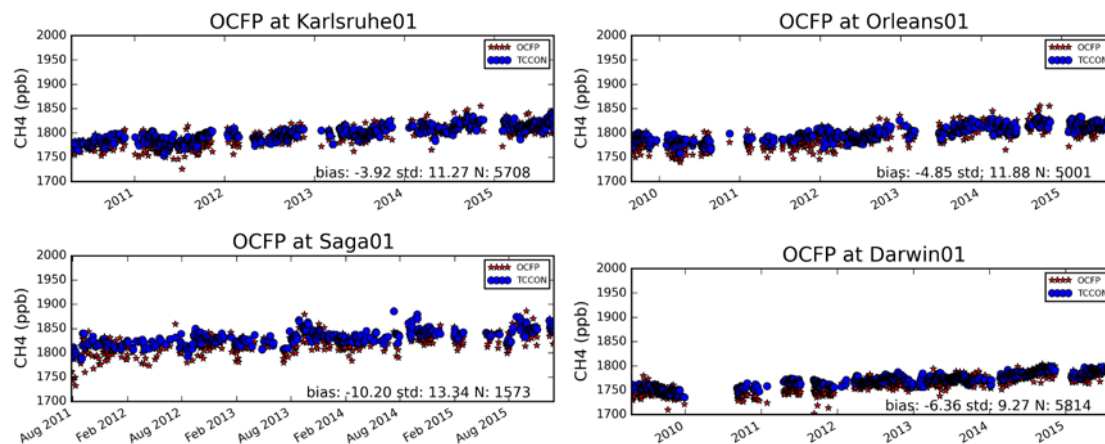


Figure 3.2.5.2: Example timeseries of daily averaged OCFP and FTIR XCH₄ data.

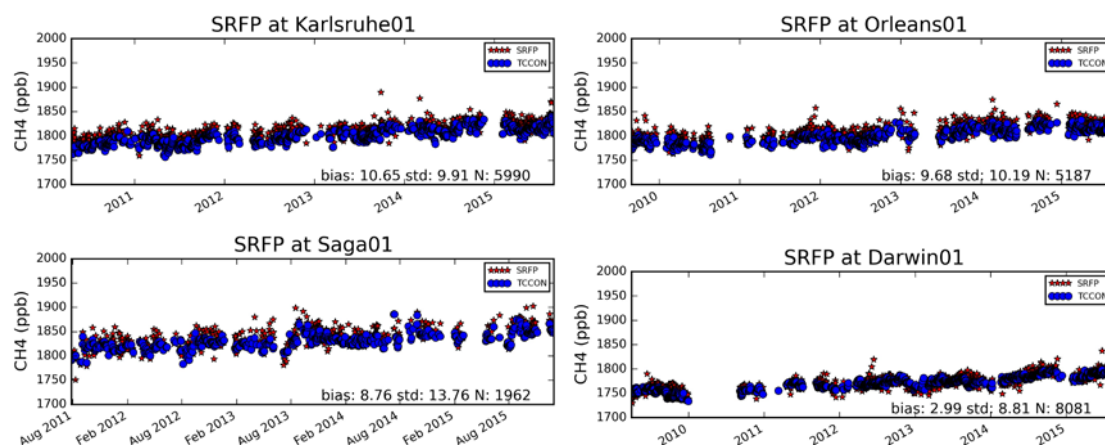


Figure 3.2.5.3: Example timeseries of daily averaged SRFP and FTIR XCH₄ data.

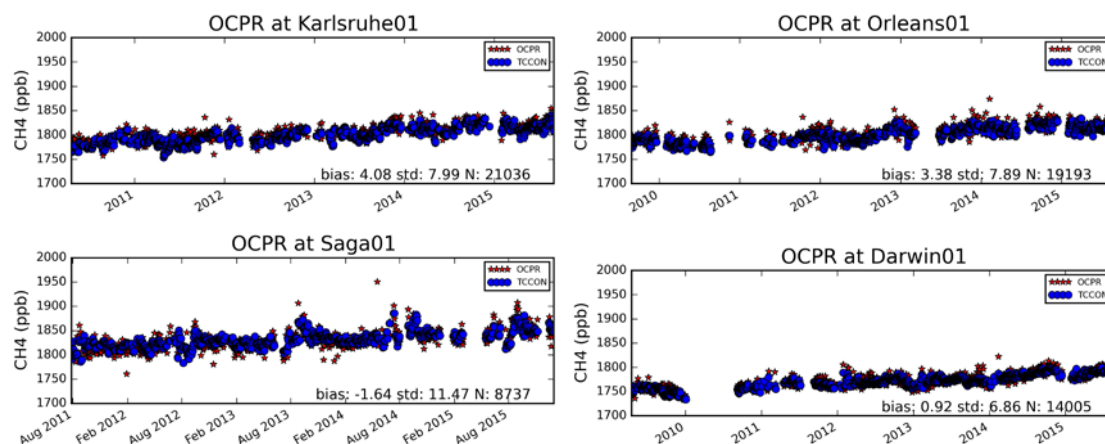


Figure 3.2.5.4: Example timeseries of daily averaged OCPR and FTIR XCH₄ data.



ESA Climate Change Initiative (CCI)

Product Validation and Intercomparison Report (PVIR)

for the Essential Climate Variable (ECV)
Greenhouse Gases (GHG)

Page 49

Version 5.0
Final

9 Feb 2017

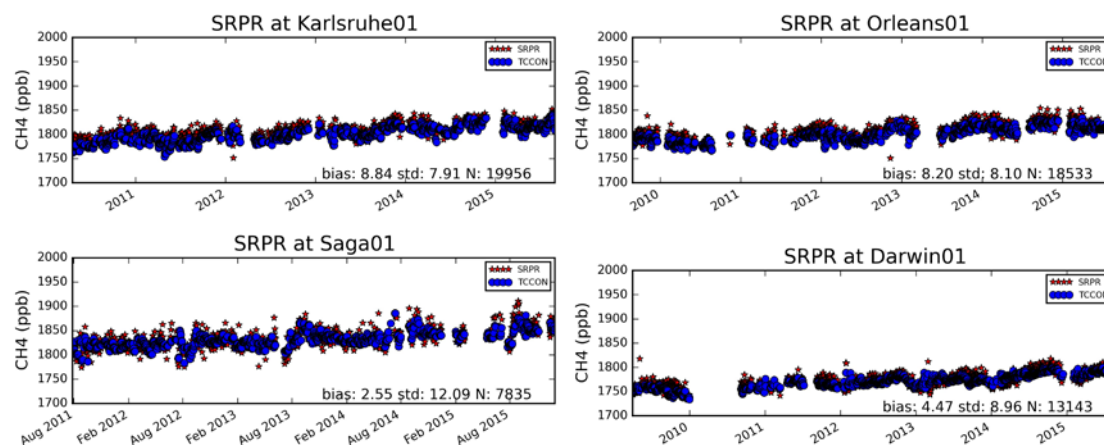


Figure 3.2.5.5: Example timeseries of daily averaged SRPR and FTIR XCH₄ data.

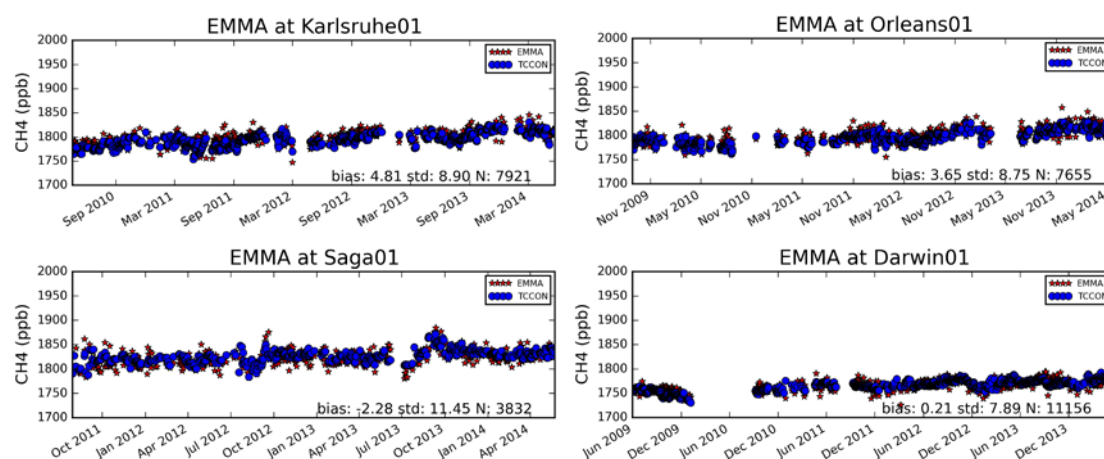


Figure 3.2.5.6: Example timeseries of daily averaged EMMA and FTIR XCH₄ data.



ESA Climate Change Initiative (CCI)

**Product Validation and
Intercomparison Report (PVIR)**

for the Essential Climate Variable (ECV)
Greenhouse Gases (GHG)

Page 50

Version 5.0
Final

9 Feb 2017

GOSAT XCH ₄ fit results												
	OCFP				SRFP				EMMA			
Stat	Slope	Slope err	Ampli	Ampli err	slope	Slope err	Ampli	Ampli err	slope	Slope err	Ampli	Ampli err
SOD	1.20	0.59	5.61	3.86	0.10	0.57	2.64	2.89	0.44	0.49	3.80	1.88
BIA	1.66	0.33	4.50	1.33	0.03	0.30	2.06	0.83	0.02	0.41	2.01	0.92
BRE	2.50	0.51	3.02	1.98	0.52	0.46	1.95	1.19	0.67	0.58	1.46	1.19
KAR	1.69	0.42	4.38	1.23	-0.93	0.38	1.93	1.05	-0.69	0.50	3.78	0.96
ORL	1.99	0.41	3.81	1.13	-0.29	0.38	1.62	1.03	0.00	0.41	2.33	0.89
GAR	2.49	0.46	2.75	1.40	0.03	0.42	1.48	1.17	0.51	0.45	1.75	1.02
PAR	2.05	0.28	1.85	0.72	0.22	0.26	3.76	0.71	0.87	0.33	2.70	0.63
LAM	0.31	0.22	1.24	0.61	-1.78	0.20	1.19	0.55	-2.21	0.25	0.50	0.51
SAG	2.08	0.93	1.56	1.88	1.12	0.95	0.88	1.63	0.16	1.19	1.43	1.50
DAR	1.38	0.29	3.02	0.87	-0.15	0.26	5.59	0.73	-0.67	0.30	5.21	0.66
REU	2.22	0.57	1.71	0.99	-0.70	0.49	3.42	0.87	-0.71	0.67	3.75	0.83
WOL	1.99	0.31	3.31	0.73	-0.19	0.26	1.16	0.62	-0.08	0.29	1.59	0.58
LAU	1.59	0.68	3.40	1.76	-0.06	0.68	3.27	2.04	1.69	0.64	1.76	1.20
N-H	1.30	0.17	3.10	0.46	-0.62	0.15	1.97	0.40	-0.70	0.18	1.33	0.36
S-H	2.35	0.22	0.33	0.57	0.46	0.19	2.40	0.52	0.08	0.22	1.83	0.45
All	1.63	0.59	5.61	3.86	-0.42	0.12	1.67	0.33	-0.60	0.14	1.92	0.27
Stability	1.54 ± 1.05 ppm/year				-0.46 ± 0.57 ppm/year				-0.36 ± 0.71 ppm/year			

GOSAT XCH ₄ fit results								
	OCPR				SRPR			
Stat	Slope	Slope err	Ampli	Ampli err	slope	Slope err	Ampli	Ampli err
SOD	0.24	0.30	4.62	1.13	-0.02	0.25	3.40	0.87
BIA	0.24	0.22	2.00	0.66	-0.16	0.21	2.47	0.60
BRE	0.85	0.33	1.46	0.99	0.22	0.32	3.63	0.90
KAR	-0.44	0.27	3.02	0.65	-1.03	0.27	0.89	0.58
ORL	-0.21	0.24	2.07	0.64	-0.79	0.24	2.27	0.60
GAR	0.40	0.27	1.53	0.73	-0.31	0.27	2.98	0.71
PAR	0.20	0.16	2.53	0.42	-0.21	0.17	5.47	0.46
LAM	-1.76	0.14	0.44	0.40	-2.24	0.15	2.69	0.41
SAG	1.12	0.55	5.49	1.02	1.32	0.61	0.60	1.02
DAR	-0.20	0.19	3.22	0.49	-0.55	0.19	8.76	0.52
REU	-0.33	0.33	2.48	0.63	-0.11	0.30	1.27	0.50
WOL	-0.23	0.19	2.33	0.46	-0.05	0.20	2.52	0.48
LAU	0.08	0.29	1.02	0.81	0.12	0.27	3.70	0.78
N-H	-0.52	0.09	2.06	0.23	-0.93	0.09	1.97	0.25
S-H	0.31	0.14	1.04	0.37	0.30	0.15	2.80	0.40
All	-0.39	0.07	1.99	0.20	-0.74	0.08	1.25	0.22
Stability	-0.30 ± 0.53 ppm/year				-0.60 ± 0.67 ppm/year			

Table 3.2.5.2: OCFP and SRFP (top), and OCPR and SRPR (bottom) XCH₄ SAT-FTS fit results for all individual stations and using all data combined (All). All units are in ppb. NH and SH are the results obtained from all Northern and Southern Hemisphere data pair. Stability is the weighted average over all station slope results, with weights=1/(slope error)². The uncertainty on the stability corresponds with the 95% confidence interval.



ESA Climate Change Initiative (CCI)

Product Validation and Intercomparison Report (PVIR)

for the Essential Climate Variable (ECV)
Greenhouse Gases (GHG)

Page 51

Version 5.0
Final

9 Feb 2017

GOASAT XCH ₄ fit results												
	OCFP				SRFP				EMMA			
Station	YtY std	95% err	YtY range	95% err	YtY std	95% err	YtY range	95% err	YtY std	95% err	YtY range	95% err
SOD	3.79	0.07	10.05	0.22	1.74	0.11	5.09	0.38	0.85	0.03	2.27	0.08
BIA	5.58	0.09	14.96	0.22	1.07	0.04	3.04	0.10	0.70	0.03	1.82	0.08
BRE	6.28	0.05	16.12	0.26	2.23	0.10	6.36	0.33	1.37	0.11	3.65	0.29
KAR	4.14	0.08	10.21	0.21	1.31	0.03	3.44	0.07	1.05	0.04	2.54	0.11
ORL	4.33	0.07	11.22	0.14	1.50	0.05	4.12	0.16	1.27	0.06	3.13	0.14
GAR	5.70	0.07	13.85	0.22	1.85	0.05	5.50	0.19	1.85	0.05	4.88	0.16
PAR	5.09	0.02	12.66	0.08	0.93	0.02	2.76	0.10	1.02	0.05	2.63	0.12
LAM	3.53	0.05	9.94	0.18	3.77	0.04	11.13	0.12	2.78	0.03	7.21	0.07
SAG	1.60	0.15	4.10	0.42	1.13	0.09	2.81	0.24	0.27	0.03	0.54	0.06
DAR	5.39	0.08	15.40	0.15	2.55	0.15	7.28	0.42	2.42	0.11	6.43	0.29
REU	1.61	0.11	4.12	0.31	1.01	0.10	2.50	0.27	0.40	0.06	0.79	0.12
WOL	4.49	0.02	10.94	0.06	0.69	0.03	1.85	0.06	0.74	0.03	1.95	0.08
LAU	4.85	0.19	13.25	0.43	1.58	0.15	4.26	0.45	1.46	0.09	3.61	0.23
N-H	4.00	0.03	10.68	0.14	1.33	0.01	3.92	0.06	0.85	0.02	2.31	0.05
S-H	5.66	0.06	13.83	0.11	1.08	0.03	3.15	0.10	0.81	0.03	2.11	0.07
All	4.35	0.03	11.04	0.12	1.17	0.01	3.51	0.04	0.87	0.01	2.31	0.02
Mean	4.34±0.88 ppb		11.29±2.30 ppb		1.64±0.50 ppb		4.63±1.53 ppb		1.24± 0.45 ppb		3.19±1.21 ppb	

GOSAT XCH ₄ fit results								
	OCPR				SRPR			
Station	YtY std	95% err	YtY range	95% err	YtY std	95% err	YtY range	95% err
SOD	0.94	0.01	2.52	0.05	0.76	0.01	2.18	0.04
BIA	1.00	0.02	2.61	0.05	1.30	0.03	3.74	0.07
BRE	2.54	0.04	7.17	0.11	1.93	0.09	5.34	0.31
KAR	0.71	0.02	1.84	0.07	1.50	0.02	3.63	0.06
ORL	1.13	0.04	3.24	0.12	1.36	0.02	3.58	0.08
GAR	1.91	0.03	5.10	0.08	1.90	0.05	5.07	0.14
PAR	1.18	0.03	3.31	0.08	1.83	0.02	4.98	0.04
LAM	3.72	0.03	11.34	0.10	4.42	0.05	13.56	0.15
SAG	1.37	0.14	3.45	0.36	1.07	0.10	2.66	0.25
DAR	2.02	0.08	6.01	0.24	2.64	0.06	7.84	0.18
REU	1.09	0.05	2.77	0.15	0.87	0.05	2.09	0.12
WOL	1.00	0.04	2.91	0.13	0.81	0.04	2.20	0.10
LAU	0.86	0.07	2.62	0.23	0.94	0.04	2.48	0.12
N-H	1.06	0.01	3.32	0.04	1.99	0.01	5.68	0.07
S-H	0.92	0.04	2.77	0.13	0.97	0.05	2.83	0.14
All	0.90	0.00	2.76	0.02	1.68	0.01	5.02	0.07
Mean	1.50±0.52 ppb		4.22±1.59 ppb		1.64 ± 0.61 ppb		4.56 ± 1.92 ppb	

Table 3.2.5.3: OCFP, SRFP, EMMA, OCPR and SRPR XCH₄ SAT-FTS year-to-year stability results for all individual stations and using all data combined (All). All units are in ppm. NH and SH are the results obtained from all Northern and Southern Hemisphere data pair.



ESA Climate Change Initiative (CCI)

Product Validation and Intercomparison Report (PVIR)

for the Essential Climate Variable (ECV)
Greenhouse Gases (GHG)

Page 52

Version 5.0
Final

9 Feb 2017

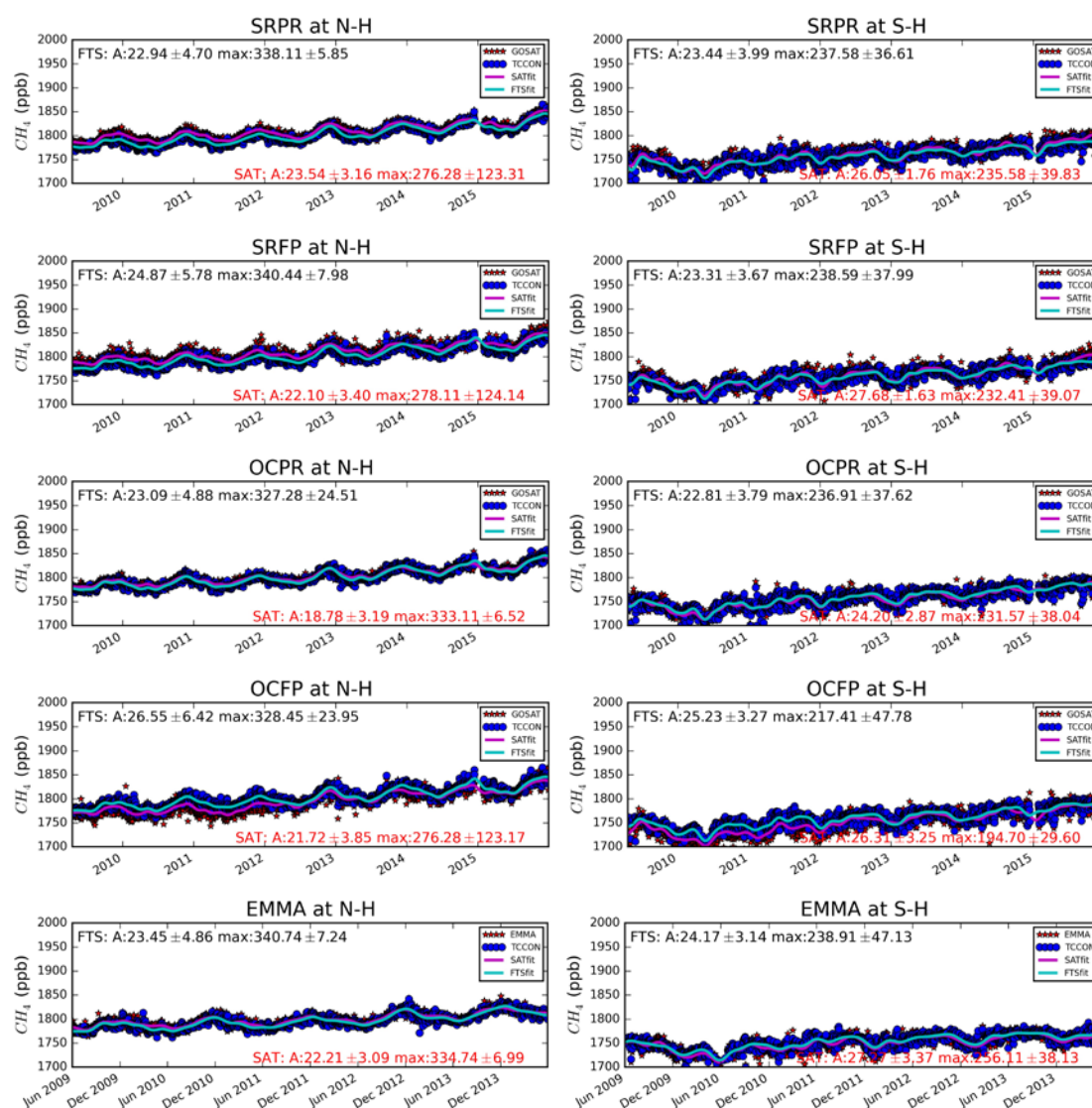


Figure 3.2.5.5: Northern and Southern Hemisphere timeseries of daily averaged OCFP, SRFP, SRPR, SRPR, EMMA and TCCON XCH₄ data, including trend and seasonal fit results.



ESA Climate Change Initiative (CCI)

Product Validation and Intercomparison Report (PVIR)

for the Essential Climate Variable (ECV)
Greenhouse Gases (GHG)

Page 53

Version 5.0
Final

9 Feb 2017

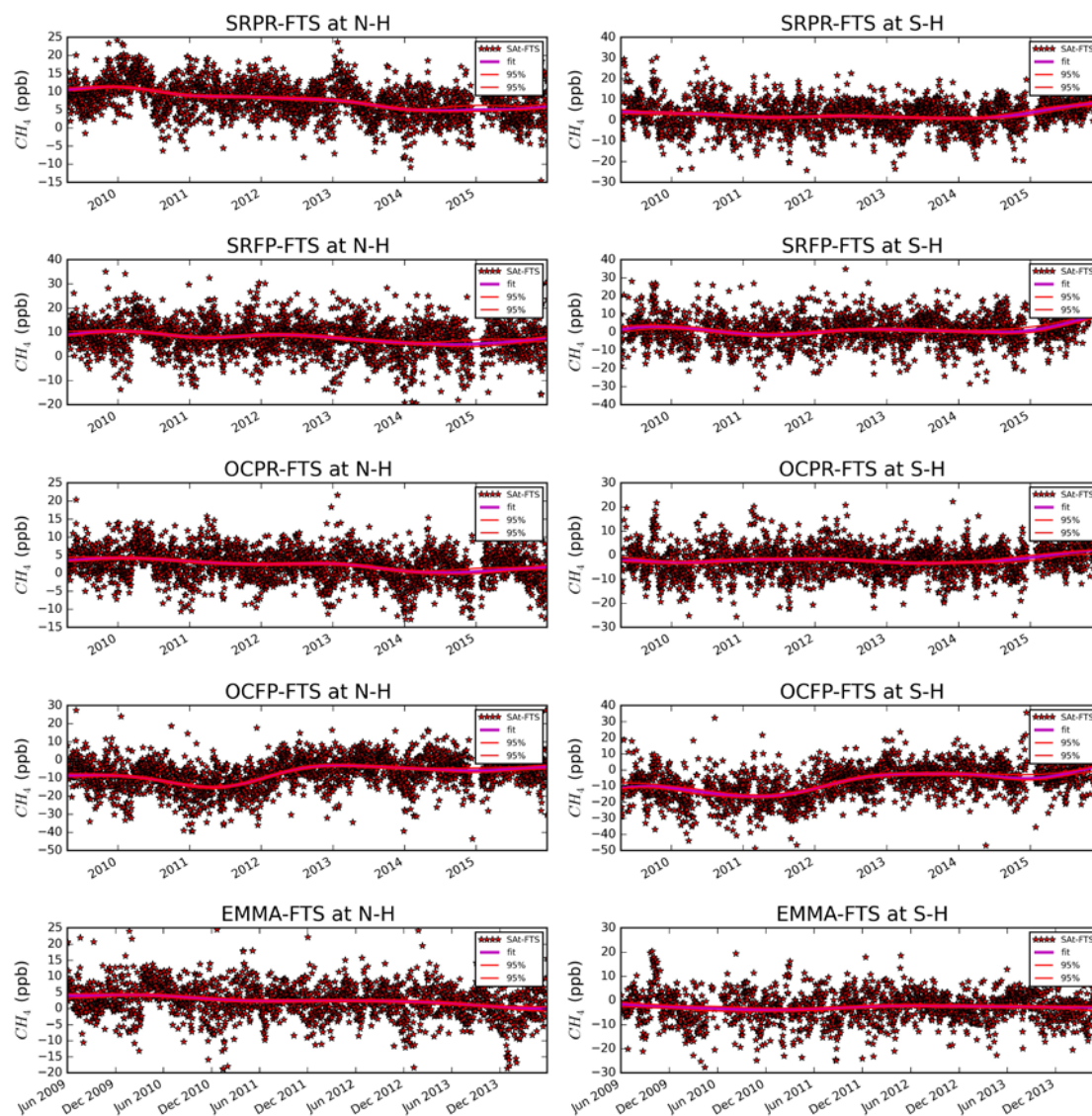


Figure 3.2.5.5: Northern and Southern Hemisphere timeseries of daily averaged OCFP, SRFP, SRPR, SRPR, EMMA - TCCON Bias XCH₄ data, including trend fit results.

3.2.6 GLINT XCO₂

Relative GOSAT GLINT XCO ₂ results								
	OCFP-OCFP glint				SRFP-SRFP glint			
Station	Bias	Scatter	R	N	Bias	Scatter	R	N
TSU	1.85	-0.14	0.00	1449	1.89	0.54	-0.03	2085
JPL	0.88	-0.75	0.21	10711	-0.03	0.57	-0.02	11692
SAG	1.36	-0.23	0.10	1413	1.91	0.78	-0.06	1755
IZA	0.31	-0.41	0.05	6699	0.42	0.60	-0.07	1722
ASC	0.38	-0.37	0.17	-2681	0.13	0.94	-0.10	-827
DAR	0.50	-0.62	0.08	5509	0.48	0.11	0.00	8488
REU	0.60	-0.30	0.02	-698	0.51	0.62	-0.09	1384
WOL	-0.54	-0.44	0.02	11427	-0.26	0.29	-0.04	15407
LAU	0.32	0.04	-0.04	748	-0.20	0.75	-0.11	573
N-H	0.11	-0.28	0.13	17591	0.20	1.01	-0.08	16427
S-H	0.04	-0.47	0.04	16986	-0.05	0.34	-0.04	25852
All	0.08	-0.37	0.07	34577	0.10	0.62	-0.04	42279
RA	0.85-0.92				0.86-0.55			
Seas	0.20-0.36				0.17-0.16			
SRA	0.99-1.06				0.81-0.62			

Table 3.2.6.1: OCFP and SRFP XCO₂ relative (land-glint) validation results for all individual stations and using all data combined (ALL). All units apart from R and N are in ppm. NH and SH are the results obtained from all Northern and Southern Hemisphere data pairs. The RA, Seas and SRA results are the explicit results (Land – Glint).

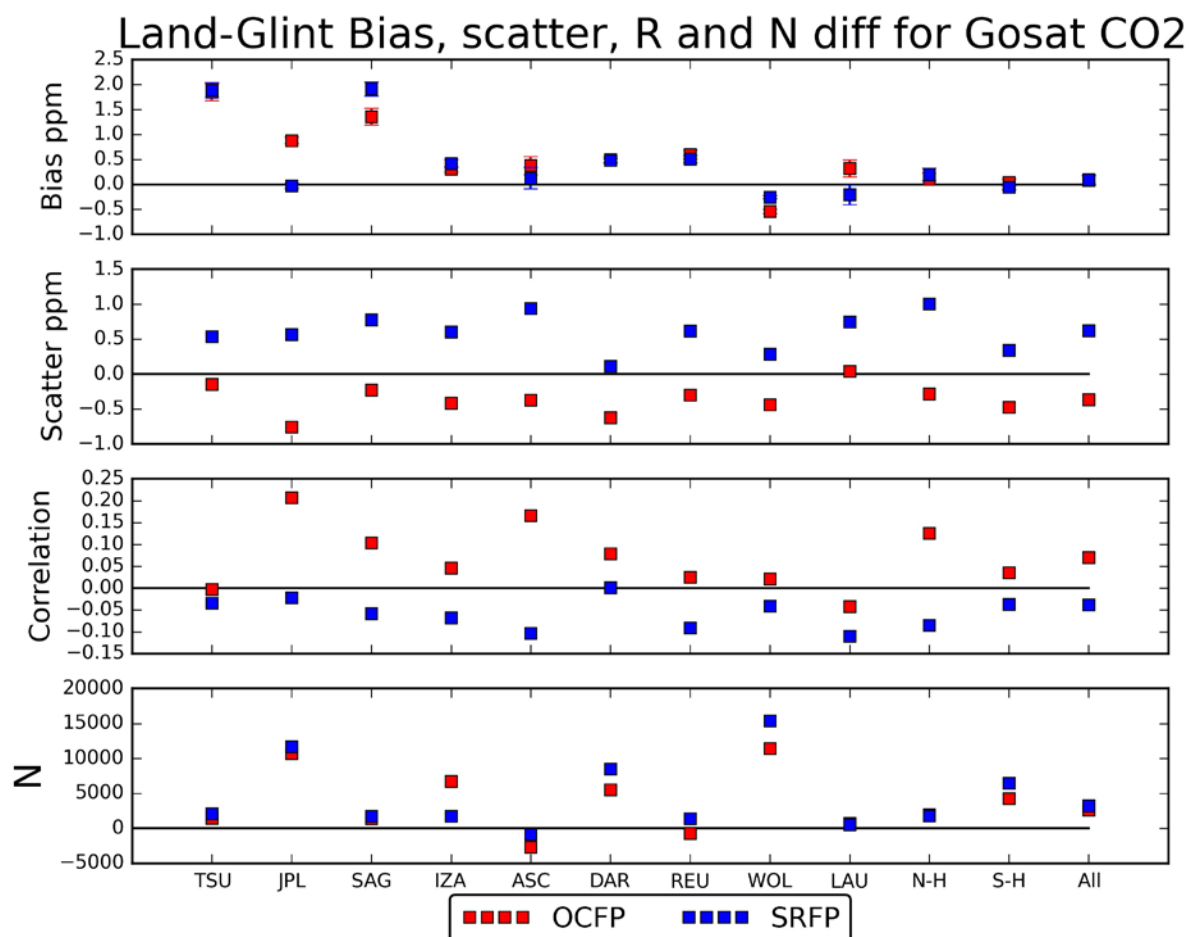


Figure 3.2.6.1: OCFP-OCFP glint and SRFP-SRFP glint validation results for all individual stations, Northern and Southern hemisphere (NH and SH respectively) and using all data combined (All). All units apart from R and N are in ppm. a) Bias, b) scatter, c) correlation and d) number of datapairs. Note that NH,SH and All correspond with the average number per station. Shown here are the difference in these obtained parameters (Bias, scatter, Correlation, N)



ESA Climate Change Initiative (CCI)

Product Validation and Intercomparison Report (PVIR)

for the Essential Climate Variable (ECV)
Greenhouse Gases (GHG)

Page 56

Version 5.0
Final

9 Feb 2017

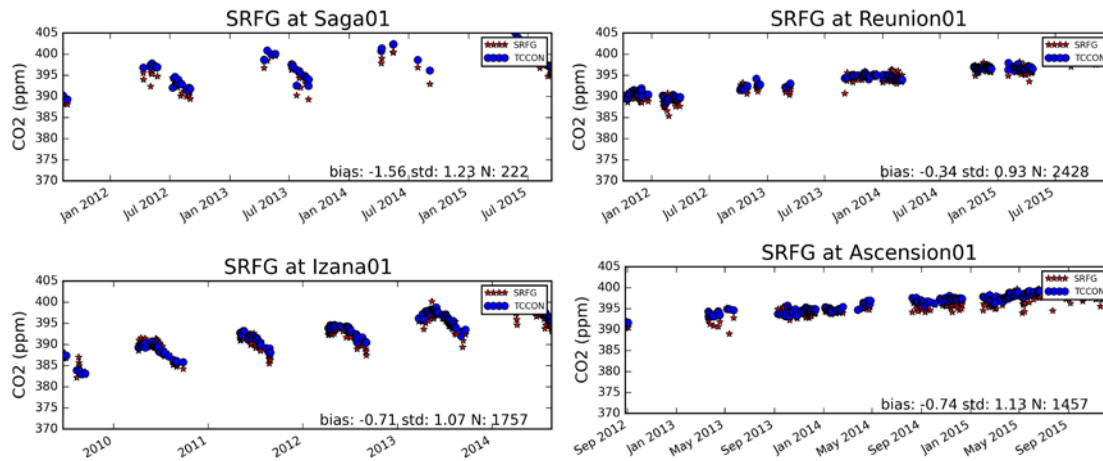


Figure 3.2.6.2: Example timeseries of daily averaged SRFG and FTIR XCO₂ data.

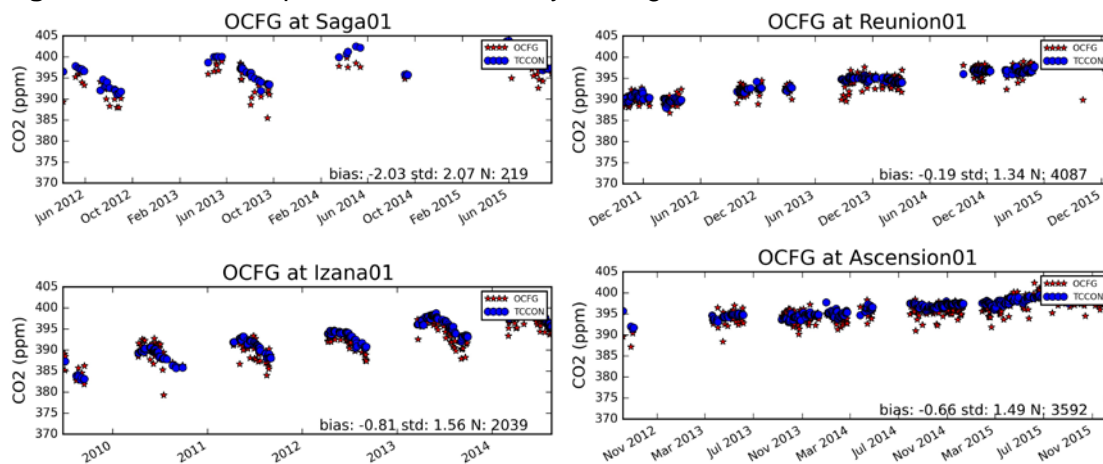


Figure 3.2.6.3: Example timeseries of daily averaged OCFG and FTIR XCO₂ data.



ESA Climate Change Initiative (CCI)

Product Validation and Intercomparison Report (PVIR)

for the Essential Climate Variable (ECV)
Greenhouse Gases (GHG)

Page 57

Version 5.0
Final

9 Feb 2017

GLINT XCO ₂ fit results								
Station	OCFG				SRFG			
	Slope	Slope err	Ampli	Ampli err	slope	Slope err	Ampli	Ampli err
TSU	-0.87	0.44	1.13	0.76	-1.13	0.42	-2.20	2.61
JPL	-0.30	0.22	-0.62	0.65	-0.07	0.15	-2.68	0.76
SAG	-0.06	0.43	0.87	1.42	-0.16	0.22	-1.50	1.20
IZA	-0.33	0.11	-0.30	0.37	-0.31	0.07	-0.87	0.45
ASC	0.04	0.17	-0.54	0.23	0.01	0.17	-0.34	0.22
DAR	-0.19	0.15	-0.79	0.50	0.01	0.12	-0.73	0.27
REU	0.11	0.10	-0.29	0.33	0.17	0.07	0.14	0.14
WOL	-0.02	0.11	-0.78	0.95	0.19	0.08	-1.10	0.82
LAU	0.07	0.17	-1.44	2.53	0.23	0.17	0.97	4.86
N-H	-0.24	0.08	0.39	0.20	-0.15	0.06	-0.04	0.15
S-H	0.02	0.06	0.15	0.19	0.16	0.05	0.52	0.21
All	-0.12	0.05	0.49	0.13	0.00	0.04	0.19	0.10
Stability	-0.08 ± 0.18 ppm/year				0.00 ± 0.18 ppm/year			

Table 3.2.6.2: OCFG and SRFG XCH₄ SAT-FTS fit results for all individual stations and using all data combined (All). All units are in ppb. NH and SH are the results obtained from all Northern and Southern Hemisphere data pair. Stability is the weighted average over all station slope results, with weights=1/(slope error)². The uncertainty on the stability corresponds with the 95% confidence interval.

GLINT XCO ₂ fit results								
Station	OCFG				SRFG			
	YtY std	95% err	YtY range	95% err	YtY std	95% err	YtY range	95% err
TSU	0.93	0.11	2.13	0.26	1.58	0.09	3.57	0.22
JPL	0.58	0.03	1.40	0.08	0.53	0.05	1.31	0.13
SAG	0.54	0.10	1.26	0.23	0.33	0.05	0.79	0.12
IZA	0.57	0.03	1.51	0.08	0.44	0.04	1.14	0.12
ASC	0.18	0.01	0.37	0.03	0.09	0.04	0.19	0.10
DAR	0.51	0.02	1.42	0.07	0.47	0.05	1.34	0.14
REU	0.22	0.02	0.57	0.06	0.13	0.02	0.34	0.05
WOL	0.30	0.03	0.83	0.09	0.36	0.02	0.97	0.04
LAU	NULL	NULL	NULL	NULL	NULL	NULL	NULL	NULL
N-H	0.52	0.05	1.46	0.14	0.39	0.04	1.13	0.12
S-H	0.34	0.01	0.91	0.04	0.25	0.01	0.66	0.02
All	0.43	0.01	1.27	0.03	0.24	0.01	0.68	0.02
Mean	0.48±0.20 ppb		1.19±0.44 ppb		0.49 ± 0.39 ppb		1.21 ± 1.28 ppb	

Table 3.2.6.3: OCFG and SRFG XCO₂ SAT-FTS year-to-year stability results for all individual stations and using all data combined (All). All units are in ppm. NH and SH are the results obtained from all Northern and Southern Hemisphere data pair.



ESA Climate Change Initiative (CCI)

Product Validation and Intercomparison Report (PVIR)

for the Essential Climate Variable (ECV)
Greenhouse Gases (GHG)

Page 58

Version 5.0
Final

9 Feb 2017

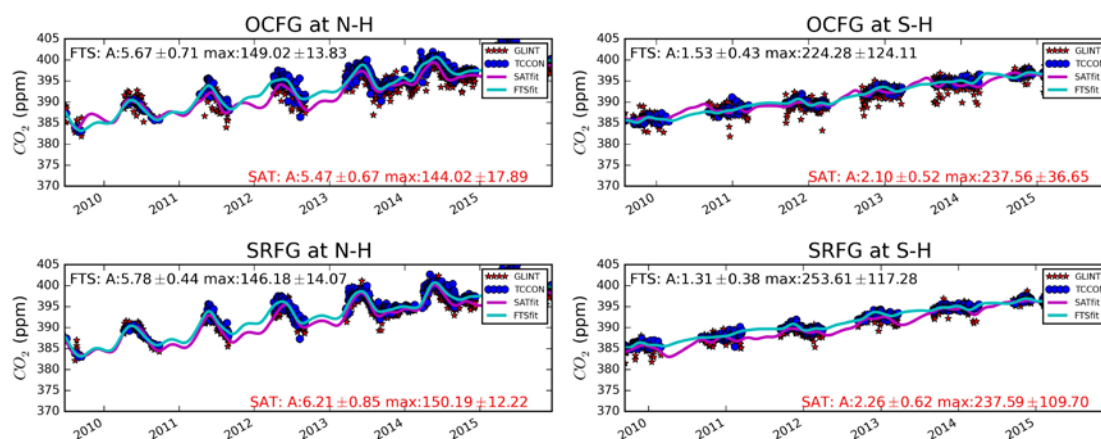


Figure 3.2.6.4: Northern and Southern Hemisphere timeseries of daily averaged OCFG, SRFG and TCCON XCO₂ data, including trend and seasonal fit results.

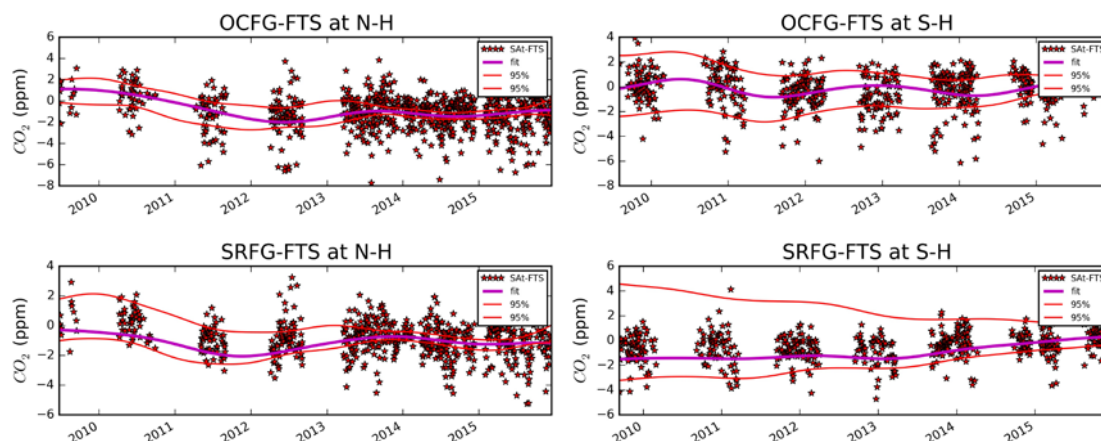


Figure 3.2.6.5: Northern and Southern Hemisphere timeseries of daily averaged OCFG, SRFG - TCCON Bias XCO₂ data, including trend fit results.



ESA Climate Change Initiative (CCI)

**Product Validation and
Intercomparison Report (PVIR)**

for the Essential Climate Variable (ECV)
Greenhouse Gases (GHG)

Page 59

Version 5.0
Final

9 Feb 2017

3.2.7 GLINT XCH₄

Relative GOSAT GLINT XCH ₄ results								
	OCFP-OCFP glint				SRFP-SRFP glint			
Station	Bias	Scatter	R	N	Bias	Scatter	R	N
TSU	18.98	-1.56	0.12	1375	20.42	3.04	-0.13	2033
JPL	12.67	0.28	0.18	11139	10.27	3.36	-0.02	12855
SAG	14.45	-0.82	0.08	1304	20.71	2.69	-0.11	1777
IZA	-1.14	-1.19	0.09	5429	12.09	2.29	0.00	1059
ASC	9.32	-0.46	0.13	-2549	1.78	1.92	-0.08	-622
DAR	2.43	-4.45	0.28	3276	-0.78	-1.30	0.09	6635
REU	11.26	-1.54	0.06	1015	8.20	1.51	-0.11	2932
WOL	1.33	0.61	-0.01	8920	-0.28	1.06	-0.06	12919
LAU	2.74	3.88	-0.14	504	1.10	2.96	-0.18	330
N-H	3.97	0.37	0.21	16698	8.67	2.78	-0.05	17102
S-H	2.68	-0.17	0.07	13715	-0.81	1.88	-0.05	22816
All	3.21	0.07	0.06	30413	3.94	1.60	0.03	39918
RA	5.02-6.70				5.00-6.27			
Seas	0.77-2.37				0.37-3.18			
SRA	5.43-6.98				5.24-6.64			
Relative GOSAT GLINT XCH ₄ results								
	OCPR-OCPR glint				SRPR-SRPR glint			
Station	Bias	Scatter	R	N	Bias	Scatter	R	N
TSU	6.75	2.55	-0.10	7611	9.18	1.98	-0.10	7095
JPL	5.23	2.89	-0.01	27905	9.11	2.76	0.00	26317
SAG	4.95	3.14	-0.10	7491	8.42	3.27	-0.06	6508
IZA	2.97	-1.61	0.07	14455	14.50	-2.02	0.06	9849
ASC	-0.06	-0.76	0.08	-8186	1.01	-0.76	0.15	-10344
DAR	-0.28	-1.61	0.05	4905	0.25	-1.40	0.02	1834
REU	6.32	-0.74	0.00	-621	9.37	-1.62	0.02	-64
WOL	3.56	-0.80	0.01	21840	3.76	-1.43	0.04	22661
LAU	7.05	0.72	-0.08	2636	8.43	0.17	-0.09	2530
N-H	0.79	1.92	0.03	49276	6.56	1.25	-0.01	39425
S-H	0.37	-0.36	0.02	28760	1.62	-0.53	0.03	26961
All	0.65	1.11	0.01	78036	4.44	0.51	0.03	66386
RA	3.52-4.12				3.72-4.17			
Seas	0.43-1.07				0.64-2.34			
SRA	4.18-4.25				4.88-4.94			

Table 3.2.7.1: Relative OCFP,OCPR,SRFP and SRPR land – glint XCH₄ validation results for all individual stations and using all data combined (ALL). All units apart from R and N are in ppm. NH and SH are the results obtained from all Northern and Southern Hemisphere data pairs.

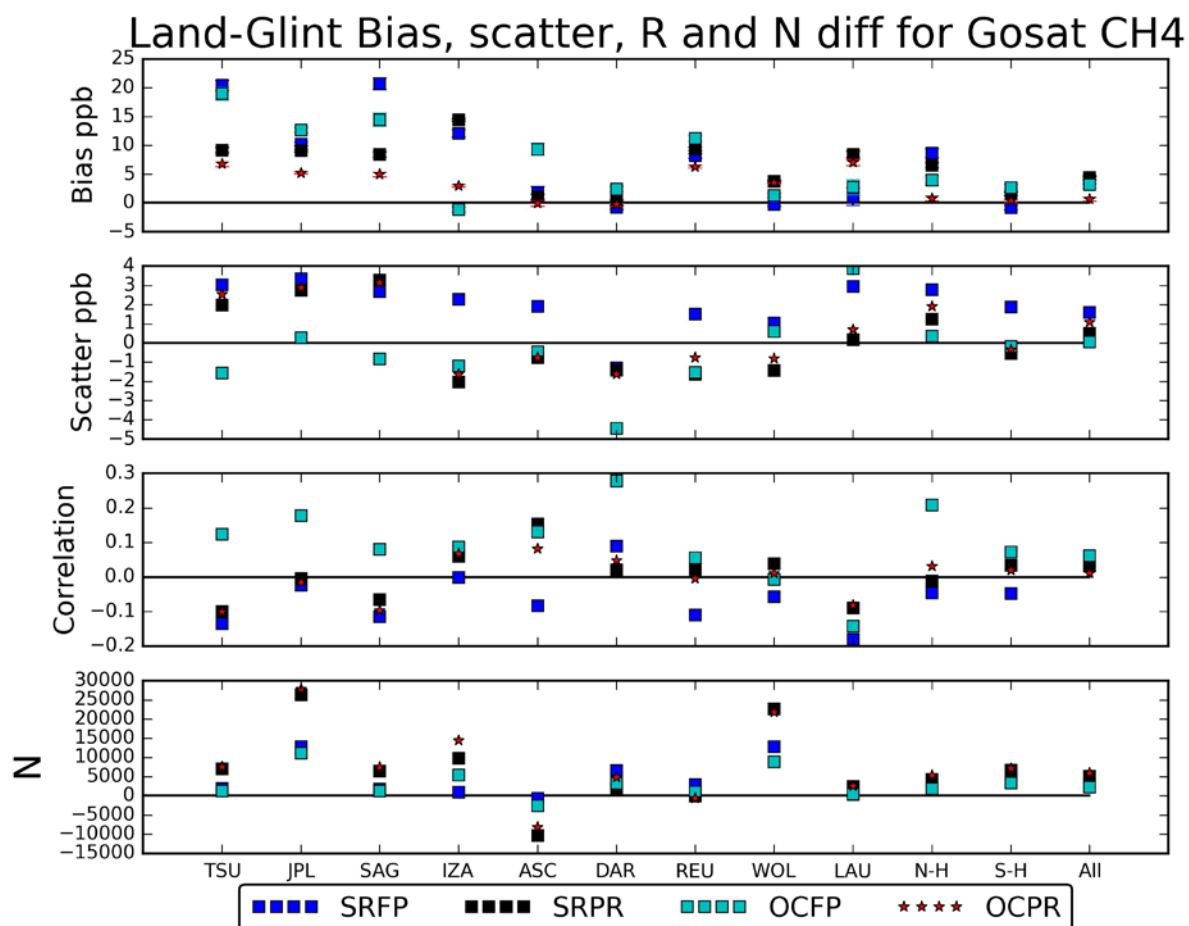


Figure 3.2.7.1: SRFP, SRPR, OCFP and OCPR land -glint validation results for all individual stations, Northern and Southern hemisphere (NH and SH respectively) and using all data combined (All). All units apart from R and N are in ppm. a) Bias, b) scatter, c) correlation and d) number of datapairs. Note that NH,SH and All correspond with the average number per station. Shown here are the difference in these obtained parameters (Bias, scatter, Correlation, N)

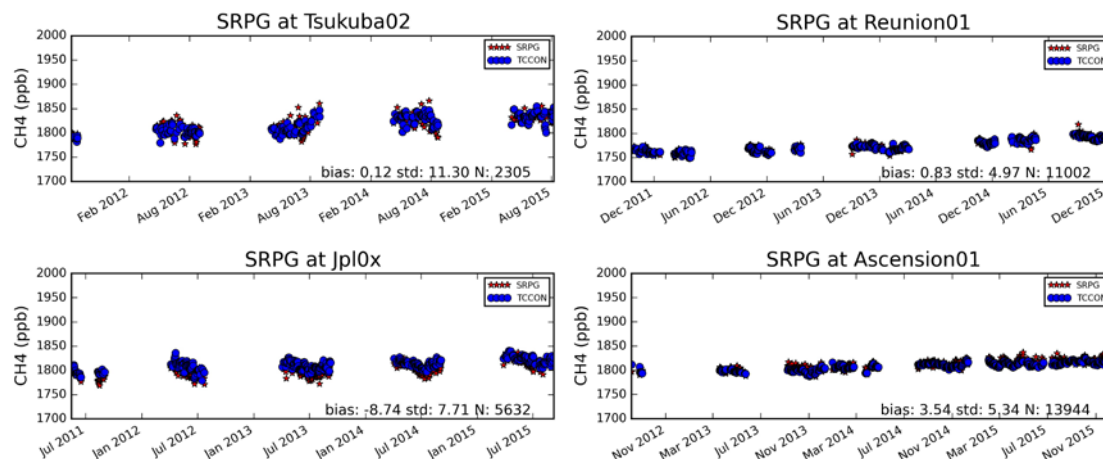


Figure 3.2.7.2: Example timeseries of daily averaged SRPG and FTIR XCH₄ data.

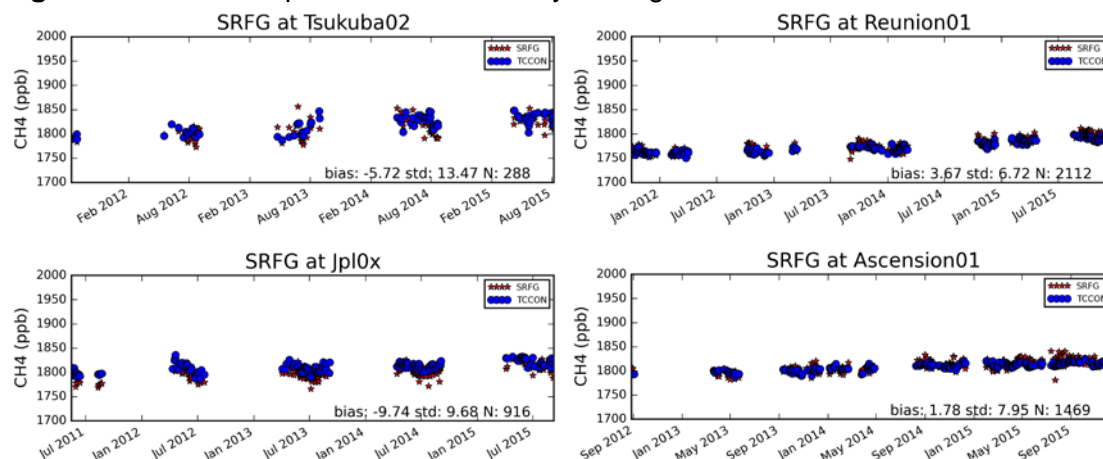


Figure 3.2.7.3: Example timeseries of daily averaged SRFG and FTIR XCH₄ data.

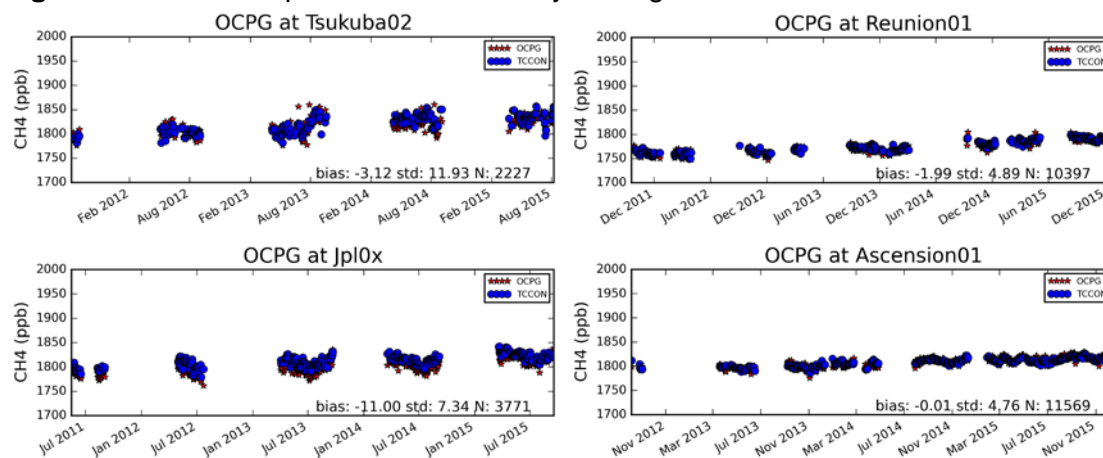


Figure 3.2.7.4: Example timeseries of daily averaged OCPG and FTIR XCH₄ data.



ESA Climate Change Initiative (CCI)

**Product Validation and
Intercomparison Report (PVIR)**

for the Essential Climate Variable (ECV)
Greenhouse Gases (GHG)

Page 62

Version 5.0
Final

9 Feb 2017

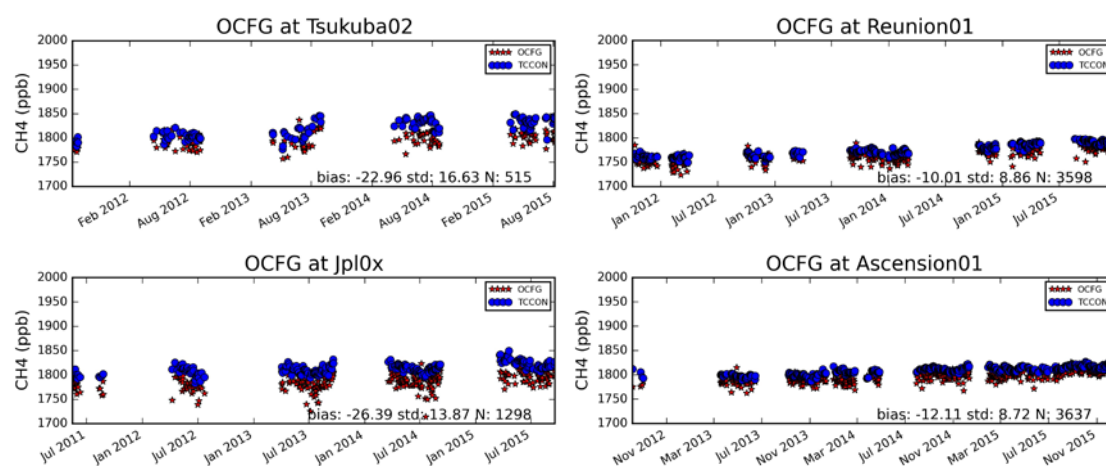


Figure 3.2.7.5: Example timeseries of daily averaged OCFG and FTIR XCH₄ data.



ESA Climate Change Initiative (CCI)

**Product Validation and
Intercomparison Report (PVIR)**

for the Essential Climate Variable (ECV)
Greenhouse Gases (GHG)

Page 63

Version 5.0
Final

9 Feb 2017

GLINT XCH ₄ fit results								
	OCFG				SRFG			
Station	Slope	Slope err	Ampli	Ampli err	slope	Slope err	Ampli	Ampli err
TSU	-6.01	2.26	2.41	8.97	-4.16	2.28	-11.24	4.50
JPL	0.38	1.45	-1.92	6.13	2.24	1.04	-5.91	3.62
SAG	-1.93	2.39	9.69	7.89	-0.61	2.61	-7.55	8.77
IZA	-1.83	0.75	-4.18	3.39	-1.47	0.66	-2.69	3.37
ASC	0.50	0.96	4.09	1.28	1.52	1.03	-4.68	1.41
DAR	-1.46	0.60	6.08	1.56	-0.42	0.59	6.30	1.39
REU	-0.50	0.66	-1.98	1.31	0.60	0.53	2.27	1.03
WOL	-1.08	0.66	-5.29	5.52	1.10	0.58	19.08	6.48
LAU	0.36	1.18	4.87	20.72	1.50	1.23	-21.13	39.56
N-H	-1.21	0.51	3.55	1.20	0.74	0.45	3.72	1.25
S-H	-0.87	0.34	-4.08	0.98	0.62	0.33	-4.81	1.12
All	-1.16	0.30	3.96	0.75	0.52	0.29	4.65	0.74
Stability	-0.97 ± 1.14 ppb/year				0.31 ± 0.98 ppb/year			

GLINT XCH ₄ fit results								
	OCPG				SRPG			
Station	Slope	Slope err	Ampli	Ampli err	slope	Slope err	Ampli	Ampli err
TSU	-3.94	1.20	3.93	5.84	-2.82	1.16	-8.04	4.60
JPL	1.28	0.60	2.11	2.64	1.48	0.59	4.06	2.29
SAG	-0.06	1.25	1.54	2.20	0.32	1.28	-3.34	3.86
IZA	-0.53	0.42	3.51	1.89	-0.59	0.43	3.14	2.21
ASC	0.88	0.47	-1.60	0.63	0.80	0.56	-0.77	0.70
DAR	-1.00	0.30	3.63	0.80	-0.89	0.32	6.93	0.74
REU	-0.60	0.32	-1.93	0.89	-0.09	0.33	2.03	0.75
WOL	-0.46	0.41	-5.44	2.85	0.05	0.49	-9.14	4.86
LAU	-0.45	0.77	-6.12	12.76	-0.03	0.83	-0.77	18.69
N-H	-0.42	0.24	2.76	0.62	0.64	0.25	5.11	0.69
S-H	-0.73	0.20	-5.21	0.78	-0.55	0.22	-6.27	0.69
All	-0.40	0.17	1.89	0.46	0.06	0.19	3.99	0.49
Stability	-0.44 ± 0.75 ppm/year				-0.20 ± 0.65 ppm/year			

Table 3.2.7.2: OCFG, SRFG, OCPG and SRPG XCH₄ SAT-FTS fit results for all individual stations and using all data combined (All). All units are in ppb. NH and SH are the results obtained from all Northern and Southern Hemisphere data pair. Stability is the weighted average over all station slope results, with weights=1/(slope error)². The uncertainty on the stability corresponds with the 95% confidence interval.



ESA Climate Change Initiative (CCI)

**Product Validation and
Intercomparison Report (PVIR)**

for the Essential Climate Variable (ECV)
Greenhouse Gases (GHG)

Page 64

Version 5.0
Final

9 Feb 2017

GLINT XCH ₄ fit results								
	OCFG				SRFG			
Station	YtYstd	95% err	YtY range	95% err	YtYstd	95% err	YtY range	95% err
TSU	6.01	0.14	13.76	0.45	1.73	0.50	3.99	1.13
JPL	1.81	0.18	4.63	0.51	2.11	0.26	5.11	0.69
SAG	5.66	0.75	13.23	1.85	4.46	0.70	11.20	1.81
IZA	3.69	0.24	9.38	0.67	2.48	0.21	6.64	0.56
ASC	0.51	0.08	1.05	0.19	2.03	0.21	4.12	0.43
DAR	5.00	0.08	12.78	0.18	4.11	0.14	10.94	0.50
REU	1.94	0.23	4.85	0.54	1.78	0.11	4.50	0.25
WOL	2.99	0.12	8.24	0.39	1.94	0.13	5.44	0.38
LAU	NULL	NULL	NULL	NULL	NULL	NULL	NULL	NULL
N-H	3.46	0.30	9.70	0.87	3.29	0.15	8.88	0.49
S-H	2.37	0.13	6.78	0.39	1.30	0.07	4.10	0.28
All	2.84	0.13	8.58	0.40	1.61	0.10	4.77	0.33
Mean	3.45±1.67 ppb		8.49±3.39 ppb		0.49 ± 0.39 ppb		1.21 ± 1.28 ppb	

GLINT XCH ₄ fit results								
	OCPG				SRPG			
Station	YtYstd	95% err	YtY range	95% err	YtYstd	95% err	YtY range	95% err
TSU	3.68	0.16	8.43	0.41	2.86	0.15	6.67	0.35
JPL	1.74	0.13	4.20	0.33	1.66	0.16	4.10	0.35
SAG	2.28	0.19	5.56	0.46	1.91	0.17	4.63	0.41
IZA	1.03	0.04	2.64	0.13	1.23	0.04	3.00	0.14
ASC	0.45	0.08	0.98	0.21	0.30	0.06	0.64	0.14
DAR	2.91	0.10	8.22	0.38	2.87	0.09	8.01	0.35
REU	1.26	0.07	3.01	0.16	1.71	0.14	4.37	0.36
WOL	2.33	0.12	6.33	0.35	1.94	0.09	5.62	0.27
LAU	NULL	NULL	NULL	NULL	NULL	NULL	NULL	NULL
N-H	1.41	0.11	3.93	0.32	2.49	0.05	6.91	0.24
S-H	1.05	0.06	3.00	0.19	1.44	0.06	4.67	0.23
All	1.17	0.04	3.35	0.13	1.28	0.06	3.41	0.15
Mean	1.96±0.88 ppb		4.92±2.43 ppb		1.81 ± 0.70 ppb		4.63 ± 2.06 ppb	

Table 3.2.7.3: OCFG, SRFG, OCPG and SRPG XCH₄ SAT-FTS year-to-year stability results for all individual stations and using all data combined (All). All units are in ppm. NH and SH are the results obtained from all Northern and Southern Hemisphere data pair.



ESA Climate Change Initiative (CCI)

Product Validation and Intercomparison Report (PVIR)

for the Essential Climate Variable (ECV)
Greenhouse Gases (GHG)

Page 65

Version 5.0
Final

9 Feb 2017

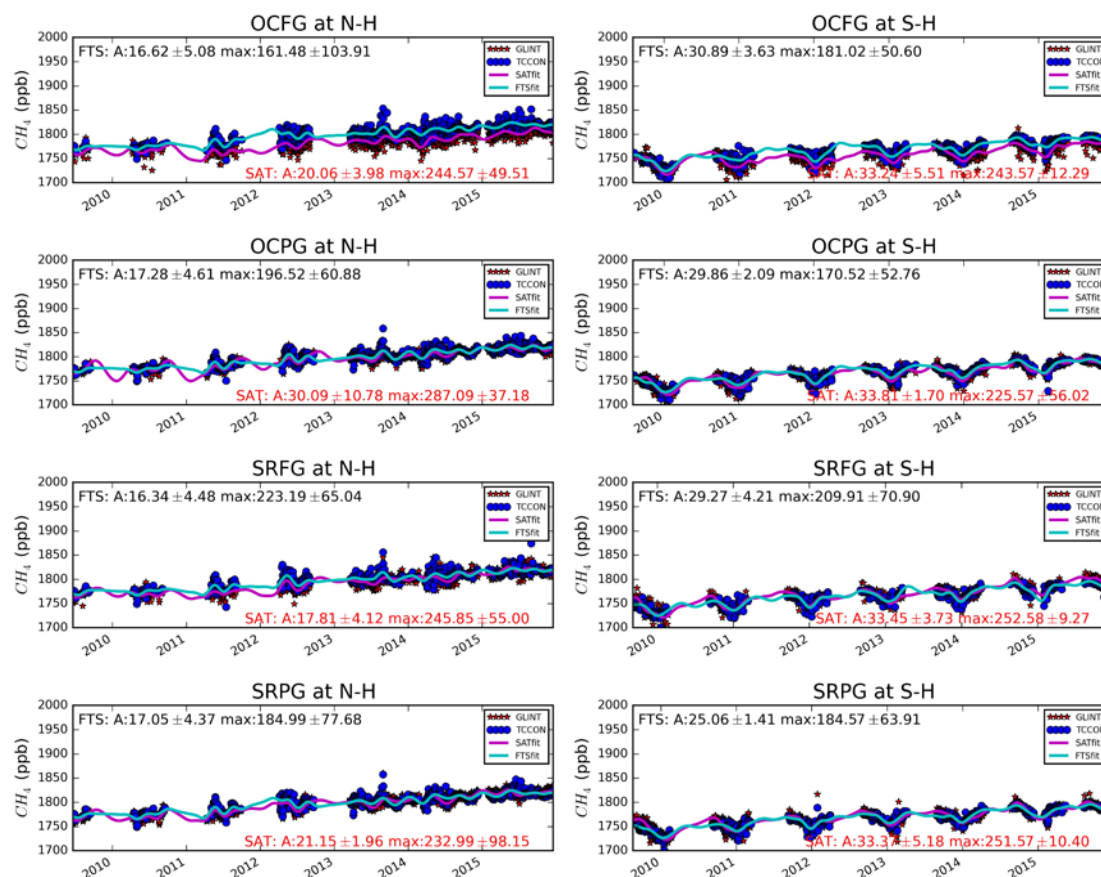


Figure 3.2.7.6: Northern and Southern Hemisphere timeseries of daily averaged OCFG, SRFG, OCPG, SRFP and TCCON XCO₂ data, including trend and seasonal fit results.



ESA Climate Change Initiative (CCI)

Product Validation and Intercomparison Report (PVIR)

for the Essential Climate Variable (ECV)
Greenhouse Gases (GHG)

Page 66

Version 5.0
Final

9 Feb 2017

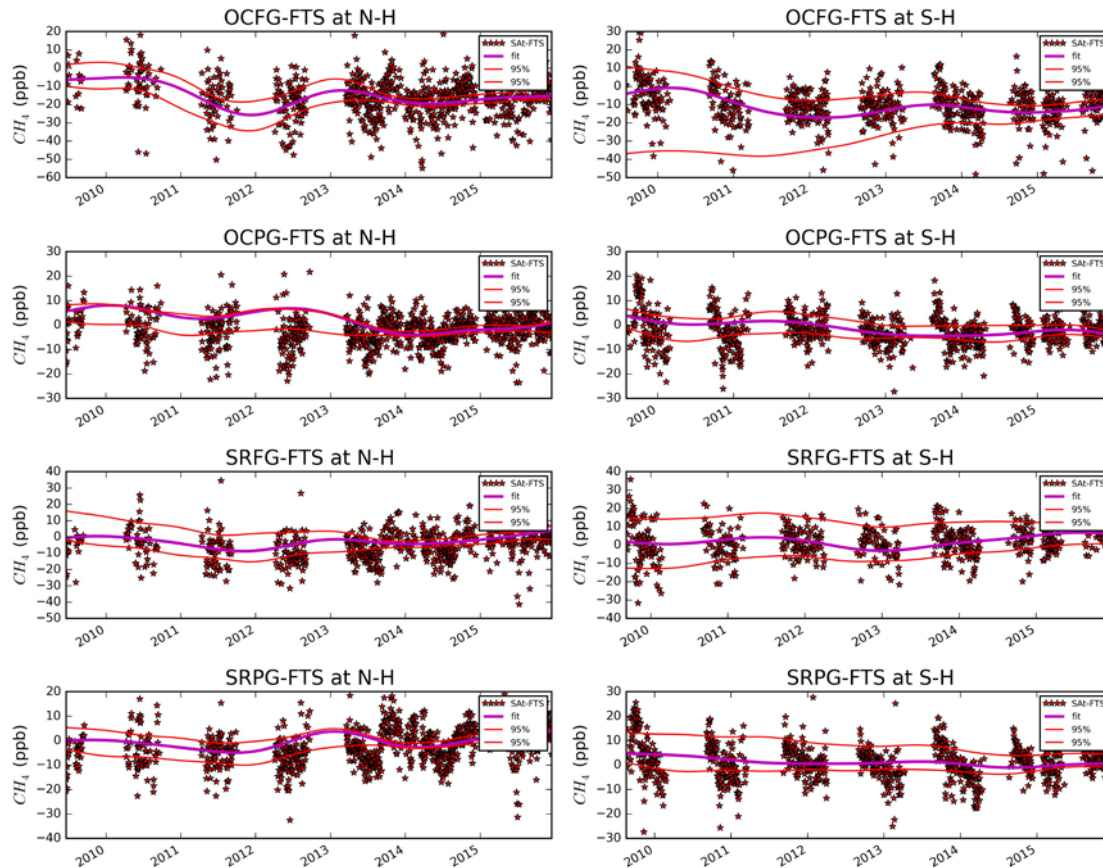


Figure 3.2.7.7: Northern and Southern Hemisphere timeseries of daily averaged OCFG, SRFG, OCPG, SRFP - TCCON Bias XCO_2 data, including trend fit results.



3.2.8 Overall Results

Tables 3.2.8.1 and 3.2.8.2 give an overview of the overall results. The first table lists Bias, Scatter, Correlation (R) and number of data pairs (N), as well as the results of the error assessment analysis. Sat Error corresponds with the mean single measurement precision as set forward by the algorithm developers. This is compared with our obtained scatter, taking into account the precision of the FTS measurements. This yields the so called Delta E, the difference between the measured scatter and what can be derived from the reported uncertainty. When positive, the retrieval teams have underestimated the uncertainty on their measurements. If negative, the actual uncertainty is smaller than predicted. Also listed is NH-SH, which corresponds with the Northern-Southern hemisphere bias. Notice that OCFP and SRFP XCO₂ are featured twice in the tables. The second entry (in italics), matches EMMA's temporal coverage. The first entry uses the entire dataset (clipped to a common timeframe).

Overall results								
Algo	Molec	Bias	Scatter	R	Sat Error	Delta E	NH-SH	N
BESD	CO ₂	0.03±0.01	1.95	0.91	1.85	0.04	-0.43	262090
WFMD	CO ₂	-0.15±0.01	2.67	0.87	2.99	-0.36	0.71	536388
OCFP	CO ₂	0.12±0.01	1.82	0.93	1.73	-0.03	0.22	80069
SRFP	CO ₂	-0.11±0.01	1.99	0.92	1.69	0.23	0.42	91522
EMMA	CO ₂	0.42±0.02	2.03	0.80	2.23	-0.25	0.39	41667
EMMB	CO ₂	0.44±0.02	1.72	0.86	1.93	-0.26	0.27	33470
EMMC	CO ₂	0.34±0.02	1.72	0.86	1.94	-0.27	0.38	31771
OCFP	CO ₂	0.25±0.02	1.81	0.84	1.84	-0.09	0.40	29778
SRFP	CO ₂	-0.18±0.02	1.92	0.87	1.63	0.23	0.45	45510
IMAP	CH ₄	10.28±0.10	45.43	0.43	60.15	-14.83	15.08	833878
WFMD	CH ₄	8.81±0.19	76.04	0.27	76.59	-0.63	13.67	605821
OCFP	CH ₄	-6.32±0.10	14.86	0.86	13.55	0.78	1.11	84583
OCPR	CH ₄	1.66±0.05	13.69	0.87	10.80	2.29	5.21	272863
SRFP	CH ₄	6.33±0.09	14.14	0.87	11.68	1.86	6.39	97977
SRPR	CH ₄	6.64±0.05	13.98	0.86	11.18	2.20	5.00	281892
EMMA	CH ₄	1.24±0.07	13.44	0.86	15.53	-2.52	5.17	133049

Table 3.2.8.1: Overview table, listing all overall (ALL) results. The listed uncertainties on the bias correspond with the 0.95 confidence interval. XCO₂ bias and scatter in ppm, XCH₄ bias and scatter in ppb. Sat Error, is the mean error as reported by the retrieval teams, Delta E, is the difference between the measured (SAT-FTS) Scatter and the calculated error based on the reported SAT uncertainty and observed TCCON variability), if positive the reported Satellite error is underestimated, if negative it is overestimated. NH-SH is the Northern-Southern hemisphere bias.

Table 3.2.8.2 yields the overall stability assessment results. Stability is the (weighed) average linear drift in the SAT-TCCON bias. The uncertainty corresponds with the 95% confidence interval on the mean. A(NH) corresponds with the Northern Hemisphere Amplitude of the Satellite-TCCON difference fit. YtY_std and YtY_range are the average (over all stations) year to year variability and range (and their corresponding 95% confidence interval).



ESA Climate Change Initiative (CCI)

**Product Validation and
Intercomparison Report (PVIR)**

for the Essential Climate Variable (ECV)
Greenhouse Gases (GHG)

Page 68

Version 5.0
Final

9 Feb 2017

Overall Results: Stability					
Algo	Molec	Stability	A(NH)	YtY_std	YtY_range
BESD	CO ₂	0.03±0.06	0.14±0.08	0.32±0.08	0.82±0.30
WFMD	CO ₂	-0.03±0.10	0.12±0.09	0.31±0.11	0.80±0.35
OCFP	CO ₂	-0.07±0.07	0.21±0.06	0.29±0.06	0.79±0.19
SRFP	CO ₂	0.02±0.04	0.45±0.06	0.27±0.12	0.75±0.18
EMMA	CO ₂	-0.08±0.22	0.13±0.10	0.18±0.12	0.36±0.25
EMMB	CO ₂	-0.08±0.20	0.15±0.09	0.16±0.11	0.32±0.22
EMMC	CO ₂	-0.14±0.20	0.20±0.08	0.16±0.12	0.33±0.23
OCFP	CO ₂	-0.20±0.26	0.06±0.05	0.20±0.15	0.41±0.32
SRFP	CO ₂	0.05±0.11	0.51±0.05	0.20±0.12	0.41±0.24
IMAP	CH ₄	0.69±0.77	4.68±1.15	3.34±1.28	8.69±4.11
WFMD	CH ₄	1.09±1.23	1.89±2.15	4.16±1.34	10.54±4.00
OCFP	CH ₄	1.54±1.05	3.10±0.46	4.34±0.88	11.29±2.30
OCPR	CH ₄	-0.30±0.53	2.06±0.23	1.50±0.52	4.22±1.59
SRFP	CH ₄	-0.46±0.57	1.97±0.40	1.64±0.50	4.63±1.53
SRPR	CH ₄	-0.60±0.67	1.97±0.25	1.64±0.61	4.56±1.92
EMMA	CH ₄	-0.36±0.71	1.33±0.36	1.24±0.45	3.19±1.21

Table 3.2.8.2: Overview table, listing the overall stability, year-to-year standard deviation and range derived from all individual station results. The stability corresponds with the temporal drift of the algorithm, its error with the 95% confidence band, A (NH) is the amplitude of the seasonal component of the Satellite-TCCON bias timeseries, its error with the 95% confidence band. YtY std is the overall year to year standard deviation (with 95% confidence interval) and YtY range is the year to year range (highest-smallest value, again with the 95% confidence interval)


Table 3.2.8.3 lists the secondary FoM, their 95% confidence interval and for each validation round, the likelihood that these parameters are actually different samples of the same overall population, i.e. the probability that the variances are identical or $P(\sigma^2=\sigma^2)$. When smaller than 0.05, one can say that both algorithms indeed produce significantly different results. This is not the case for any of the algorithms. For all parameters the confidence in their difference is less than 95%. Only the SRA difference in the EMMA and SCIAMACHY XCO₂ values come close to being significant. On the other hand the SRA values for GOSAT XCH₄ are near indistinguishable ($P > 0.50$). For RA the latter holds also true for GOSAT XCO₂ and all XCH₄ algorithms.

VALT results										
Station	Mol	RA	RA 95%	P ($\sigma^2=\sigma^2$)	Seas	Seas 95%	P ($\sigma^2=\sigma^2$)	SRA	SRA 95%	P ($\sigma^2=\sigma^2$)
BESD	CO ₂	0.37	0.28-0.64	0.15	0.17	0.11-0.73	0.88	0.56	0.47-0.70	0.10
WFMD	CO ₂	0.57	0.42-0.97		0.15	0.10-0.66		0.71	0.59-0.89	
OCFP	CO ₂	0.36	0.27-0.62	0.98	0.15	0.10-0.64	0.43	0.58	0.49-0.73	0.39
SRFP	CO ₂	0.36	0.27-0.62		0.24	0.16-1.05		0.51	0.43-0.64	
EMMA	CO ₂	0.37	0.28-0.64	0.69	0.11	0.07-0.46	0.77	0.45	0.37-0.56	0.07
EMMB	CO ₂	0.29	0.21-0.49		0.11	0.07-0.47		0.38	0.32-0.48	
EMMC	CO ₂	0.30	0.22-0.51		0.12	0.08-0.52		0.39	0.33-0.50	
OCFP	CO ₂	0.35	0.26-0.60		0.14	0.09-0.60		0.52	0.44-0.66	
SRFP	CO ₂	0.41	0.31-0.71		0.21	0.14-0.89		0.52	0.44-0.66	
IMAP	CH ₄	8.75	6.53-15.04	0.97	4.02	2.63-17.32	0.97	8.99	7.54-11.44	0.45
WFMD	CH ₄	8.84	6.60-15.19		3.93	2.57-16.91		10.07	8.44-12.82	
OCFP	CH ₄	4.68	3.50-8.05	0.82	1.73	1.13-7.47	0.70	4.81	4.06-6.06	0.70
OCPR	CH ₄	4.09	3.05-7.02		1.18	0.77-5.10		4.31	3.64-5.42	
SRFP	CH ₄	4.83	3.60-8.30		0.94	0.61-4.03		5.11	4.31-6.43	
SRPR	CH ₄	3.78	2.82-6.50		0.95	0.62-4.07		4.77	4.02-6.00	
EMMA	CH ₄	4.03	3.01-6.93	0.95	1.02	0.67-4.40	0.86	4.39	3.70-5.53	0.64

Table 3.2.8.3: Overview table, listing the “Relative Accuracy” (RA), overall “Seasonality” (Seas) and “Seasonal Relative Accuracy” (SRA), together with their 0.95 confidence interval (RA 95%, Seas 95% and SRA 95%) and the probability that the obtained sample variances all stem from the same population (P).

Looking at the Glint XCO₂ results we see some remarkable differences between the algorithms. SRFP glint has better scatter, R, RA and SRA values than SRFP land. For OCFP the opposite is true (better values for land). Tsukuba and Saga yield particularly strong differences in the bias. This is probably collocation related where the land measurement also sample measurements over mainland China. Looking at the stability, neither glint measurements shown a significant drift.

For XCH₄, scatter is generally lower for the glint measurements (most pronounced for SRFP). Correlation for the SRFP stations is generally also better for glint (but not for all measurements combined). The inverse is generally true for the other algorithms. All glint measurements yield somewhat worse for the RA and SRA values than their land counterparts. The proxy algorithms yield better RA and SRA values than their full physics counterparts.

	ESA Climate Change Initiative (CCI)	Page 70
	Product Validation and Intercomparison Report (PVIR)	
	for the Essential Climate Variable (ECV) Greenhouse Gases (GHG)	Version 5.0 Final
		9 Feb 2017

3.3 Summary and conclusions TCCON validation of ECA products

This chapter gives an overview of the validation results obtained by VALT. As detailed in **Sect. 3.1**. When we compare the above tables in the overall results with the GCOS and URD quality requirements (see **Table S-3**) we can draw the following conclusions:

Concerning the overall Bias: Of less importance (since it can be more readily corrected) than the variability of the bias, the magnitude of the bias, using all individual collocated measurements, still yields useful information on the quality nevertheless. For XCO₂ BESD has the lowest absolute bias at 0.03 ppm, while WFMD and the GOSAT algorithms range between 0.11 and 0.15 ppm (again absolute values). EMMA values range between 0.34 and 0.44 ppm and are thus slightly higher.

For XCH₄ we can again make out three groups. High absolute values for IMAP (10.3 ppb) and WFMD (8.8 ppb), lower values ranging between 6.6 and 6.3 ppb for OCFP, SRFP and SRPR, and low values for OCPR (1.7 ppb) and EMMA (1.2 ppb)

Concerning the Random Error: The scatter (standard deviation on the individual sat-fts biases) for XCO₂ ranges between 1.7 and 2.7 ppm. The latter value corresponds with WFMD, while all other algorithms feature values at or below 2 ppm. This is below the Breakthrough URD requirement of 3 ppm.


For XCH₄ we see a large difference between the GOSAT algorithms (ranging between 13.4 and 14.9 ppb) and the SCIAMACHY algorithms (45.4 ppb for IMAP and 76.0 ppb for WFMD). Here we have to note that most TCCON stations became operational after the SCIAMACHY detector degradation and thus this value represents the post-degradation single measurement precision. Compared to the URD requirements (<34 ppb), none of the SCIA algorithms meet this requirement, while the GOSAT algorithms even meet the breakthrough value (<17 ppb)

Concerning the Northern-Southern Hemisphere Bias: For XCO₂ most algorithms yield biases between 0.3 and 0.4 ppm. Notable exception is WFMD with a 0.7 ppm bias between hemispheres. OCFP yields a lower value at 0.22 ppm (but this becomes 0.4 when using the EMMA timeseries overlap).

For XCH₄, we see a noticeable difference between the SCIA and GOSAT algorithms, with the first (IMAP (15.1 ppb) and WFMD (13.7 ppb)) yielding considerably higher biases than the latter (ranging between 5 and 6.4 ppb apart from OCFP at 1.1 ppb).

Concerning the assessment of the reported single measurement precision: Delta E, see **Table 3.2.8.1**, is the difference between the measured (SAT-FTS) Scatter and the calculated error based on the reported SAT uncertainty and observed TCCON variability), if positive the reported Satellite error is underestimated, if negative it is overestimated. The highest value (regardless of sign) for XCO₂ can be found for WFMD (-0.36 ppm, thus a slight overestimation of the error), the lowest for BESD (0.04 ppm) and OCFP (-0.03 ppm). The others all hover around 0.25 ppm (all negative apart from SRFP which yields a positive thus underestimation of the SMP).

For XCH₄, we observe a rather large (-14.6 ppb Delta E value). The other algorithms all range (absolute values) between 0.6 and 2.5 ppb.

	ESA Climate Change Initiative (CCI)		Page 71
	Product Validation and Intercomparison Report (PVIR)		
	for the Essential Climate Variable (ECV) Greenhouse Gases (GHG)		Version 5.0 Final
			9 Feb 2017

Concerning Accuracy: This is an estimate of the stability of the bias over space and time. A large but stable bias can be easily corrected in inverse modelling studies, while a small but unstable bias causes severe problems. In our analysis we both compute the variability of the bias between stations (our so-called Relative Accuracy (RA)) and our so-called Seasonal Relative Accuracy (SRA), which captures the variability in the bias between stations and season. Given that our SRA is probably a better value to compare with the accuracy requirements we will focus on this parameter.


SRA values for XCO₂ range between 0.38 and 0.71 ppm. Typically BESD and the 2 GOSAT algorithms are slightly higher than 0.5 ppm, the EMMA algorithms without WFMD are even lower than 0.4 (which corresponds with the TCCON network uncertainty), while WFMD is slightly higher at 0.71. This implies, looking at the raw numbers, that only EMMA meets the GCOS and URD requirements (<0.5 ppm). However taking the analysis uncertainty and TCCON uncertainty into account all algorithms could very well have passed this test.

SRA values for XCH₄ range between 4.3 and 10.1 ppb. This implies that all algorithms may have passed the URD (<10 ppb) requirements (again taking the analysis uncertainty into account). The more stringent <5 ppb GCOS requirement is only met by the GOSAT algorithms (SRFP is slightly higher at 5.1 ppb but its uncertainty interval well overlaps the threshold).


Concerning Stability: Looking at the long term drift (Stability in **Table 3.2.8.2**) none of the algorithms yield a statistically significant drift apart from OCFP XCH₄ at 1.54 ± 1.05 ppb/year. This value is lower than the URD requirement (3 ppb/year), but higher than the very strict GCOS (<0.7 ppb/year) requirements. Looking at the **Figure 3.2.5.5** we see an offset in the bias timeseries occurring around the beginning of 2012. Somewhat higher (with respect to competitors) amplitudes in the residual timeseries (indicating a seasonality in the sat-FTS bias residual) can be found in SRFP (for XCO₂, 0.45 ppm, others are 0.21 and lower), IMAP (SCIA XCH₄, 4.7 ppb), and OCFP (GOSAT CH₄, 3.1 ppb). Other XCH₄ algorithms have amplitudes at 2.1 ppb and below.

Stability can also be interpreted as the overall variability between years. This is probably best captured by the YtY_std in **Table 3.2.8.2**. Unlike the drift, all the obtained results are statistically significant. For XCO₂, the YtY_std values range between 0.16 and 0.32 ppm (1 sigma). Thus all XCO₂ algorithms pass the URD requirements (<0.5 ppm), but none (apart EMMA if we take the uncertainty into account) meet the very strict (<0.15 ppm/year) GCOS requirement. Here we have to keep in mind that EMMA's timeseries is shorter. Given a timeperiod like EMMA, for instance, OCFP's YtY_std drops from 0.29 ± 0.06 to 0.20 ± 0.15 ppm/year (it's confidence interval now overlaps with our GCOS threshold). For XCH₄, values range between 4.3 and 1.2 ppb/year. Again all values are statistically significant. OCFP, SRFP and SRPR all have very similar values (~1.5 ppb). EMMA has an even lower value but benefits from a shorter timeseries (1.2 ppb). All the above meet the URD requirements of <3 ppb/year. Taking the confidence interval into account, also IMAP and WFMD (although the latter only very narrowly) overlap with this threshold. Only OCFP's confidence interval falls outside. The GCOS requirements of <0.7 ppb/year is not met by any of the algorithms.

However, the above interpretation of the numbers assumes that there is absolutely no year to year variability in the TCCON data itself. This is simply not the case. There are known drifts and changes in the TCCON instruments, due to changes in the Instrumental Line Shape (ILS) and ghosts. Version GGG2014 fixed the ghost issue, but changes in the ILS over time is still an issue, prompting the operators at times to re-align their instruments to

	ESA Climate Change Initiative (CCI)	Page 72
	Product Validation and Intercomparison Report (PVIR)	
	for the Essential Climate Variable (ECV) Greenhouse Gases (GHG)	Version 5.0 Final
		9 Feb 2017

avoid any truly long-term drift. It is extremely difficult to assess to what extent these drifts in the instrument alignment cause year-to-year offsets in the timeseries but is probably safe to say that TCCON's variability is a non-negligible component in our observed YtY_std values. Therefore, final judgement on whether the algorithms have met the GCOS requirements have to be withheld until TCCON either accurately quantifies and/or corrects for these ILS changes (scheduled for the next release of TCCON GGG).

	ESA Climate Change Initiative (CCI)	Page 73
	Product Validation and Intercomparison Report (PVIR)	
	for the Essential Climate Variable (ECV) Greenhouse Gases (GHG)	Version 5.0 Final
		9 Feb 2017

3.3.1 SCIAMACHY XCO₂

Other than the data density, which is significantly higher for WFMD, BESD (consistent with previous analysis) still outperforms WFMD on almost every other front: smaller biases, less scatter, higher correlation, better relative accuracy. However, given the small differences between algorithms and the limited dataset used, observed differences in the validation parameters often turn out to lack statistical significance. In fact in this analysis none of the parameters for (Seasonal) Relative Accuracy reach a 95% confidence margin. Here, we still see one of the most distinct differences among the observed algorithms though. The difference in relative accuracies (RA and SRA) reaches 85% and 90% confidence, respectively.

Neither algorithm clearly reaches the 0.5 ppm threshold for the Accuracy Requirement as set forward by the URD. BESD's RA does reach 0.37 ppm, but it's SRA (a more accurate representation of the user threshold) does not (although its confidence band overlaps 0.47-0.70). If we take into account the uncertainty on the collocation we cannot state with confidence that the BESD algorithm does not meet the requirements. Neither can we say this for the WFMD algorithm since its SRA confidence band overlaps the 0.70 threshold (which apart from the user's 0.5 ppm threshold takes into account the TCCON network uncertainty)

The time series show no obvious deviations for either algorithm. Fit results of the Northern-hemisphere data yields a slight advantage to BESD. As for the stability, or the weighted average of all drift results obtained through fitting a trend and seasonal fit through the daily sat-TCCON bias results, both algorithms yield small and very similar values, neither of which are significant. The year-to-year stability figures are likewise near identical, the significance of which has been discussed in above in Section 3.3.


Looking at figures 3.2.1.5 (Bias timeseries), the only noticeable feature is a slight bump in the 2010 Southern Hemisphere WFMD timeseries.

Overall summary BESD:

- Single measurement precision: 1.95 ppm (1-sigma)
- Relative accuracy, Seasonal Relative accuracy: 0.37, 0.56 ppm
- Stability:
 - Linear trend: 0.03 ± 0.06 ppm / year
 - Year-to-year stability (1-sigma): 0.32 ± 0.08 ppm


Overall summary WFMD:

- Single measurement precision: 2.67 ppm (1-sigma)
- Relative accuracy, Seasonal Relative accuracy: 0.57, 0.71 ppm
- Stability:
 - Linear trend: -0.03 ± 0.10 ppm / year
 - Year-to-year stability (1-sigma): 0.31 ± 0.11 ppm

	ESA Climate Change Initiative (CCI)	Page 74
	Product Validation and Intercomparison Report (PVIR)	
	for the Essential Climate Variable (ECV) Greenhouse Gases (GHG)	Version 5.0 Final
		9 Feb 2017

Summary table:

Estimates of achieved data quality: CRDP#4 CO2_SCI_BESD and WFMD					
Sensor	Algorithm	Random error [ppm]	Systematic error [ppm]	Stability [ppm / year]	Comments
SCIAMACHY on ENVISAT	BESD v02.01.02	1.95	0.37 – 0.56 RA - SRA	Linear trend: 0.03 ± 0.06 Year-to-year: [0.32 +/- 0.08]	Stability: Significance?: Trend: no Year-to-year: yes
SCIAMACHY on ENVISAT	WFMD V4.0	2.67	0.57 - 0.71 RA - SRA	Linear trend: -0.03 ± 0.10 Year-to-year: [0.31 +/- 0.11]	Stability: Significance?: Trend: no Year-to-year: yes (2010 SH feature?)
All values are 1-sigma (except for trend and range); The uncertainties given correspond with the 95% confidence intervals. Note: "Year-to-year" stability refers to assessment results related to the extended definition of stability as given in URDv2.1, which now also covers "inter-annual error changes"					

	ESA Climate Change Initiative (CCI)	Page 75
	Product Validation and Intercomparison Report (PVIR)	
	for the Essential Climate Variable (ECV) Greenhouse Gases (GHG)	Version 5.0 Final
		9 Feb 2017

3.3.2 GOSAT XCO₂


The differences between these datasets are very small. Both biases are similar but on opposing ends (+0.12 ppm for OCFP and -0.11 ppm for SRFP). SRFP's scatter is only marginally higher. Correlations are similar (0.93 and 0.92). This time SRFP has slightly more data (used to be different in previous version) (91522 vs. 80069). The resemblance in RA and SRA is still very strong, in fact they yield the same RAs (the probability of them being equal is 98% and 39% for the SRA respectively). Since the previous analysis this similarity has increased for RA but decreased for the SRA. SRFP has a slightly better SRA. Looking at the SRA, neither algorithm reaches the 0.5 quality thresholds. Looking at the confidence interval both algorithms do overlap the 0.5 criteria, while, if taking into account the collocation error, both algorithms yield SRAs smaller than 0.7 ppm. Regarding stability, neither show a substantial drift and comparable year-to-year stability results. Nor are there distinct features in the Bias timeseries (see **Fig 3.2.2.5**) apart from a seasonal residual in the SRFP Northern Hemisphere plots. At 0.45 ppm, SRFP yields the highest residual amplitude of all the XCO₂ algorithms, more than twice as high OCFP (see **Table 3.2.8.2**).

Overall summary OCFP:

- Single measurement precision: 1.82 ppm (1-sigma)
- Relative accuracy, Seasonal Relative accuracy: 0.36, 0.58 ppm
- Stability:
 - Linear trend: -0.07 ± 0.07 ppm / year
 - Year-to-year stability (1-sigma): 0.29 ± 0.06 ppm


Overall summary SRFP:

- Single measurement precision: 1.99 ppm (1-sigma)
- Relative accuracy, Seasonal Relative accuracy: 0.36, 0.51 ppm
- Stability:
 - Linear trend: 0.02 ± 0.04 ppm / year
 - Year-to-year stability (1-sigma): 0.27 ± 0.12 ppm

	ESA Climate Change Initiative (CCI)	Page 76
	Product Validation and Intercomparison Report (PVIR)	
	for the Essential Climate Variable (ECV) Greenhouse Gases (GHG)	Version 5.0 Final
		9 Feb 2017

Summary table:

Estimates of achieved data quality: CRDP#4 CO2_GOS_OCFP and SRFP					
Sensor	Algorithm	Random error [ppm]	Systematic error [ppm]	Stability [ppm / year]	Comments
TANSO on GOSAT	OCFP v7 (UoL-FP)	1.82	0.36 – 0.58 RA - SRA	Linear trend: -0.07 ± 0.07 Year-to-year: [0.29 +/- 0.06]	Stability: Significance?: Trend: no Year-to-year: yes
TANSO on GOSAT	SRFP v2.3.8 (RemoTeC)	1.99	0.36 - 0.51 RA - SRA	Linear trend: 0.02 ± 0.04 Year-to-year: [0.27 +/- 0.12]	Stability: Significance?: Trend: no Year-to-year: yes Seasonal cycle in residuals
All values are 1-sigma (except for trend and range); The uncertainties given correspond with the 95% confidence intervals. Note: "Year-to-year" stability refers to assessment results related to the extended definition of stability as given in URDv2.1, which now also covers "inter-annual error changes"					

	ESA Climate Change Initiative (CCI)	Page 77
	Product Validation and Intercomparison Report (PVIR)	
	for the Essential Climate Variable (ECV) Greenhouse Gases (GHG)	Version 5.0 Final
		9 Feb 2017

3.3.3 EMMA XCO₂

The 3 versions of EMMA have been inter-compared and with OCFP and SRFP using the same EMMA time period. As expected, differences between the EMMA runs are relatively small. Scatter improves when moving from v2.2a to 2.2b, but not between b and c. This is due to the exclusion of WFMD in the 2.2b ensemble. V2.2c excludes all SCIAMACHY data, but the exclusion of BESD seems to have no impact on the scatter. The evolution of the correlation coefficient follows suit.

Likewise the SRA improves from 0.45 to 0.38 and 0.39 and the RA from 0.37(EMMA) to 0.29 (EMMB) and 0.30 (EMMC). The differences between the EMMA versions and OCFP and SRFP in terms of the RA are not significant, but in terms of the SRA, the likelihood that they are from the same sample decreases to 7%. Both OCFP and SRFP yield SRAs (both 0.52) that are higher than the lowest EMMB 0.38 value, with only marginal overlap in their confidence bands. Statistically however we still cannot claim significant differences here. Also note that the observed SRA's for EMMB and EMMC are smaller than the TCCON network accuracy (0.4 ppm)!

EMMB (and EMMC) do seem to perform better than the other algorithms but never to a statistically significant degree.

All of the EMMA products reach the combined 0.7 ppb threshold and so does OCFC and SRFC. In fact all EMMA products even reach the 0.5 threshold


None of the long term drifts yield significant numbers. The YtY_std is statistically significant for all versions and while the actual values are slightly higher than the GCOS requirement of <0.15 their 95% confidence interval overlaps with this value.

Overall summary EMMAv2.2a:

- Single measurement precision: 2.03 ppm (1-sigma)
- Relative accuracy, Seasonal Relative accuracy: 0.37, 0.45 ppm
- Stability:
 - Linear trend: -0.08 ± 0.22 ppm / year
 - Year-to-year stability (1-sigma): 0.18 +/- 0.12 ppm

Overall summary EMMAv2.2b:

- Single measurement precision: 1.72 ppm (1-sigma)
- Relative accuracy, Seasonal Relative accuracy: 0.29, 0.38 ppm
- Stability:
 - Linear trend: -0.08 ± 0.20 ppm / year
 - Year-to-year stability (1-sigma): 0.16 +/- 0.11 ppm


	ESA Climate Change Initiative (CCI)	Page 78
	Product Validation and Intercomparison Report (PVIR)	
	for the Essential Climate Variable (ECV) Greenhouse Gases (GHG)	Version 5.0 Final
		9 Feb 2017

Overall summary EMMAv2.2c:

- Single measurement precision: 1.72 ppm (1-sigma)
- Relative accuracy, Seasonal Relative accuracy: 0.30, 0.39 ppm
- Stability:
 - Linear trend: -0.14 ± 0.20 ppm / year
 - Year-to-year stability (1-sigma): 0.16 ± 0.12 ppm

Summary table:

Estimates of achieved data quality: CRDP#4 EMMA XCO ₂					
Sensor	Algorithm	Random error [ppm]	Systematic error [ppm]	Stability [ppm / year]	Comments
Mixed	EMMA v2.2a	2.03	0.37 - 0.45 RA - SRA	Linear trend: -0.08 ± 0.22 Year-to-year: [0.18 +/- 0.12]	Stability: Significance?: Trend: no Year-to-year: yes
Mixed	EMMA v2.2b	1.72	0.29 - 0.38 RA - SRA	-0.08 ± 0.20 [0.16 +/- 0.11]	Stability: Significance?: Trend: no Year-to-year: yes
TANSO on GOSAT	EMMA v2.2c	1.72	0.30 - 0.39 RA - SRA	-0.14 ± 0.20 [0.16 +/- 0.12]	Stability: Significance?: Trend: no Year-to-year: yes
All values are 1-sigma (except for trend and range); The uncertainties given correspond with the 95% confidence intervals. Note: "Year-to-year" stability refers to assessment results related to the extended definition of stability as given in URDv2.1, which now also covers "inter-annual error changes"					

	ESA Climate Change Initiative (CCI)	Page 79
	Product Validation and Intercomparison Report (PVIR)	
	for the Essential Climate Variable (ECV) Greenhouse Gases (GHG)	Version 5.0 Final
		9 Feb 2017

3.3.4 SCIAMACHY XCH₄

IMAP has superior scatter, correlation and data density. Previous versions of IMAP had issues with a bias jump around the year 2010. This issue seems to be resolved. This has a beneficial impact on the RA and SRA values (both have become smaller). In fact now IMAP yields slightly better SRA values although the difference in statistical terms is negligible. In fact that observation can be pretty much made for all parameters save the three mentioned above. WFMD does seem to have incorporated a better estimate of their single measurement precision and it does a better job at capturing the seasonal cycle (lower amplitude on the bias fit). This is visible in **Figure 3.2.4.5** where the Northern Hemisphere bias plot for IMAP features a seasonal pattern and in **Table 3.2.8.2** where it has the highest A(NH) value (4.68 ppb) of all the XCH₄ algorithms.


None of the algorithms feature a significant drift in the timeseries.

Overall summary WFMD:

- Single measurement precision: 76.04 ppb (1-sigma)
- Relative accuracy, Seasonal Relative accuracy: 8.8, 10.1 ppb
- Stability:
 - Linear trend: 1.09 ± 1.23 ppb / year
 - Year-to-year stability: 4.16 ± 1.34 ppb


Overall summary IMAP:

- Single measurement precision: 45.43 ppb (1-sigma)
- Relative accuracy, Seasonal Relative accuracy: 8.8, 9.0 ppb
- Stability:
 - Linear trend: 0.69 ± 0.77 ppb / year
 - Year-to-year stability: 3.34 ± 1.28 ppb

	ESA Climate Change Initiative (CCI)	Page 80
	Product Validation and Intercomparison Report (PVIR)	
	for the Essential Climate Variable (ECV) Greenhouse Gases (GHG)	Version 5.0 Final
		9 Feb 2017

Summary table:

Estimates of achieved data quality: CRDP#4 CH ₄ _SCI_WFMD and IMAP					
Sensor	Algorithm	Random error [ppb]	Systematic error [ppb]	Stability [ppb / year]	Comments
SCIAMACHY on ENVISAT	WFMD V4.0	76.0	8.8 – 10.1 RA - SRA	Linear trend: 1.09 ± 1.23 Year-to-year: [4.16 +/- 1.34]	Stability: Significance?: Trend: no Year-to-year: yes
SCIAMACHY on ENVISAT	IMAP v7.2	45.4	RA - SRA 8.8 – 9.0	0.69 ± 0.77 [3.34 +/- 1.28]	Stability: Significance?: Trend: no Year-to-year: yes Seasonal cycle in residual
All values are 1-sigma (except for trend and range); The uncertainties given correspond with the 95% confidence intervals. Note: "Year-to-year" stability refers to assessment results related to the extended definition of stability as given in URDv2.1, which now also covers "inter-annual error changes"					

	ESA Climate Change Initiative (CCI)	Page 81
	Product Validation and Intercomparison Report (PVIR)	
	for the Essential Climate Variable (ECV) Greenhouse Gases (GHG)	Version 5.0 Final
		9 Feb 2017

3.3.5 GOSAT XCH₄

As with GOSAT XCO₂, the differences between the algorithms are very small. Note that we have not listed the results of EMMA separately in this case. This is because the results yielded little differences when clipping the timeseries so as to overlap that with EMMA. In terms of RA and SRA, the likelihood that they essentially are the same is 95% and 64% respectively (when including EMMA). The lowest bias and scatter are for EMMA and OCPR. Correlations are near identical. The best RA is for SRPR, while the best SRA is for OCPR (but as said with very small overall differences. The lowest interhemispheric difference is for OCFP, while the largest is for SRFP. OCFP is the only algorithm which features a statistically significant bias drift (1.54 ppb/year) although it still falls within the URD requirements of <3 ppb/year but is higher than the <0.7ppb/year GCOS requirement. Also its seasonal amplitude on the residual is the largest (after IMAF XCH₄). Looking at the Bias timeseries in **Figure 3.2.5.6** we see a rather significant jump in the beginning of 2012 in the OCFP bias timeseries.

Overall summary OCFP:

- Single measurement precision: 14.9 ppb (1-sigma)
- Relative accuracy, Seasonal Relative accuracy: 4.7, 4.8 ppb
- Stability:
 - Linear trend: 1.54 ± 1.05 ppb / year
 - Year-to-year stability: 4.34 ± 0.88 ppb
 -

Overall summary OCPR:

- Single measurement precision: 13.7 ppb (1-sigma)
- Relative accuracy, Seasonal Relative accuracy: 4.1, 4.3 ppb
- Stability:
 - Linear trend: -0.30 ± 0.53 ppb / year
 - Year-to-year stability: 1.50 ± 0.52 ppb

Overall summary SRFP:

- Single measurement precision: 14.1 ppb (1-sigma)
- Relative accuracy, Seasonal Relative accuracy: 4.8, 5.1 ppb
- Stability:
 - Linear trend: -0.46 ± 0.57 ppb / year
 - Year-to-year stability: 1.64 ± 0.50 ppb

Overall summary SRPR:

- Single measurement precision: 14.0 ppb (1-sigma)
- Relative accuracy, Seasonal Relative accuracy: 3.8, 4.8 ppb
- Stability:
 - Linear trend: -0.60 ± 0.67 ppb / year
 - Year-to-year stability: 1.64 ± 0.61 ppb



ESA Climate Change Initiative (CCI)

**Product Validation and
Intercomparison Report (PVIR)**

for the Essential Climate Variable (ECV)
Greenhouse Gases (GHG)


Page 82

Version 5.0
Final

9 Feb 2017

Summary table:

Estimates of achieved data quality: CRDP#4 CH ₄ _GOS_OCPR, SRFP, SRPR					
Sensor	Algorithm	Random error [ppb]	Systematic error [ppb]	Stability [ppb / year]	Comments
TANSO on GOSAT	OCFP v2.02 (UoL-PR)	14.9	4.7 – 4.8 RA - SRA	Linear trend: 1.54 ± 1.05 Year-to-year: [4.34 +/- 0.88]	Stability: Significance?: Trend: yes Year-to-year: yes (2012 jump)
TANSO on GOSAT	OCPR v7 (UoL-PR)	13.7	4.1 – 4.3 RA - SRA	-0.30 ± 0.53 [1.50+/-0.52]	Stability: Significance?: Trend: no Year-to-year: yes
TANSO on GOSAT	SRFP v2.3.8 (RemoTeC)	14.1	4.8 – 5.1 RA - SRA	-0.46 ± 0.57 [1.64+/-0.50]	Stability: Significance?: Trend: no Year-to-year: yes
TANSO on GOSAT	SRPR v2.3.8 (RemoTeC)	14.0	3.8 – 4.8 RA - SRA	-0.60 ± 0.67 [1.64 +/- 0.61]	Stability: Significance?: Trend: no Year-to-year: yes
All values are 1-sigma (except for trend and range); The uncertainties given correspond with the 95% confidence intervals. Note: "Year-to-year" stability refers to assessment results related to the extended definition of stability as given in URDv2.1, which now also covers "inter-annual error changes"					

	ESA Climate Change Initiative (CCI)	Page 83
	Product Validation and Intercomparison Report (PVIR)	
	for the Essential Climate Variable (ECV) Greenhouse Gases (GHG)	Version 5.0 Final
		9 Feb 2017

3.3.6 EMMA XCH₄


As already mentioned in **Section 3.3.5** the differences between EMMA and the other GOSAT algorithms (apart maybe OCFP which exhibits some stability issues) are very small. It's RA and SRA values are in line with its counterparts as well as Bias, scatter and stability.

Overall summary EMMA:

- Single measurement precision: 13.4 ppb (1-sigma)
- Relative accuracy, Seasonal Relative accuracy: 4.0, 4.4 ppb
- Stability:
 - Linear trend: -0.36 ± 0.71 ppb / year
 - Year-to-year stability: 1.24 ± 0.45 ppb / year

Summary table:

Estimates of achieved data quality: CRDP#4 EMMA					
Sensor	Algorithm	Random error [ppb]	Systematic error [ppb]	Stability [ppb / year]	Comments
TANSO on GOSAT	EMMA v1.2	13.4	4.0 – 4.4 RA - SRA	-0.36 ± 0.71 [1.24 +/- 0.45]	Stability: Significance?: Trend: no Year-to-year: yes
All values are 1-sigma (except for trend and range); The uncertainties given correspond with the 95% confidence intervals. Note: "Year-to-year" stability refers to assessment results related to the extended definition of stability as given in URDv2.1, which now also covers "inter-annual error changes"					

	ESA Climate Change Initiative (CCI)	Page 84
	Product Validation and Intercomparison Report (PVIR)	
	for the Essential Climate Variable (ECV) Greenhouse Gases (GHG)	Version 5.0 Final
		9 Feb 2017

4 Validation of ECA products using NDACC (no update)

This section was present in **/PVIRv2 CRDP#1/** generated for CRDP#1 during GHG-CCI Phase 1.

This section has been kept to avoid changing the section numbering with respect to previous PVIR versions.


This activity has not been continued within GHG-CCI Phase 2 and therefore no updates are reported here.

5 Verification using ground-based in-situ measurements (no update)

This section was present in **/PVIRv2 CRDP#1/** generated for CRDP#1 during GHG-CCI Phase 1.

This section has been kept to avoid changing the section numbering with respect to the previous PVIR.

This activity has not been continued within GHG-CCI Phase 2 and therefore no updates are reported here.

	ESA Climate Change Initiative (CCI)	Page 85
	Product Validation and Intercomparison Report (PVIR)	
	for the Essential Climate Variable (ECV) Greenhouse Gases (GHG)	Version 5.0 Final
		9 Feb 2017

6 Retrieval team assessments of CRDP#4

In this section validation and inter-comparison results as obtained by the data providers (DP) ("retrieval team") are presented and discussed.

In **Section 6.1** the XCO₂ product assessments are presented, in **Section 6.2** the XCH₄ assessment results, and in **Section 6.3** the ACA assessment results.

Consistency aspects are addressed in **Section 6.4** for XCO₂ and in **Section 6.5** for XCH₄.

6.1 Assessment of XCO₂ data products

6.1.1 Assessment of SCIAMACHY BESD (and WFMD) XCO₂

The results shown in this section have been generated by the SCIAMACHY BESD retrieval team. Validation results of BESD v02.01.02, which is part of CRDP#4, and model comparisons are part of this section.

As can be seen in **Figure 6.1.1.1** to **Figure 6.1.1.5**, BESD reproduces large scale features such as the north/south gradient, the annual increase, and the seasonal cycle as expected: i) Due to anthropogenic emissions BESD observes a continues increase of just under 2 ppm per year. ii) As these emissions are primarily on the northern hemisphere, BESD observes a north/south gradient with larger values on the northern hemisphere during end of the northern hemispheric growing season. iii) As expected BESD observes a much larger seasonal cycle on the northern hemisphere as on the southern hemisphere because of the distribution of vegetated land masses.

However, a closer look at **Figure 6.1.1.1** reveals too large values in the first half of 2003. The reason for this behaviour was found in an instrument issue resulting in a slight correlation between instrumental throughput and retrieved XCO₂. The current bias correction scheme cannot account for this because the throughput in this period lies outside the range of trained values. Expanding the training dataset to throughput values as found in 2003 is not possible with the current approach because most TCCON sites started operation after or in 2004. The bias correction scheme of future versions may overcome this issue by the use of model data instead of TCCON data.

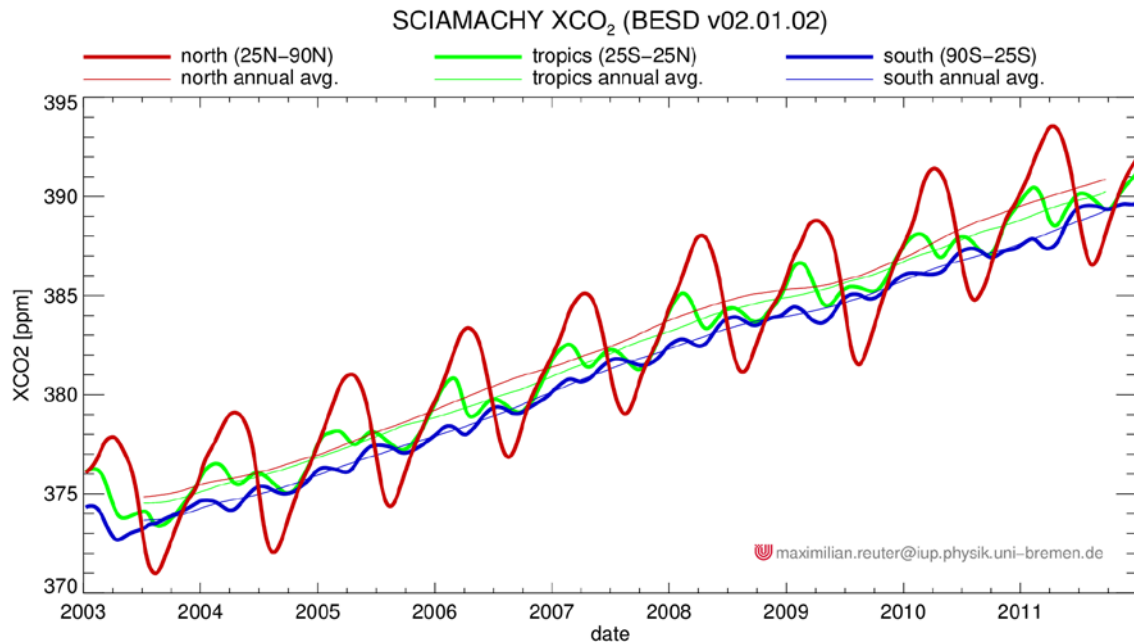


Figure 6.1.1.1: BESD northern hemispheric, southern hemispheric, and tropical seasonal cycle smoothed by convolution with a Hann-function with an effective width of two months as well as corresponding 12 monthly running averages.

Figure 6.1.1.2 to Figure 6.1.1.5 show that the large scale features are also in reasonable agreement with model results (CarbonTracker, MPI BGC Jena, LSCE MACC). However, these figures also show that differences become larger, i.e., a few ppm, when looking at smaller scales but it is interesting to note that the differences BESD vs. model appear to be not larger than the differences between the individual models. As an example, the Asian pattern of the BESD anomaly in April/May/June is very similar to the LSCE model but CarbonTracker and then MPI model simulate considerably lower values here (**Figure 6.1.1.3**). As another example, the July/August/September anomaly shows that there is overall disagreement about the partitioning of the southern hemispheric tropical source in Africa and South America (**Figure 6.1.1.4**).

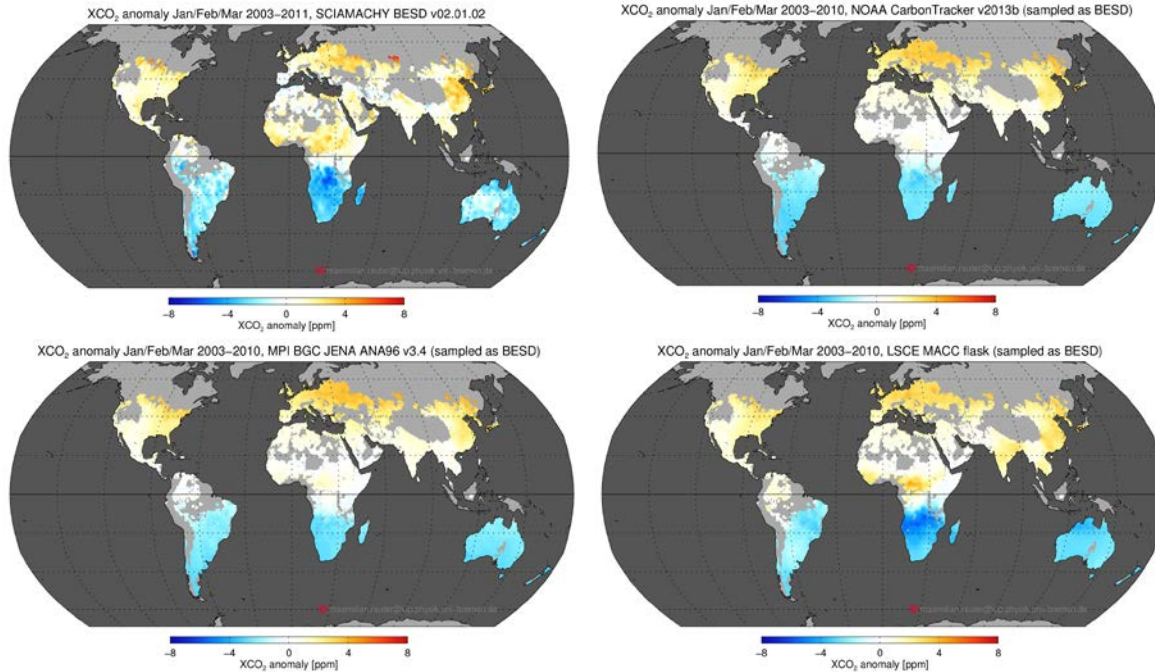


Figure 6.1.1.2: Average seasonal anomaly January/February/March of BESD (top left) and co-located model results (top right CarbonTracker 2013b, bottom left MPI BGC Jena ANA96 v3.4, bottom right LSCE MACC) smoothed by convolution with a Hann-function with an effective width of 2°x2°.

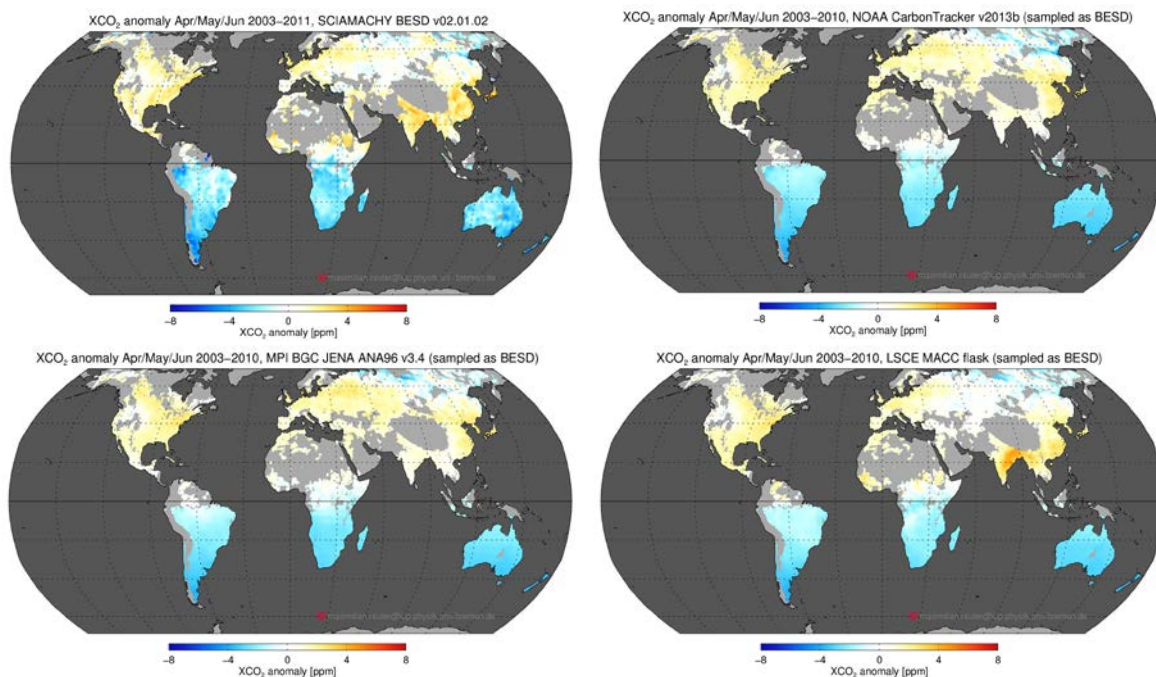


Figure 6.1.1.3: As Figure 6.1.1.2 but for April/May/June.

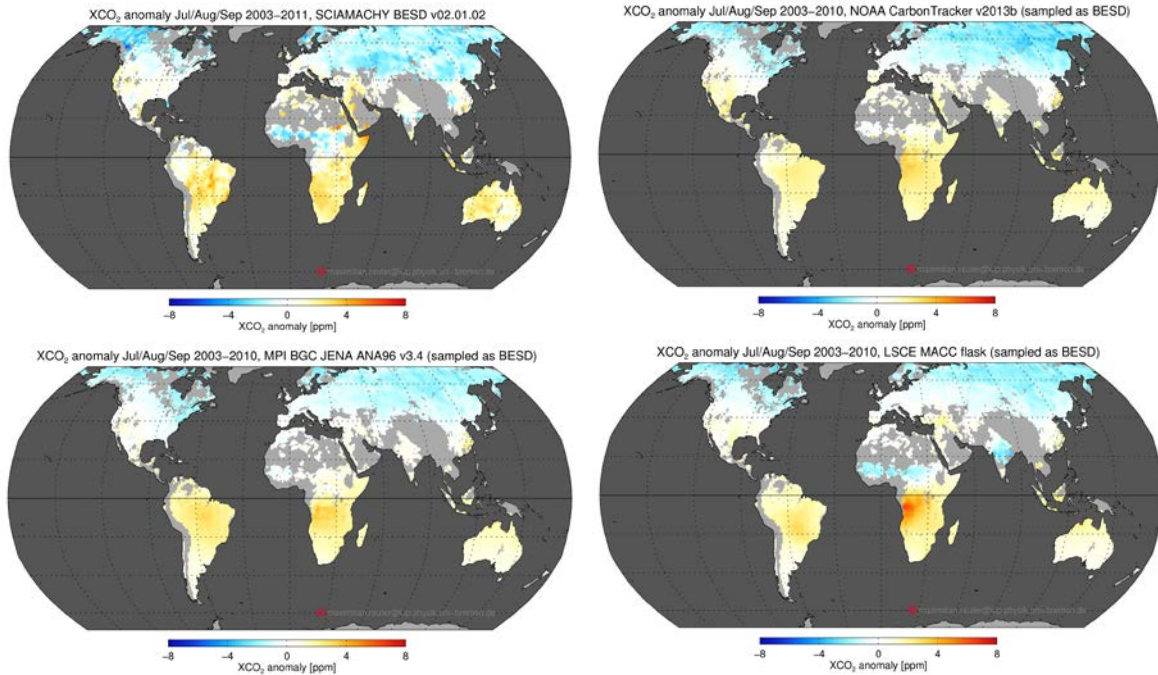


Figure 6.1.1.4: As **Figure 6.1.1.2** but for July/August/September.

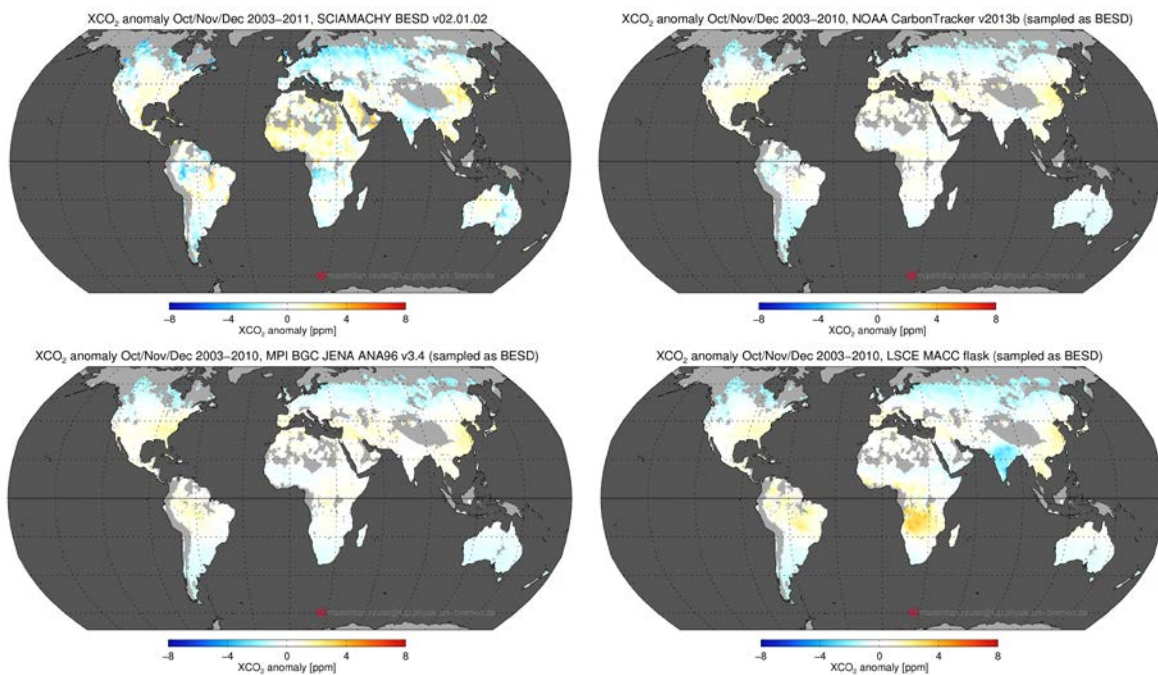



Figure 6.1.1.5: As **Figure 6.1.1.2** but for October/November/December.

	ESA Climate Change Initiative (CCI)	Page 89
	Product Validation and Intercomparison Report (PVIR)	
	for the Essential Climate Variable (ECV) Greenhouse Gases (GHG)	Version 5.0 Final
		9 Feb 2017

BESD has been validated with TCCON (using version GGG2014 R0/1) measurements in a similar way as done by **/Reuter et al. 2011/**. The co-location criteria are defined by a maximal time difference of two hours, a maximal spatial distance of 500km, and a maximal surface elevation difference of 250m. **Figure 6.1.1.6** shows all co-located BESD and TCCON retrievals in the years 2006-2011 for TCCON sites with more than 250 co-locations and covering a time period of at least one year. One can see that BESD captures the year-to-year increase and the seasonal features. For each station, the performance statistics number of co- locations, station bias, seasonal bias, linear drift, and single measurement precision were calculated.


The station bias is defined as average difference to TCCON and the single measurement precision as standard deviation of the difference to TCCON. Seasonal bias and linear drift have been derived by fitting the following trend model:

$$\Delta X = a_0 + a_1 t + a_2 \sin(2\pi t + a_3) + \varepsilon$$

Here, ΔX represents the difference satellite minus TCCON, ε the residual, and a_{0-3} the free fit parameters. Specifically, a_1 represents the linear drift and a_2 the amplitude of the seasonal bias. However, as the seasonal cycles at several TCCON sites can have large data gaps, seasonal biases at each TCCON site are estimated by the standard deviation of $a_2 \sin(2\pi t + a_3)$.

Based on the per station statistics, the following summarizing statistics have been calculated: Total number of co-locations used for validation, (quadratic) average single measurement precision, station-to-station bias (standard deviation of the station biases), average seasonal bias (standard deviation of the seasonal bias term), and average linear drift. As the linear drift can be assumed to be globally constant, the station-to-station standard deviation of the linear drift is a measure for its uncertainty.

Additionally, a measure for the year-to-year stability has been computed: For each TCCON site, the residual difference (satellite - TCCON) which is not explained by station bias, seasonal bias, and/or linear drift has been derived by subtracting the fit of the trend model ΔX from the satellite minus TCCON difference. These time series were smoothed by a running average of 365 days. Only days where more than 10 co-locations contributed to the running average of at least 5 TCCON sites have been further considered. At these days, the station-to-station average has been calculated. The corresponding expected uncertainty has been computed from the standard error of the mean (derived from the station-to-station standard deviation and the number of stations) and by error propagation of the reported single sounding uncertainties. For BESD (**Figure 6.1.1.8**) the average is always between about -0.25ppm and 0.35ppm (WFMD: -0.45 – 0.30, **Figure 6.1.1.9**) with an uncertainty of typically 0.20ppm (WFMD: 0.25ppm). Most of the time, the average is not significantly different from zero (for BESD and WFMD), i.e., its one sigma uncertainty is larger than its absolute value. Due to the relatively large uncertainty, we decided to compute not the

	ESA Climate Change Initiative (CCI)	Page 90
	Product Validation and Intercomparison Report (PVIR)	
	for the Essential Climate Variable (ECV) Greenhouse Gases (GHG)	Version 5.0 Final
		9 Feb 2017

maximum minus minimum as a measure for the year-to-year stability because this quantity can be expected to increase with length of the time series simply due to statistics. Therefore, we estimate the year-to-year stability by randomly selecting pairs of dates with a time difference of at least 365 days. For each selection we computed the difference modified by a random component corresponding to the estimated uncertainty. From 1000 of such pairs we compute the standard deviation as estimate for the year-to-year stability. We repeat this experiment 1000 times and compute the average (BESD: 0.34ppm, WFMD: 0.46ppm) and standard deviation (see **Figure 6.1.1.8** and **Figure 6.1.1.9**).

Per station statistics and overall performance estimates are listed in **Table 6.1.1.1** and **Table 6.1.1.2**.

The purpose of this document is not only product validation but also its inter-comparison. Therefore, validation results for WFMD (derived with the same method) are also listed in the same table and shown in **Figure 6.1.1.6** and **Figure 6.1.1.7**. More inter-comparisons also with GOSAT algorithms can be found in **Sect. 6.1.5**.

Table 6.1.1.1: Validation statistics for all TCCON sites with more than 250 co-locations and covering a time period of at least one year with number of co-locations (#), single measurement precision (σ), station bias (Δ), seasonal bias (s) and linear drift (d). Values in **red** are valid of BESD v02.01.02 and values in **green** for WFMD v4.0. The last row contains the overall statistics. In this row σ represents the (quadratic) average single measurement precision, Δ the station-to-station bias (i.e., the standard deviation of the station biases), s the average seasonal bias, and d the average drift plus minus its standard deviation.

Station	#	σ [ppm]	Δ [ppm]	s [ppm]	d [ppm/a]
Bialystok	1662 / 3732	1.95 / 3.05	-0.20 / -0.40	0.83 / 0.68	0.17 / 0.19
Bremen	999 / 1537	1.75 / 2.87	0.02 / 0.09	0.09 / 0.29	-0.12 / -0.01
Darwin	6630 / 8562	1.79 / 1.90	-0.63 / -1.10	0.24 / 0.54	-0.09 / -0.11
Garmisch	392 / 1162	2.16 / 3.47	-0.19 / -0.16	0.14 / 0.32	0.13 / 0.38
Karlsruhe	1287 / 1644	2.21 / 3.01	0.43 / 1.38	0.86 / 0.47	0.78 / 0.54
Lamont	9662 / 19520	1.73 / 2.41	-0.34 / -0.81	0.47 / 0.59	-0.11 / 0.02
Orleans	1242 / 1484	1.84 / 2.38	-0.01 / 0.89	0.40 / 0.30	0.38 / 0.24
Park Falls	3462 / 13525	1.95 / 3.12	0.13 / -0.10	0.19 / 0.61	-0.01 / 0.07
Sodankylä	254 / 854	1.87 / 3.55	0.70 / 0.47	0.22 / 1.31	0.21 / 0.22
Wollongong	1354 / 1540	1.80 / 2.32	0.08 / -0.27	0.61 / 0.86	-0.04 / -0.09
total	26944	1.91	0.38	0.40	0.13±0.28
	53560	2.85	0.75	0.60	0.14±0.21

In total, ~27000 co-located BESD measurements have been used for the validation exercise (WFMD: ~54000). The overall single measurement precision is 1.91 ppm (WFMD: 2.85 ppm) and station-to-station biases amount to 0.38 ppm (WFMD: 0.75 ppm).

In the context of station-to-station biases, it shall be noted that **Wunch et al., 2010, 2011/** specifies the accuracy (1σ) of TCCON to be about 0.4 ppm. This means it cannot be expected to find regional biases considerably less than 0.4 ppm using TCCON as reference.

Seasonal cycle biases amount to 0.40 ppm on average (WFMD: 0.60 ppm) and no significant drift can be found for BESD (0.13±0.28 ppm/a) or WFMD (0.14±0.21 ppm/a).



ESA Climate Change Initiative (CCI)

Product Validation and Intercomparison Report (PVIR)

for the Essential Climate Variable (ECV)
Greenhouse Gases (GHG)

Page 92

Version 5.0
Final

9 Feb 2017

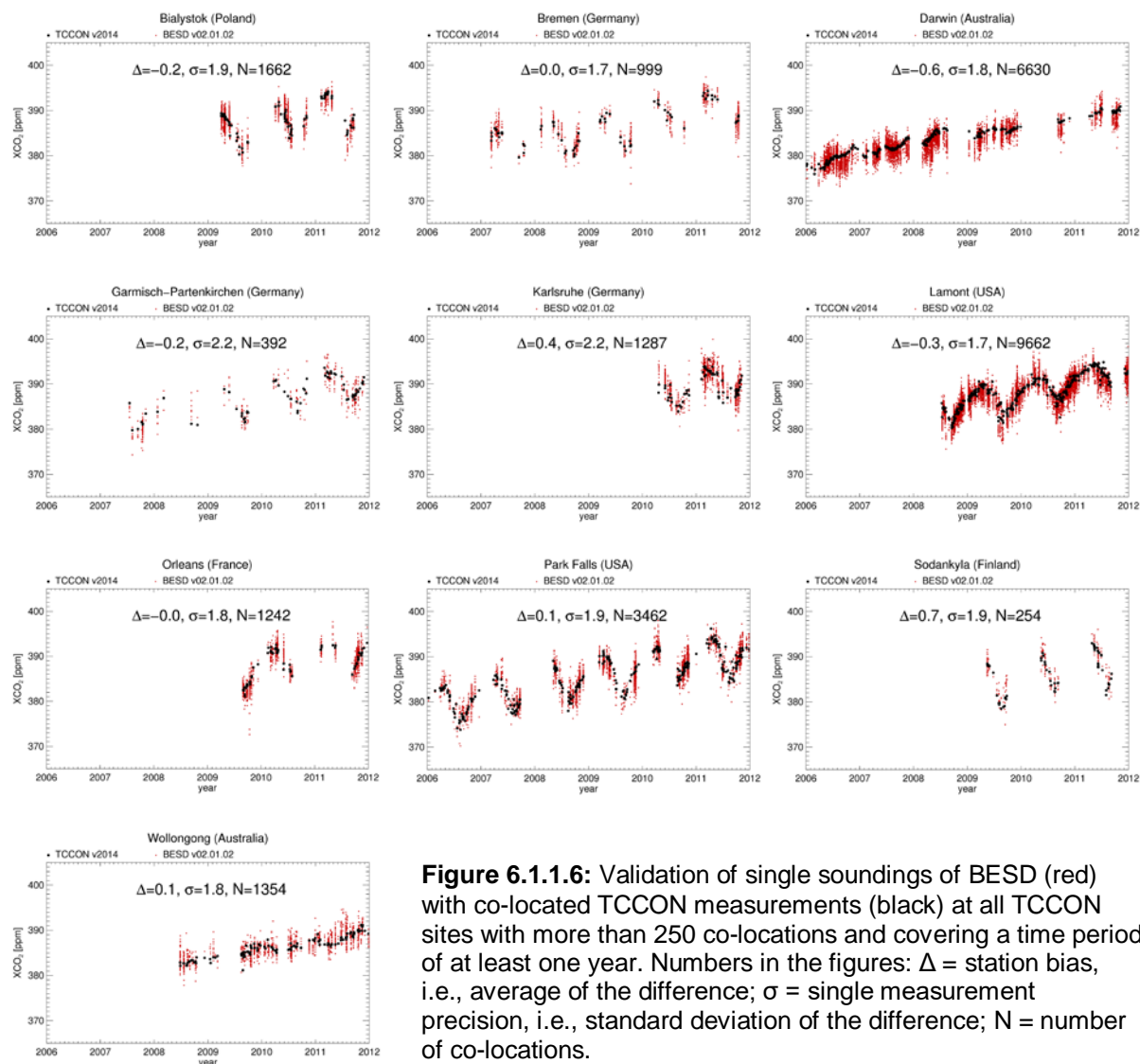


Figure 6.1.1.6: Validation of single soundings of BESD (red) with co-located TCCON measurements (black) at all TCCON sites with more than 250 co-locations and covering a time period of at least one year. Numbers in the figures: Δ = station bias, i.e., average of the difference; σ = single measurement precision, i.e., standard deviation of the difference; N = number of co-locations.



ESA Climate Change Initiative (CCI)

Product Validation and Intercomparison Report (PVIR)

for the Essential Climate Variable (ECV)
Greenhouse Gases (GHG)

Page 93

Version 5.0
Final

9 Feb 2017

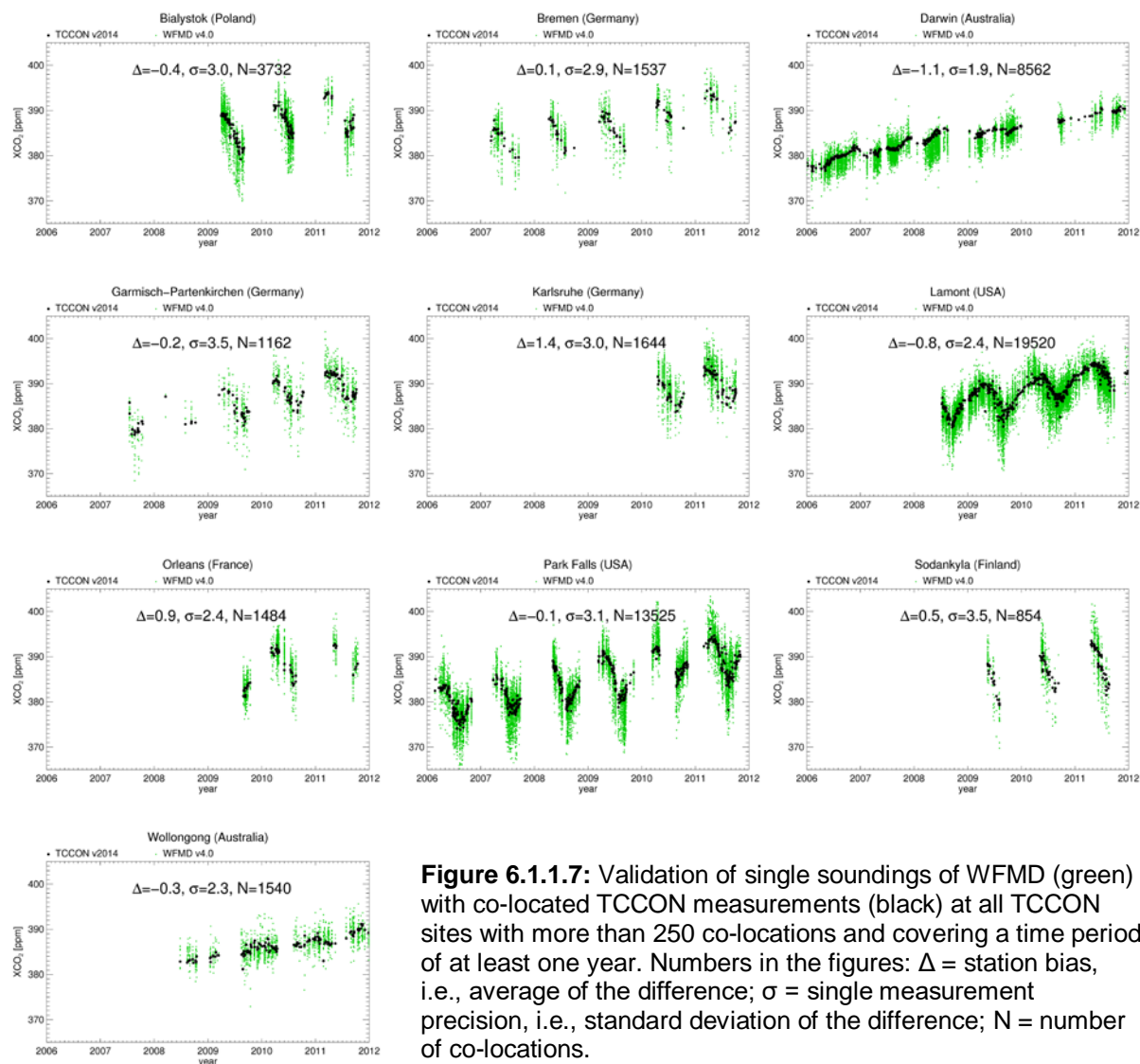


Figure 6.1.1.7: Validation of single soundings of WFMD (green) with co-located TCCON measurements (black) at all TCCON sites with more than 250 co-locations and covering a time period of at least one year. Numbers in the figures: Δ = station bias, i.e., average of the difference; σ = single measurement precision, i.e., standard deviation of the difference; N = number of co-locations.

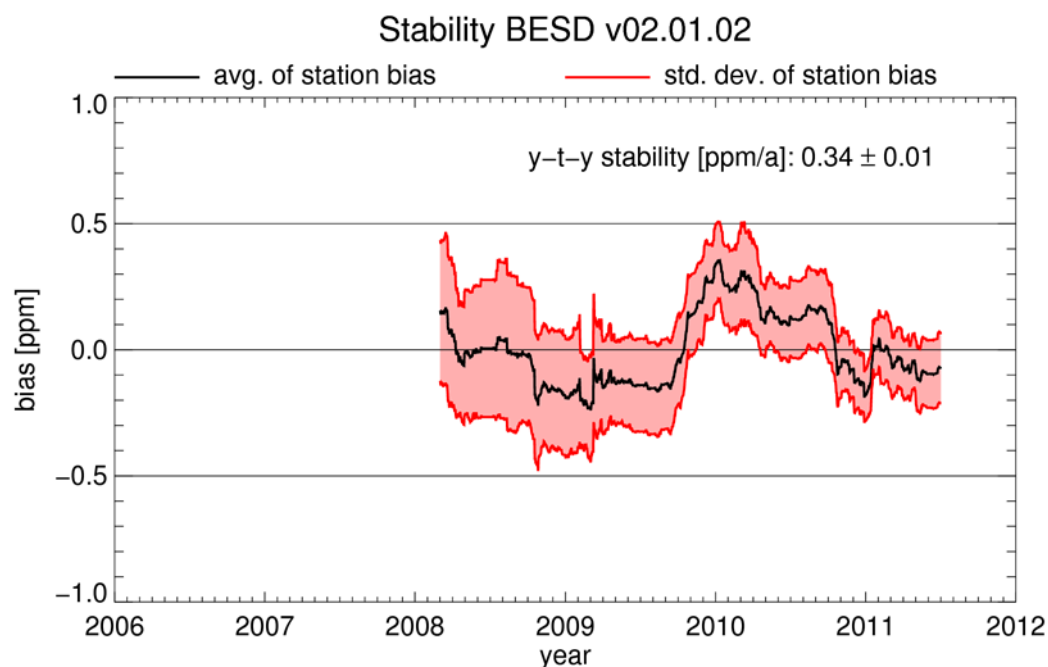


Figure 6.1.1.8: Stability analyses for BESD. The black curve shows the average station bias and the red curves its uncertainty represented by the station-to-station standard deviation and error propagation from single sounding measurement noise.

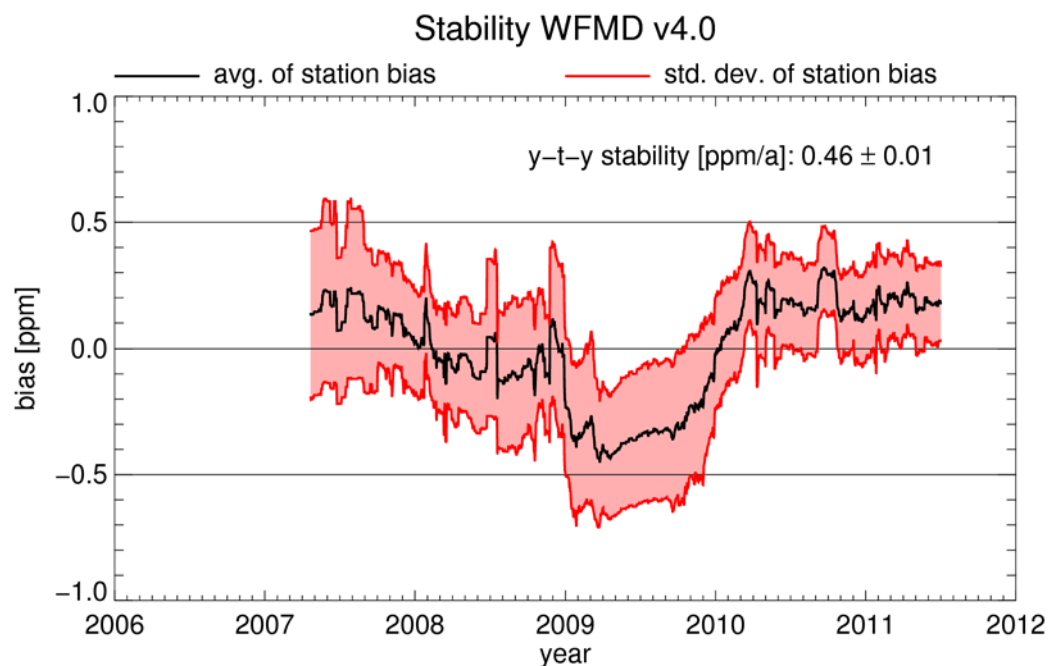


Figure 6.1.1.9: Same as **Figure 6.1.1.8** but for WFMD.


	ESA Climate Change Initiative (CCI)	Page 95
	Product Validation and Intercomparison Report (PVIR)	
	for the Essential Climate Variable (ECV) Greenhouse Gases (GHG)	Version 5.0 Final
		9 Feb 2017

Table 6.1.1.2: Summary table SCIAMACHY XCO₂ BESD v02.01.02 and WFMD v4.0.

Estimates of achieved data quality: CRDP#4 CO2_SCI_BESD and WFMD					
Sensor	Algorithm	Random error [ppm]	Systematic error [ppm]	Stability [ppm / year]	Comments
SCIAMACHY on ENVISAT	BESD v02.01.02	1.91	0.38 RA 0.40 SA	Linear trend: 0.13±0.28 Year-to-year: 0.34	2006-2011 10 TCCON sites Stability: Significance?: Unclear
SCIAMACHY on ENVISAT	WFMD V4.0	2.85	0.75 RA 0.60 SA	Linear trend: 0.14±0.21 Year-to-year: 0.46	2006-2011 10 TCCON sites Stability: Significance?: Unclear
All values are 1-sigma (except for stability); Note: "Year-to-year" stability refers to assessment results related to the extended definition of stability as given in URDv2.1, which now also covers "inter-annual error changes".					

6.1.2 Assessment of SCIAMACHY WFMD XCO₂

Validation and intercomparison results for WFMDv4.0, which is part of the CRDP#4 are summarised in this section.

The carbon dioxide mole fractions as a function of latitude and time are shown in **Figure 6.1.2.1** demonstrating the pronounced seasonal cycle in the northern hemisphere due to the temporally varying imbalance between photosynthesis and respiration of vegetation and the global steady increase of atmospheric carbon dioxide primarily caused by the burning of fossil fuels.

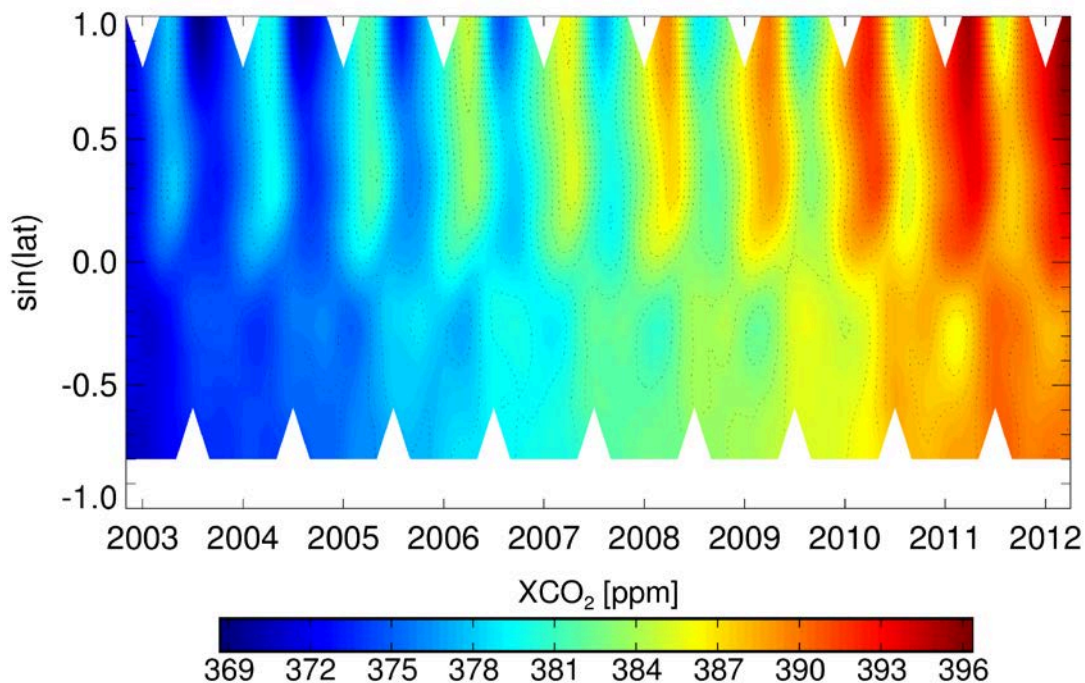


Figure 6.1.2.1: Overview of the WFMDv4.0 carbon dioxide data set; shown are column-averaged dry air mole fractions as a function of latitude and time.

A comparison of the spatial XCO₂ distribution of SCIAMACHY and the assimilation system CarbonTracker (CT2013B) /Peters et al., 2007/ is shown in **Figure 6.1.2.2**. Also shown are the locations of the seven observational sites used in the soft calibration based on multivariate linear regression to minimise correlations of the difference of the WFMD retrievals to CarbonTracker with state vector elements and instrument parameters /Schneising et al., 2014a/. The chosen sites meet the following requirements: 1) the mismatch of modelled CarbonTracker values and assimilated data is small; 2) they span a wide range of retrieval conditions (e.g. low and high albedo or atmospheric water vapour). By construction, this post-processing calibration is completely independent of TCCON data

and is not performed at TCCON sites directly. This prevents overfitting and unrepresentative improvements of the validation results, which can occur when the same data sets are used in calibration and validation. Hence, the used approach with independent data sets increases the diagnostic value of the validation results.

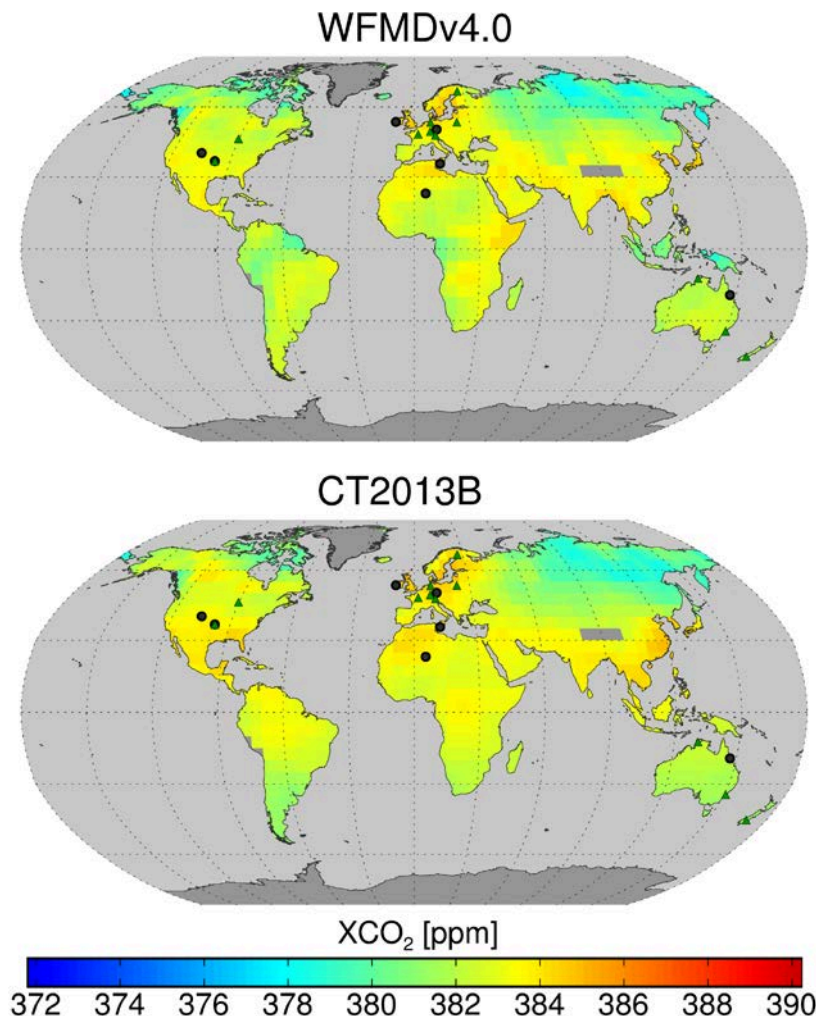


Figure 6.1.2.2: Spatial distribution of SCIAMACHY and CarbonTracker XCO₂ for the year 2007. CarbonTracker has been sampled at the time and location of the SCIAMACHY measurements. The grey circles illustrate the seven observational sites used to derive the linear regression parameters in the soft calibration. The green triangles represent the TCCON sites used in the validation.

From the validation with the 2014 release of ground-based Fourier Transform Spectroscopy (FTS) measurements of the Total Carbon Column Observing Network (TCCON) /Wunch et al., 2011/ (see **Figure 6.1.2.3**) and comparison with the assimilation system CarbonTracker (CT2015) /Peters et al., 2007/ (see **Figure 6.1.2.4**) at 11 TCCON sites, namely Sodankylä



ESA Climate Change Initiative (CCI)

Product Validation and Intercomparison Report (PVIR)

for the Essential Climate Variable (ECV)
Greenhouse Gases (GHG)

Page 98

Version 5.0
Final

9 Feb 2017

(Finland), Bialystok (Poland), Bremen (Germany), Karlsruhe (Germany), Orleans (France), Garmisch (Germany), Park Falls (USA), Lamont (USA), Darwin (Australia), Wollongong (Australia), and Lauder (New Zealand), realistic error estimates of the satellite data are provided and summarised in **Table 6.1.2.1**. For Karlsruhe R0 TCCON data are used to have a consistent validation data set obtained with the same algorithm for all sites. The relevant parameters for quality assessment are the global offset which is defined as the mean of the local offsets d at the individual sites, the random error relative to the reference which is the standard deviation of the differences using all data combined after subtraction of the respective regional biases, and the spatial systematic error which is the standard deviation of the local offsets d relative to TCCON or CarbonTracker at the individual sites. Also given is the seasonal systematic error which is the standard deviation of the 4 overall seasonal offsets (using all sites combined after subtraction of the respective local offsets d). The temporal long-term drift stability is determined by a linear fit of the differences relative to the reference (using all data combined after subtraction of the respective regional biases) with time.

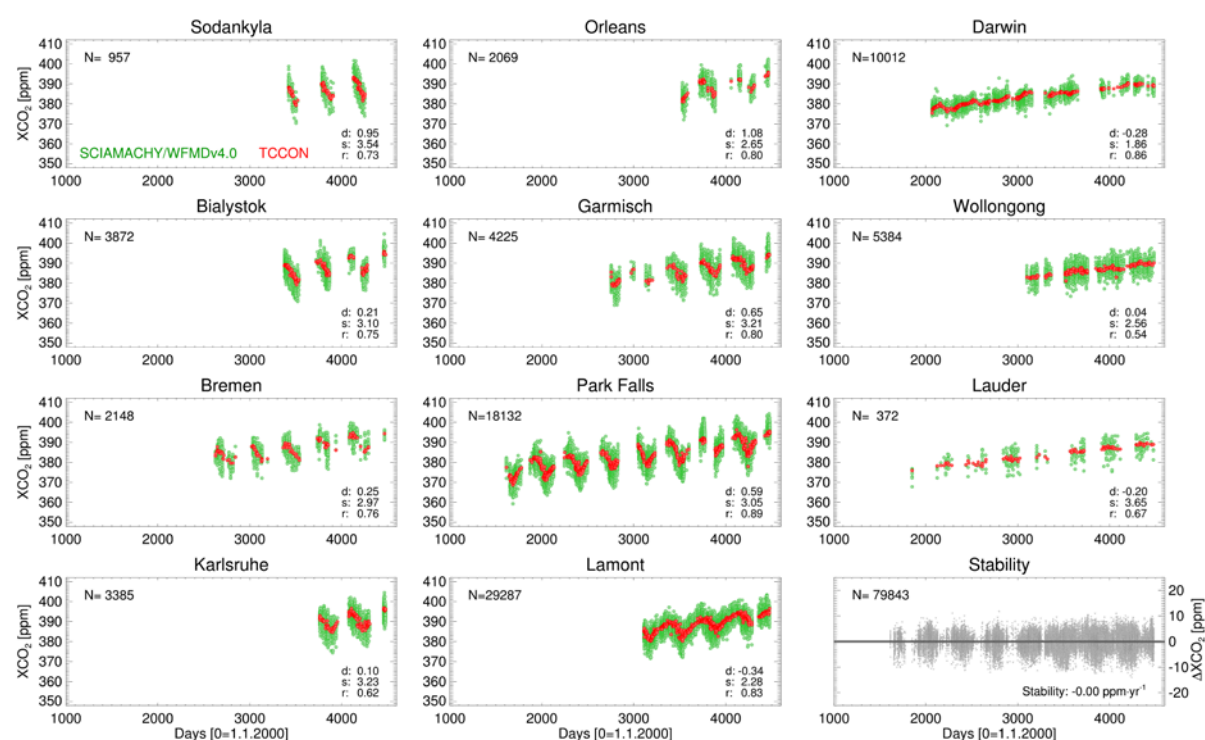


Figure 6.1.2.3: Validation of the WFMDv4.0 carbon dioxide data set with TCCON.



ESA Climate Change Initiative (CCI)

**Product Validation and
Intercomparison Report (PVIR)**

for the Essential Climate Variable (ECV)
Greenhouse Gases (GHG)

Page 99

Version 5.0
Final

9 Feb 2017

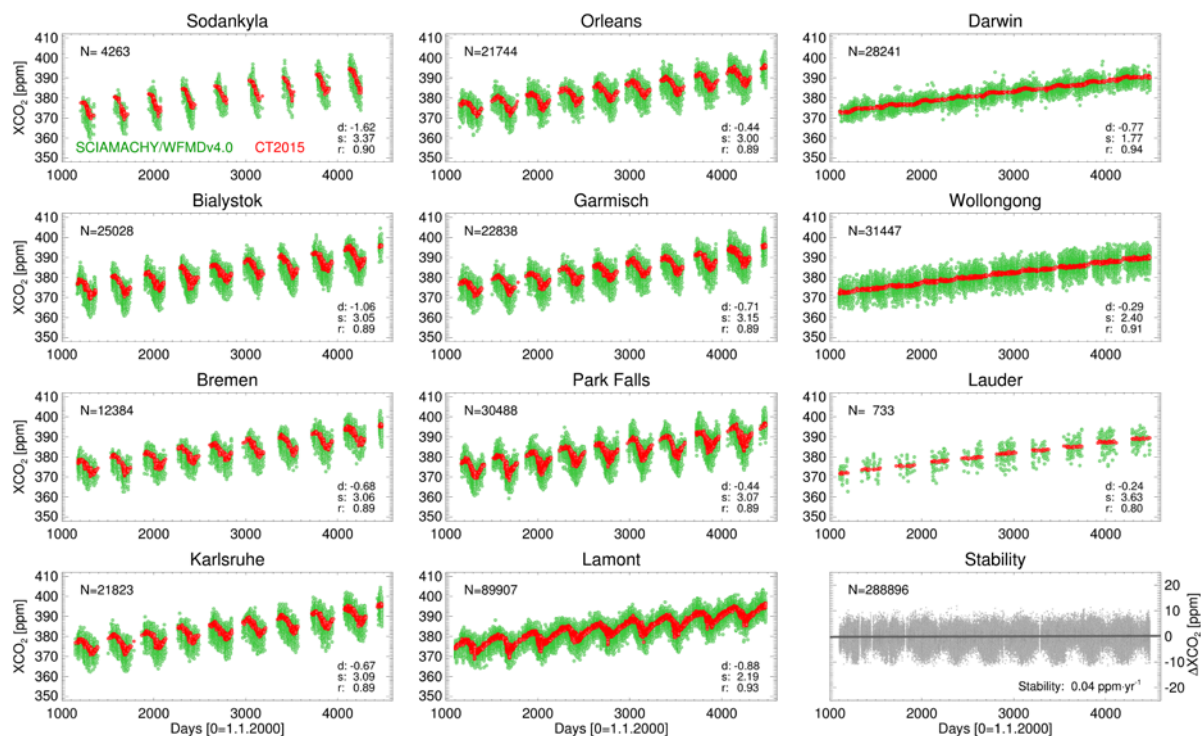


Figure 6.1.2.4: Comparison of the WFMDv4.0 carbon dioxide data set with CarbonTracker at TCCON sites.

The year-to-year stability is assessed in the following way: The one-year moving average of the differences relative to the reference (using all data combined and subtracting respective regional biases and the global long-term drift) is generated. For a given point in time t , let $\sigma_{yr}(t)$ be defined as the standard deviation of this deseasonalised difference within a one-year window around t . This results in two curves (referring to TCCON and CarbonTracker, see **Figure 6.1.2.5**) as a function of time, considering only those time periods where data of at least four sites are available. The deviations of these two curves are interpreted as the uncertainty of the corresponding mean curve (shaded gray area around black curve in **Figure 6.1.2.5**) and the year-to-year stability is then defined as the maximum of σ_{yr} over time. The proposed approach allows to detect potential jumps in the time series.

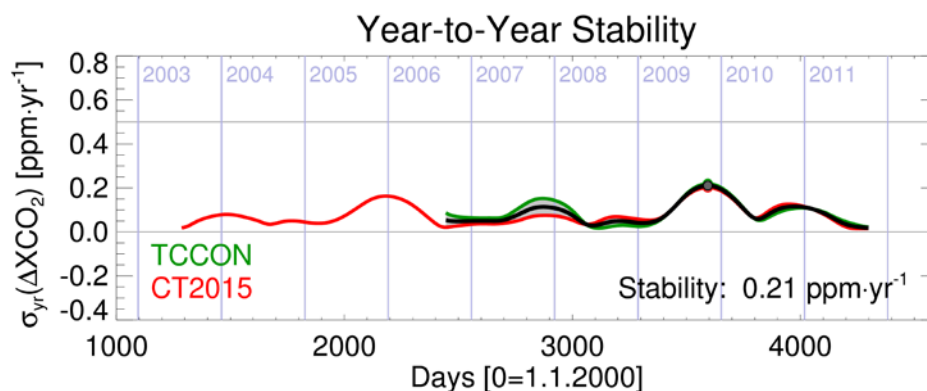


Figure 6.1.2.5: Year-to-year stability of the WFMDv4.0 carbon dioxide data set relative to TCCON and CarbonTracker at TCCON sites.

	SCIA - TCCON	SCIA - CT
Global Offset [ppm]	0.3	-0.7
Random error [ppm]	2.64	2.65
Spatial Systematic error [ppm]	0.48	0.39
Seasonal Systematic error [ppm]	0.04	0.13
Long-term Drift Stability [ppm/yr]	0.00	0.04
Year-to-Year Stability [ppm/yr]	0.21	

Table 6.1.2.1: Validation and comparison results for WFMDv4.0 XCO₂ based on single measurements between January 2003 and April 2012.

Please note, that the random error defined above includes systematic components and is therefore an upper bound of the actual single measurement precision characterising the repeatability of the measurements. The single ground pixel retrieval precision derived from averaging daily standard deviations of the retrieved XCO₂ for several locations distributed around the globe provides an estimate of the single measurement precision of about 2.2 ppm.

The long-term drift stability of the data set is also reflected in the very good agreement of the SCIAMACHY and CarbonTracker growth rates for hemispheric means (see **Figure 6.1.2.6**), which differ by less than 0.04 ppm/yr in the multiyear mean.

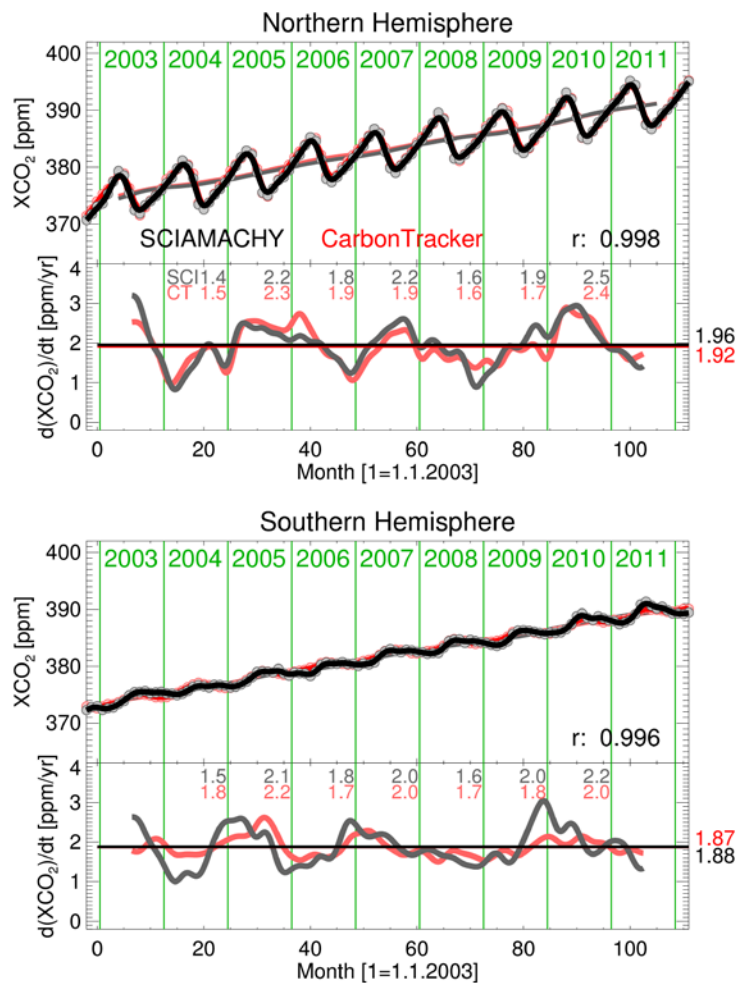



Figure 6.1.2.6: Comparison of hemispheric means of the SCIAMACHY (black) and CarbonTracker (red) XCO₂ based on monthly data (coloured circles). The saturated solid lines have been smoothed using a four-month Hann window (which has a similar frequency response to a two-month boxcar filter). The pale solid lines represent the corresponding deseasonalised trends. Shown below are the derivatives of these deseasonalised curves.

	ESA Climate Change Initiative (CCI)	Page 102
	Product Validation and Intercomparison Report (PVIR)	
	for the Essential Climate Variable (ECV) Greenhouse Gases (GHG)	Version 5.0 Final
		9 Feb 2017

Summary for assessment of SCIAMACHY WFMD XCO₂ product

Summary table:

Estimates of achieved data quality: CRDP#4 CO ₂ _SCI_WFMD					
Sensor	Algorithm	Random error [ppm]	Systematic error [ppm]	Stability [ppm / year]	Comments
SCIAMACHY on ENVISAT	WFMD V4.0	2.64	Spatial: 0.39-0.48 Seasonal: 0.04-0.13 Spatial+Seasonal: 0.52	Linear trend: [0.00, 0.04] Year-to-year: 0.21	Stability: Significance?: Unclear
All values are 1-sigma (except for stability); Note: "Year-to-year" stability refers to assessment results related to the extended definition of stability as given in URDv2.1, which now also covers "inter-annual error changes"					



6.1.3 Assessment of GOSAT OCFP XCO₂

Validation and inter-comparison of results for OCFPv7.0, submitted as University of Leicester's contribution to CRDP4, are summarised in this section. This includes presentation of seasonal mean maps and comparisons with Total Column Carbon Observing Network (TCCON) and MACC model. All OCFPv7.0 data shown make use of the filtered XCO₂ product.

Spatial distributions of OCFPv7.0 XCO₂ seasonal means are presented in **Fig. 6.1.3.1**, along with differences to MACC 14r1 model data (only available until 2014) in **Fig. 6.1.3.2**. Spatial distribution and magnitudes of OCFPv7.0 are in line with expected values for each season, as shown by comparison to MACC data, where major deviations (± 3.0 ppm) from model data do not occur over any great portion of the globe. More significant differences are observed over Central- Eastern Asia which might be related to the occurrence of high aerosol loadings. Also, summer 2014 shows unusually large regional differences.

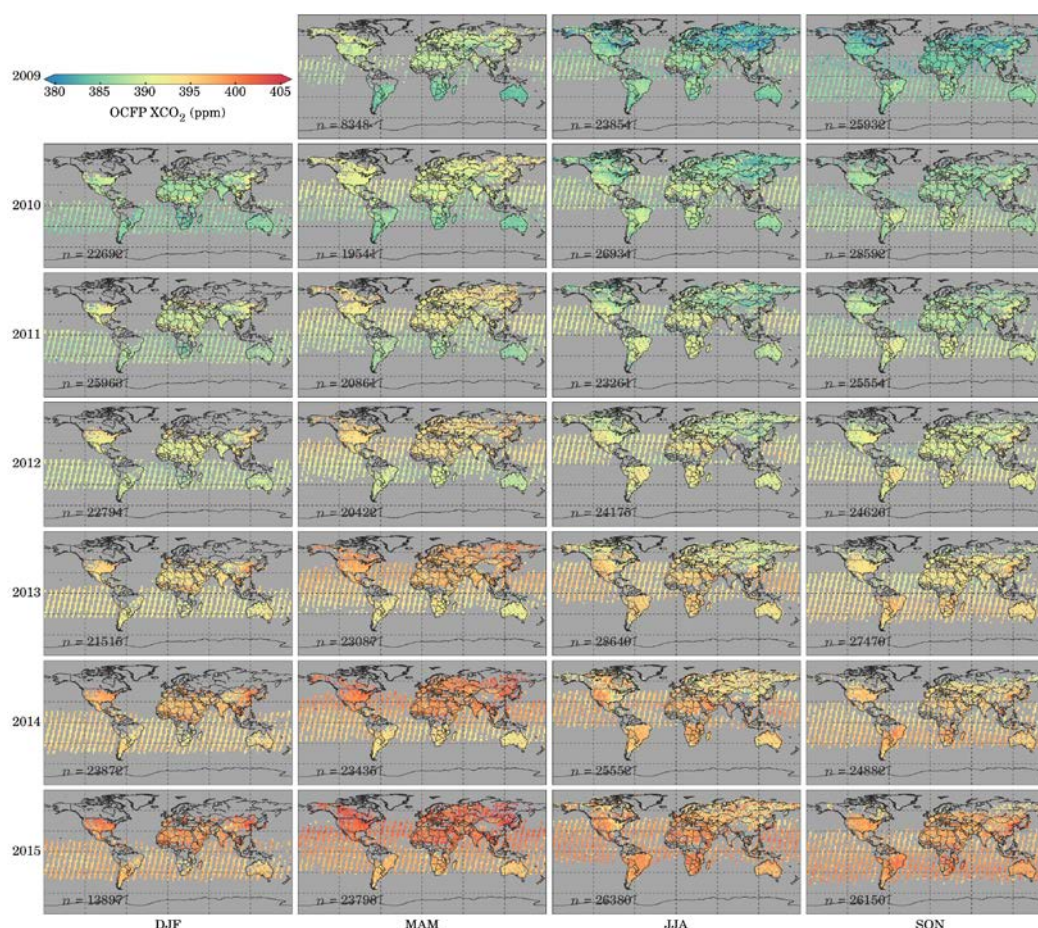


Figure 6.1.3.1. Seasonal means of filtered OCFPv7.0 XCO₂ for 2009–2015.



ESA Climate Change Initiative (CCI)

**Product Validation and
Intercomparison Report (PVIR)**

for the Essential Climate Variable (ECV)
Greenhouse Gases (GHG)

Page 104

Version 5.0
Final

9 Feb 2017

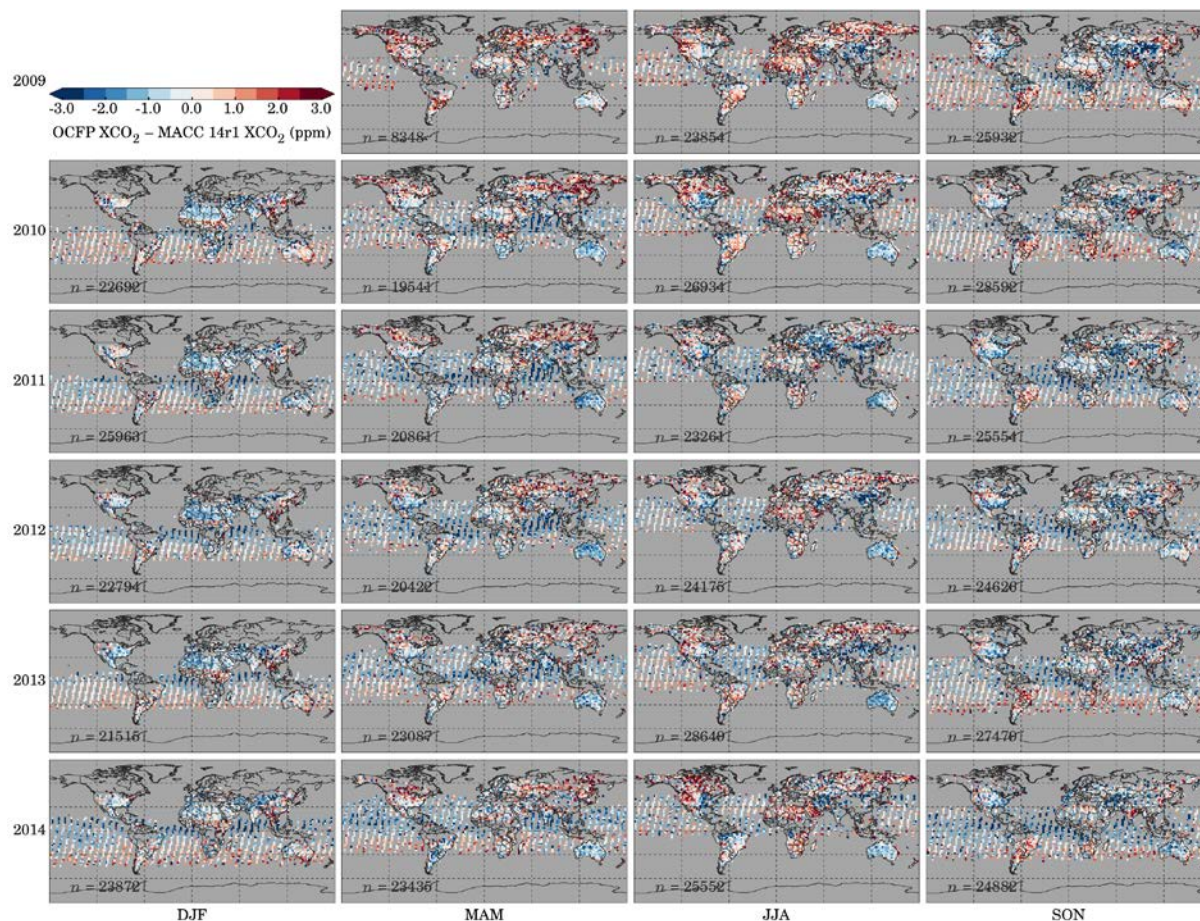


Figure 6.1.3.2. Seasonal means of differences between OCFPv7.0 (as above) and MACC 14r1 XCO₂

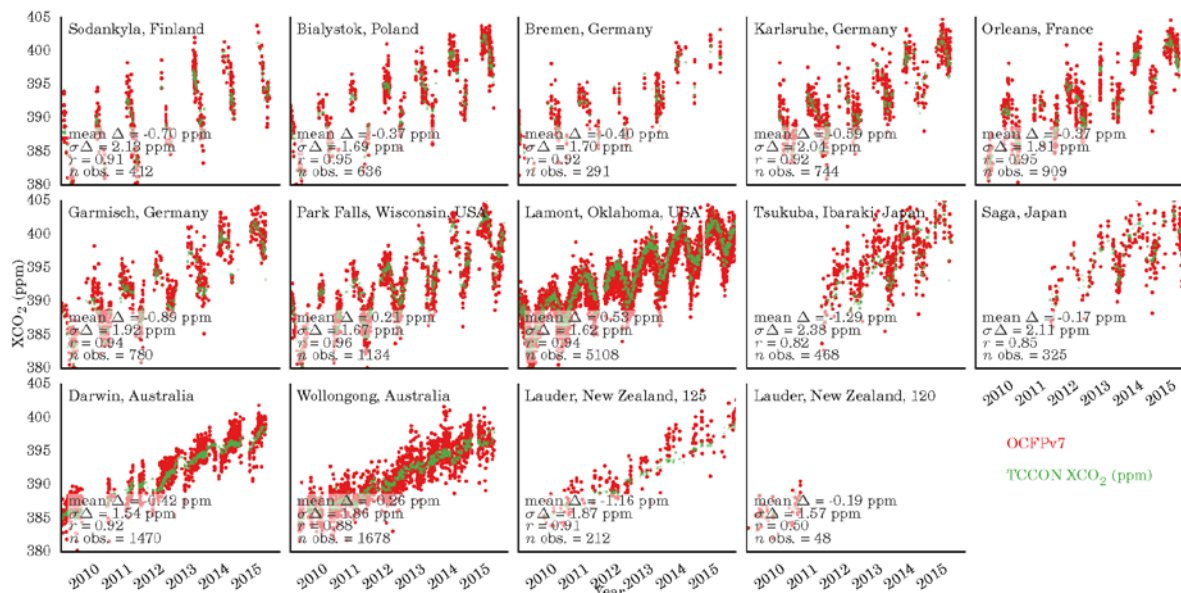


Figure 6.1.3.3 demonstrates validation of OCFPv7.0 with TCCON observations of XCO_2 , encompassing Fourier transform spectroscopy measurements made at 14 TCCON sites available within the GGG2014 dataset. Bias (calculated as $\text{TCCON} - \text{OCFPv7.0}$), correlation, and standard deviation of the bias are annotated on each sub-plot per site, and repeated in **Tab. 6.1.3.1**. Measurement parameters relating to OCFPv7.0 stability are presented in **Tab. 6.1.3.2**. **Figure 6.1.3.4** details OCFPv7.0 observations and MACC 14r1 modelled XCO_2 interpolated to time and location of OCFP measurements, subset to Transcom regions. For TCCON and MACC comparisons, OCFPv7.0 is seen to capture the seasonal cycle well, albeit with a slight low bias for OCFPv7.0 against MACC data in equatorial and tropical regions of the globe.



ESA Climate Change Initiative (CCI)

**Product Validation and
Intercomparison Report (PVIR)**

for the Essential Climate Variable (ECV)
Greenhouse Gases (GHG)

Page 106

Version 5.0
Final

9 Feb 2017

Site	Mean Δ	$\sigma\Delta$	r	n obs.
Sodankyla, Finland	-0.704	2.132	0.91	412
Bialystok, Poland	-0.367	1.694	0.95	636
Bremen, Germany	-0.400	1.695	0.92	291
Karlsruhe, Germany	-0.589	2.041	0.92	744
Orleans, France	-0.372	1.809	0.95	909
Garmisch, Germany	-0.889	1.923	0.94	780
Park Falls, Wisconsin, USA	0.211	1.666	0.96	1134
Lamont, Oklahoma, USA	0.529	1.625	0.94	5108
Tsukuba, Ibaraki, Japan, 125HR	-1.289	2.381	0.82	468
Saga, Japan	-0.165	2.106	0.85	325
Darwin, Australia	-0.425	1.544	0.92	1470
Wollongong, Australia	-0.260	1.863	0.88	1678
Lauder, New Zealand, 125HR	-1.161	1.868	0.91	212
Lauder, New Zealand, 120HR	-0.195	1.571	0.50	48

Table 6.1.3.1. Site statistics for OCFP comparisons against TCCON, with mean Δ and $\sigma\Delta$ in ppb.



ESA Climate Change Initiative (CCI)

Product Validation and Intercomparison Report (PVIR)

for the Essential Climate Variable (ECV)
Greenhouse Gases (GHG)

Page 107

Version 5.0
Final

9 Feb 2017

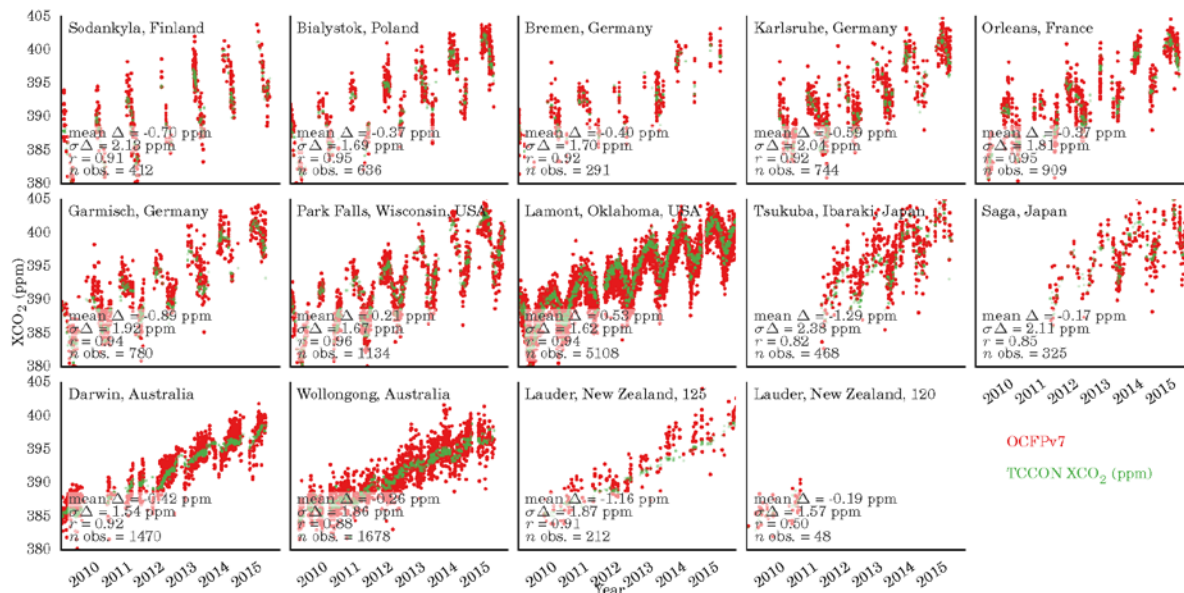


Figure 6.1.3.3. TCCON GGG2014 (green) and OCFPv7.0 (red) XCO₂ observations; OCFP observations are co-located with TCCON sites using a <550km spatial and ±2 hour temporal criteria.

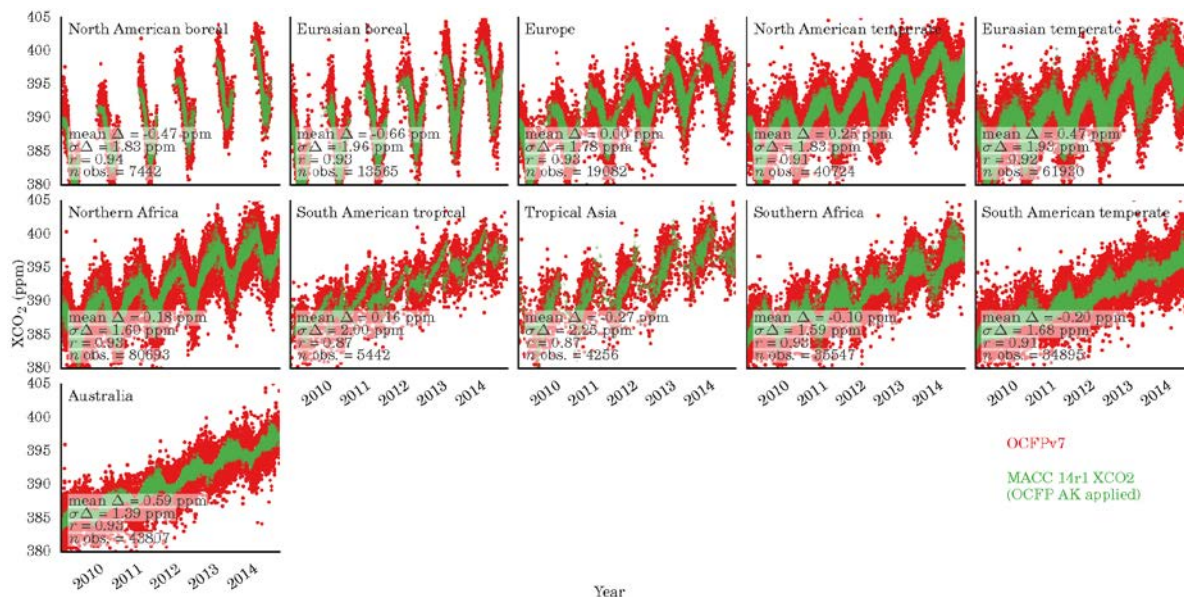


Figure 6.1.3.4. Subset to Transcom basis map regions, OCFPv7.0 (red) and MACC 14r1 XCO₂ (green) interpolated to OCFP time and location (with OCFP averaging kernel applied).

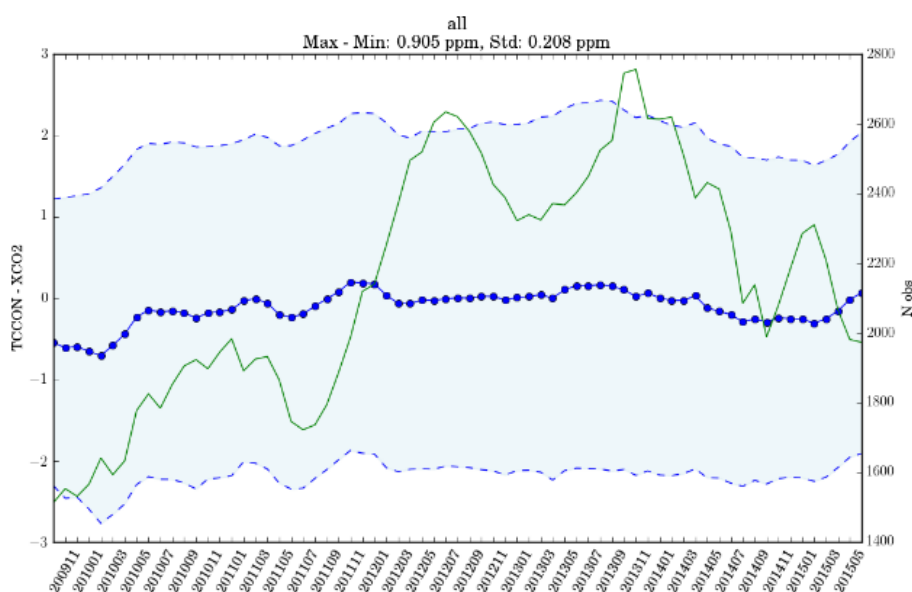



Figure 6.1.3.5: Year-to-year Stability of the TCCON-OCFPv7.0 XCO₂ bias calculated with for +/-6 month averaging window for each month of the GOSAT time series between June 2010 and June 2015. The thick blue symbols give the mean bias for a 12 month period and the shaded area indicates the standard deviation of the data. The green lines gives the number of data points per 12 month period.

We have inferred the year-to-year variability of the stability as the maximum-minimum difference between the bias between GOSAT and TCCON for any 12 month period calculated for each month between June 2010 and June 2015. The mean bias for a 12 month period is inferred from all GOSAT-TCCON pairs for all TCCON stations after subtracting the mean bias for the data for each station. Note that the variable number of data points and the variable temporal coverage will have an impact on the inferred max-min value.

Global offset	Single meas. precision	Relative accuracy	Product stability
-0.08	1.85	0.47	Linear trend: 0.11 Max-Min (between any 12 month period): 0.905

Table 6.1.3.2. Summary statistics (all units in ppm) for the nearly 7 year OCFPv7.0 XCO₂ dataset as validated with TCCON GGG2014 XCO₂; mean of per-site TCCON mean bias (global offset), standard deviation of all co-located OCFPv7.0-TCCON differences (single measurement precision), standard deviation of per-site OCFPv7.0-TCCON biases (relative accuracy), linear fitting of all OCFPv7.0-TCCON biases and max-min of the OCFPv7.0-TCCON biases for a 12month period (product stability).

	ESA Climate Change Initiative (CCI)	Page 109
	Product Validation and Intercomparison Report (PVIR)	
	for the Essential Climate Variable (ECV) Greenhouse Gases (GHG)	Version 5.0 Final
		9 Feb 2017

6.1.4 Assessment of GOSAT SRFP (RemoTeC) XCO₂

The GOSAT SRFP (RemoTeC) XCO₂ data were obtained using the L1B data of v201 and later as input for the Full Physics retrieval using RemoTeC v2.3.8. Posterior filters as described in the Product User Guide were applied to produce quality flags for the gain H, gain M and sunglint data. These data were then compared to the TCCON XCO₂ measurements based on the following co-location criteria:

- modelled XCO₂ (Basu et al., 2013) for GOSAT sounding < 0.25 ppm different than model XCO₂ at TCCON site, as described in Guerlet et al. (2013a).
- GOSAT sounding within ± 2 hrs of TCCON measurement.

Figure 6.1.4.1 - Figure 6.1.4.5 show the time series comparison between the SRFP/RemoTeC product and TCCON for gain-H, gain-M and sunglint data. **Table 6.1.4.1 – 6.1.4.3** show an overview of the validation.

For the bias correction, we investigated the correlation of the GOSAT-TCCON differences with different geophysical and retrieval parameters. After extensive testing, we found that the best bias correction is obtained by applying a correction with the aerosol filter parameter and solar zenith angle for gain H, aerosol filter parameter for gain M and derived O₂ ratio for sunglint measurements. In all three cases a linear correlation was used.

Gain H: $XCO_2_biascorr / XCO_2 = 0.999995 + 2.8204e-5 \cdot (\text{aerosol filter parameter}) + 7.287e-5 \cdot (\text{solar zenith angle})$

Gain M: $XCO_2_biascorr / XCO_2 = 1.004228 - 3.00868e-6 \cdot (\text{aerosol filter parameter})$

Sunglint: $XCO_2_biascorr / XCO_2 = 1.283633 - 0.28368 \cdot RO_2$

One important note for the sunglint and gain M data is that the total number of data points used to derive the bias correction is limited. For gain M we have added the Izana TCCON station to include a wider variety of gain M scenes. This addition resulted in more accurate gain M retrievals over the Sahara and Middle East scenes and resulted in a more accurate gain M bias correction in general.

The previous product (v2.3.7) also suffered from an incorrect Instrument Line Shape (ILS) after the Solar Paddle array failure in May 2014. This has been corrected in the new version v2.3.8 (see System Verification Report CRDP#4 SRFP XCO₂).

A more detailed assessment of the SRFP XCO₂ v2.3.8 product can be found in the CECR CRDP#4 SRFP XCO₂ document.

The average offset w.r.t TCCON before bias correction is around - 2 ppm.




TCCON site	Number of co-locations [-]	Mean difference [ppm]	Standard deviation of difference [ppm]
Bialystok, Poland	1419	-0.13	2.08
Bremen, Germany	535	0.16	1.89
Darwin, Australia	4831	0.07	1.58
Garmisch, Germany	723	0.33	2.22
Karlsruhe, Germany	1028	0.19	2.12
Lamont, USA	7896	-0.40	1.77
Lauder, New Zealand	111	1.24	3.26
Orleans, France	1013	-0.03	2.08
Park Falls, USA	3398	0.23	1.96
Saga, Japan	438	0.67	2.12
Sodankyla, Finland	298	0.91	1.93
Wollongong, Australia	2994	0.21	2.03
TOTAL	24684	0.02	1.91

Table 6.1.4.1: Overview of the SRFP/RemoTeC XCO₂ validation with TCCON for gain H (after bias correction). Standard deviations are based on comparison of individual data points.

TCCON site	Number of co-locations [-]	Mean difference [ppm]	Standard deviation of difference [ppm]
Darwin, Australia	187	0.18	1.31
Dryden, USA	225	-0.69	2.03
Izana	411	0.03	1.79
Wollongong, Australia	1052	0.06	1.59
TOTAL	1875	-0.01	1.69

Table 6.1.4.2: Overview of the SRFP/RemoTeC XCO₂ validation with TCCON for gain M (after bias correction). Standard deviations are based on comparison of individual data points.

	ESA Climate Change Initiative (CCI)	Page 111
	Product Validation and Intercomparison Report (PVIR)	
	for the Essential Climate Variable (ECV) Greenhouse Gases (GHG)	Version 5.0 Final
		9 Feb 2017

TCCON site	Number of co-locations [-]	Mean difference [ppm]	Standard deviation of difference [ppm]
Ascension Island	705	0.03	1.36
Darwin, Australia	453	-0.34	1.26
Reunion Island	727	0.16	1.26
Wollongong, Australia	205	-0.25	1.46
TOTAL	2090	-0.01	1.33

Table 6.1.4.3: Overview of the SRFP/RemoTeC XCO₂ validation with TCCON for sunglint (after bias correction). Standard deviations are based on comparison of individual data points.



ESA Climate Change Initiative (CCI)

Product Validation and Intercomparison Report (PVIR)

for the Essential Climate Variable (ECV)
Greenhouse Gases (GHG)

Page 112

Version 5.0
Final

9 Feb 2017

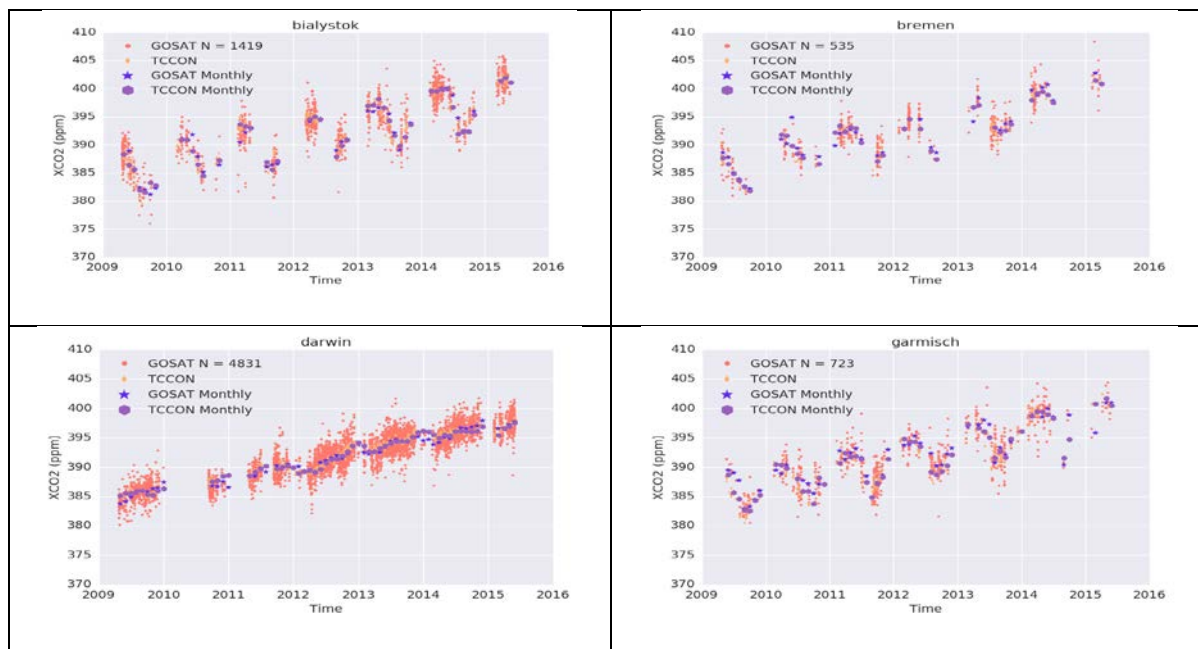


Figure 6.1.4.1: Difference between TCCON and GOSAT (after bias correction) for gain H and TCCON stations 1-4.

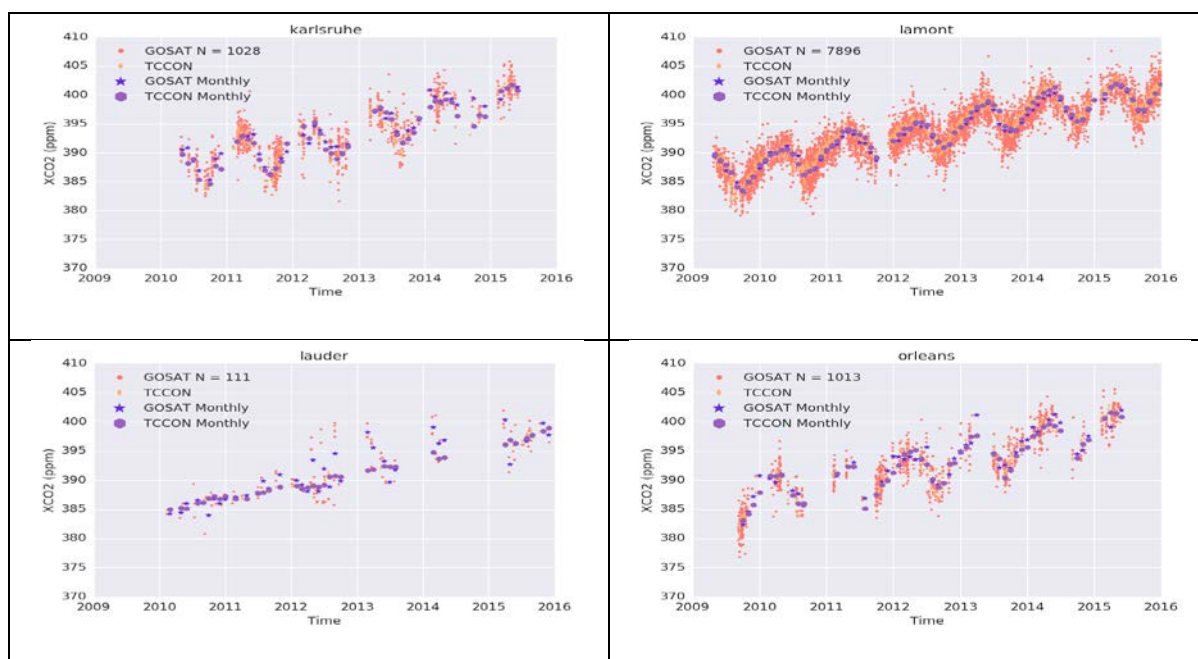


Figure 6.1.4.2: Difference between TCCON and GOSAT (after bias correction) for gain H and TCCON stations 5-8.



ESA Climate Change Initiative (CCI)

Product Validation and Intercomparison Report (PVIR)

for the Essential Climate Variable (ECV)
Greenhouse Gases (GHG)

Page 113

Version 5.0
Final

9 Feb 2017

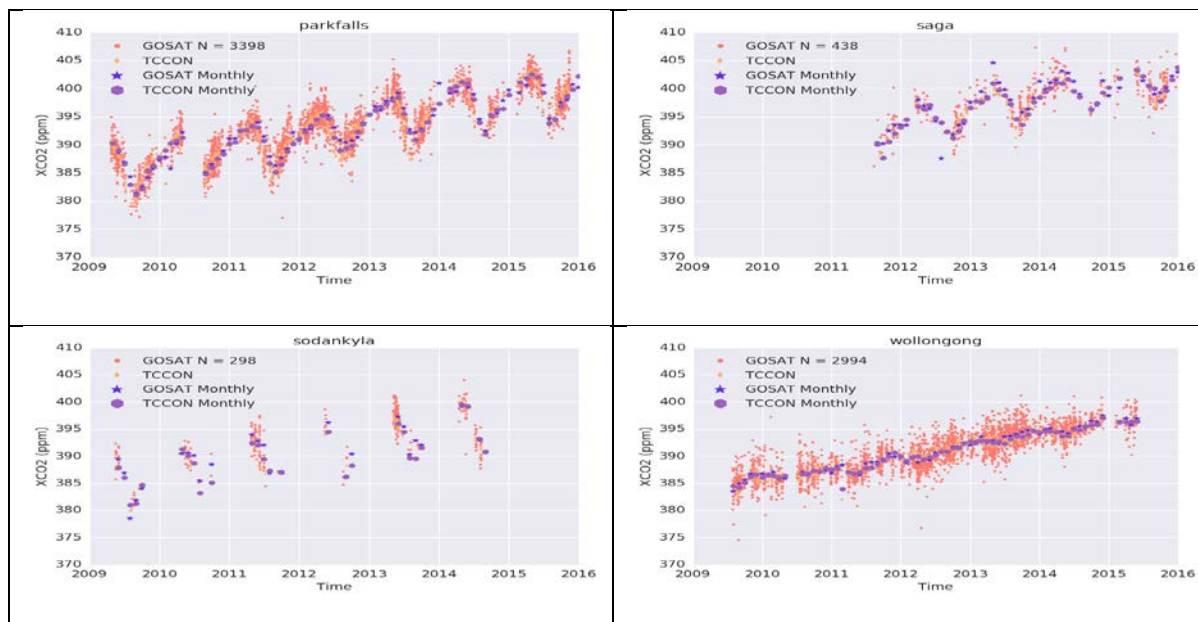


Figure 6.1.4.3: Difference between TCCON and GOSAT (after bias correction) for gain H and TCCON stations 9-12.

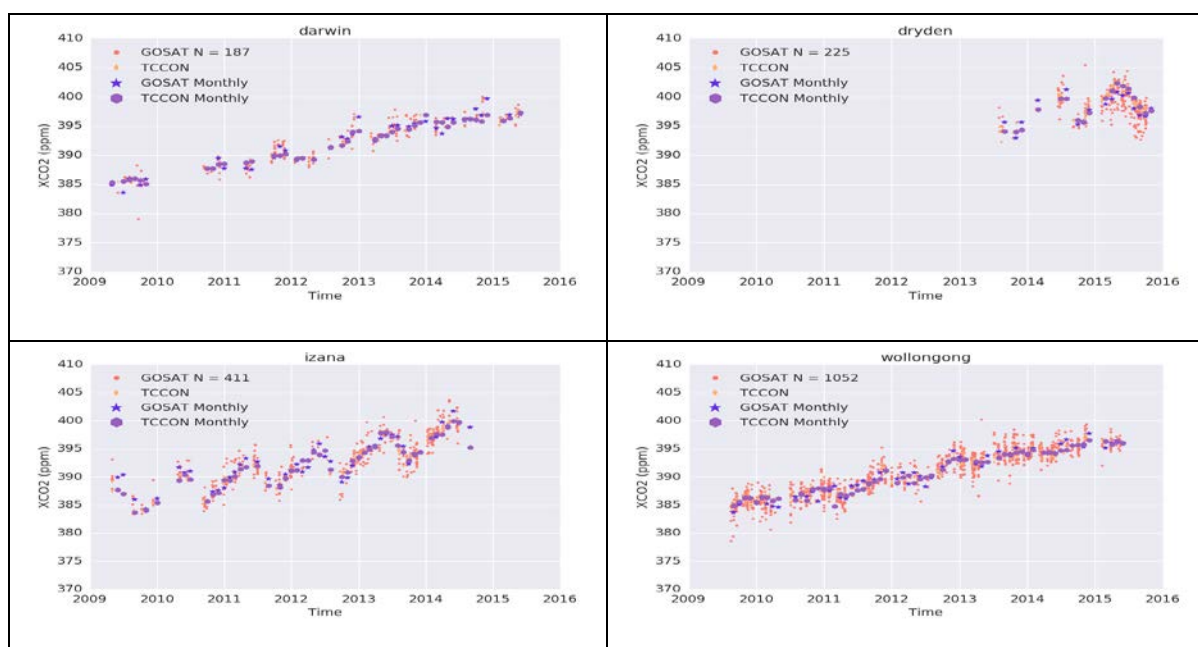


Figure 6.1.4.4: Difference between TCCON and GOSAT (after bias correction) for gain M.



ESA Climate Change Initiative (CCI)

**Product Validation and
Intercomparison Report (PVIR)**

for the Essential Climate Variable (ECV)
Greenhouse Gases (GHG)

Page 114

Version 5.0
Final

9 Feb 2017

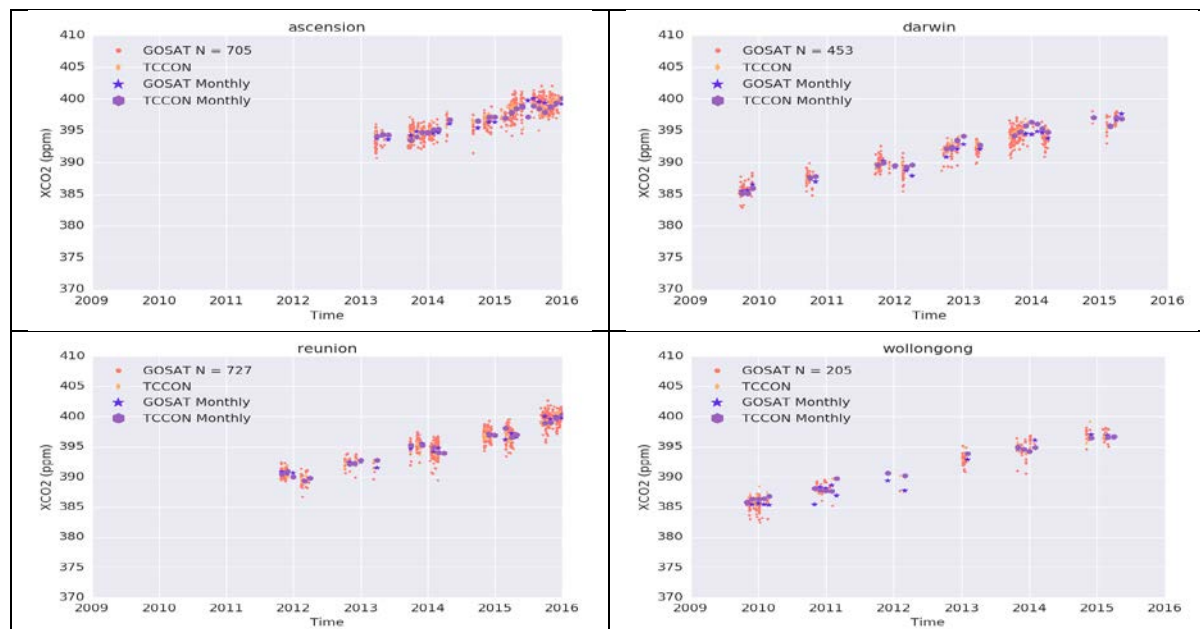



Figure 6.1.4.5: Difference between TCCON and GOSAT (after bias correction) for sunglint observations.

	ESA Climate Change Initiative (CCI)	Page 115
	Product Validation and Intercomparison Report (PVIR)	
	for the Essential Climate Variable (ECV) Greenhouse Gases (GHG)	Version 5.0 Final
		9 Feb 2017

Summary for assessment of GOSAT SRFP XCO₂ product


We have assessed the GOSAT SRFP XCO₂ product against ground-based TCCON observations for each of the three different observation settings (gain H, gain M and sunglint). Compared to the previous version (v2.3.7) of the data, we see an improvement in the gain M bias correction due to the inclusion of the Izana TCCON station.

The SRFP XCO₂ v.2.3.8 product shows no significant linear trend over the whole period (2009-2015). The year-to year variability has been obtained by calculating the maximum peak to peak difference of the GOSAT –TCCON remaining bias, yearly averaged, for the 7 year period.

The obtained year-to year variability is 0.34 ± 0.12 ppm. By itself the variability is significant, however it is not certain that this is caused by any instrument variability, as the sampling of TCCON varies from year to year due to a non-uniform co-location and measurement density of TCCON and GOSAT.

Summary table:

Estimates of achieved data quality: CRDP#4 CO ₂ _GOS_SRFP					
Sensor	Algorithm	Random error [ppm]	Systematic error [ppm]	Stability [ppm / year]	Comments
TANSO on GOSAT	SRFP v2.3.8 (RemoTeC)	1.9	0.43	Linear trend: -0.05 ± 0.12 ppm Year-to-year: 0.34 ± 0.12 ppm	Stability: Significance?: Trend: no Year-to-year: yes
All values are 1-sigma (except for stability); Note: "Year-to-year" stability refers to assessment results related to the extended definition of stability as given in URDv2.1, which now also covers "inter-annual error changes"					

	ESA Climate Change Initiative (CCI)	Page 116
	Product Validation and Intercomparison Report (PVIR)	
	for the Essential Climate Variable (ECV) Greenhouse Gases (GHG)	Version 5.0 Final
		9 Feb 2017

6.1.5 Assessment of SCIAMACHY/GOSAT EMMA XCO₂

The XCO₂ Level 2 data product generated with the ensemble algorithm EMMA is part of CRDP#4 and, therefore, its quality has been assessed as for each other algorithms in CRDP#4. Additionally, this section contributes not only to the algorithm validation but also to the algorithm inter-comparison. EMMA includes many individual algorithms and handles them in a standardized way. Moreover, **/Reuter et al., 2013/** showed that EMMA is relatively in-sensitive to outliers and performs well in respect to TCCON and CarbonTracker.

The latest version of EMMA is v2.2. It includes only the most recent algorithm versions and spans over a period of up to four years. Like the versions before (used for CRDP#3), it comes in three different flavours:

V2.2a) ACOS v7.3r01, BESD v02.01.02, NIES v02.21, RemoTeC v2.3.8, UOL-FP v7.0, WFMD v4.0. Minimum number of algorithms used for median calculation: 4 (of 6). Period: 06/2009 – 03/2012

V2.2b) ACOS v7.3r01, BESD v02.01.02, NIES v02.21, RemoTeC v2.3.8, UOL-FP v7.0. Minimum number of algorithms used for median calculation: 3 (of 5). Period: 06/2009 – 03/2012

V2.2c) ACOS v7.3r01, NIES v02.21, RemoTeC v2.3.8, UOL-FP v7.0. Minimum number of algorithms used for median calculation: 2 (of 4). Period: 05/2009 – 05/2014


If not otherwise stated, the results shown in this section correspond to EMMA v2.2a as only this version includes all retrieval algorithms assessed in the GHG-CCI II project.

Most of the shown figures are updated versions of figures shown in the publication of **/Reuter et al. 2013/**. In this publication more information can be found on EMMA's algorithm selection method and on the interpretation of the shown figures. See also <http://www.iup.uni-bremen.de/~mreuter/emma.php> for more information.

Emma as well as individual algorithms have been validated with TCCON as described by **/Reuter et al., 2013/**. The overall statistics per algorithm are summarized in **Table 6.1.5.1** and individual validation results are shown in **Figure 6.1.5.1** and **Figure 6.1.5.2**.

All validation results are valid only for the corresponding EMMA period but can be used to assess whether there is consistency with more sophisticated validation experiments of the validation team.

The individual algorithms have a single measurement precision in the range of 1.67 ppm - 2.06 ppm except for WFMD which has a single measurement precision of 2.96 ppm. EMMA has a single measurement precision of 2.35 ppm which is slightly larger than most of the

	ESA Climate Change Initiative (CCI)	Page 117
	Product Validation and Intercomparison Report (PVIR)	
	for the Essential Climate Variable (ECV) Greenhouse Gases (GHG)	Version 5.0 Final
		9 Feb 2017

individual algorithms due to the WFMD contribution (1.80 ppm for EMMA v2.2b). EMMA's station-to-station biases (0.40 - 0.54 ppm) are usually on the lower end of the range of the individual algorithms (0.39 ppm to 0.62 ppm).

Additionally to **Table 6.1.5.1**, **Figure 6.1.5.3** shows the anomaly of station biases of the used seven algorithms. One can see that most satellite retrievals have a high bias of about 0.5 ppm at the Garmisch-Partenkirchen and Karlsruhe TCCON sites and low bias of similar magnitude in Darwin and Lamont. This feature considerably contributes to the algorithms station-to-station bias statistics. Currently, it is unclear whether this discrepancy comes from the satellite retrievals or the TCCON.

Figure 6.1.5.3 shows that not only the station bias has some common features among the various retrieval algorithms at some TCCON sites. The scatter (standard deviation of the difference to TCCON) is a few tenth of a ppm larger in Karlsruhe which may be explained with local sources and a few tenth of a ppm lower in Darwin and Lamont, which may (in the case of Darwin) be explained by a smaller representation error on the southern hemisphere.

The drift analysis shows more or less consistent negative trends of about -0.3ppm/a at the sites Lamont and Darwin and positive trends of the same magnitude at Orleans and Park Falls. This is a bit surprising because three of the sites are located in similar latitude bands.

No pronounced similarities in the anomaly of the seasonal cycle biases were found.



ESA Climate Change Initiative (CCI)

Product Validation and Intercomparison Report (PVIR)

for the Essential Climate Variable (ECV)
Greenhouse Gases (GHG)

Page 118

Version 5.0
Final

9 Feb 2017

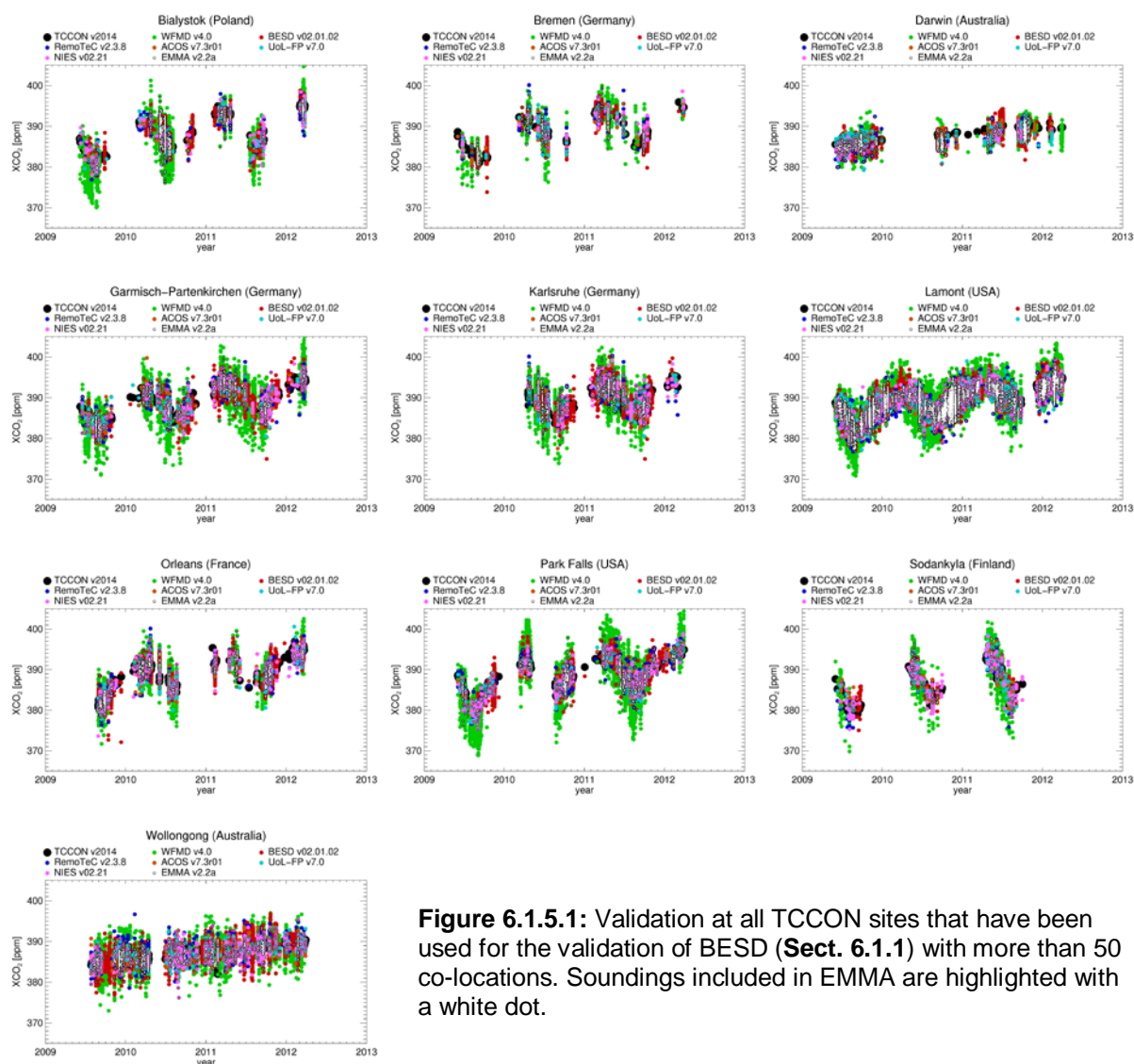


Figure 6.1.5.1: Validation at all TCCON sites that have been used for the validation of BESD (**Sect. 6.1.1**) with more than 50 co-locations. Soundings included in EMMA are highlighted with a white dot.



ESA Climate Change Initiative (CCI)

Product Validation and Intercomparison Report (PVIR)

for the Essential Climate Variable (ECV)
Greenhouse Gases (GHG)

Page 119

Version 5.0
Final

9 Feb 2017

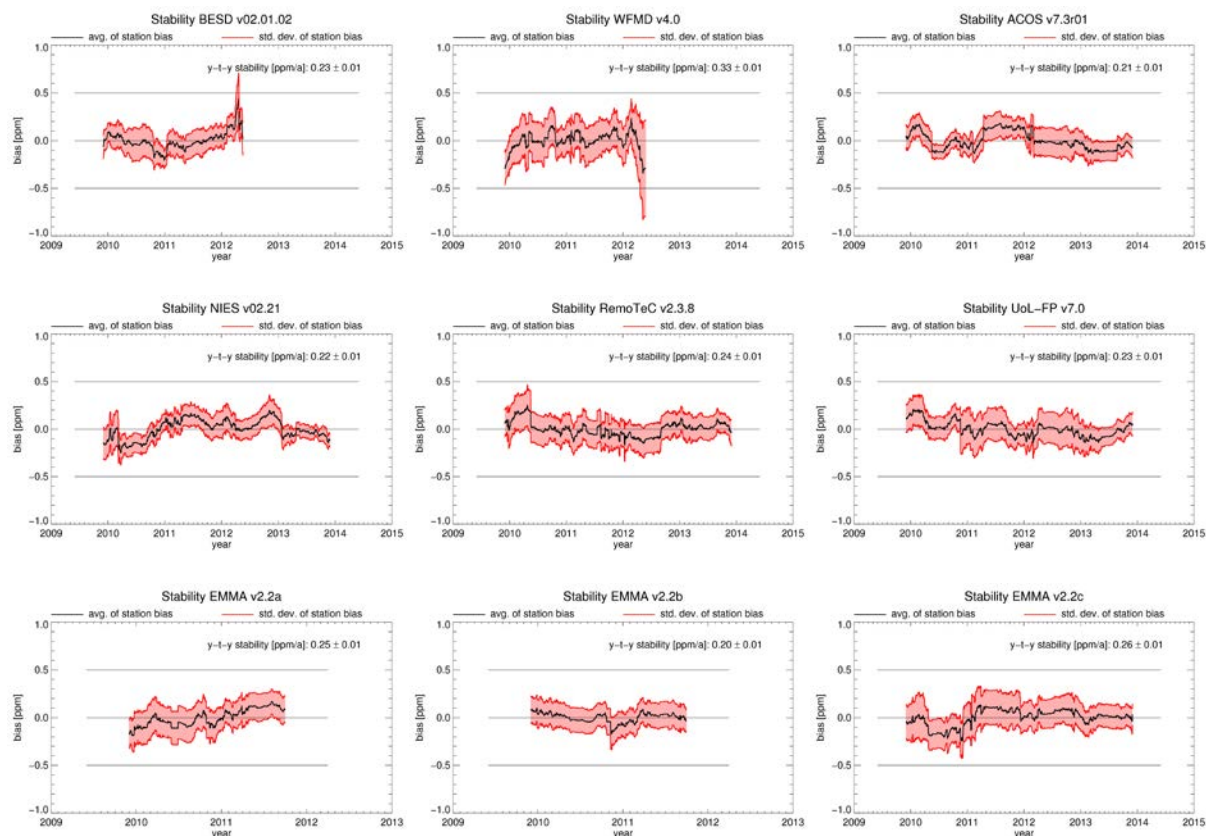


Figure 6.1.5.2: Stability analyses for EMMA and the contributing individual algorithms. The black curve shows the average station bias and the red curves its uncertainty represented by the station-to-station standard deviation and error propagation from single sounding measurement noise.


	ESA Climate Change Initiative (CCI)	Page 120
	Product Validation and Intercomparison Report (PVIR)	
	for the Essential Climate Variable (ECV) Greenhouse Gases (GHG)	Version 5.0 Final
		9 Feb 2017

Table 6.1.5.2: Summarizing validation statistics for all TCCON sites that have been used for the validation of BESD (**Sect. 6.1.1**) with more than 50 co-locations. Listed are the number of co-locations (#), average single measurement precision, regional and seasonal accuracy, linear trend, and year-to-year stability.

Algorithm	#	Precision	Accuracy [ppm]		Stability [ppm/a]	
		[ppm]	Regional	Seasonal	Trend	Year2Year
WFMD v4.0	46466	2.96	0.60	0.63	0.23±0.42	0.33
BESD v02.01.02	23725	1.97	0.39	0.43	-0.02±0.33	0.23
RemoTeC v2.3.8	9657	2.06	0.48	0.28	0.00±0.16	0.24
ACOS v7.3r01	10359	1.67	0.57	0.30	-0.11±0.12	0.21
UOL-FP v7.0	8142	1.79	0.42	0.36	-0.15±0.11	0.23
NIES v02.21	8059	1.92	0.62	0.27	0.03±0.15	0.22
EMMA v2.2a	9771	2.35	0.54	0.47	-0.30±0.64	0.25
EMMA v2.2b	4813	1.80	0.40	0.32	-0.13±0.42	0.20
EMMA v2.2c	8473	1.81	0.44	0.24	-0.04±0.16	0.26

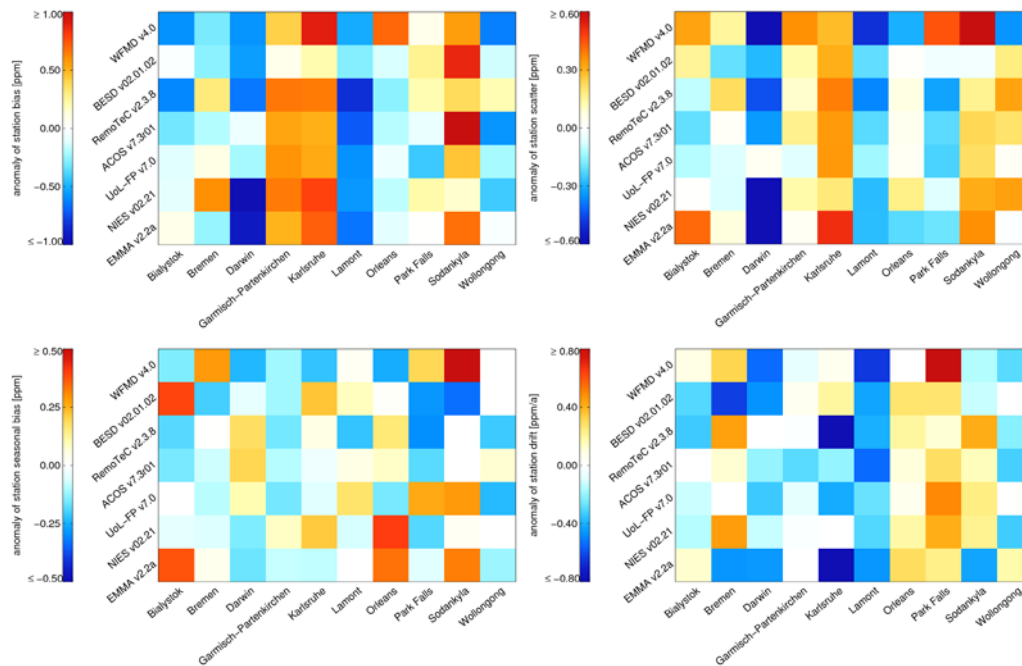


Figure 6.1.5.3: Anomaly of station biases (top, left), station scatter (top, right), seasonal biases per station (bottom, left), and station drift (bottom, right).


As in previous EMMA versions, all algorithms reproduce large scale features well, however, there are still differences of a few ppm when looking into details (**Figure 6.1.5.4** to **Figure 6.1.5.6**).

All algorithms see consistently larger seasonal amplitudes than CarbonTracker. The satellite retrieved seasonal amplitudes are generally in better agreement with TCCON than with CarbonTracker (**Figure 6.1.5.7**, top left).

Comparison of the north/south gradients show similar performances when comparing against CarbonTracker and TCCON. However, this should not be over interpreted because TCCON contributes only to few grid boxes especially on the southern hemisphere (**Figure 6.1.5.7**, top right).

Emma outperforms all individual algorithms in terms of frequency of potential outliers and standard deviation of the difference to CarbonTracker and TCCON (**Figure 6.1.5.7**, bottom).

ACOS has the fewest fractions of outliers (difference larger than 2.5 ppm) in respect to EMMA (**Figure 6.1.5.7**, bottom left).

	ESA Climate Change Initiative (CCI)	Page 122
	Product Validation and Intercomparison Report (PVIR)	
	for the Essential Climate Variable (ECV) Greenhouse Gases (GHG)	Version 5.0 Final
		9 Feb 2017

WFMD (26%) and BESD (25%) provide the largest part of the integrated data fraction of EMMA v2.2a. The smallest contribution (10%) has NIES (**Figure 6.1.5.8**).



ESA Climate Change Initiative (CCI)

**Product Validation and
Intercomparison Report (PVIR)**

for the Essential Climate Variable (ECV)
Greenhouse Gases (GHG)

Page 123

Version 5.0
Final

9 Feb 2017

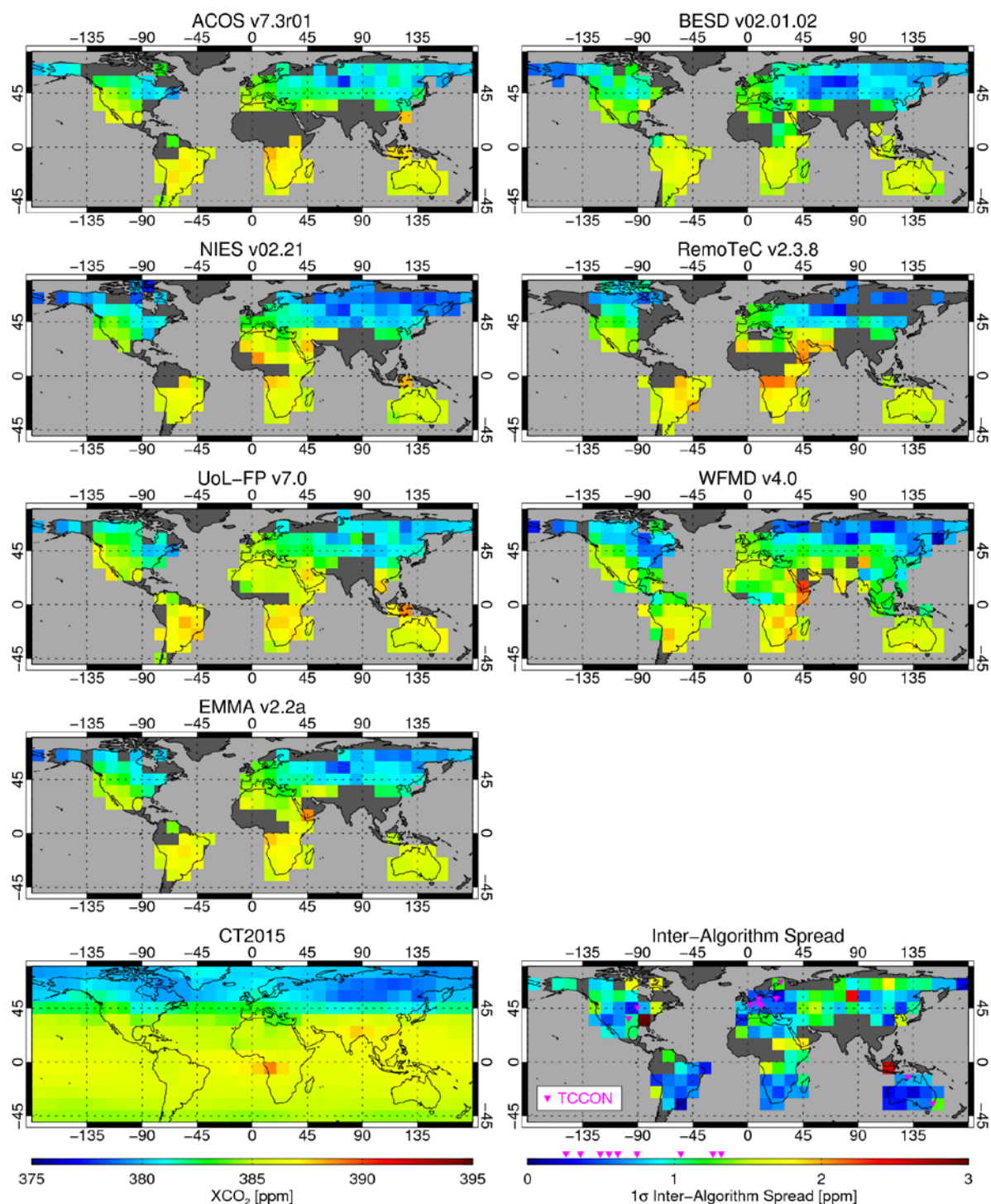


Figure 6.1.5.4: Typical monthly gridded averages (August 2009) of the seven algorithms, EMMA, and CT2015 as well as corresponding inter-algorithm spread, i.e., the inter-algorithm standard deviation.



ESA Climate Change Initiative (CCI)

**Product Validation and
Intercomparison Report (PVIR)**

for the Essential Climate Variable (ECV)
Greenhouse Gases (GHG)

Page 124

Version 5.0
Final

9 Feb 2017

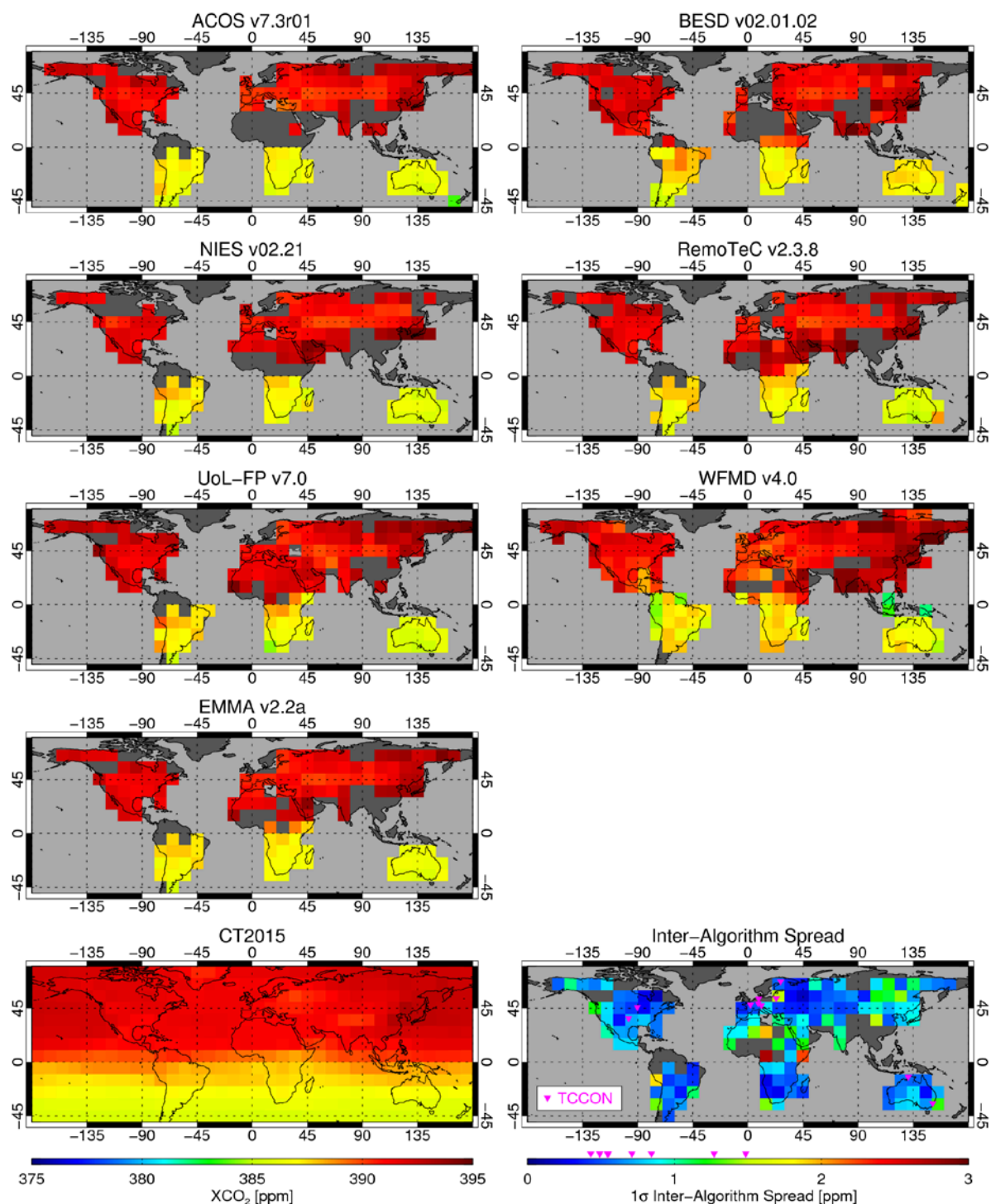


Figure 6.1.5.5: As Figure 6.1.5.4 but for May 2010.

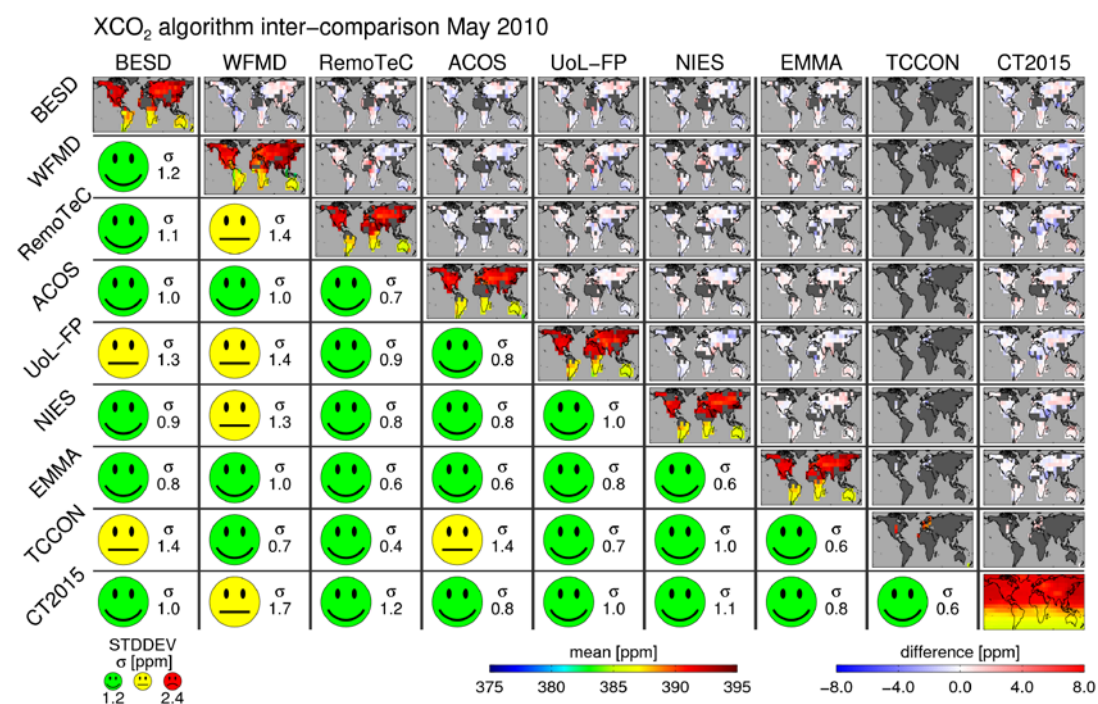
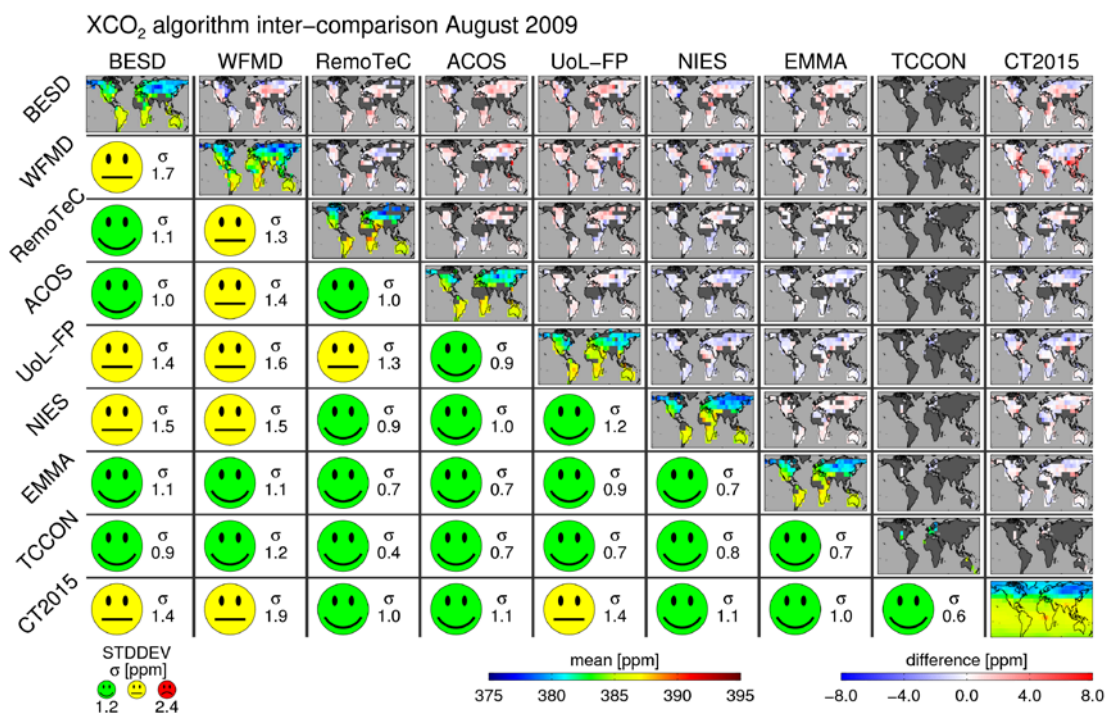


Figure 6.1.5.6: Algorithm inter-comparison matrix for August 2009 (top) and May 2010 (bottom).



ESA Climate Change Initiative (CCI)

Product Validation and Intercomparison Report (PVIR)

for the Essential Climate Variable (ECV)
Greenhouse Gases (GHG)

Page 126

Version 5.0
Final

9 Feb 2017

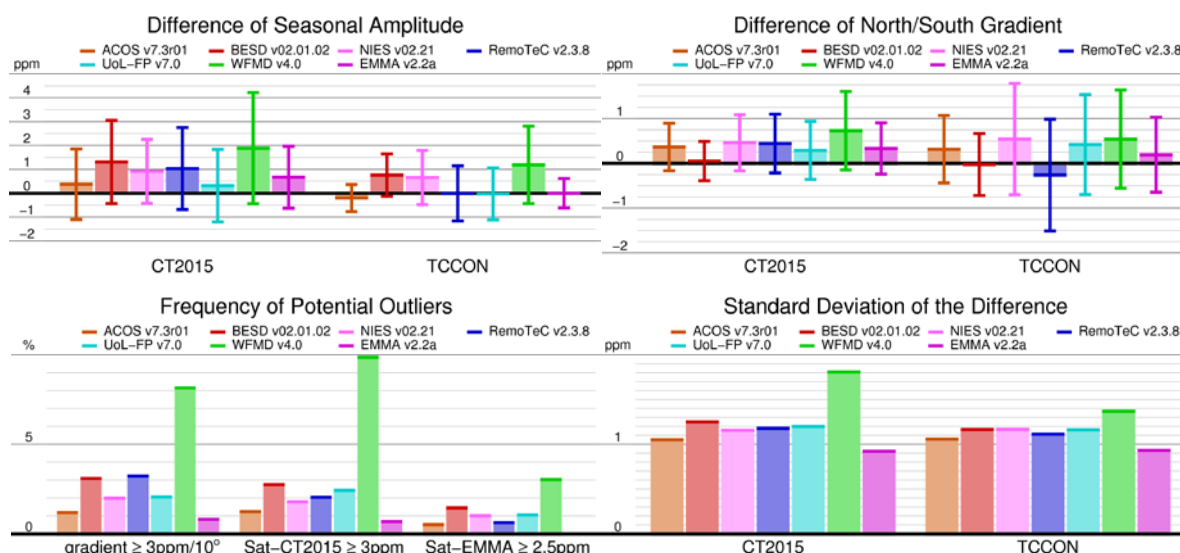


Figure 6.1.5.7: Top left: Difference of seasonal cycle amplitude of all individual algorithms as well as EMMA compared with CarbonTracker v2015 and TCCON v2014. Top right: Difference of north/south gradient of all individual algorithms as well as EMMA compared with CarbonTracker v2015 and TCCON. Bottom left: Frequency of potential outliers estimated by large gradients, large difference to CarbonTracker, and large difference to EMMA. Bottom right: Standard deviation of the difference of all algorithms and EMMA to CarbonTracker and TCCON.

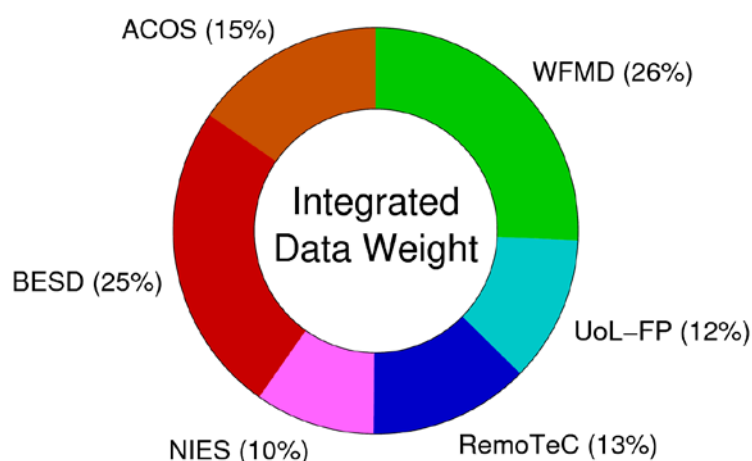


Figure 6.1.5.8: Integrated data weight of each algorithm within the EMMA database defined as $\sum 1/\sigma_i^2$ where σ_i is the (scaled) individual sounding error derived from TCCON comparisons.



The average inter-algorithm spread has values between 0.4 ppm and 1.6 ppm and is typically below 0.9 ppm (**Figure 6.1.5.9**). The largest inter-algorithm spreads are observed in the tropics, Asia, and in high latitudes. Only a small fraction of the inter-algorithm spread can be explained with differences expected due to measurement noise so that most of the differences can be considered systematic errors. Only in high latitudes and at some coast-lines measurement noise is expected to explain a significant part of the inter-algorithm spread.

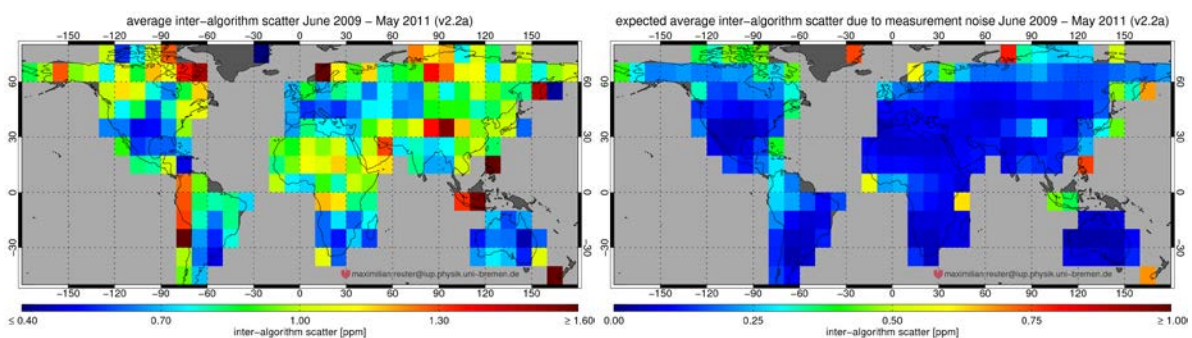


Figure 6.1.5.9: Average inter-algorithm scatter of monthly $10^{\circ} \times 10^{\circ}$ averages from June 2009 till May 2011 of the most recent algorithm versions of ACOS, NIES operational, RemoTeC, UOL-FP, BESD, and WFMD (left) and corresponding expected contribution of measurement noise (right).

It is interesting to note that (till now) the average inter-algorithm spread reduces with every new EMMA version (always including the most recent algorithm versions, **Figure 6.1.5.10**). This means that EMMA observes a kind of convergence among the individual algorithms. It is not entirely clear where this is coming from and many effects may contribute to the explanation: Algorithms are improved and bugs are removed but algorithms may also become more similar by using the same input data (e.g., spectroscopy, elevation model).

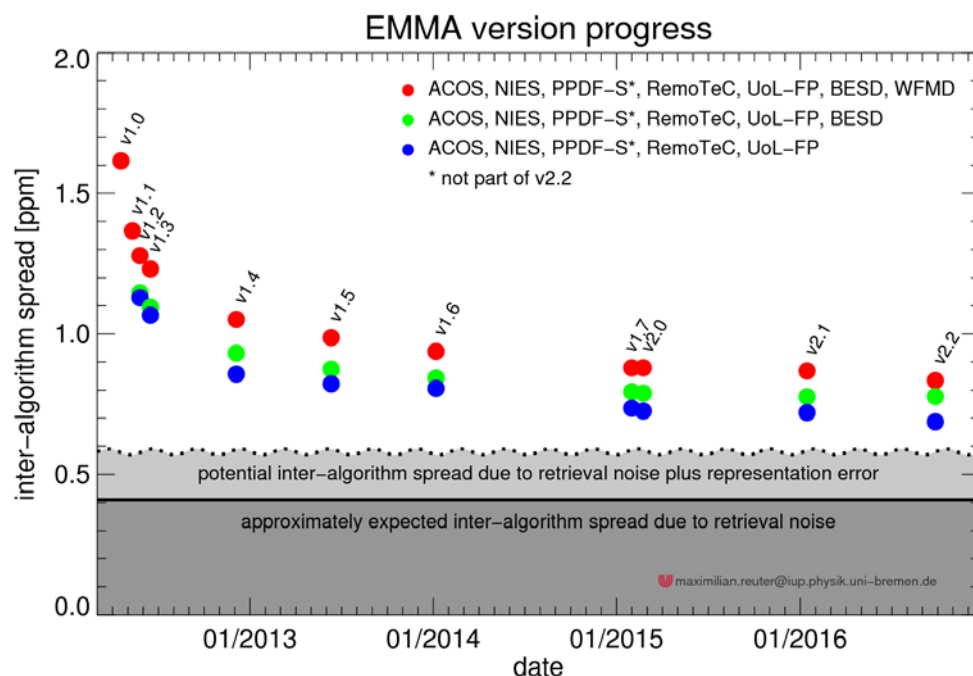



Figure 6.1.5.10: Average inter-algorithm spread of all EMMA versions compared with the approximately expected contribution of retrieval noise and a rough estimate of the representation error.

	ESA Climate Change Initiative (CCI)	Page 129
	Product Validation and Intercomparison Report (PVIR)	
	for the Essential Climate Variable (ECV) Greenhouse Gases (GHG)	Version 5.0 Final
		9 Feb 2017

Summary for assessment of EMMA and related XCO₂ product:

Table 6.1.5.2: Summary table EMMA v2.2a/b/c and contributing algorithms. Note: Stability: Significance?: Unclear.

Estimates of achieved data quality: CRDP#4 CO2_v2.2x_EMMA (and contributing algorithms)					
Sensor	Algorithm	Random error [ppm]	Systematic error [ppm]	Stability [ppm / year]	Comments
SCIAMACHY and GOSAT	EMMA v2.2a	2.35	0.54 RA 0.47 SA	-0.30±0.64 TR 0.25 YTY	06/2009-03/2012 10 TCCON sites
SCIAMACHY and GOSAT	EMMA v2.2b	1.80	0.40 RA 0.32 SA	-0.13±0.42 TR 0.20 YTY	
GOSAT	EMMA v2.2c	1.81	0.44 RA 0.24 SA	-0.04±0.16 TR 0.26 YTY	06/2009-05/2014 10 TCCON sites
SCIAMACHY	WFMD v4.0	2.96	0.60 RA 0.63 SA	0.23±0.42 TR 0.33 YTY	06/2009-03/2012 10 TCCON sites
SCIAMACHY	BESD v02.01.02	1.97	0.39 RA 0.43 SA	-0.02±0.33 TR 0.23 YTY	
GOSAT	RemoTeC v2.3.8	2.06	0.48 RA 0.28 SA	0.00±0.16 TR 0.24 YTY	06/2009-05/2014 10 TCCON sites
GOSAT	ACOS v7.3r01	1.67	0.57 RA 0.30 SA	-0.11±0.12 TR 0.21 YTY	
GOSAT	UOL-FP v7.0	1.79	0.42 RA 0.36 SA	-0.15±0.11 TR 0.23 YTY	
GOSAT	NIES v02.21	1.92	0.62 RA 0.27 SA	0.03±0.15 TR 0.22 YTY	

All uncertainty estimates represent 1-sigma (except for stability). Note: "Year-to-year" stability refers to assessment results related to the extended definition of stability as given in URDv2.1, which now also covers "inter-annual error changes".



6.2 Assessment of XCH₄ data products

6.2.1 Assessment of SCIAMACHY WFMD XCH₄

Validation and intercomparison results for WFMDv4.0, which is part of the CRDP#4 are summarised in this section.

The methane mole fractions as a function of latitude and time are shown in **Figure 6.2.1.1**. The retrieved methane results show that after years of stability, atmospheric methane has started to rise again in recent years which is consistent with surface measurements /Rigby et al., 2008/, /Dlugokencky et al., 2009/.

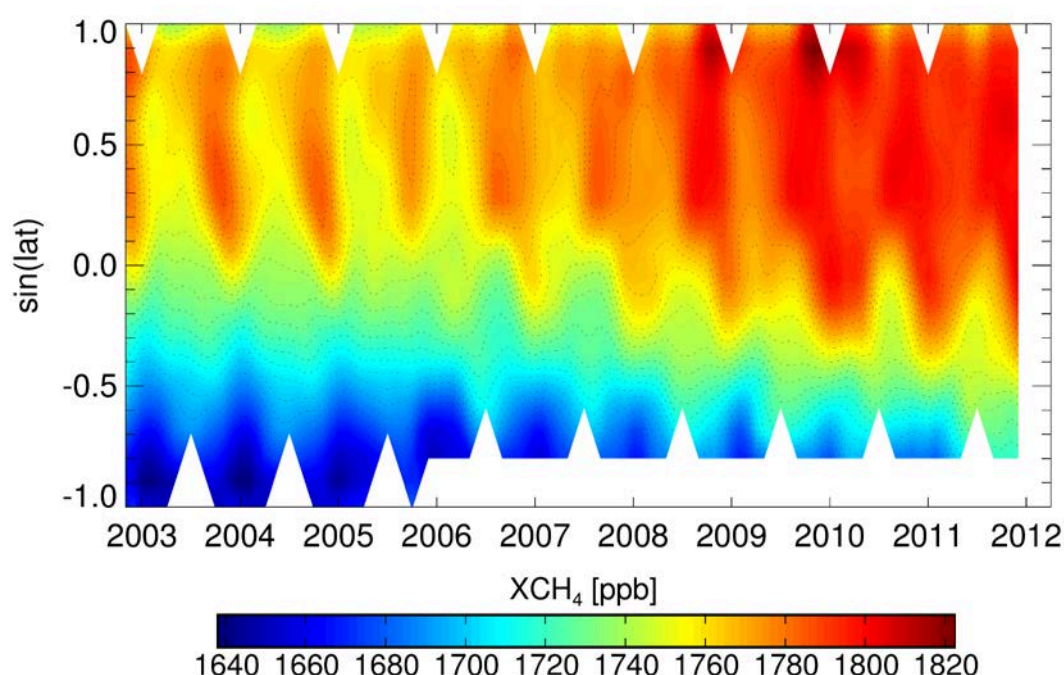


Figure 6.2.1.1: Overview of the long-term global WFMDv4.0 methane data set; shown are column-averaged dry air mole fractions as a function of latitude and time.

**Product Validation and
Intercomparison Report (PVIR)**Version 5.0
Finalfor the Essential Climate Variable (ECV)
Greenhouse Gases (GHG)

9 Feb 2017

Major methane source regions like the Sichuan Basin in China which is famous for rice cultivation and the interhemispheric gradient with larger methane concentrations in the Northern Hemisphere are clearly visible in the data (see **Figure 6.2.1.2**).

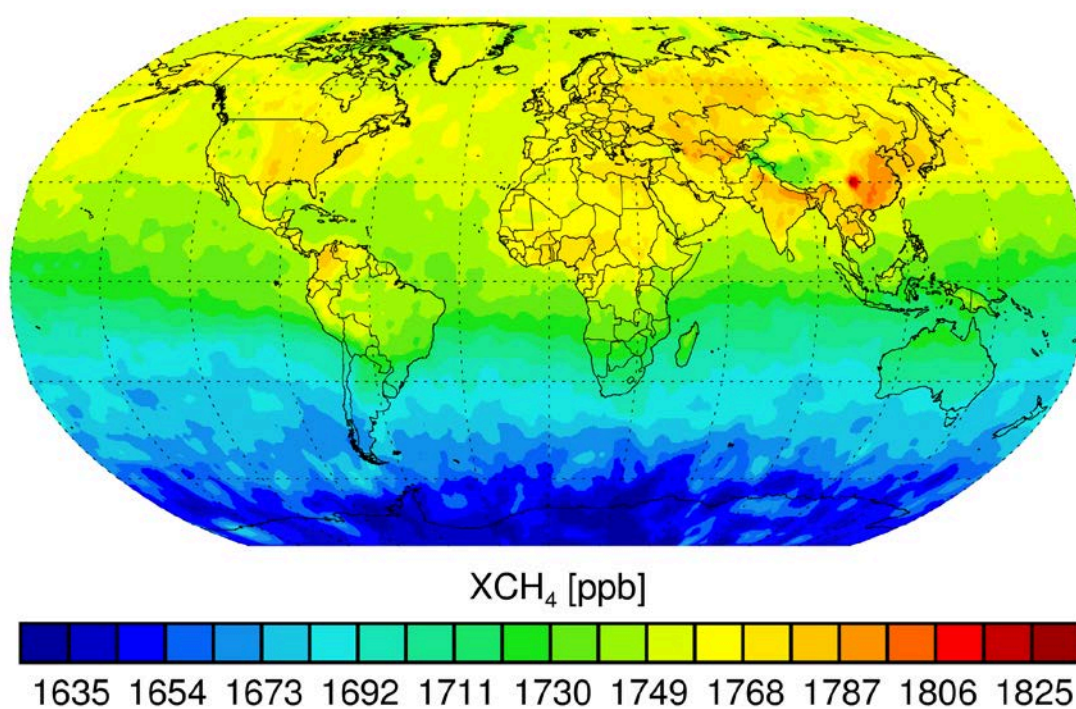


Figure 6.2.1.2: Three years mean (2003-2005) of retrieved SCIAMACHY WFMDv4.0 methane.

From the validation with the 2014 release of ground-based Fourier Transform Spectroscopy (FTS) measurements of the Total Carbon Column Observing Network (TCCON) **/Wunch et al., 2011/** (see **Figure 6.2.1.3**) and comparison with the TM5-4DVAR model **/Bergamaschi et al., 2009/**, **/Bergamaschi et al., 2010/** (see **Figure 6.2.1.4**) at 11 TCCON sites, namely Sodankylä (Finland), Bialystok (Poland), Bremen (Germany), Karlsruhe (Germany), Orleans (France), Garmisch (Germany), Park Falls (USA), Lamont (USA), Darwin (Australia), Wollongong (Australia), and Lauder (New Zealand), realistic error estimates of the satellite data are provided and summarised in **Table 6.2.1.1**. For Karlsruhe R0 TCCON data are used to have a consistent validation data set obtained with the same algorithm for all sites. The relevant parameters for quality assessment are the global offset which is defined as the mean of the local offsets d at the individual sites, the random error relative to the reference which is the standard deviation of the differences using all data combined after subtraction of the respective regional biases, and the spatial systematic error which is the standard deviation of the local offsets d relative to TCCON or TM5-4DVAR at the individual sites. Also given is the seasonal systematic error which is the standard deviation of the 4 overall seasonal offsets (using all sites combined after subtraction of the respective local offsets d). The temporal long-term drift stability is determined by a linear fit of the differences relative to the reference (using all data combined after subtraction of the respective regional biases) with time. In particular, the TCCON comparison is dominated by the period with detector issues (after October 2005) worsening the quality of the satellite retrievals.

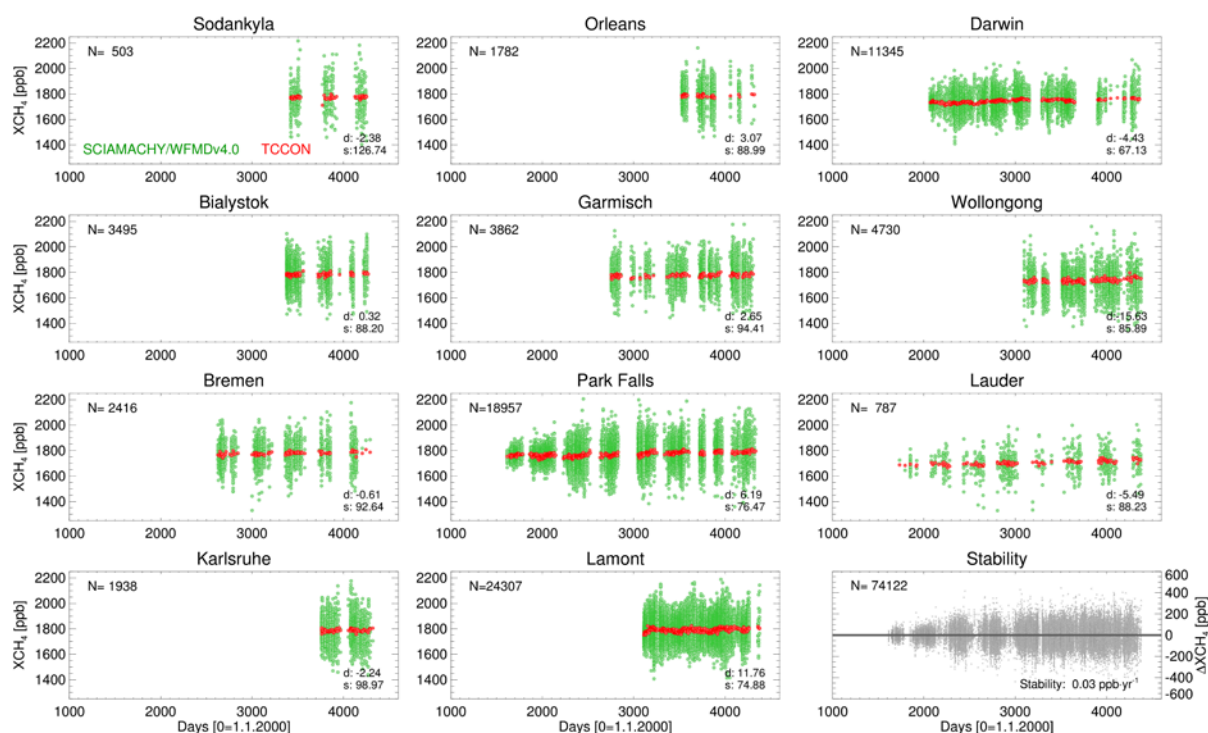


Figure 6.2.1.3: Validation of the WFMDv4.0 methane data set with TCCON.



ESA Climate Change Initiative (CCI)

**Product Validation and
Intercomparison Report (PVIR)**

for the Essential Climate Variable (ECV)
Greenhouse Gases (GHG)

Page 133

Version 5.0
Final

9 Feb 2017

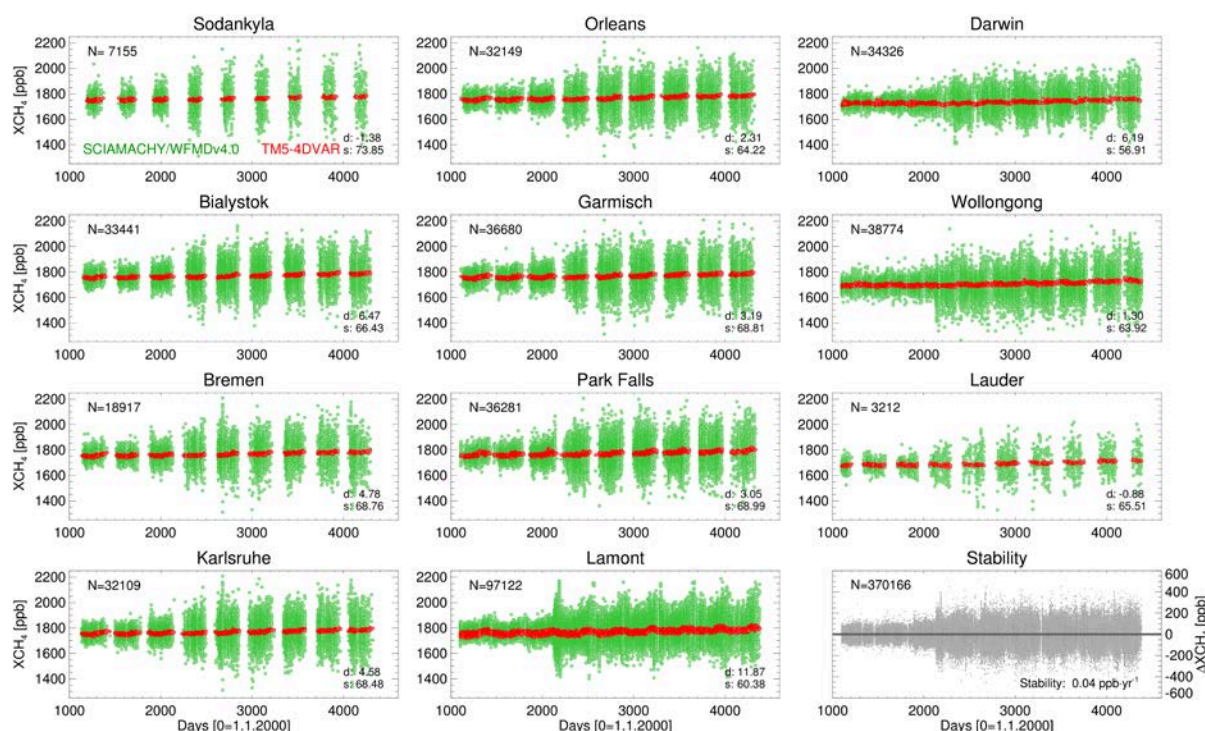


Figure 6.2.1.4: Comparison of the WFMDv4.0 methane data set with TM5-4DVAR.

The year-to-year stability is assessed in the following way: The one-year moving average of the differences relative to the reference (using all data combined and subtracting respective regional biases and the global long-term drift) is generated. For a given point in time t , let $\sigma_{yr}(t)$ be defined as the standard deviation of this deseasonalised difference within a one-year window around t . This results in two curves (referring to TCCON and TM5-4DVAR, see **Figure 6.2.1.5**) as a function of time, considering only those time periods where data of at least four sites are available. The deviations of these two curves are interpreted as the uncertainty of the corresponding mean curve (shaded gray area around black curve in **Figure 6.2.1.5**) and the year-to-year stability is then defined as the maximum of σ_{yr} over time. The proposed approach allows to detect potential jumps in the time series.

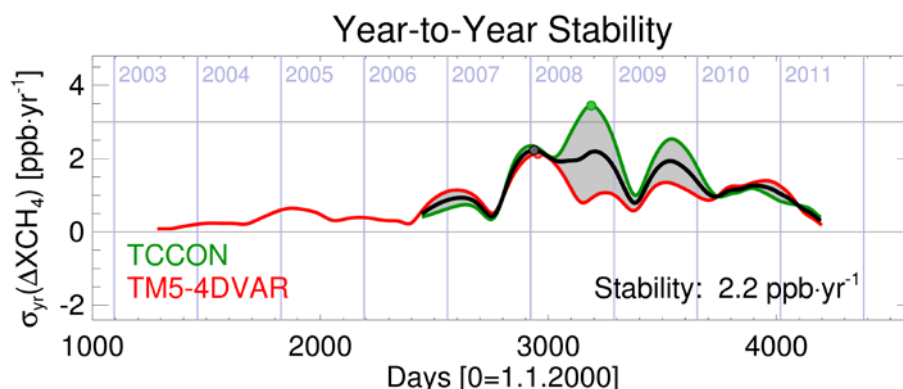


Figure 6.2.1.5: Year-to-year stability of the WFMDv4.0 carbon dioxide data set relative to TCCON and TM5-4DVAR at TCCON sites.

	SCIA - TCCON	SCIA - TM5
Global Offset [ppb]	-1	4
Random Error [ppb]	79	65 (32; 80)
Spatial Systematic Error [ppb]	7.0	3.7
Seasonal Systematic Error [ppb]	1.3	1.5
Long-term Drift Stability [ppb/yr]	0.03	0.04
Year-to-Year Stability [ppb/yr]	2.2	

Table 6.2.1.1: Validation and comparison results for WFMDv4.0 XCH₄ based on single measurements between 2003 and 2011. Note that the TCCON validation focuses on the period after the pixel mask change as a consequence of lack of TCCON measurements before November 2005. For the TM5 comparison, the values in brackets correspond to the two periods before and after the pixel mask change at the beginning of November 2005.

Please note, that the random error defined above includes systematic components and is therefore an upper bound of the actual single measurement precision characterising the repeatability of the measurements. The single ground pixel retrieval precision derived from averaging daily standard deviations of the retrieved XCH₄ for several locations distributed around the globe provides an estimate of the single measurement precision of about 30 ppb before and 70 ppb after the pixel mask change due to detector degradation at the beginning of November 2005.



To examine the renewed methane increase in recent years more quantitatively, **Figure 6.2.1.6** shows the temporal evolution of retrieved SCIAMACHY and modelled TM5-4DVAR methane based on monthly means. The anomaly since 2007 is derived from the difference of the mean values of the derivative of the deseasonalised trend after and before middle of 2006. A consistent estimate of about 5-6 ppb/yr is obtained for both, SCIAMACHY and TM5-4DVAR. The consistency of this estimate also confirms the stability of the SCIAMACHY data.

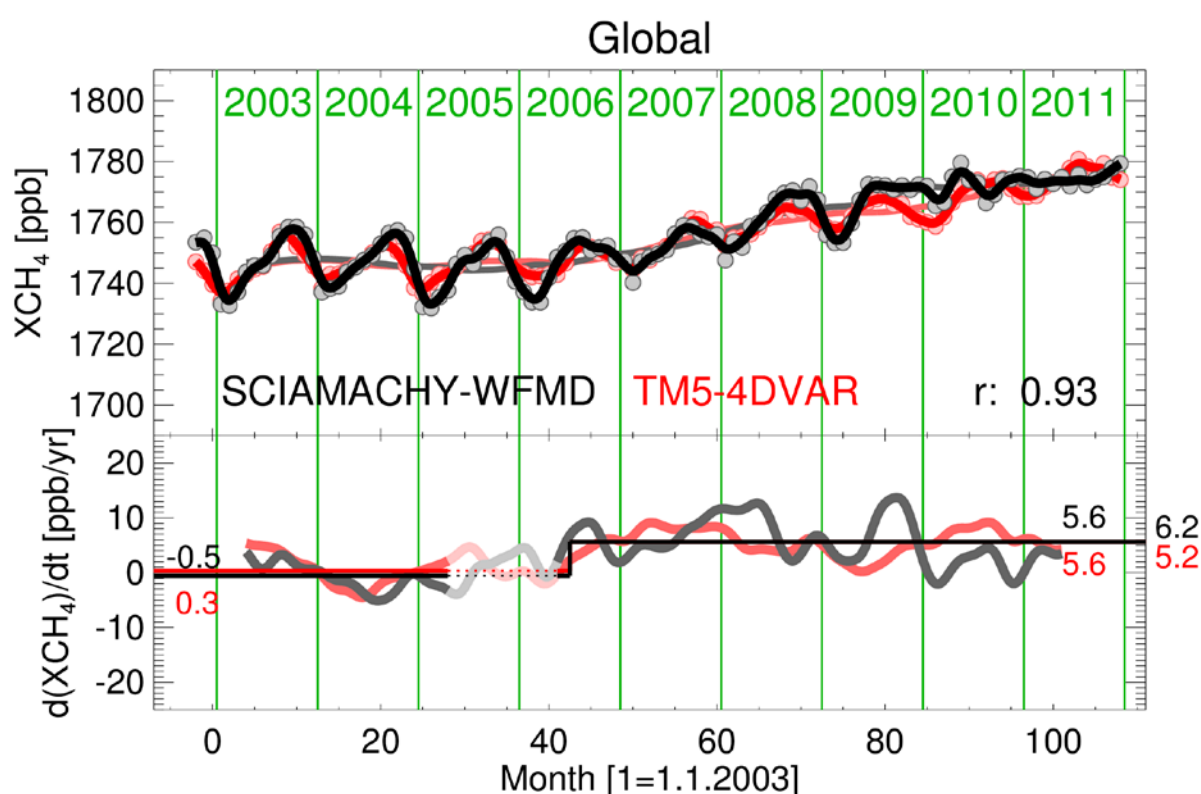




Figure 6.2.1.6: Timeseries of SCIAMACHY and TM5-4DVAR methane. Also shown are the deseasonalised trends and their derivatives. The estimated anomaly since 2007 is noted on the right hand side.

	ESA Climate Change Initiative (CCI)	Page 136
	Product Validation and Intercomparison Report (PVIR)	
	for the Essential Climate Variable (ECV) Greenhouse Gases (GHG)	Version 5.0 Final
		9 Feb 2017

Summary for assessment of SCIAMACHY WFMD XCH₄ product:

Summary table:

Estimates of achieved data quality: CRDP#4 CH₄_SCI_WFMD					
Sensor	Algorithm	Random error [ppb]	Systematic error [ppb]	Stability [ppb / year]	Comments
SCIAMACHY on ENVISAT	WFMD V4.0	79 (32)	Spatial: 3.7-7.0 Seasonal: 1.3-1.5 Spatial+Seasonal: 5.2-8.3	Linear trend: [0.03, 0.04] Year-to-year: 2.2	The values in brackets () correspond to the period before November 2005 Stability: Significance?: Unclear
All values are 1-sigma (except for stability); Note: "Year-to-year" stability refers to assessment results related to the extended definition of stability as given in URDv2.1, which now also covers "inter-annual error changes"					

	ESA Climate Change Initiative (CCI)	Page 137
	Product Validation and Intercomparison Report (PVIR)	
	for the Essential Climate Variable (ECV) Greenhouse Gases (GHG)	Version 5.0 Final
		9 Feb 2017

6.2.2 Assessment of SCIAMACHY IMAP XCH₄

The SCIAMACHY IMAP XCH₄ product v7.2 is similar to its previous version 7.1/7.0 but incorporates an empirical bias correction using water vapor abundance as the driving variable, which is now implemented as the standard version (was an added variable in 7.1). The main inconsistency in v7.0/7.1, namely an apparent positive jump of about 20 ppb as of mid 2010 is now corrected in v7.2 using a postprocessing bias correction. It was also found that additional filtering was necessary as spurious days can affect the retrieval, mostly related to either decontamination periods or anomalous dark current obtained during the eclipse of the orbit. This filtering, which was not properly done in v7.1, is more stringent in v7.2

In addition, IMAP v7.2 was tested against GOSAT SRON proxy XCH₄ retrievals and bias corrections based on monthly means comparing the two independent datasets.

The main differences between versions are summarized below:

v7.2 changes over v7.1/7.0:

- Bias corrected XCH₄ is now the standard product in v7.1 (and was only provided as auxiliary variable in v7.0).
- H₂O bias correction was updated, using a linear scaling factor of the H₂O water vapor column
- A small AMF bias factor correction was added as well
- A high basis after June 2010 was applied
- The XCO₂ rescaling for the proxy method is now based on CarbonTracker 2015 data, not CarbonTracker 2011, for which data had to be extrapolated into the future for a larger part of the SCIAMACHY time-series after 2010.

Results

The main verification results are shown in **Figures 6.2.2.1-6.2.2.5**. Results are very similar to v7.1 but a more consistent time-series beyond 2010 is now achieved. There is also very good agreement in latitudinal cross sections between GOSAT and SCIAMACHY in 2009 test data.

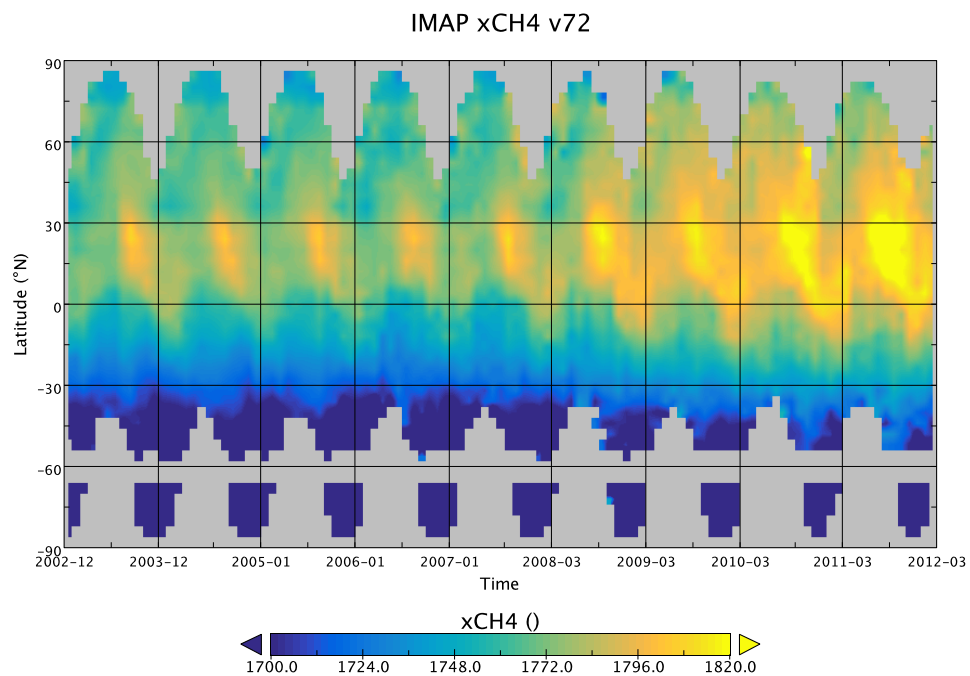


Figure 6.2.2.1: Carpet plot of IMAP v72 data.

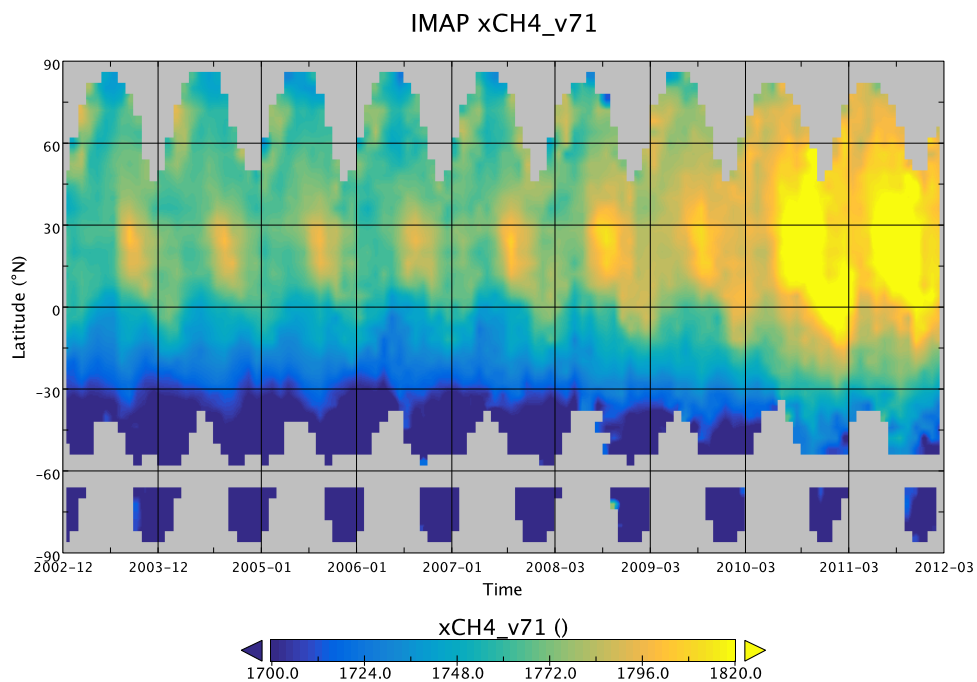


Figure 6.2.2.1: Carpet plot of SCIA v71 data, showing the abnormal jump in mid 2010 but otherwise very similar behaviour to v72.

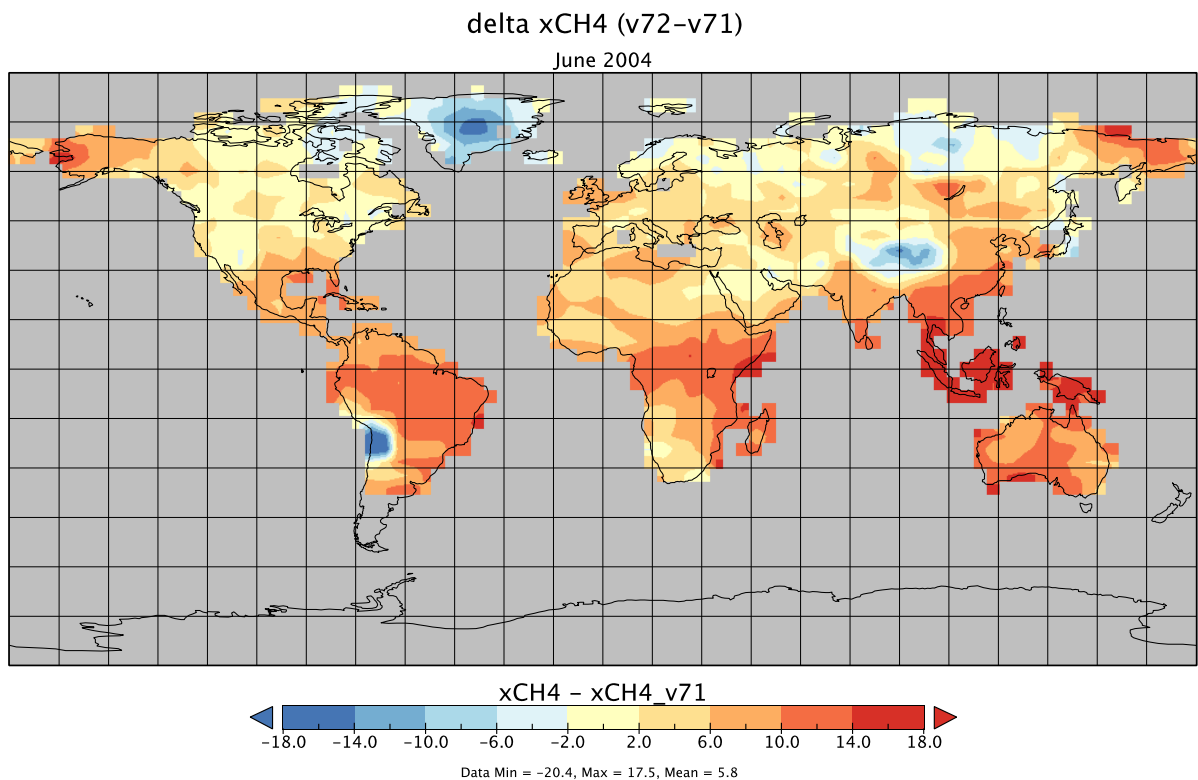


Figure 6.2.2.1 Difference between v72 and v71 in June 2004, strongest difference in very dry regions, where v71 might have over-corrected data due to the log(h2o) correction.



ESA Climate Change Initiative (CCI)

**Product Validation and
Intercomparison Report (PVIR)**

for the Essential Climate Variable (ECV)
Greenhouse Gases (GHG)

Page 140

Version 5.0
Final

9 Feb 2017

delta xCH₄ (v72-v71)
December 2004

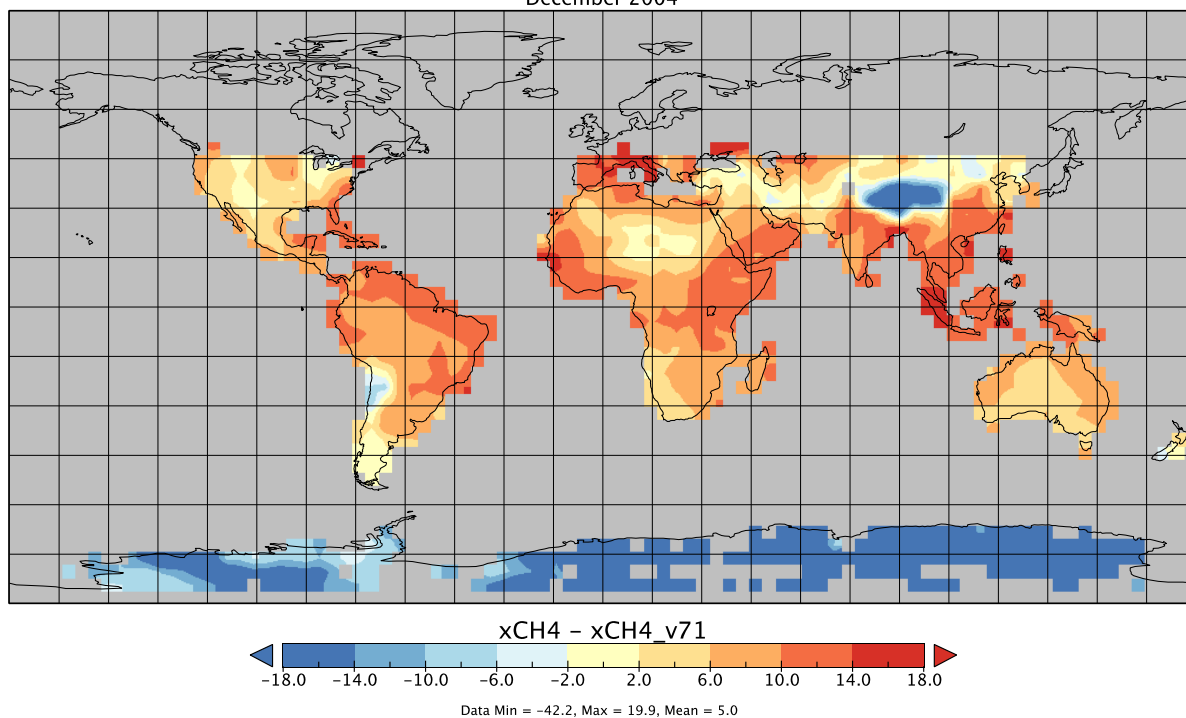


Figure 6.2.2.4 Difference between v72 and v71 in December 2004, strongest difference in very dry regions, where v71 might have over-corrected data due to the log(h₂o) correction.



ESA Climate Change Initiative (CCI)

Product Validation and Intercomparison Report (PVIR)

for the Essential Climate Variable (ECV)
Greenhouse Gases (GHG)

Page 141

Version 5.0
Final

9 Feb 2017

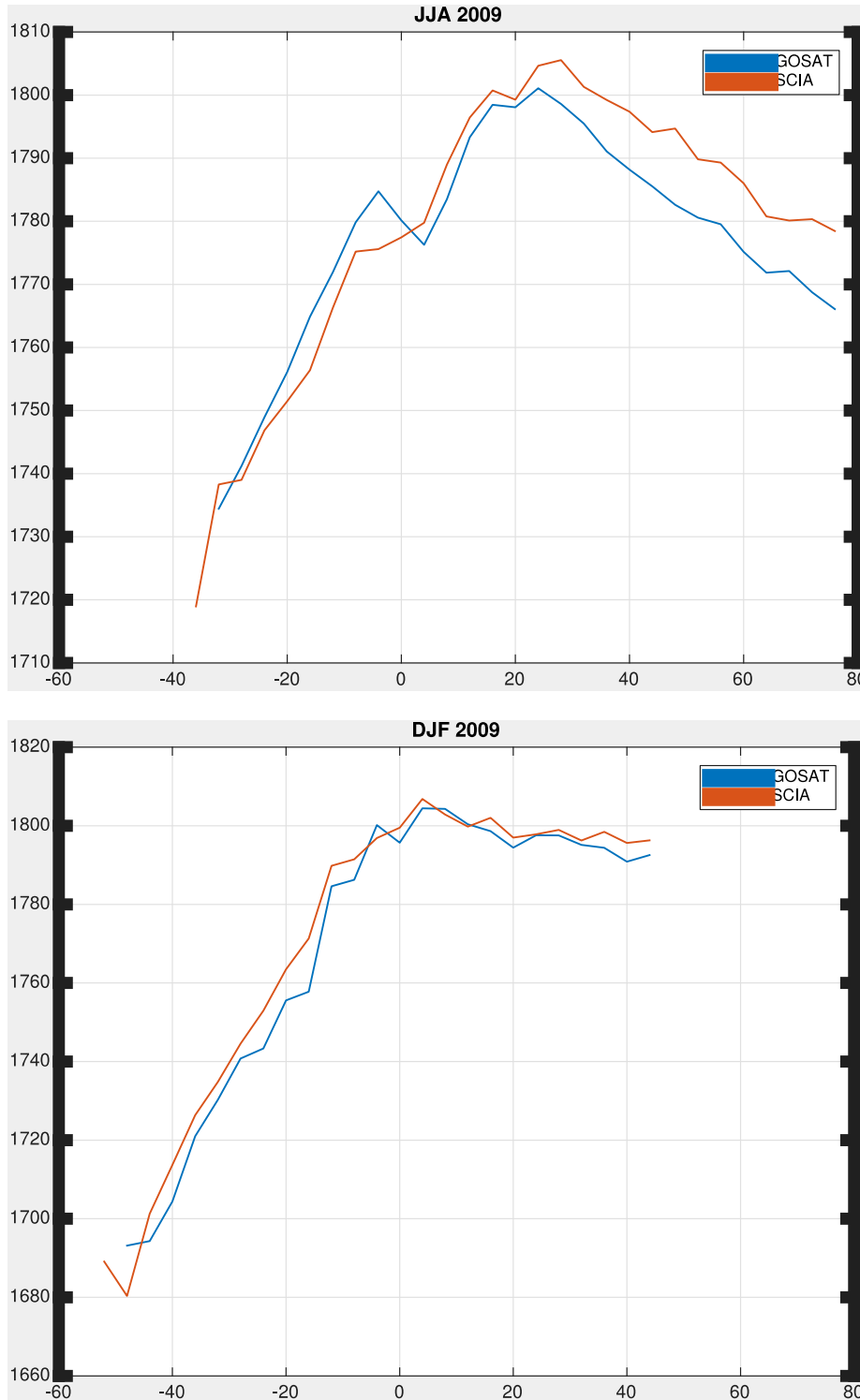



Figure 6.2.2.5 Latitudinal cross sections of SCIA v72 and GOSAT in JJA and DJF 2009, showing excellent agreement.

	ESA Climate Change Initiative (CCI)	Page 142
	Product Validation and Intercomparison Report (PVIR)	
	for the Essential Climate Variable (ECV) Greenhouse Gases (GHG)	Version 5.0 Final
		9 Feb 2017


Summary and conclusions

The SCIAMACHY IMAP XCH₄ product v7.2 can be considered the final IMAP XCH₄ product and incorporates changes to alleviate the major concerns observed in v7.1, most notably the larger bias after 2010 as well as some bad retrievals, which were not filtered properly. Also, a new XCO₂ scaling was applied, which should result in more realistic XCH₄ values as actual XCO₂ CarbonTracker with a consistent version throughout the entire time series is now applied.

Summary for assessment of SCIAMACHY IMAP XCH₄ product

Summary table:

Estimates of achieved data quality: CRDP#4 CH ₄ _SCI_IMAP					
Sensor	Algorithm	Random error [ppb]	Systematic error [ppb]	Stability [ppb / year]	Comments
SCIAMACHY on ENVISAT	IMAP V7.2	50 (32)	<10	Linear trend: Not observed Year-to-year: Not significant (but enhanced noise after 2005)	The values in brackets () correspond to the period before November 2005 Trend: no Year-to-year: unclear
All values are 1-sigma (except for stability); Note: "Year-to-year" stability refers to assessment results related to the extended definition of stability as given in URDv2.1, which now also covers "inter-annual error changes"					

	ESA Climate Change Initiative (CCI)	Page 143
	Product Validation and Intercomparison Report (PVIR)	
	for the Essential Climate Variable (ECV) Greenhouse Gases (GHG)	Version 5.0 Final
		9 Feb 2017

6.2.3 Assessment of GOSAT OCPR XCH₄

Validation and inter-comparison of results for OCPRv7.0, submitted as University of Leicester's contribution to CRDP4, are summarised in this section. This includes presentation of seasonal mean maps and comparison with Total Column Carbon Observing Network (TCCON) and MACC model data. All OCPRv7.0 data shown make use of the filtered XCH₄ product.

Spatial distributions of OCPRv7.0 XCH₄ seasonal means are presented in **Fig. 6.2.3.1**, along with differences to MACC S1NOAAv10 model data (available only until end of 2012) in **Fig. 6.2.3.2**. Note that the stratospheric column in MACC has been replaced with calculations by the TOMCAT model. Spatial distribution and magnitudes of OCPRv7.0 are in general agreement with calculations by the MACC model, where major deviations (± 30.0 ppb) from model data do not occur over any great portion of the globe. Notable exceptions are seen over regions where fluxes are uncertain such as South-East Asia in autumn or southern Africa in winter (DJF).



ESA Climate Change Initiative (CCI)

**Product Validation and
Intercomparison Report (PVIR)**

for the Essential Climate Variable (ECV)
Greenhouse Gases (GHG)

Page 144

Version 5.0
Final

9 Feb 2017

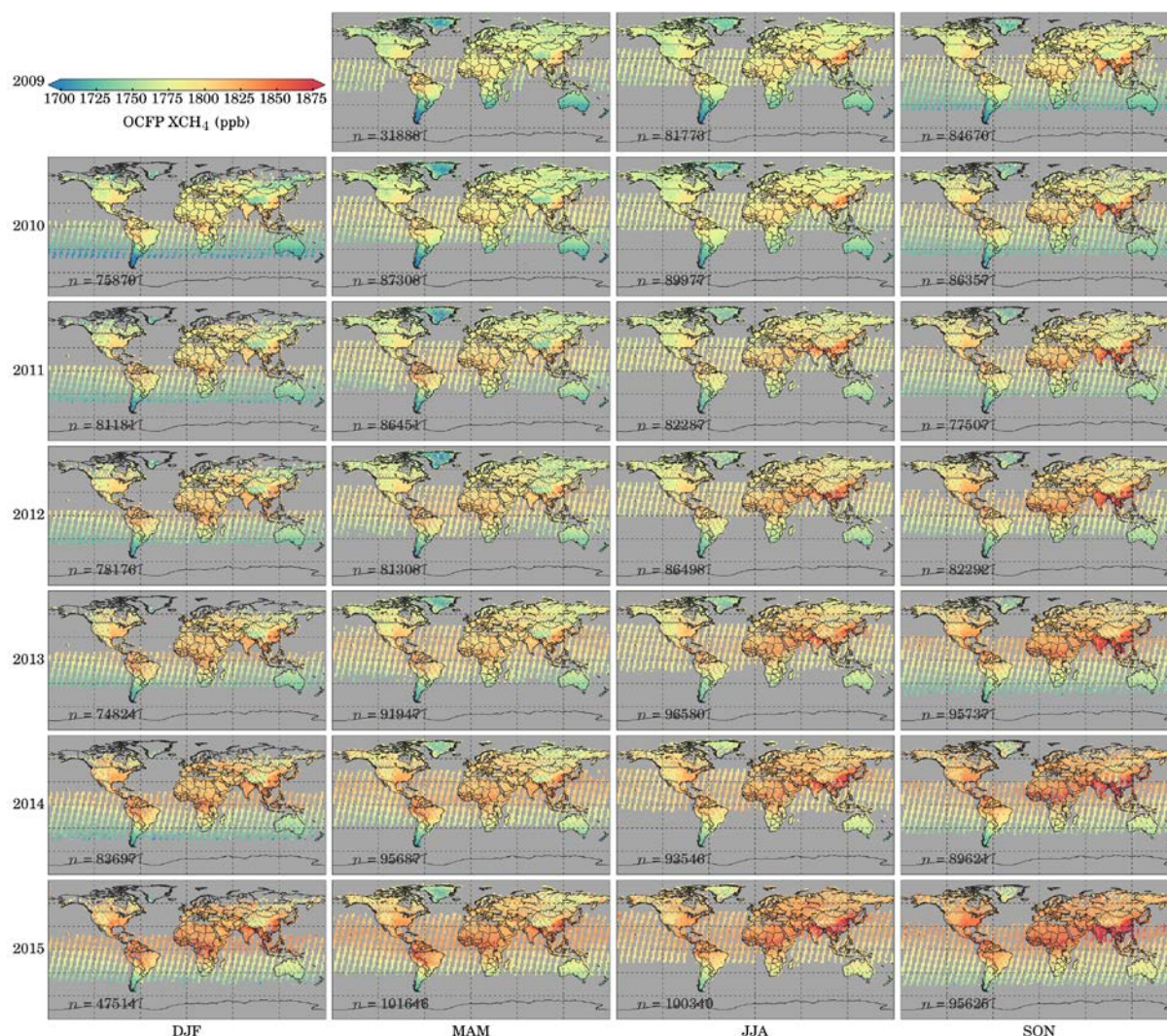


Figure 6.2.3.1. Seasonal means of filtered OCPRv7.0 XCH₄ for 2009–2015.

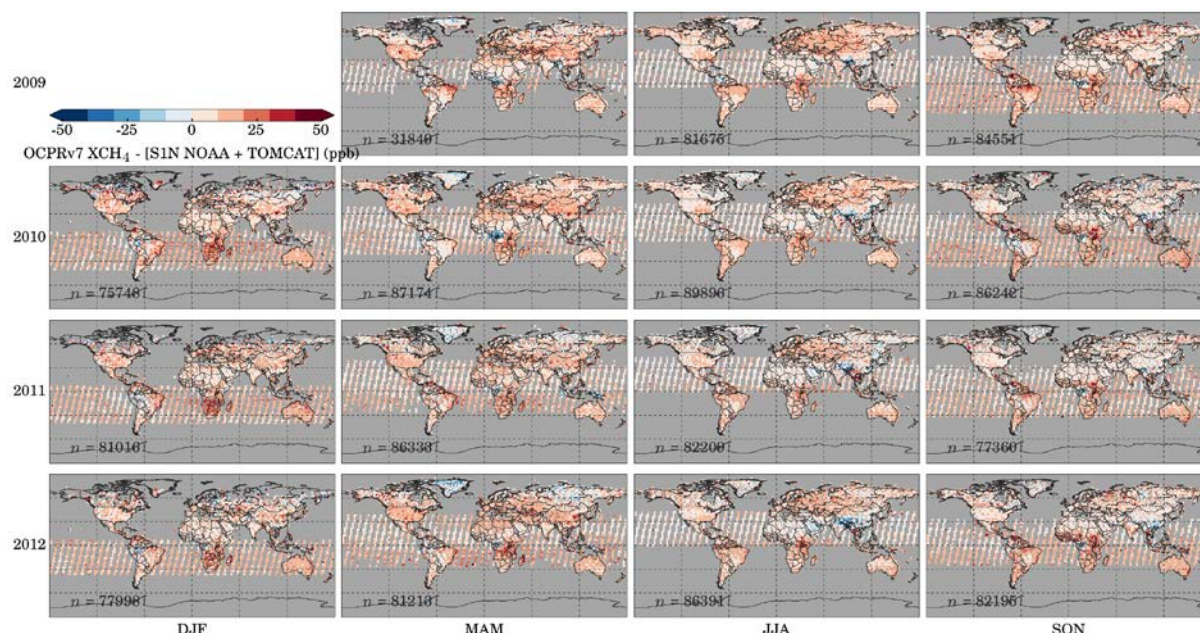


Figure 6.2.3.2. Seasonal means of differences between OCPRv7.0 (as above) and MACC S1NOAAv10 XCH₄

Figure 6.2.3.3 demonstrates validation of OCPRv7.0 with TCCON observations of XCH₄, encompassing Fourier transform spectroscopy measurements made at 14 TCCON sites available within the GGG2014 dataset. Bias (calculated as TCCON–OCPRv7.0), correlation, and standard deviation of the bias are annotated on each sub-plot per site, and repeated in **Tab. 6.2.3.1**. Measurement parameters relating to OCPRv7.0 stability are presented in **Tab. 6.2.3.2**. **Figure 6.2.3.4** details OCPRv7.0 observations and MACC S1NOAAv10 modelled XCH₄ interpolated to time and location of OCPR measurements, subset to Transcom regions. For TCCON and MACC comparisons, OCPRv7.0 is seen to capture the seasonal cycle well, albeit with a high bias for OCPRv7.0 against MACC data.



ESA Climate Change Initiative (CCI)

**Product Validation and
Intercomparison Report (PVIR)**

for the Essential Climate Variable (ECV)
Greenhouse Gases (GHG)

Page 146

Version 5.0
Final

9 Feb 2017

Site	Mean Δ	$\sigma\Delta$	r	n obs.
Sodankyla, Finland	-6.79	15.95	0.72	2433
Bialystok, Poland	-5.32	13.74	0.75	2848
Bremen, Germany	-3.94	12.82	0.75	984
Karlsruhe, Germany	-3.82	14.42	0.68	2931
Orleans, France	-1.76	12.93	0.72	3067
Garmisch, Germany	-8.79	15.13	0.67	3175
Park Falls, Wisconsin, USA	-7.46	12.79	0.76	4472
Lamont, Oklahoma, USA	-1.15	13.14	0.80	11139
Tsukuba, Ibaraki, Japan, 125HR	-2.37	13.03	0.74	2041
Saga, Japan	2.96	13.37	0.77	1263
Darwin, Australia	0.40	8.06	0.83	2791
Wollongong, Australia	5.80	11.93	0.70	4384
Lauder, New Zealand, 125HR	0.55	9.84	0.83	914
Lauder, New Zealand, 120HR	-0.98	9.90	0.77	151

Table 6.2.3.1. Site statistics for OCPD comparisons against TCCON, with mean Δ and $\sigma\Delta$ in ppb.

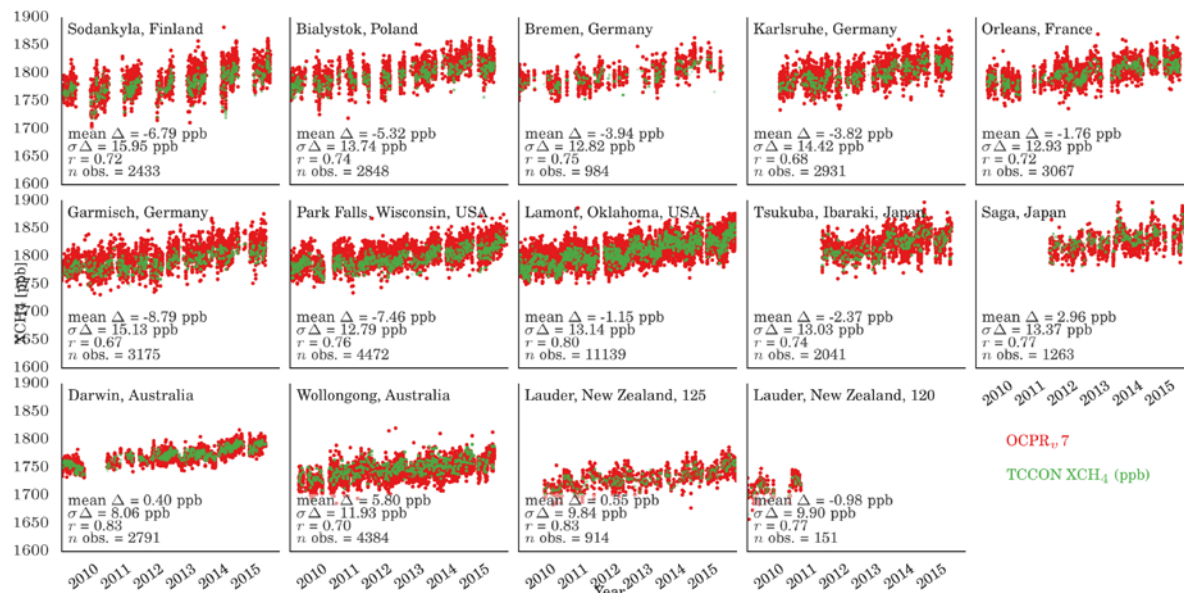


Figure 6.2.3.3. TCCON GGG2014 (green) and OCPRv7.0 (red) XCH₄ observations; OCPR observations are co-located with TCCON sites using a <550km spatial and ± 2 hour temporal criteria.

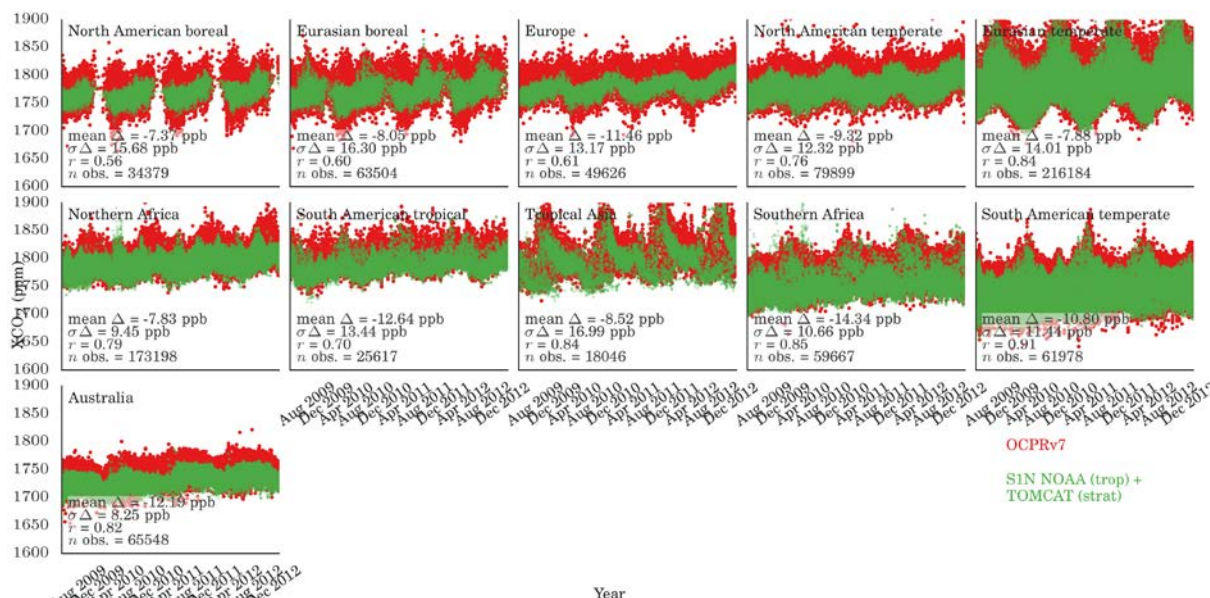


Figure 6.2.3.4. Subset to Transcom basis map regions, OCPRv7.0 (red) and MACC S1NOAAv10 XCH₄ (green) interpolated to OCPR time and location (with OCPR averaging kernel applied).

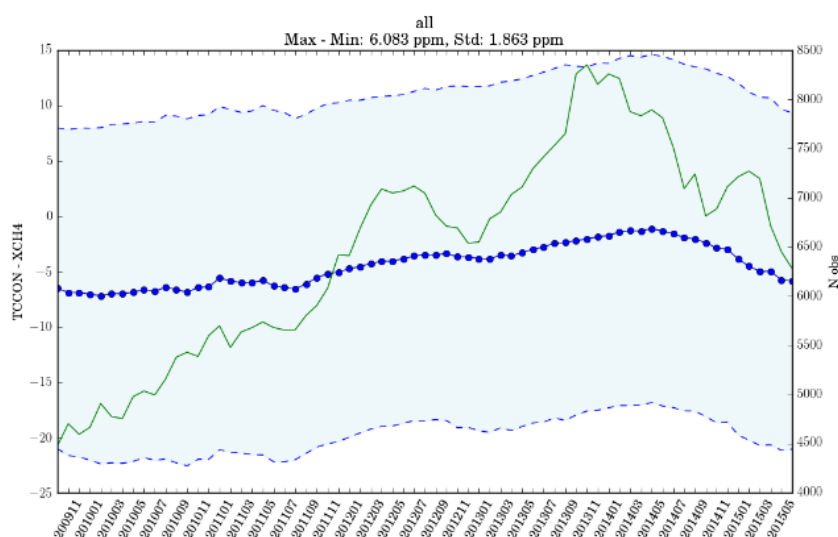


Figure 6.2.3.5: Year-to-year Stability of the TCCON-OCPRv7.0 XCH₄ bias calculated with for +/-6 month averaging window for each month of the GOSAT time series between June 2010 and June 2015. The thick blue symbols give the mean bias for a 12 month period and the shaded area indicates the standard deviation of the data. The green lines gives the number of data points per 12 month period.

The year-to-year variability of the stability has been calculated from the maximum-minimum difference between the bias between GOSAT and TCCON for any 12 month period similar to the section on OCFPv7.0 XCO₂

Global offset	Single meas. precision	Relative accuracy	Product stability
-2.33	13.71	3.92	Linear trend: 0.06 Max-Min (between any 12 month period): 6.083

Table 6.2.3.2. Summary statistics (all units in ppb) for the nearly 7 year OCPRv7.0 XCH₄ dataset as validated with TCCON GGG2014 XCH₄; mean of per-site TCCON mean bias (global offset), standard deviation of all co-located OCPRv7.0–TCCON differences (single measurement precision), standard deviation of per-site OCPRv7.0–TCCON biases (relative accuracy), linear fitting of all OCPRv7.0–TCCON biases and max-min of the OCPRv7.0–TCCON biases for a 12month period (product stability).

6.2.4 Assessment of GOSAT SRFP (RemoTeC) XCH₄

The GOSAT SRFP (RemoTeC) XCH₄ data were obtained using the L1B data of v201 and later as input for the Full Physics retrieval using RemoTeC v2.3.8. Posterior filters as described in the Product User Guide were applied to produce quality flags for the gain H, gain M and sunglint data. These data were then compared to the TCCON XCH₄ measurements based on the following co-location criteria:

- model XCO₂ for GOSAT sounding < 0.25 ppm different than model XCO₂ at TCCON site, as described in Guerlet et al. (2013a) (for gain H only).
- GOSAT sounding within +/- 5 degrees latitude and +/- 8 degrees longitude of TCCON station (for all observation modes).
- GOSAT sounding within +/- 2 hrs of TCCON observation (for all observation modes).

Figure 6.2.4.1 – 6.2.4.6 show the time series comparison between the SRFP/RemoTeC product and TCCON for gain-H, gain-M and sunglint data. **Table 6.2.4.1 – 6.2.4.3** show an overview of the validation.

For the bias correction, we investigated the correlation of the GOSAT-TCCON differences with different geophysical and retrieval parameters. After extensive testing, we found that the best bias correction is obtained by applying a correction with the aerosol filter parameter and solar zenith angle for gain H, aerosol filter parameter for gain M and derived O₂ ratio for sunglint measurements. In all three cases a linear correlation was used.

Gain H: $XCH_4_bias / XCH_4 = 0.996226 + 4.4482e-5 \cdot (\text{aerosol filter parameter}) + 6.0089e-5 \cdot (sza)$

Gain M: $XCH_4_bias / XCH_4 = 1.002728 + 1.0053e-5 \cdot (\text{aerosol filter parameter})$

Sunglint: $XCH_4_bias / XCH_4 = 1.18122 - 0.18569 \cdot RO_2$

One important note for the gain M and sunglint data is that the total number of datapoints is limited.



ESA Climate Change Initiative (CCI)

**Product Validation and
Intercomparison Report (PVIR)**

for the Essential Climate Variable (ECV)
Greenhouse Gases (GHG)

Page 150

Version 5.0
Final

9 Feb 2017

TCCON site	Number of co-locations [-]	Mean difference [ppb]	Standard deviation of difference [ppb]
Bialystok, Poland	1419	0.51	14.13
Bremen, Germany	535	0.87	15.16
Darwin, Australia	4831	-1.87	10.58
Garmisch, Germany	723	6.21	14.72
Karlsruhe, Germany	1028	1.69	13.97
Lamont, USA	7896	-1.03	15.23
Lauder, New Zealand	111	8.04	16.97
Orleans, France	1013	0.28	14.33
Park Falls, USA	3398	5.41	14.44
Saga, Japan	438	0.81	17.27
Sodankyla, Finland	298	6.31	14.34
Wollongong, Australia	2994	-2.78	14.04
TOTAL	24684	-0.35	14.30

Table 6.2.4.1: Overview of the SRFP/RemoTeC XCH₄ validation with TCCON for gain H (after bias correction). Standard deviations are based on comparison of individual data points.

TCCON site	Number of co-locations [-]	Mean difference [ppb]	Standard deviation of difference [ppb]
Darwin, Australia	185	-3.08	10.77
Dryden, USA	225	4.44	14.16
Wollongong, Australia	1052	0.28	12.99
TOTAL	1464	0.09	13.11



Table 6.2.4.2: Overview of the SRFP/RemoTeC XCH₄ validation with TCCON for gain M (after bias correction). Standard deviations are based on comparison of individual data points.

TCCON site	Number of co-locations [-]	Mean difference [ppb]	Standard deviation of difference [ppb]
Ascension Island	705	-0.84	11.73
Darwin, Australia	453	-0.25	12.87
Reunion Island	727	0.83	10.56
Wollongong, Australia	205	3.01	11.56
TOTAL	2090	-0.32	11.69

Table 6.2.4.3: Overview of the SRFP/RemoTeC XCH₄ validation with TCCON for sunglint (after bias correction). Standard deviations are based on comparison of individual data points.

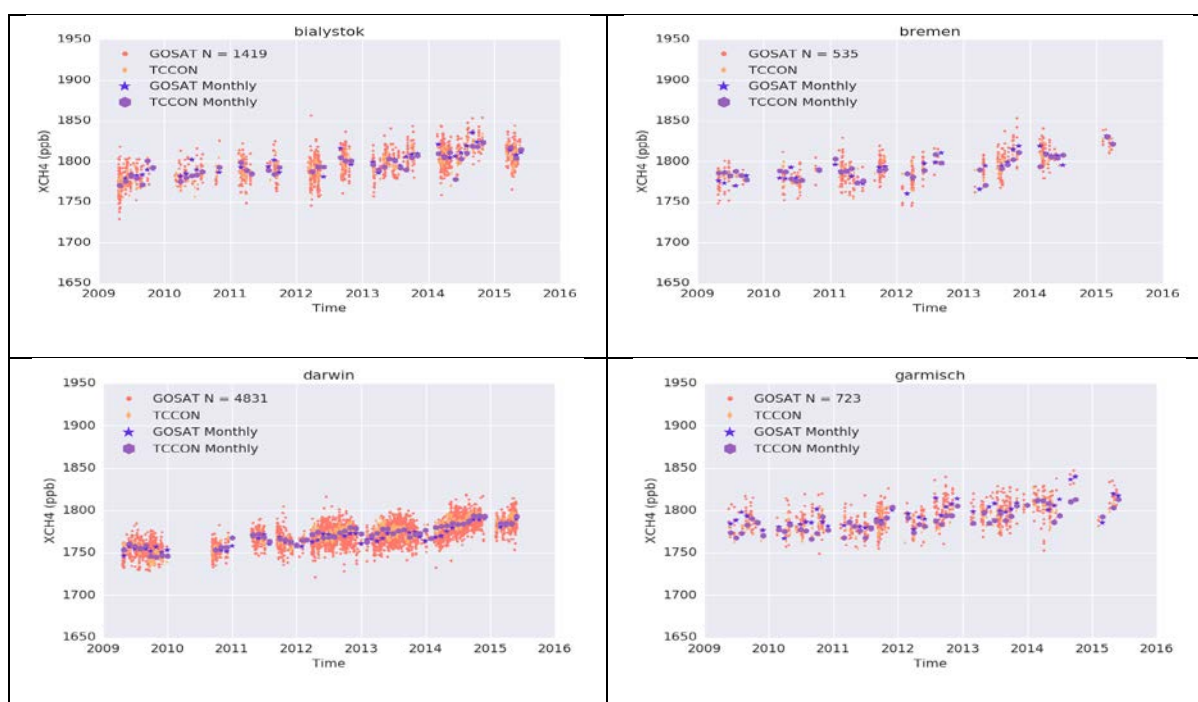


Figure 6.1.4.1: Difference between TCCON and GOSAT (after bias correction) for gain H and TCCON stations 1-4.



ESA Climate Change Initiative (CCI)

Product Validation and Intercomparison Report (PVIR)

for the Essential Climate Variable (ECV)
Greenhouse Gases (GHG)

Page 152

Version 5.0
Final

9 Feb 2017

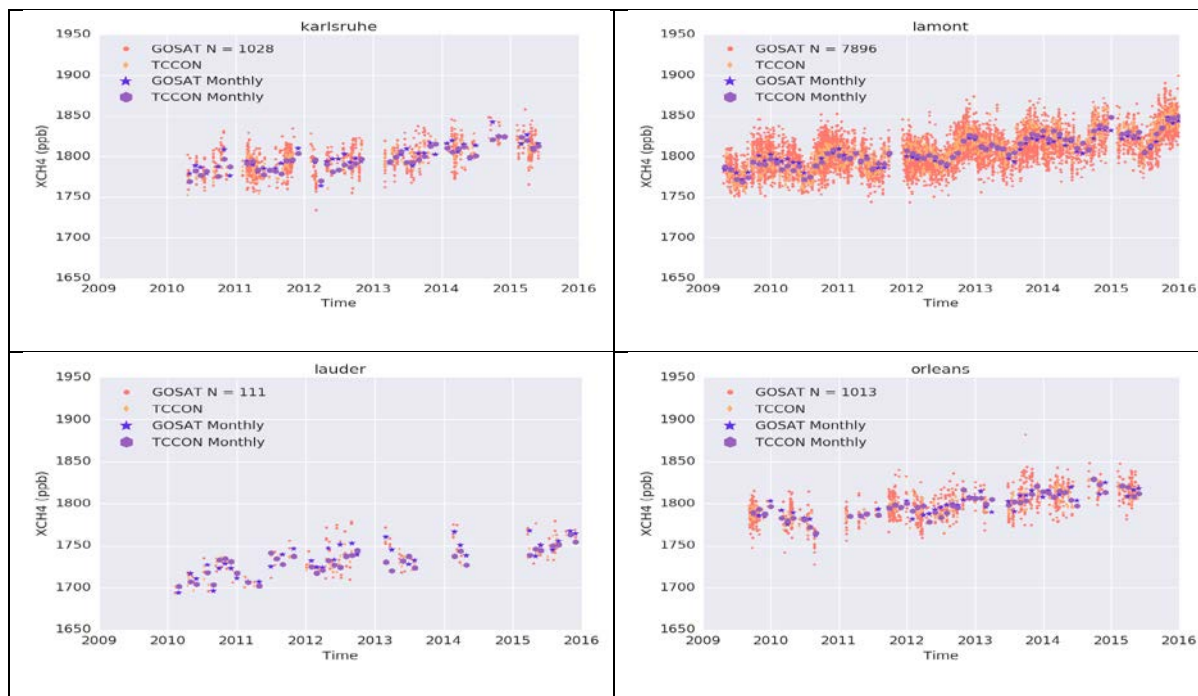


Figure 6.1.4.2: Difference between TCCON and GOSAT (after bias correction) for gain H and TCCON stations 5-8

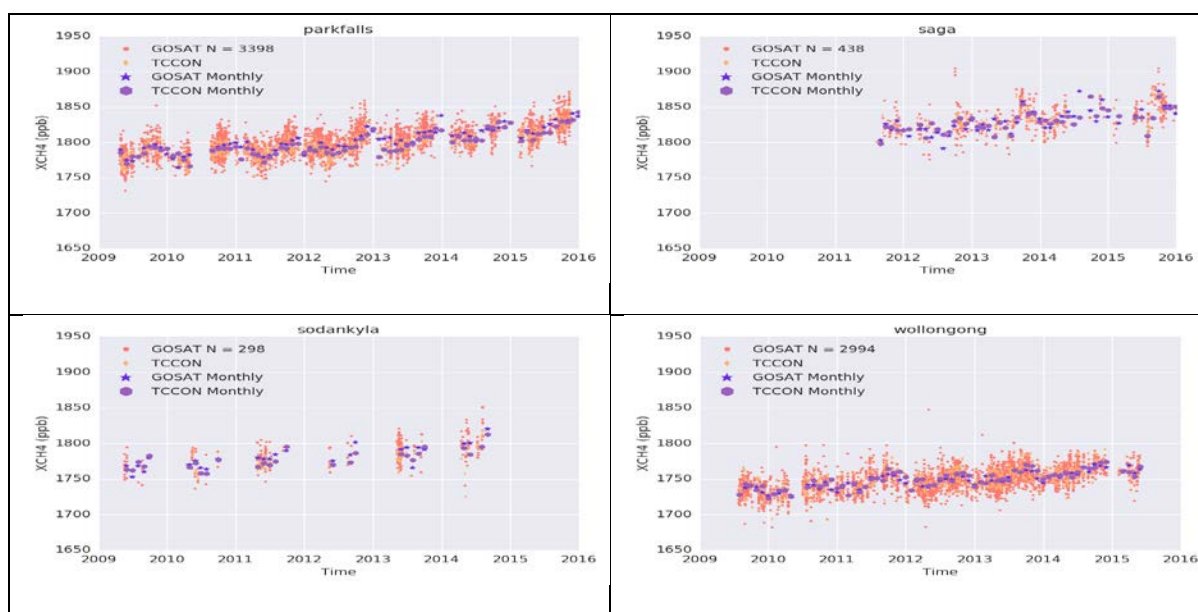


Figure 6.1.4.3: Difference between TCCON and GOSAT (after bias correction) for gain H and TCCON stations 9-12.



ESA Climate Change Initiative (CCI)

**Product Validation and
Intercomparison Report (PVIR)**

for the Essential Climate Variable (ECV)
Greenhouse Gases (GHG)

Page 153

Version 5.0
Final

9 Feb 2017

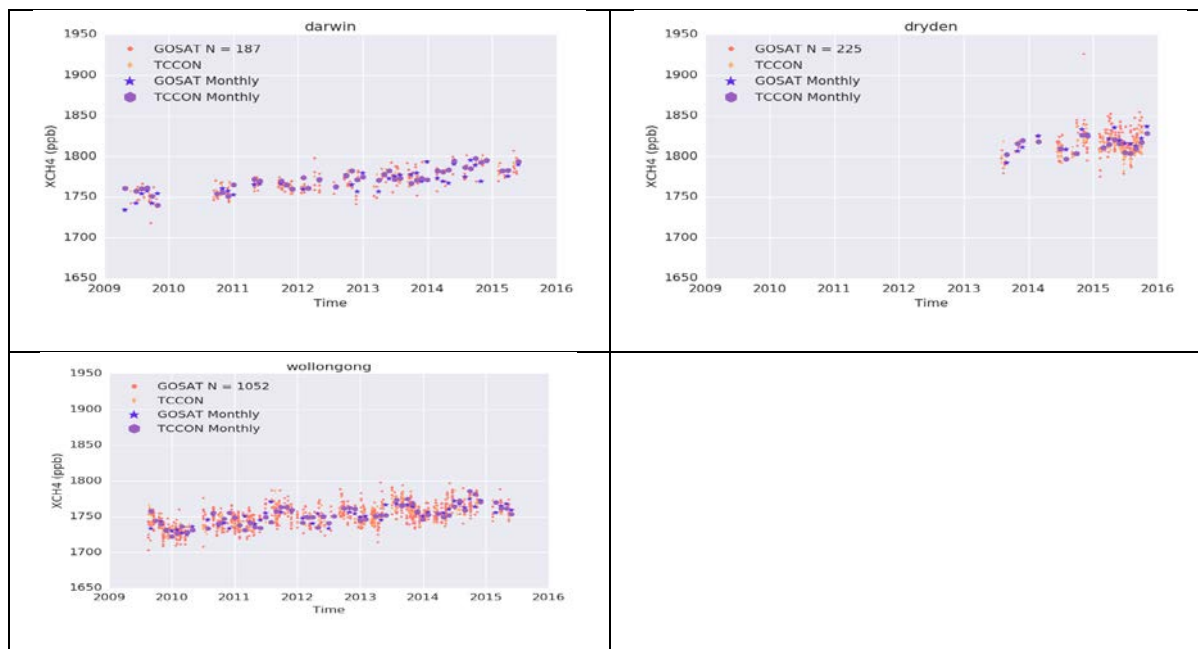


Figure 6.1.4.4: Difference between TCCON and GOSAT (after bias correction) for gain M.

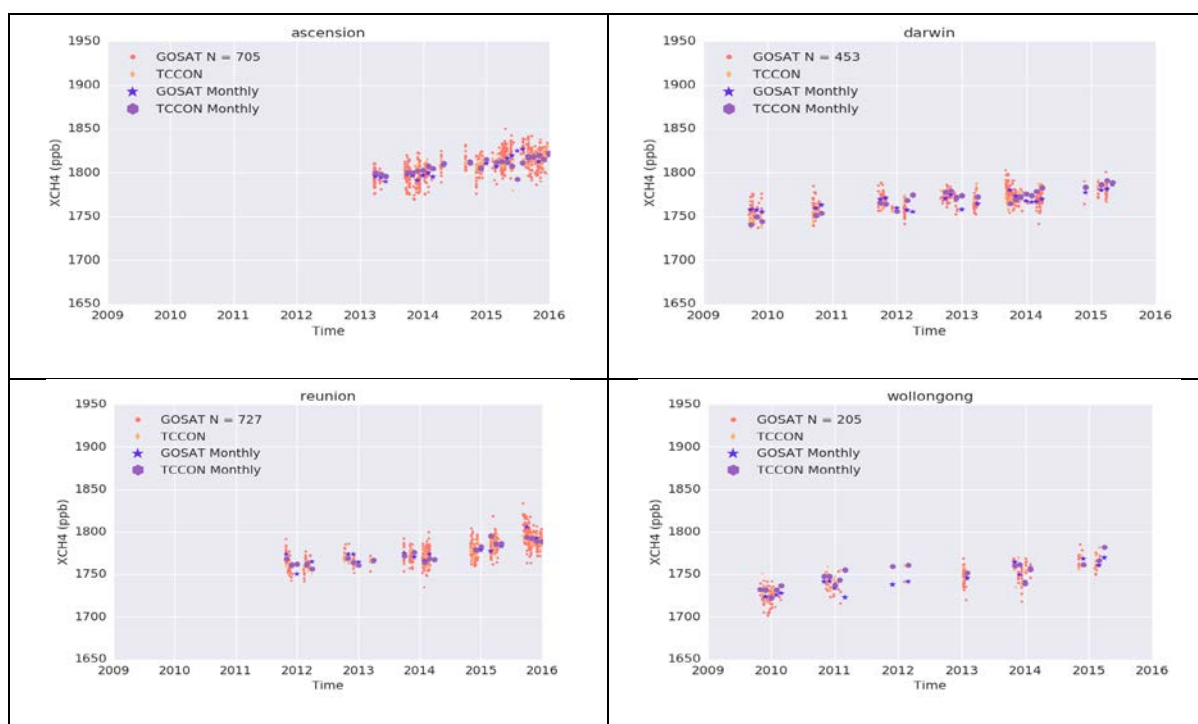



Figure 6.1.4.5: Difference between TCCON and GOSAT (after bias correction) for sunglint observations.

	ESA Climate Change Initiative (CCI)	Page 154
	Product Validation and Intercomparison Report (PVIR)	
	for the Essential Climate Variable (ECV) Greenhouse Gases (GHG)	Version 5.0 Final
		9 Feb 2017

Summary for assessment of GOSAT SRFP XCH₄ product

We have assessed the GOSAT SRFP XCH₄ product against ground-based TCCON observations for each of the three different observation settings (gain H, gain M and sunglint). The standard deviation is similar (14.3 ppb instead of 14.4 ppb) while the total bias is very similar and the stations to station bias decreased to 3.41 ppb. Sodankyla and Garmisch as well as Lauder seem to be outliers with remaining positive biases of around 6-7 ppb. Sunglint and especially gain M measurements are still hard to validate due to the lack of suitable TCCON stations at sea-level near the ocean or near high albedo scenes (i.e. deserts).

The SRFP XCH₄ v.2.3.8 product shows no significant linear trend over the whole period (2009-2015). The year-to-year variability has been obtained by calculating the maximum peak to peak difference of the GOSAT –TCCON remaining bias, yearly averaged, for the 7 year period.

The obtained year-to-year variability is 5.37 ± 1.97 ppb. By itself the variability is significant, however it is not certain that this is caused by any instrument variability, as the sampling of TCCON varies from year to year due to a non-uniform co-location and measurement density of TCCON and GOSAT.

Summary table:

Estimates of achieved data quality: CRDP#4 CH ₄ _GOS_SRFP					
Sensor	Algorithm	Random error [ppb]	Systematic error [ppb]	Stability [ppb / year]	Comments
TANSO on GOSAT	SRFP v2.3.8 (RemoTeC)	14.3	3.4	Linear trend: -0.82 ± 1.91 ppb Year-to-year: 5.37 ± 1.97 ppb	Stability: Significance?: Trend: no Year-to-year: ye
All values are 1-sigma (except for stability); Note: "Year-to-year" stability refers to assessment results related to the extended definition of stability as given in URDv2.1, which now also covers "inter-annual error changes"					

6.2.5 Assessment of GOSAT SRPR (RemoTeC) XCH₄

The GOSAT SRPR (RemoTeC) XCH₄ data were obtained using the L1B data of v201 and later as input for the Non-Scattering retrieval using RemoTeC v2.3.8. Posterior filters as described in the Product User Guide were applied to produce quality flags for the gain H, gain M and sunglint data. These data were then compared to the TCCON XCH₄ measurements based on the following co-location criteria:

- model XCO₂ for GOSAT sounding < 0.25 ppm different than model XCO₂ at TCCON site, as described in Guerlet et al. (2013a)
- GOSAT sounding within +/- 5 degrees latitude and +/- 8 degrees longitude of TCCON station.
- GOSAT sounding within +/- 2 hrs of TCCON observation

Figure 6.2.5.1 – 6.2.5.6 show the time series comparison between the SRPR/RemoTeC product and TCCON for gain-H, gain-M and sunglint data. **Table 6.2.5.1 – 6.2.5.3** show an overview of the validation.

For the bias correction, we investigated the correlation of the GOSAT-TCCON differences with different geophysical and retrieval parameters. After extensive testing, we found that the best bias correction is obtained by applying a correction with the albedo at 1.6 um parameter. In the case of gain H and gain M a linear correlation was used, while for the sunglint observations a constant offset was deemed better.

Gain H: $XCH_4_bias / XCH_4 = 0.9869 + 0.01788 \cdot (\text{albedo at } 1.6\mu\text{m parameter})$

Gain M: $XCH_4_bias / XCH_4 = 0.9845 + 0.01892 \cdot (\text{albedo at } 1.6\mu\text{m parameter})$

Sunglint: $XCH_4_bias / XCH_4 = 0.992557$

The average offset w.r.t TCCON before bias correction is around + 14 ppb



TCCON site	Number of co-locations [-]	Mean difference [ppb]	Standard deviation of difference [ppb]
Bialystok, Poland	3850	-0.70	14.99
Bremen, Germany	1392	-0.18	15.37
Darwin, Australia	7161	0.25	11.08
Garmisch, Germany	2332	4.63	14.79
Karlsruhe, Germany	2773	0.38	14.29
Lamont, USA	17962	-1.22	16.06
Lauder, New Zealand	800	4.12	11.86
Orleans, France	3502	-0.94	14.08
Park Falls, USA	10517	3.91	15.06
Saga, Japan	1614	-6.17	17.79
Sodankyla, Finland	2371	-1.12	17.31
Wollongong, Australia	6588	-101	12.44
TOTAL	60682	0.06	14.89

Table 6.2.5.1: Overview of the SRPR/RemoTeC XCH₄ validation with TCCON for gain H (after bias correction). Standard deviations are based on comparison of individual data points.

TCCON site	Number of co-locations [-]	Mean difference [ppb]	Standard deviation of difference [ppb]
Darwin, Australia	338	-6.31	12.15
Dryden, USA	987	3.66	18.39
Wollongong, Australia	1839	-1.26	12.27
TOTAL	3164	-0.36	14.88


	ESA Climate Change Initiative (CCI)	Page 157
	Product Validation and Intercomparison Report (PVIR)	
	for the Essential Climate Variable (ECV) Greenhouse Gases (GHG)	Version 5.0 Final
		9 Feb 2017

Table 6.2.5.2: Overview of the SRPR/RemoTeC XCH₄ validation with TCCON for gain M (after bias correction). Standard deviations are based on comparison of individual data points.

TCCON site	Number of co-locations [-]	Mean difference [ppb]	Standard deviation of difference [ppb]
Ascension Island	4543	0.44	12.52
Darwin, Australia	3210	0.74	13.05
Reunion Island	3832	-1.64	11.91
Wollongong, Australia	869	-6.37	12.75
TOTAL	12454	-0.63	12.66

Table 6.2.5.3: Overview of the SRPR/RemoTeC XCH₄ validation with TCCON for sunglint (after bias correction). Standard deviations are based on comparison of individual data points.



ESA Climate Change Initiative (CCI)

Product Validation and Intercomparison Report (PVIR)

for the Essential Climate Variable (ECV)
Greenhouse Gases (GHG)

Page 158

Version 5.0
Final

9 Feb 2017



Figure 6.2.5.1: Difference between TCCON and GOSAT (after bias correction) for gain H and TCCON stations 1-4.



Figure 6.2.5.2: Difference between TCCON and GOSAT (after bias correction) for gain H and TCCON stations 5-8.



ESA Climate Change Initiative (CCI)

Product Validation and Intercomparison Report (PVIR)

for the Essential Climate Variable (ECV)
Greenhouse Gases (GHG)

Page 159

Version 5.0
Final

9 Feb 2017

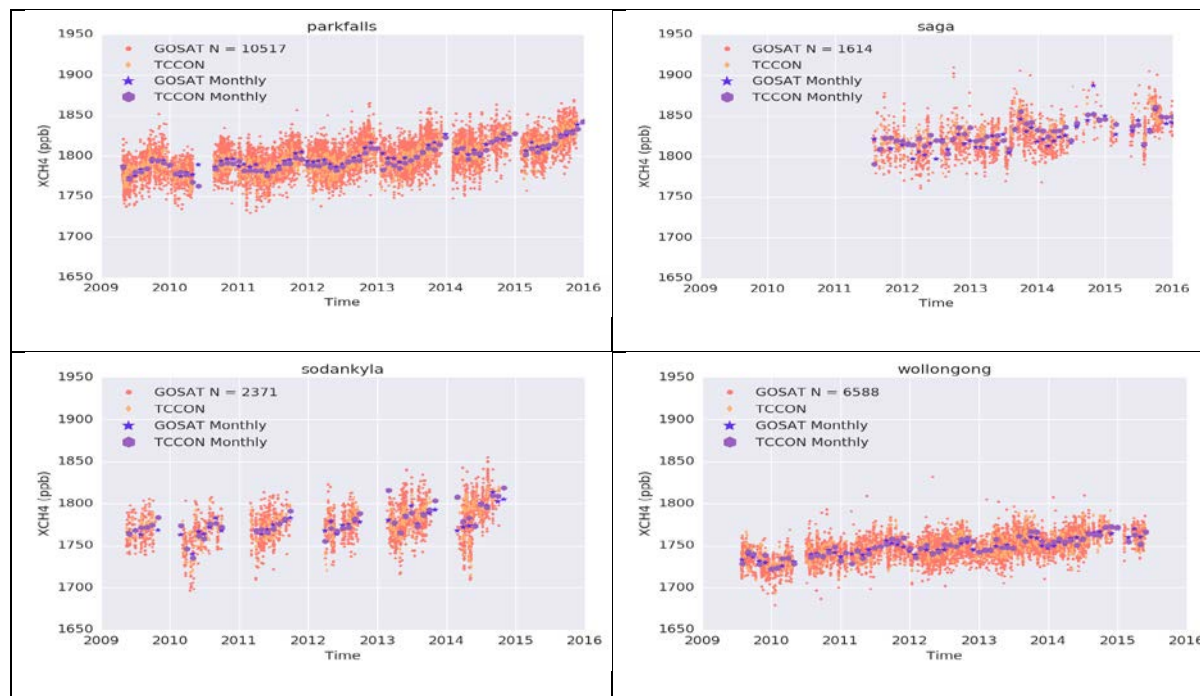


Figure 6.2.5.3: Difference between TCCON and GOSAT (after bias correction) for gain H and TCCON stations 9-12

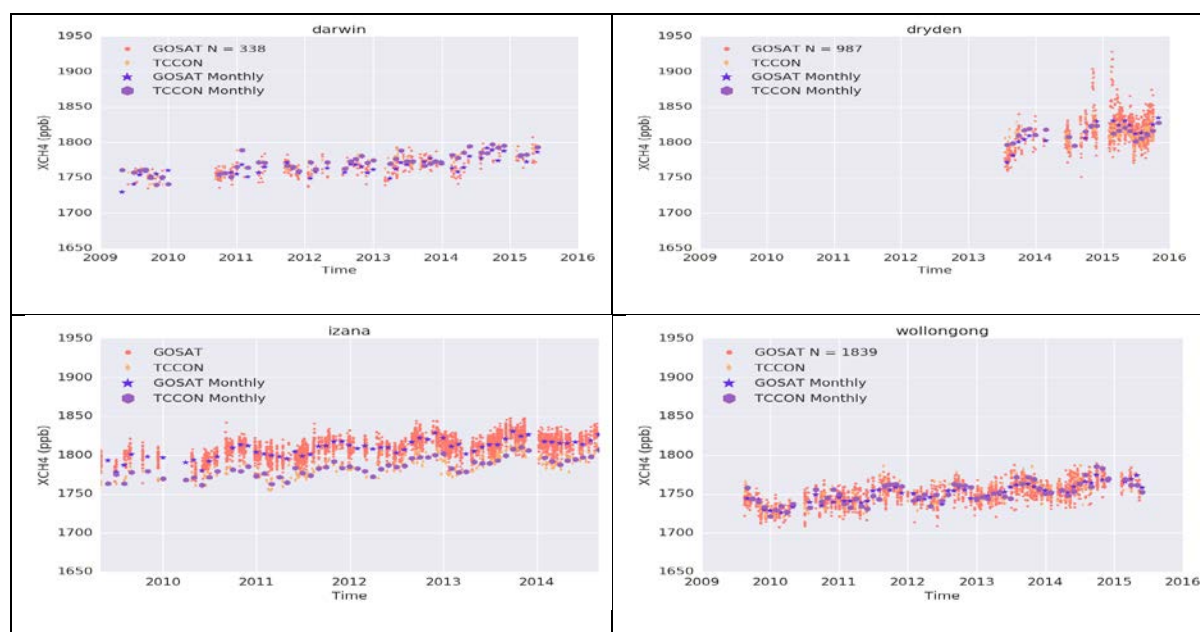


Figure 6.2.5.5: Difference between TCCON and GOSAT (after bias correction) for gain M.



ESA Climate Change Initiative (CCI)

**Product Validation and
Intercomparison Report (PVIR)**

for the Essential Climate Variable (ECV)
Greenhouse Gases (GHG)

Page 160

Version 5.0
Final

9 Feb 2017

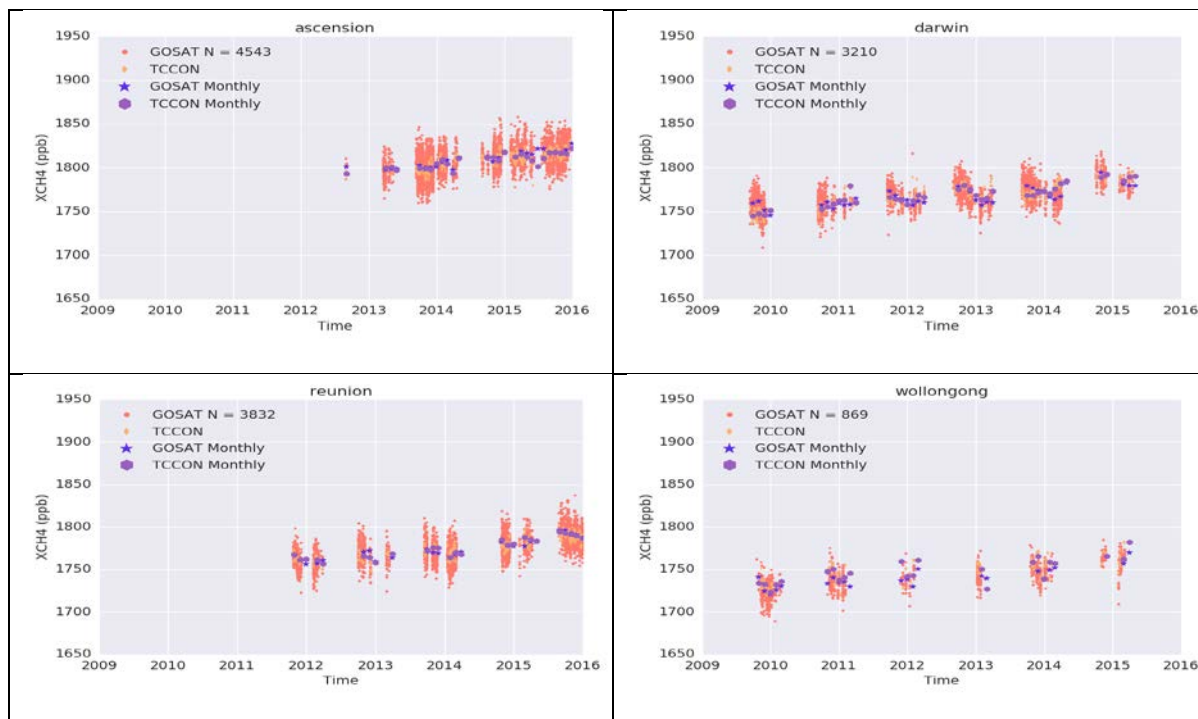



Figure 6.2.5.6: Difference between TCCON and GOSAT (after bias correction) for sunglint observations.

	ESA Climate Change Initiative (CCI)	Page 161
	Product Validation and Intercomparison Report (PVIR)	
	for the Essential Climate Variable (ECV) Greenhouse Gases (GHG)	Version 5.0 Final
		9 Feb 2017

Summary for assessment of GOSAT SRPR XCH₄ product


We have assessed the GOSAT product against ground-based TCCON observations for each of the three different observation settings (gain H, gain M and sunglint). The co-location criterion has been tightened to 0.25 ppm, resulting in a significant decrease in the number of co-locations. The standard deviation is very similar 14.9 instead of 15.0 ppb. The total bias is very similar but the station to station bias has decreased from 3.71 to 2.84 ppb. Sunglint and especially gain M measurements are still hard to validate due to the lack of suitable TCCON stations at sea-level near the ocean or near high albedo scenes (i.e. deserts).

The SRPR XCH₄ v.2.3.8 product shows no significant linear trend over the whole period (2009-2015). The year-to-year variability has been obtained by calculating the maximum peak to peak difference of the GOSAT –TCCON remaining bias, yearly averaged, for the 7 year period.

The obtained year-to-year variability is 6.10 ± 2.21 ppb. By itself the variability is significant, however it is not certain that this is caused by any instrument variability, as the sampling of TCCON varies from year to year due to a non-uniform co-location and measurement density of TCCON and GOSAT.

Summary table:

Estimates of achieved data quality: CRDP#4 CH ₄ _GOS_SRPR					
Sensor	Algorithm	Random error [ppb]	Systematic error [ppb]	Stability [ppb / year]	Comments
TANSO on GOSAT	SRPR v2.3.8 (RemoTeC)	14.9	3.7	Linear trend: -0.82 ± 2.2 ppb Year-to-year: 6.1 ± 2.2 ppb	Stability: Significance?: Trend: no Year-to-year: yes
All values are 1-sigma (except for stability); Note: "Year-to-year" stability refers to assessment results related to the extended definition of stability as given in URDv2.1, which now also covers "inter-annual error changes"					

	ESA Climate Change Initiative (CCI)	Page 162
	Product Validation and Intercomparison Report (PVIR)	
	for the Essential Climate Variable (ECV) Greenhouse Gases (GHG)	Version 5.0 Final
		9 Feb 2017

6.2.6 Assessment of GOSAT OCFP XCH₄

Validation and inter-comparison of results for OCFPv2.0, submitted as University of Leicester's contribution to CRDP4, are summarised in this section. This includes presentation of seasonal mean maps and comparisons with Total Column Carbon Observing Network (TCCON) and MACC model. All OCFPv2.0 data shown make use of the filtered XCH₄ product.

Spatial distributions of OCFPv2.0 XCH₄ seasonal means are presented in **Fig. 6.2.6.1**, along with differences to MACC S1NOAAv10 model data (available only until end 2012) in **Fig. 6.2.6.2**. As in the proxy section, the stratospheric column in MACC has been replaced with calculations by the TOMCAT model. Again, spatial distribution and magnitudes of OCFPv2.0 are in line with expected values for each season, as shown by comparison to MACC data, where major deviations (± 30.0 ppb) from model data do not occur over any great portion of the globe. Larger differences occur over South-America in spring and summer and over Arabian Peninsula and North-Eastern Africa in summer.



ESA Climate Change Initiative (CCI)

**Product Validation and
Intercomparison Report (PVIR)**

for the Essential Climate Variable (ECV)
Greenhouse Gases (GHG)

Page 163

Version 5.0
Final

9 Feb 2017

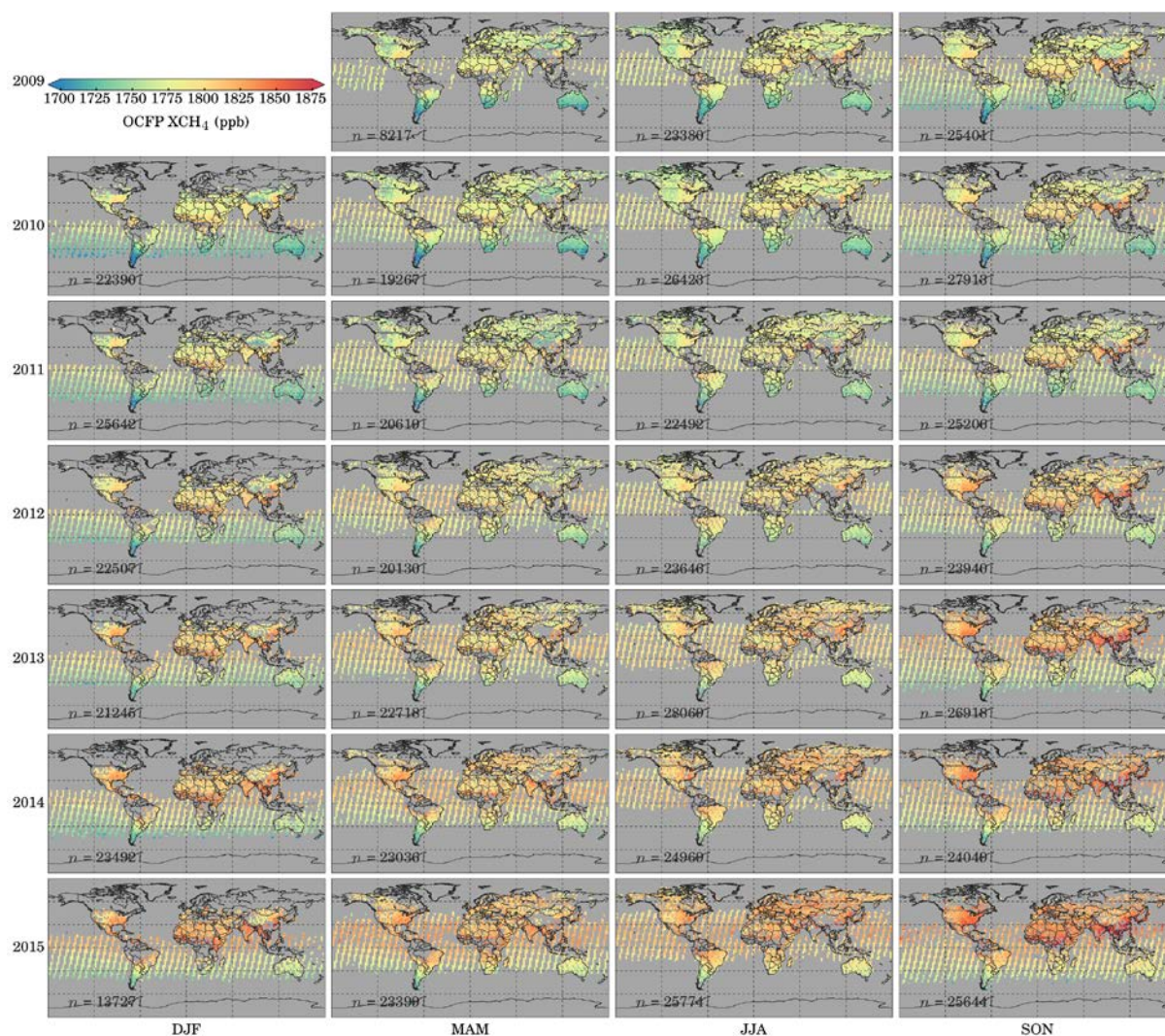


Figure 6.2.6.1. Seasonal means of filtered OCFPv2.0 XCH₄ for 2009–2015.

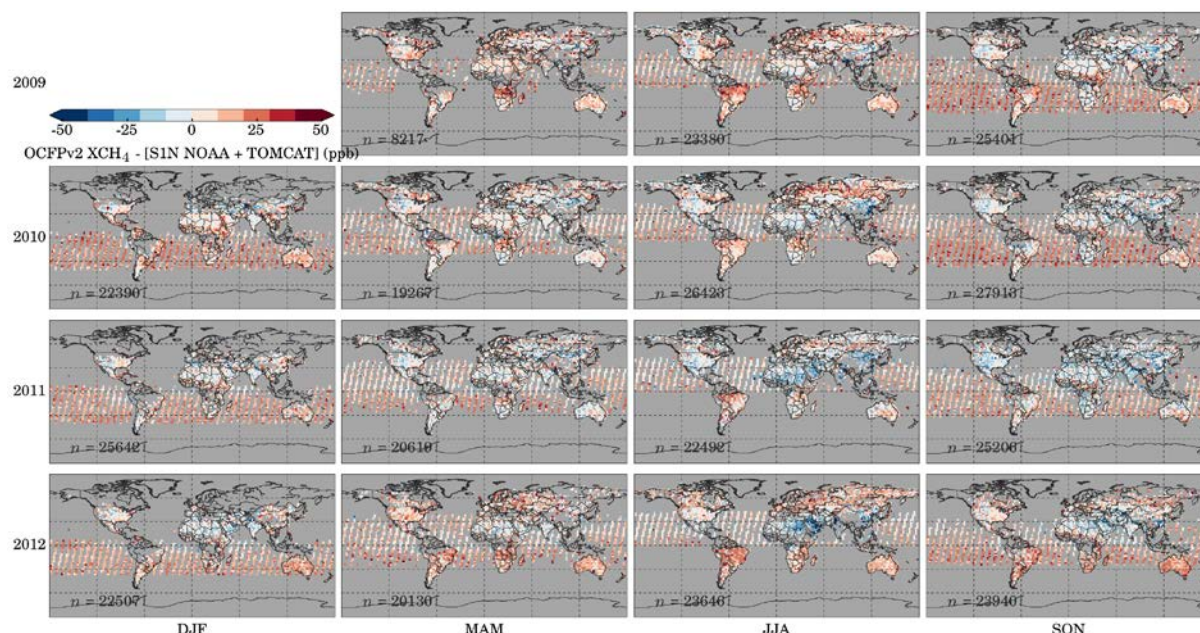


Figure 6.2.6.2. Seasonal means of differences between OCFPv2.0 (as above) and MACC S1NOAAv10 XCH₄

Figure 6.2.6.3 demonstrates validation of OCFPv2.0 with TCCON observations of XCH₄, encompassing Fourier transform spectroscopy measurements made at 14 TCCON sites available within the GGG2014 dataset. Bias (calculated as TCCON-OCFPv2.0), correlation, and standard deviation of the bias are annotated on each sub-plot per site, and repeated in **Tab. 6.2.6.1**. Measurement parameters relating to OCFPv2.0 stability are presented in **Tab. 6.2.6.2**. **Figure 6.2.6.4** details OCFPv2.0 observations and MACC S1NOAAv10 modelled XCH₄ interpolated to time and location of OCFP measurements, subset to Transcom regions. For TCCON and MACC comparisons, OCFPv2.0 is seen to capture the seasonal cycle well, albeit with a high bias for OCFPv2.0 against MACC data in the southern hemisphere.



ESA Climate Change Initiative (CCI)

**Product Validation and
Intercomparison Report (PVIR)**

for the Essential Climate Variable (ECV)
Greenhouse Gases (GHG)

Page 165

Version 5.0
Final

9 Feb 2017

Site	Mean Δ	$\sigma\Delta$	r	n obs.
Sodankyla, Finland	-7.42	16.47	0.69	413
Bialystok, Poland	-3.93	13.69	0.78	610
Bremen, Germany	-1.24	13.39	0.74	286
Karlsruhe, Germany	-3.45	14.05	0.67	724
Orleans, France	0.09	13.18	0.77	885
Garmisch, Germany	-7.14	14.25	0.69	768
Park Falls, Wisconsin, USA	-6.77	14.13	0.77	1103
Lamont, Oklahoma, USA	3.22	14.63	0.81	5002
Tsukuba, Ibaraki, Japan, 125HR	-3.31	13.60	0.75	459
Saga, Japan	0.28	14.96	0.76	317
Darwin, Australia	0.34	10.42	0.78	1427
Wollongong, Australia	3.96	15.28	0.64	1638
Lauder, New Zealand, 125HR	-1.30	11.72	0.79	209
Lauder, New Zealand, 120HR	2.53	13.46	0.47	47

Table 6.2.6.1. Site statistics for OCFP comparisons against TCCON, with mean Δ and $\sigma\Delta$ in ppb.



ESA Climate Change Initiative (CCI)

**Product Validation and
Intercomparison Report (PVIR)**

for the Essential Climate Variable (ECV)
Greenhouse Gases (GHG)

Page 166

Version 5.0
Final

9 Feb 2017

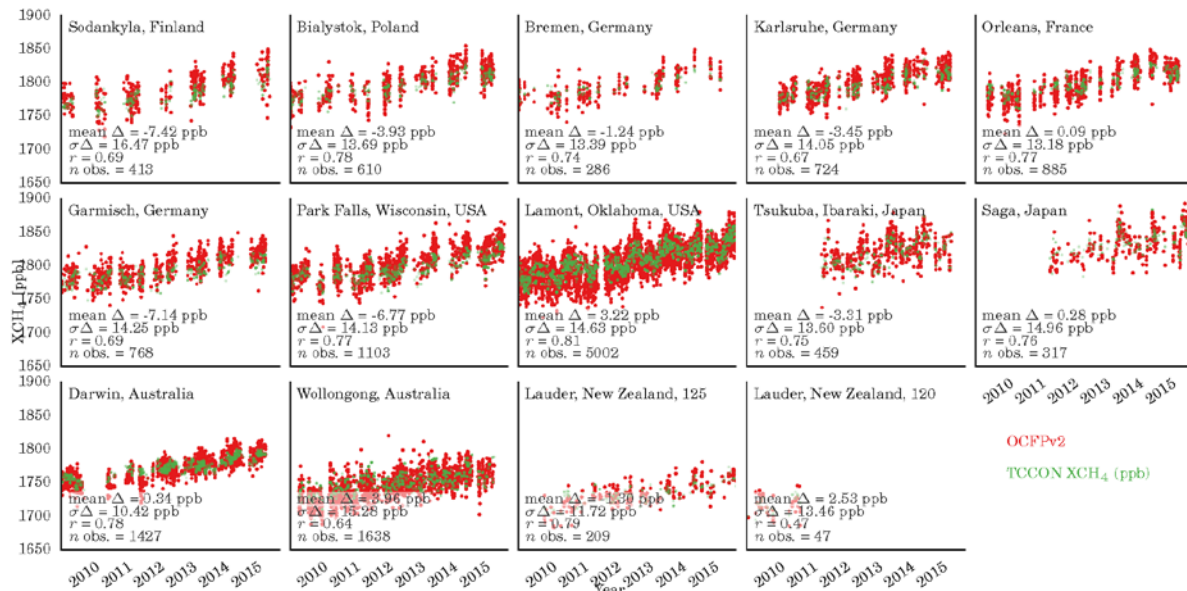


Figure 6.2.6.3. TCCON GGG2014 (green) and OCFPv2.0 (red) XCH₄ observations; OCFP observations are co-located with TCCON sites using a <550km spatial and ±2 hour temporal criteria.

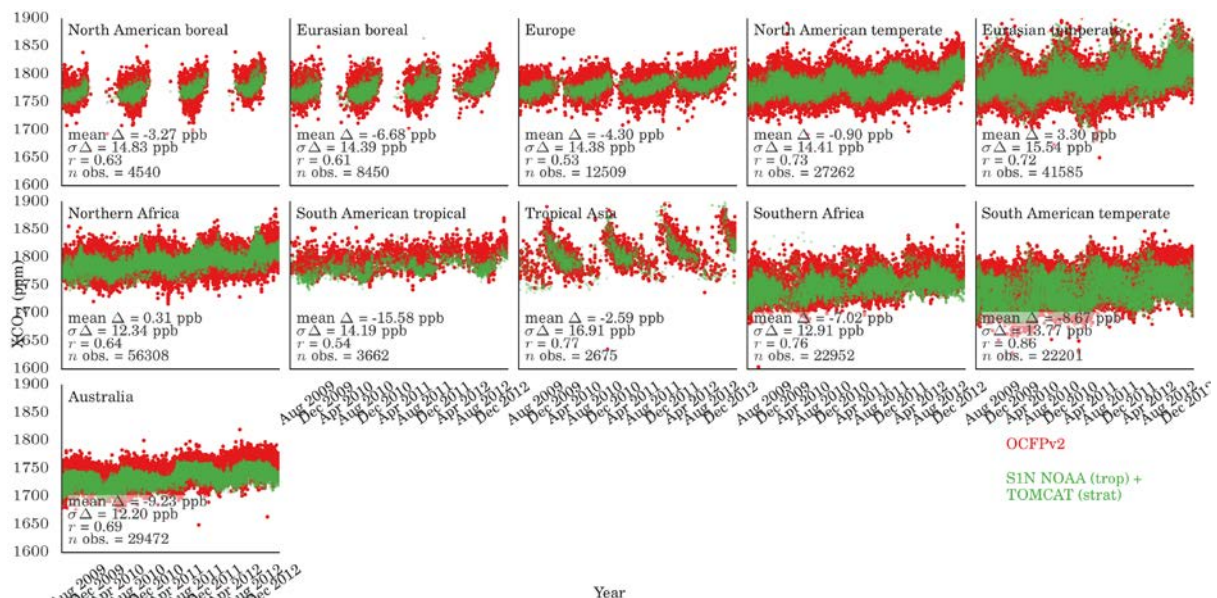


Figure 6.2.6.4. Subset to Transcom basis map regions, OCFPv2.0 (red) and MACC S1NOAAv10 XCH₄ (green) interpolated to OCFP time and location (with OCFP averaging kernel applied).



ESA Climate Change Initiative (CCI)

**Product Validation and
Intercomparison Report (PVIR)**

for the Essential Climate Variable (ECV)
Greenhouse Gases (GHG)

Page 167

Version 5.0
Final

9 Feb 2017

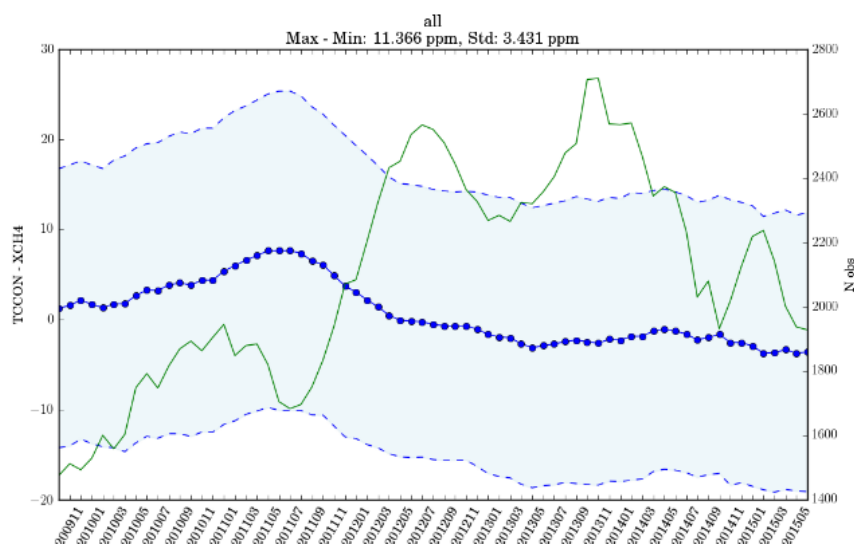



Figure 6.2.6.5. Year-to-year Stability of the TCCON-OCFPv2.0 XCH₄ bias calculated with for +/-6 month averaging window for each month of the GOSAT time series between June 2010 and June 2015. The thick blue symbols give the mean bias for a 12 month period and the shaded area indicates the standard deviation of the data. The green lines gives the number of data points per 12 month period.

The year-to-year variability of the stability has been calculated from the maximum-minimum difference between the bias between GOSAT and TCCON for any 12 month period similar to the section on OCPRv7.0 XCH₄

Global offset	Single meas. precision	Relative accuracy	Product stability
-1.72	14.61	3.63	Linear Trend: 0.43 Max-Min (between any 12 month period): 11.366

Table 6.2.6.2. Summary statistics (all units in ppb) for the nearly 6 year OCFPv2.0 XCH₄ dataset as validated with TCCON GGG2014 XCH₄; mean of per-site TCCON mean bias (global offset), standard deviation of all co-located OCFPv2.0–TCCON differences (single measurement precision), standard deviation of per-site OCFPv2.0–TCCON biases (relative accuracy), linear fitting of all OCFP2.0–TCCON biases and max-min of the OCFPv2.0–TCCON biases for a 12month period (product stability).

	ESA Climate Change Initiative (CCI)	Page 168
	Product Validation and Intercomparison Report (PVIR)	
	for the Essential Climate Variable (ECV) Greenhouse Gases (GHG)	Version 5.0 Final
		9 Feb 2017

6.3 Assessment of ACA products

6.3.1 Assessment of CO₂_AIR_NLIS (no update)

This product has been generated in GHG-CCI Phase 1 for CRDP#1. This product and its documentation (including **/PVIRv2 CRDP#1/**) is available via the GHG-CCI website (<http://www.esa-ghg-cci.org/> -> CRDP (Data)).

It is not planned to update this product within GHG-CCI Phase 2.

6.3.2 Assessment of CO₂_IAS_NLIS

Validation of CO₂_IAS_NLIS product from LMD and delivered as part of CRDP4 is summarised in this section. CO₂ partial columns covering the mid-to-upper troposphere are provided for every cloud-free field-of-view in the tropical band, together with associated vertical sensitivity.

Figure 6.3.2.1. shows the summary of validation done with aircraft measurements made in the framework of the CONTRAIL program, for which CO₂ values are provided at an altitude of ~10 km, close to the maximum sensitivity of IASI to CO₂. Over IASI-CONTRAIL co-located pairs, the comparison yields a difference of 0.57 ± 0.99 ppm.

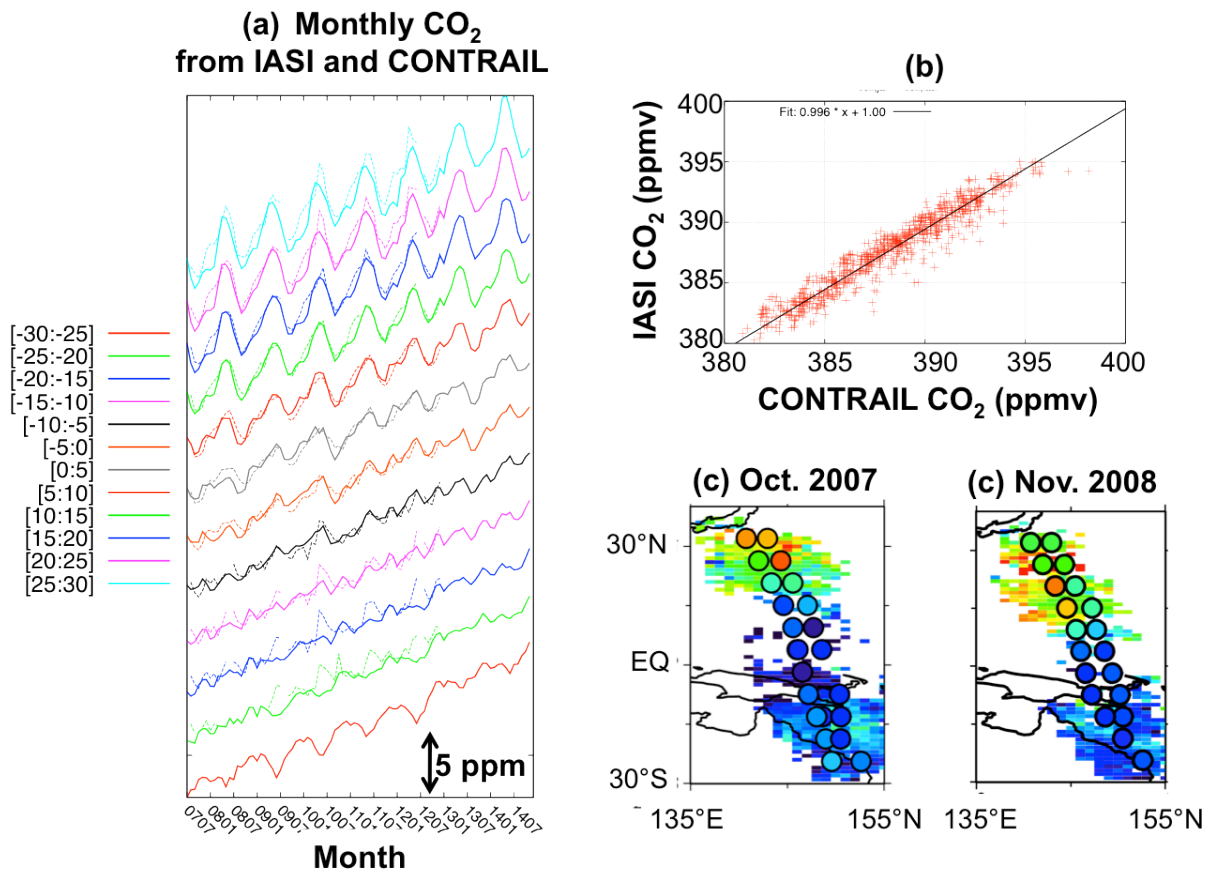



Figure 6.3.2.1. (a) Monthly evolution of CO_2 partial column from IASI and mixing ratio at 10 km measured by CONTRAIL in 12 latitudinal bands of 5° each. (b) IASI CO_2 vs. CONTRAIL CO_2 for all the 250 pairs. (c) IASI CO_2 (points) and CONTRAIL CO_2 (dots) for October 2007. (d) Same as (c) but for November 2008.

	ESA Climate Change Initiative (CCI)	Page 170
	Product Validation and Intercomparison Report (PVIR)	
	for the Essential Climate Variable (ECV) Greenhouse Gases (GHG)	Version 5.0 Final
		9 Feb 2017

6.3.3 Assessment of CO₂_ACE_CLSR (no update)

This product has been generated in GHG-CCI Phase 1 for CRDP#1 and update in Phase 2 for CRDP#2. These products and associated documentations are available via the GHG-CCI website (<http://www.esa-ghg-cci.org/> -> CRDP (Data)).

It is not planned to update this product any longer, as long as relevant spectroscopy studies concerning the N₂ continuum and the CO₂ absorption in the 4 µm band are not undertaken in order to correct the strong effects of the temperature (especially T<200 in the tropics).

6.3.4 Assessment of CO₂_SCI_ONPD (no update)

The CO₂_SCI_ONPD product described in the following has not been updated for CRDP#3, i.e., the product is identical with the CRDP#2 product. The following description and analysis is therefore identical with the previous version of this document. However, a publication for a peer-reviewed scientific journal has been written /Noël et al., 2016/.

The SCIAMACHY ONPD CO₂ stratospheric profiles have been compared with collocated CarbonTracker (CT2013) data provided by NOAA ESRL, Boulder, Colorado, USA from the website at <http://carbontracker.noaa.gov>. The results are shown in **Figure 6.3.4.1**.

SCIAMACHY ONPD CO₂ has compared to CarbonTracker on average no significant bias; this is an improvement with respect to the product version for CRDP#1. However, there is a pronounced oscillation with altitude visible in the mean difference between SCIAMACHY and CT2013. Because similar oscillations are seen for other ONPD products (see e.g. methane below), it is assumed that these altitude variations are an artefact of the ONPD retrieval. However, CarbonTracker is mainly a tropospheric model and has only a limited sampling in the stratosphere, therefore this issue needs further investigation. The amplitude of this oscillation is about 10 ppm (3%). This oscillation is currently considered to be the most limiting factor for the accuracy of the SCIAMACHY ONPD CO₂ product.

The mean error of the SCIAMACHY CO₂ product is about 4 ppm (1%) at 17 km, increasing to about 16 ppm (4%) at 45 km. These errors are significantly smaller than in the CRDP#1 product. Probably because of the larger variability of the SCIAMACHY data, the maximum correlation with CarbonTracker CO₂ is only about 0.4.



ESA Climate Change Initiative (CCI)

Product Validation and Intercomparison Report (PVIR)

for the Essential Climate Variable (ECV)
Greenhouse Gases (GHG)

Page 171

Version 5.0
Final

9 Feb 2017

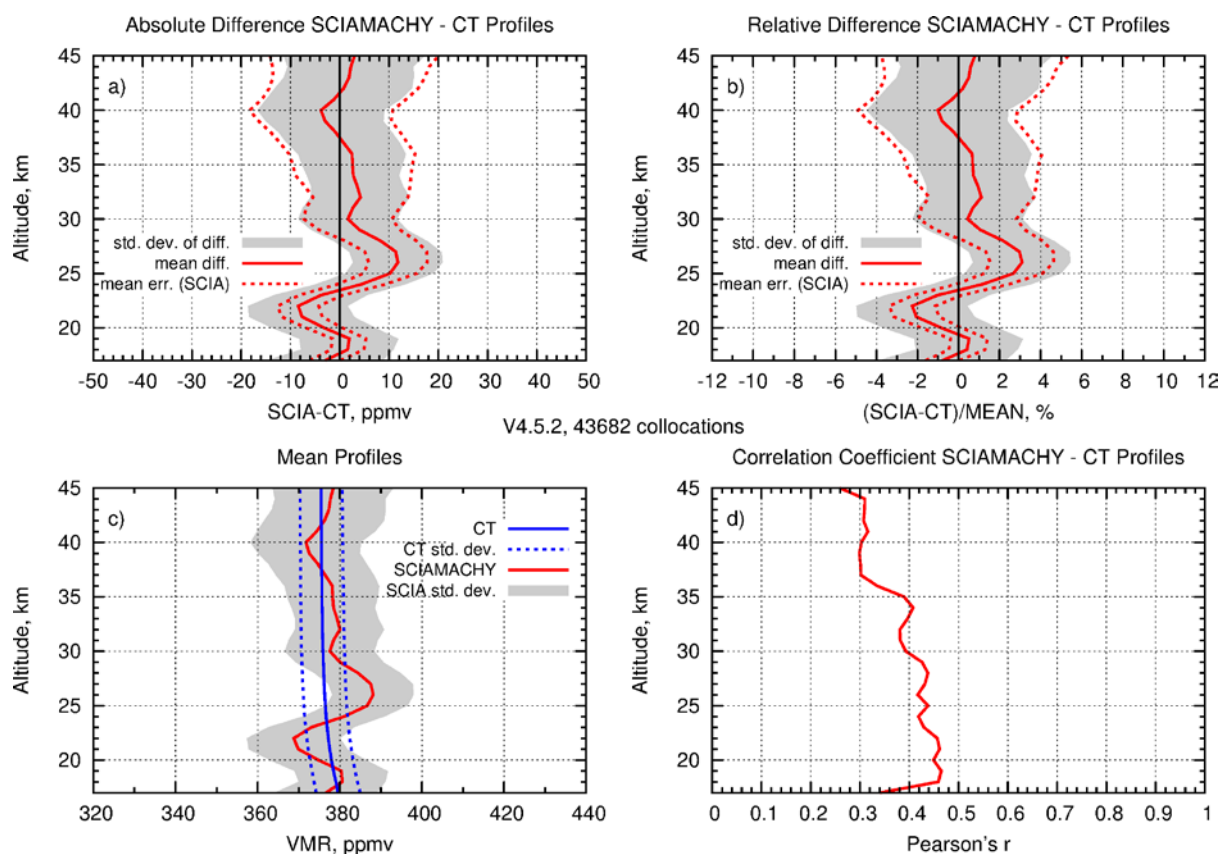



Figure 6.3.4.1: Comparison of SCIAMACHY ONPD CO₂ results (V4.5.2) with collocated Carbon Tracker (CT2013) data. a) Absolute differences and error. b) Relative differences and error. c) Mean profiles. d) Correlation coefficient.

	ESA Climate Change Initiative (CCI)	Page 172
	Product Validation and Intercomparison Report (PVIR)	
	for the Essential Climate Variable (ECV) Greenhouse Gases (GHG)	Version 5.0 Final
		9 Feb 2017

6.3.5 Assessment of CH₄_IAS_NLIS

Validation of CH₄_IAS_NLIS product from LMD and delivered as part of CRDP4 is summarised in this section. CH₄ partial columns covering the mid-troposphere are provided for every cloud-free field-of-view, together with associated vertical sensitivity. Compared to CRDP#3, two major updates have been made: (i) extension of the coverage to extra-tropical regions; (ii) processing of IASI onboard Metop-B. Four different types of validation have been carried on: (i) use of 0-30 km profiles of CH₄ measured by AirCores in Canada and Finland; (ii) use of aircraft 0-10 km profiles measured during the HIPPO campaigns; (iii) use of comparison with radiative transfer simulations; (iv) comparison between IASI/Metop-A and IASI/Metop-B retrieved values.

Figure 6.3.5.1. shows the comparison between IASI/Metop-A CH₄ columns and columns computed from 7 AirCore 0-30 km profiles to which IASI averaging kernels of co-located IASI observations have been applied. These AirCore profiles were acquired either from Timmins (Ontario, Canada) (Membrive et al., 2016) or Sodankylä (Finland). The comparison yields a difference of -2.0 ± 7.9 ppb.

Figure 6.3.5.2 shows the same comparison as for figure 6.3.5.1 but with aircraft profiles from the 5 HIPPO campaigns. Since these profiles stop at ~10 km of altitude, use has been made of LMDz simulated profiles that have been co-located to HIPPO flights. The comparison with IASI CH₄ partial columns yields a difference of 3.0 ± 15.0 ppb in the tropics, but a very large difference of XX in the northern hemisphere. This is attributed to a strong over-estimation of CH₄ by LMDz in the stratosphere, which is confirmed by a direct comparison between LMDz profiles and AirCore profiles. When imposing stratospheric values closer to what is measured by the AirCores, the bias between IASI and HIPPO+LMDz CH₄ comes down to ~5 ppbv.

Figure 6.3.5.3 shows the validation of CH₄_IAS_NLIS product based on radiative transfert simulations. Atmospheric situations from the Analyzed Radio-Sounding Archive (ARSA) developed at LMD and described by their atmospheric profiles of temperature and water vapor are used as inputs to the radiative transfer code 4A/OP to simulate IASI radiances which are then compared to IASI observed radiances for co-located observations. All together, ~100 IASI-ARSA pairs are available per month, which gives extremely robust statistics. An example of the monthly evolution of calc-obs spectral residuals for one of the IASI channels sensitive to CH₄ is plotted in the figure for 2 different inputs: when CH₄ is kept at 1860 ppb (red) and when CH₄ is the one retrieved from IASI. For the former, the trend and seasonality of CH₄ is well seen on the residual, whereas for the latter both have disappeared, with a variation of ~0.1 K over the whole period, which confirms that the corresponding signal as well been extracted from the radiances (Crevoisier et al., submitted, 2016). It has to be stated that, as opposed to retrieval methods based on Bayesian techniques that aim at reducing the bias between observations and simulations from a forward radiative transfer code, the minimization of such differences is not part of the retrieval process used in this study.



Figure 6.3.5.4 shows the seasonal maps (3 month average) of mid-tropospheric CH₄ for the year 2014 retrieved from Metop-A and Metop-B, as well as the difference between the two and the associated standard deviation. The Metop-A and -B derived fields are close to each other. However, a small but negative bias over tropical oceans and a small but positive bias over Africa and to a lesser extent Australia can be observed on the map. These biases appear to be constant throughout the year. Such constant biases might be due to the fact that the systematic radiances for Metop-B used in the retrieval process have been computed over a reduced period, with very few radiosoundings over sea and without taking into account any potential scan dependency. The availability of more years of observations to compute the radiative biases will help clarifying this point. The consistency of cloud detections between both satellites should also be assessed.

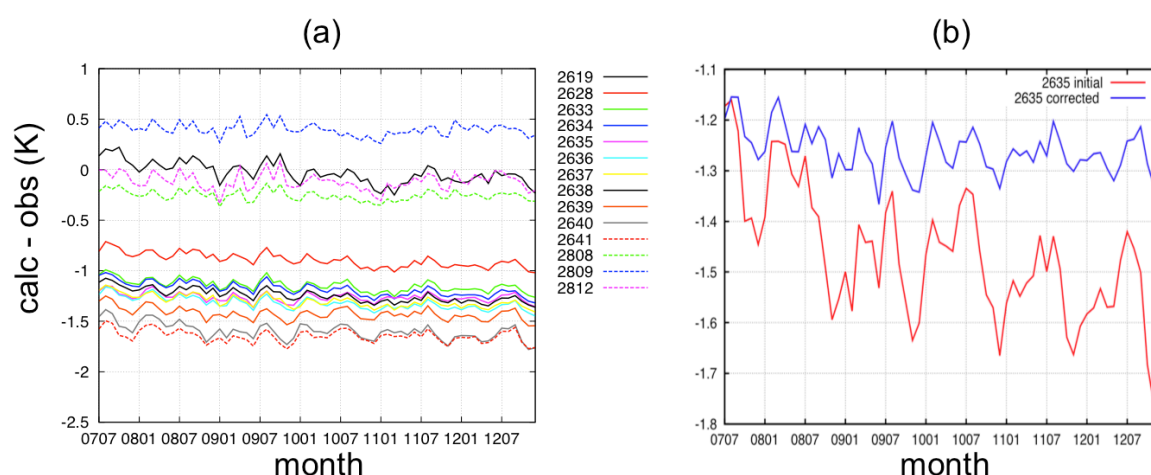


Figure 6.3.5.3. (a) Monthly evolution of calc-obs radiative residuals (K) computed over collocated IASI-ARSA situations with retrieved CH₄ mixing ratio used as input to the radiative transfer code, for daytime observations over land for the 14 IASI channels used in the retrieval scheme. **(b)** Same as (a) but for channel 2635 only with fixed (red) or retrieved (blue) CH₄ used as inputs to the radiative transfer code.

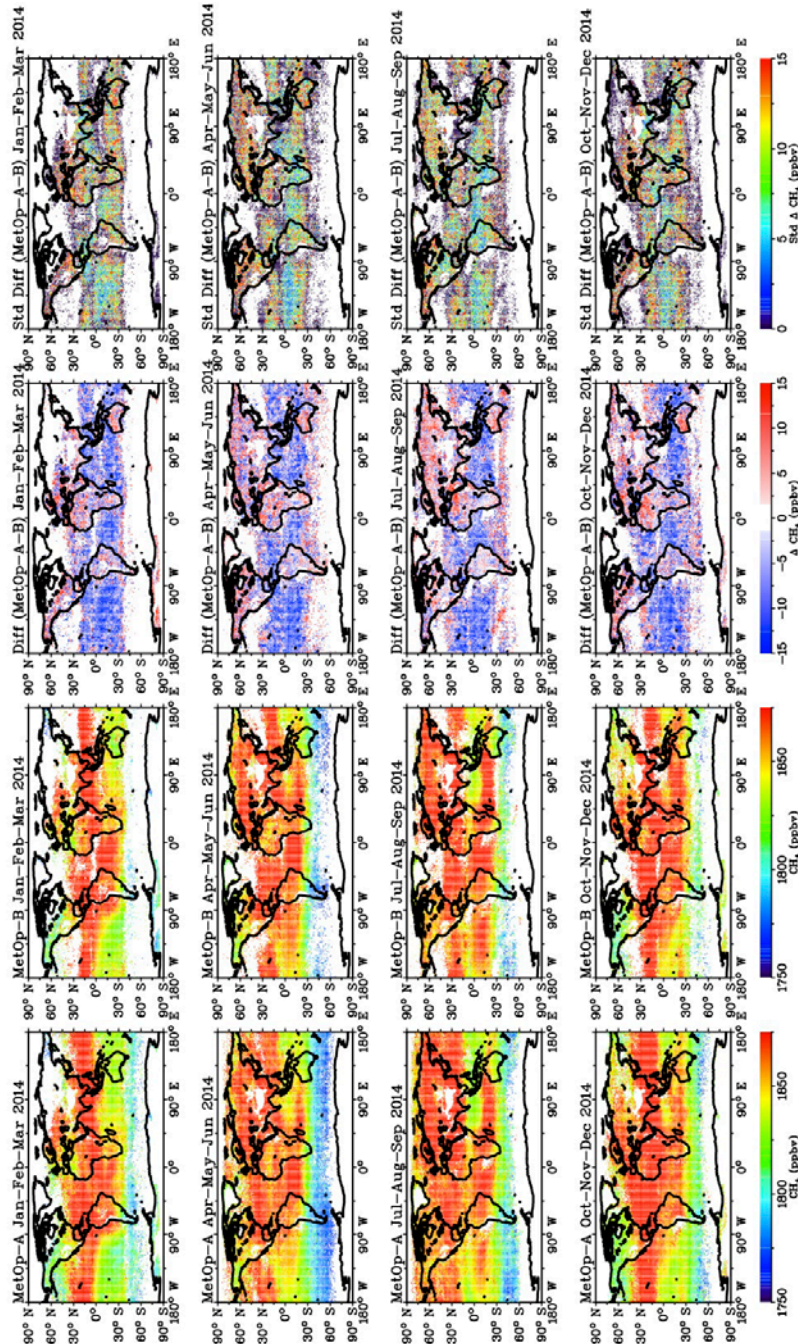


Figure 3.6.5.4. Seasonal maps (3 month average) of mid-tropospheric CH₄ as retrieved from Metop-A (1st column), Metop-B (2nd column), and mean (3rd column) and standard deviation (4th column) of the difference between Metop-A and Metop-B for the year 2014.



6.3.6 Assessment of CH₄_SCI_ONPD (no update)

The CH₄_SCI_ONPD product described in the following has not been updated for CRDP#3, i.e., the product is identical with the CRDP#2 product. The following description and analysis is therefore identical with the previous version of this document. However, a publication for a peer-reviewed scientific journal has been written /Noël et al., 2016/.

The ONPD results have been compared with 925 collocated ACE-FTS data between 2004 and October 2010 (collocation criteria: maximum spatial distance 800 km, maximum temporal distance 6 h; however actual temporal distance is usually below 1 h because only sunset data are used for both instruments). The Atmospheric Chemistry Experiment (ACE), also known as SCISAT, is a Canadian-led mission mainly supported by the Canadian Space Agency and the Natural Sciences and Engineering Research Council of Canada.

The results of this inter-comparison are shown in **Figure 6.3.6.1**. Overall, the two data sets agree within about 5-10%, which is within the expected accuracy of the products. The differences show a small oscillation with altitude, which might be related to the onion peeling approach. The estimated error of the SCIAMACHY CH₄ product is about 0.05 ppm below 35 km (smaller than the standard deviation of the difference between the two data sets) and increasing for altitudes above. Especially from 20 to 40 km the correlation between SCIAMACHY and ACE-FTS methane is high, reaching about 0.95 between 30 and 35 km.

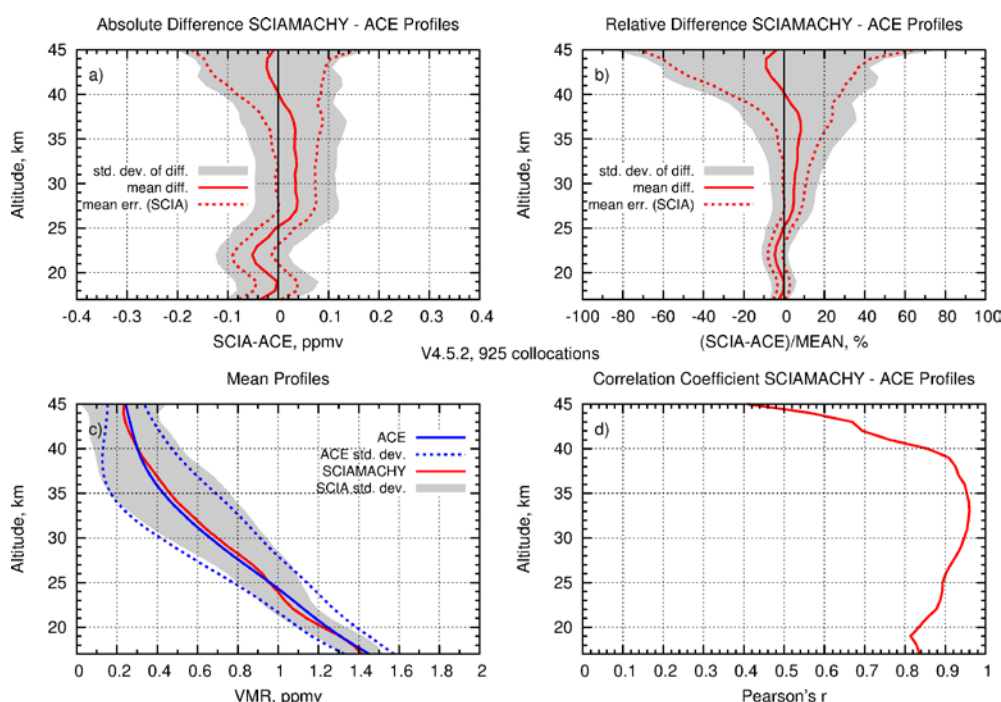




Figure 6.3.6.1: Comparison of SCIAMACHY ONPD CH₄ results (V4.5.2) with collocated ACE-FTS V3 data. a) Absolute differences and error. b) Relative differences and error. c) Mean profiles. d) Correlation coefficient.

A similar comparison has been performed with MIPAS methane data provided by KIT (see **Figure 6.3.6.2**). The MIPAS data used here are V5H_CH4_20 for the time interval from 2002 to 2004 in combination with V5R_CH4_222 (for January 2005 – April 2011) and V5R_CH4_223 (for May 2011 – April 2012). Collocation criteria are 800 km / 9h maximum distance. Only closest collocations have been used.

The average agreement between SCIAMACHY and MIPAS is almost perfect above 25 km. Below this altitude, the deviation between SCIAMACHY and MIPAS data increases with decreasing altitude, reaching about -0.2 ppmv (10–15%) at 17 km. This negative bias of SCIAMACHY towards MIPAS is in line with the about 0.2 ppmv positive bias of MIPAS in this altitude range (Laeng et al., 2013). The correlation between MIPAS and SCIAMACHY methane is somewhat lower than for SCIAMACHY vs. ACE-FTS, which is related to the different effective collocation criteria, especially the larger time differences between the MIPAS limb measurements and the SCIAMACHY occultation measurements.

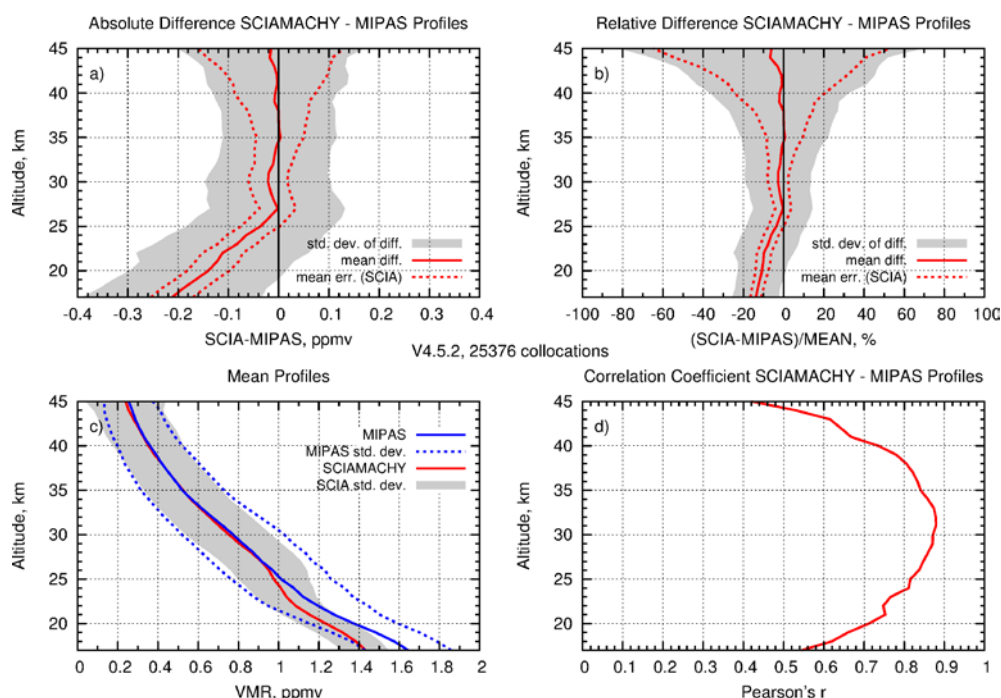


Figure 6.3.6.2: Comparison of SCIAMACHY ONPD CH₄ results (V4.5.2) with collocated MIPAS data. a) Absolute differences and error. b) Relative differences and error. c) Mean profiles. d) Correlation coefficient.

6.3.7 Assessment of CH₄_MIP_IMK

Methane profiles retrieved from MIPAS-ENVISAT spectra using the IMK/IAA retrieval processor have been validated in our work (Plieninger et al., 2016). The new versions V5H_CH₄_21 (full resolution period, FR), V5R CH₄_224 and V5R CH₄_225 (reduced resolution period, RR) are described in Plieninger et al. (2015). These profiles have been compared to collocated methane profiles from ACE-FTS, HALOE and SCIAMACHY. Generally a good agreement can be found. In the lower part of the profiles, a positive bias of the order of 0.1 to 0.2 ppmv has been found. This bias is lower than that of the previous data versions V5H_CH₄_20 (FR), V5R CH₄_222 (RR) and V5R CH₄_223 (RR). The latter two versions (for RR) have been validated by Laeng et al. (2015). The reduction of the bias of the new versions for RR is of the order of 0.08 to 0.15 ppmv. The comparison of the different MIPAS measurement periods FR and RR suggest, that the RR data leads to slightly higher volume mixing ratios.

As an example for our comparisons, in **Fig. 6.3.7.1** the profiles of MIPAS and ACE-FTS for the MIPAS FR measurement period are shown. The comparison is based on 253 pairs of collocated profiles. The general agreement of the mean profiles and their standard deviation is good. Below 20 km there are regions, where MIPAS shows higher values. This bias is largest at around 17 km and amounts to 0.12 ppmv. The right panel shows the combined estimated errors both with and without an extended example error budget for MIPAS. The estimate without this extended error budget contains noise only. There also is shown the standard deviation of the difference. Since in a difference of collocated profiles, atmospheric variation should cancel out, this is a measure of the statistical error and hence should agree with the error estimates. For the MIPAS – ACE-FTS comparison there is agreement between the estimates even though at least one of the instruments seems to underestimate its error. In **Fig. 6.3.7.2**, the comparison for the RR period is shown. The agreement between the profiles is good, but a positive bias of MIPAS can be observed. It is largest at around 13 to 15 km and amounts to about 0.15 ppmv. The error estimates are slightly overestimated below 20 km and underestimated above that altitude.

In general we are positive, that our efforts to improve the retrieval setup with respect to the bias reduction were successful, even though there still remains a small bias below 20 km. Further discussions can be found in Plieninger et al. (2016).

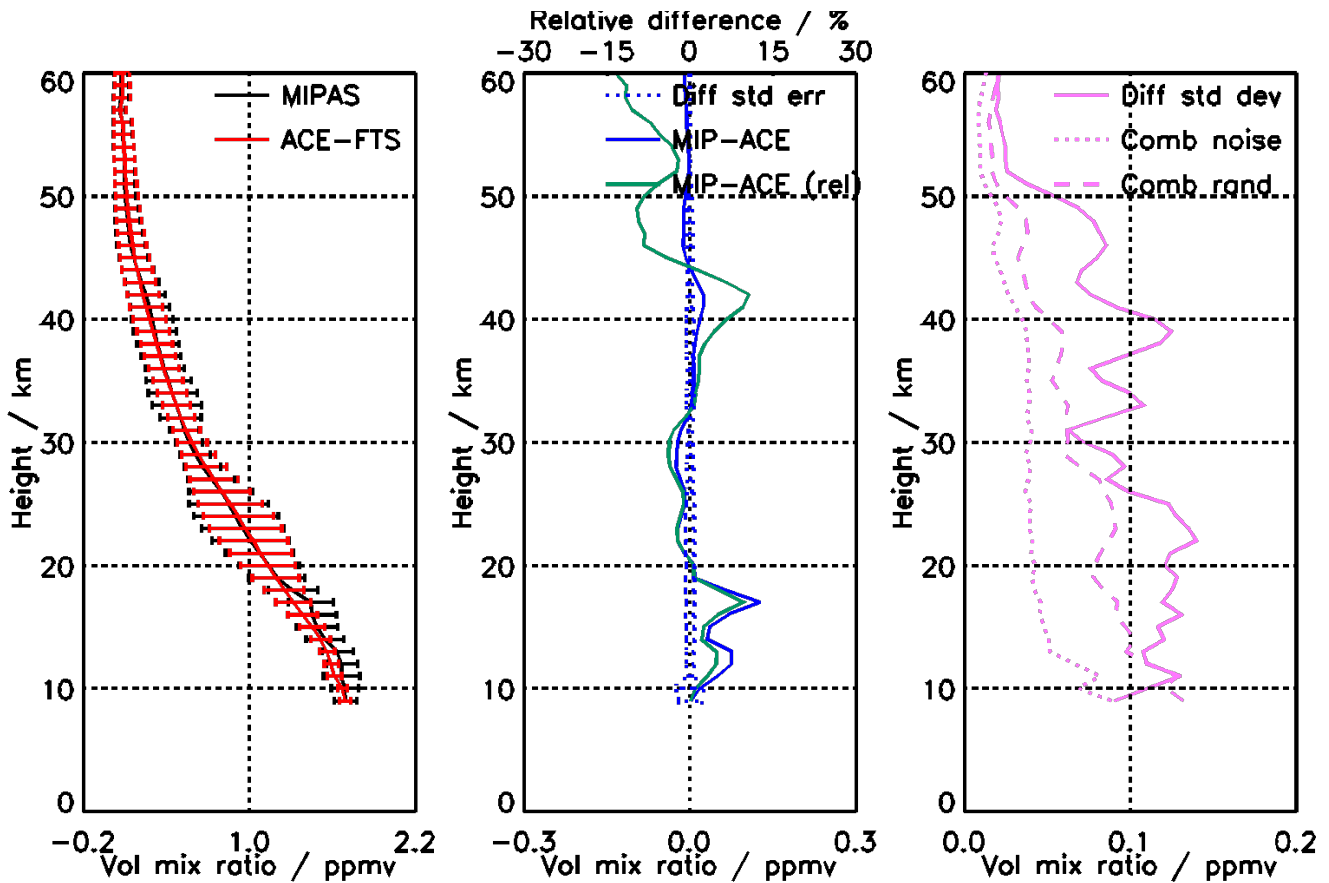


Fig. 6.3.7.1: Comparison of CH₄ from ACE-FTS and MIPAS full resolution (V5H_CH4_21). Left panel: Mean profiles of MIPAS (black) and its standard deviation (horizontal bars). Middle panel: Mean difference MIPAS minus ACE-FTS (blue solid), standard error of the difference (blue dotted), mean relative difference MIPAS minus ACE-FTS relative to ACE-FTs (green, upper axis). Right panel: combined mean estimated statistical error of the difference (pink dotted, contains MIPAS instrument noise only), combined mean estimated statistical error of the difference (pink dashed, contains MIPAS example random error budget), standard deviation of the difference (pink solid). Taken from Plieninger et al. (2016).

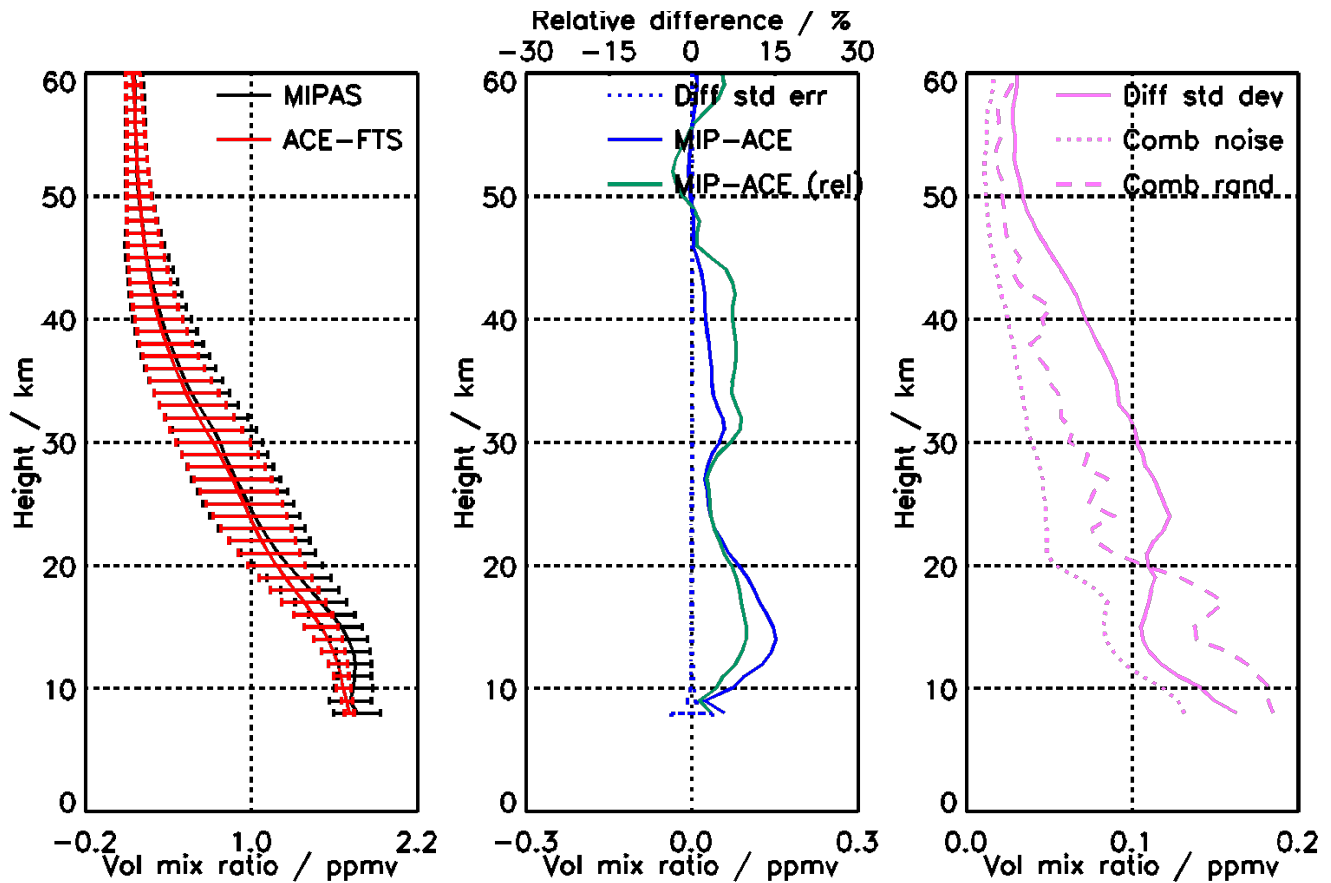



Fig. 6.3.7.2: As Fig. 6.3.7.1, but for MIPAS reduced resolution (V5R_CH4_224 and V5R_CH4_225).

	ESA Climate Change Initiative (CCI)	Page 180
	Product Validation and Intercomparison Report (PVIR)	
	for the Essential Climate Variable (ECV) Greenhouse Gases (GHG)	Version 5.0 Final
		9 Feb 2017

6.3.8 Assessment of CH₄_IAS_ASMT

The CH₄_IAS_ASMT product became part of GHG-CCI Phase 2 and a first dataset has been generated for CRDP#4. The CH₄_IAS_ASMT product provides CH₄ profiles, together with averaging kernels which give information on the vertical sensitivity of the retrieved profile. Overall 1 independent piece of information is retrieved, with a good sensitivity in the altitude range 4-17 km.

The CH₄_IAS_ASMT product has been validated with co-located ground-based NDACC FTIR observations. NDACC FTIR CH₄ profiles have good sensitivity in the troposphere and stratosphere with 2 to 3 independent pieces of information. Note, the NDACC CH₄ retrieval is not fully harmonized for all the NDACC stations.

For this validation exercise, CH₄ partial columns between 4 and 17 are compared at 13 NDACC stations for the years 2011 to 2014 (the CRDP#4 dataset). The NDACC FTIR profiles are smoothed with the CH₄_IAS_ASMT averaging kernel and the same *a priori* profile is used for the CH₄_IAS_ASMT and NDACC retrievals.

The average is taken of IASI pixels selected within 3 hours of the NDACC FTIR measurement, in a 0.5° latitude -1.5° longitude-box centred around the point on the line of sight where the FTIR measurement has maximum sensitivity.

Fig. 6.3.8.1 summarizes the results in a bar chart giving the relative difference of CH₄_IAS_ASMT and smoothed NDACC partial columns (4-17 km) at the different NDACC stations. The mean (CH₄_IAS_ASMT - NDACC)/NDACC (Δ) and standard deviation of the difference (σ) is given for each station.

We see an overall small negative bias of the CH₄_IAS_ASMT product between -0.28 and 2.27% (of which 7 stations out of 10 below 1%) with exception of the stations Altimoni, Mauna Loa and Thule, which show a positive bias. The standard deviation of the difference lies in the range 1.40 to 3.65%.

CH₄_IAS_ASMT shows a small positive bias at Mauna Loa (0.67%), and high positive biases are found at Altimoni (a relatively recent NDACC station) and the high-latitude Thule station of around 4%.



ESA Climate Change Initiative (CCI)

Product Validation and Intercomparison Report (PVIR)

for the Essential Climate Variable (ECV)
Greenhouse Gases (GHG)

Page 181

Version 5.0
Final

9 Feb 2017

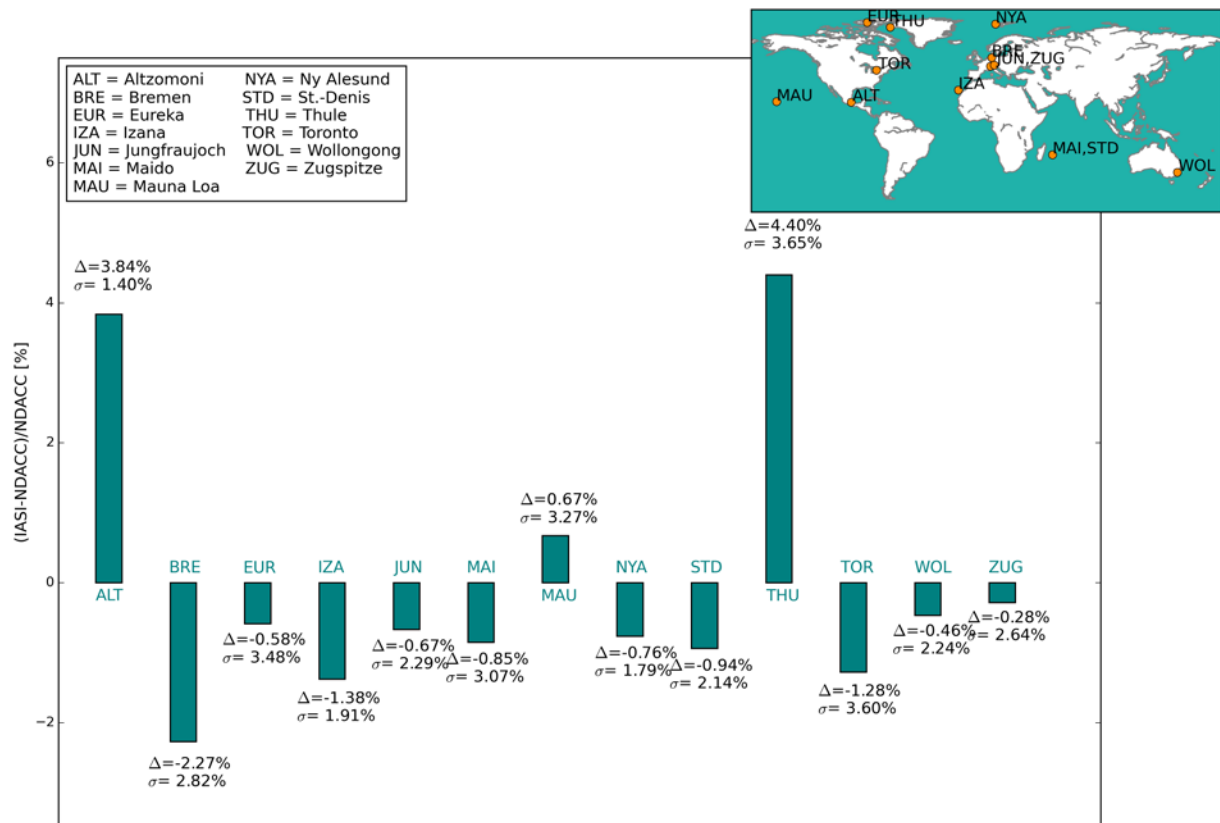


Fig. 6.3.8.1 : Bar chart with relative differences (Δ) and standard deviation of the differences (σ) between IASI and smoothed NDACC partial columns (4-17 km) at 13 NDACC stations for the CH4_IAS_ASMT CRDP#4 dataset (spanning the years 2011 to 2014). The 3-letter abbreviation of each NDACC station is given on top or below each bar, the station names are given in the legend and its location visualised on the map. These results are also summarized in Table 6.3.8.1.

Fig. 6.3.8.2 shows the scatter plots of the collocated partial columns, where we find very good correlations ($R = 0.77-0.9$) for the **high-latitude** stations (Eureka, Ny Alesund and Thule). Very good correlations ($R > 0.9$) are found as well for the **mid-latitude** stations Jungfrauoch and Zugspitze, while the mid-latitude stations Bremen and Toronto perform poorer with correlation coefficients of 0.54 and 0.42 respectively.

The **tropical** island stations La Reunion (2 stations) and Mauna Loa show poor correlations ($R = 0.42-0.52$) although absolute biases are below 1% for these stations. Izaña however shows a very good correlation of 0.9.

For the most Southern station Wollongong (34°S) we have a correlation coefficient of 0.77.

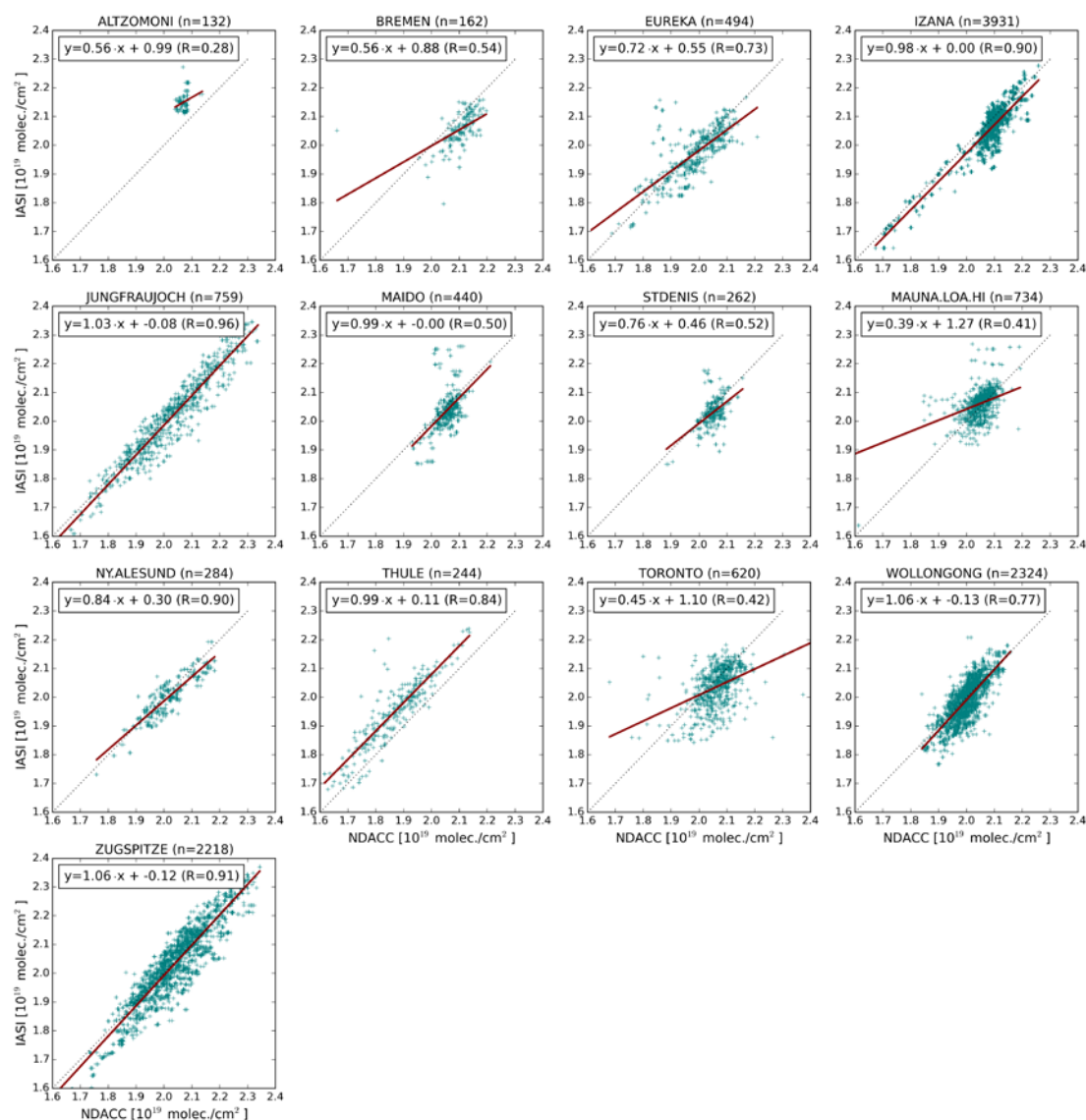


Fig. 6.3.8.2 : Correlation plots of smoothed NDACC and CH₄_IAS_ASMT CH₄ partial columns (4-17 km) at 13 NDACC stations for the period 2011-2014. The number of collocations (n) is given for each NDACC station in the title. The red lines are the linear regressions between the data points and the dashed black line is the unity slope, shown for comparison. The values of the linear regression and the correlation coefficient (R) are given for each station and summarized in Table 6.3.8.1.



ESA Climate Change Initiative (CCI)

**Product Validation and
Intercomparison Report (PVIR)**

for the Essential Climate Variable (ECV)
Greenhouse Gases (GHG)


Page 183

Version 5.0
Final

9 Feb 2017

Table 6.3.8.1 : Statistics of the comparison between the CH₄_IAS_ASMT and smoothed NDACC CH₄ 4-17km partial columns for the period 2011-2014. For each location, the mean difference (IASI-NDACC)/NDACC (**Mean Δ**) and standard deviation of the difference (**σ**) is given in percentage, the correlation coefficient (**R**) and the number of observations (**n**).

NDACC station	Latitude	Mean Δ [%]	σ [%]	R	n
Altzomoni	19°N	3.84	1.40	0.28	132
Bremen	53°N	-2.27	2.82	0.54	162
Eureka	80°N	-0.58	3.48	0.73	494
Izaña	28°N	-1.38	1.91	0.90	3931
Jungfraujoch	47°N	-0.67	2.29	0.96	759
La Reunion Mado	21°S	-0.85	3.07	0.50	440
La Reunion St. Denis	21°S	-0.94	2.14	0.52	262
Mauna Loa	20°N	0.67	3.27	0.41	734
Ny Alesund	79°N	0.76	1.79	0.90	284
Thule	77°N	4.40	3.65	0.84	244
Toronto	44°N	-1.28	3.60	0.42	620
Wollongong	34°S	-0.46	2.24	0.77	2324
Zugspitze	47°N	-0.28	2.64	0.91	2218

	ESA Climate Change Initiative (CCI)	Page 184
	Product Validation and Intercomparison Report (PVIR)	
	for the Essential Climate Variable (ECV) Greenhouse Gases (GHG)	Version 5.0 Final
		9 Feb 2017

Summary :

The CH₄_IAS_ASMT product entered Phase 2 of GHG-CCI and delivers CH₄ profiles, together with averaging kernels which give information on the vertical sensitivity of the retrieved profile. The CH₄_IAS_ASMT product has been validated with smoothed NDACC FTIR CH₄ partial columns between 4 and 17 at 13 NDACC stations for the years 2011 to 2014.

We have an overall small negative bias of the CH₄_IAS_ASMT product between -0.28 and 2.27% with exception of 3 NDACC stations, which show a positive bias. The standard deviation of the difference lies in the range 1.40 to 3.65%.

Very good correlations are found for 7 out of the 13 NDACC stations with correlation coefficients between 0.73 and 0.96. Particularly for the 3 high-latitude stations we find a very good correlation, as well as for the 2 high-quality mid-latitude stations Jungfraujoch and Zugspitze. Poorer correlations are found for the stations Bremen, La Reunion, Mauna Loa and Toronto with correlation coefficients in the range 0.4-0.5.



6.4 Consistency of XCO₂ data products

Here we present some figures showing comparison of the GHG-CCI XCO₂ data products. **Figures 6.4.1** and **6.4.2** show comparisons of monthly averages of northern and southern hemispheric XCO₂ of the four XCO₂ products retrieved from SCIAMACHY (WFMD and BESD) and GOSAT (SRFP and OCFP).

As can be seen, the agreement is quite good. Note that perfect agreement is not to be expected, as the data products have been used (averaged) “as is”, i.e., without any corrections for their (somewhat different) averaging kernels and without considering their different spatio-temporal sampling in the shown regions within each month (to what extent this explains the difference of the seasonal cycle amplitudes, in particular between SCIAMACHY and GOSAT as shown in **Figure 6.4.1**, remains to be investigated).

Figures 6.4.1 and **6.4.2** indicate a high level of stability of the SCIAMACHY and GOSAT XCO₂ products and the good to reasonable consistency of these products for large scale averages.

GHG-CCI CRDP#4

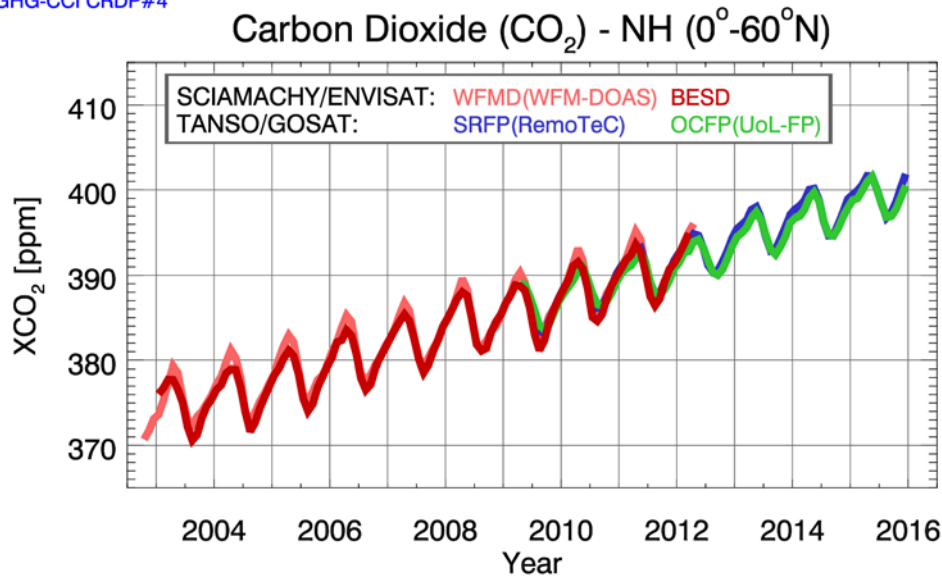
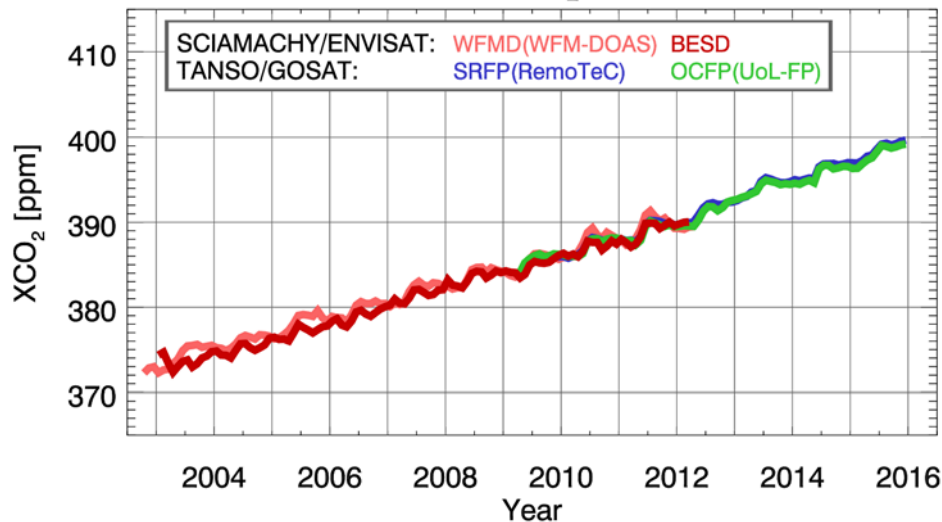


Fig. 6.4.1: Comparison of monthly averages of northern hemispheric XCO₂ (0° - 60°N) between the four XCO₂ products retrieved from SCIAMACHY (WFMD and BESD) and GOSAT (SRFP and OCFP).



GHG-CCI CRDP#4

Carbon Dioxide (CO₂) - SH (60°S-0°)



Michael.Buchwitz@iup.physik.uni-bremen.de 3-Nov-2016 cmp:direct filter:all

Fig. 6.4.2: As Fig. 6.4.1 but for southern hemispheric XCO₂ (0° - 60°S).

Figures 6.4.3 – 6.4.6 show latitude – time plots of the four data products. Shown is XCO₂ (top) but also the mean value of the reported uncertainty (middle) and the number of observations per grid cell (bottom; monthly and within 10° latitude bands). As can be seen, all products agree reasonable well. Again, perfect agreement is not to be expected, for the reasons already explained above.

As expected the WFMD product has larger values of the reported uncertainty compared to BESD, as the very fast WFMD algorithm is somewhat less precise (~3 ppm) compared to the computationally very demanding BESD algorithm (precision ~2 ppm), but - as also can be seen - WFMD has much more data.

The reported uncertainty of GOSAT/SRFP is typically 1-2 ppm. The number of data points per grid cell is less than for BESD (note the scale change). For GOSAT/OCFP the reported uncertainty is somewhat larger (~2 ppm) compared to SRFP (~1.5-2 ppm). However, the number of data points is somewhat higher for OCFP, depending on latitude and month.

Figures 6.4.7 – 6.4.10 show spatial maps for monthly averaged data (here: August 2009). As can be seen, the four XCO₂ products are quite consistent. Note again that perfect agreement is not expected for the reasons already explained above.



GHG-CCI CRDP#4

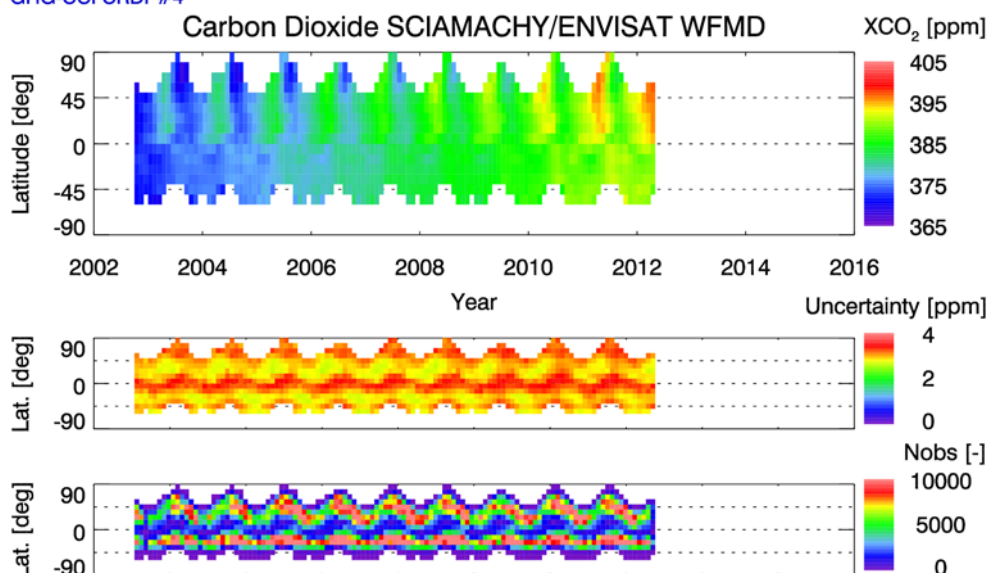


Fig. 6.4.3: Latitude – time plots of SCIAMACHY/WFMD XCO₂. Top: XCO₂ with spatio-temporal averaging within 10 deg latitude bands and monthly time intervals. Middle: Mean value of reported uncertainty. Bottom: Number of observations per grid cell.

GHG-CCI CRDP#4

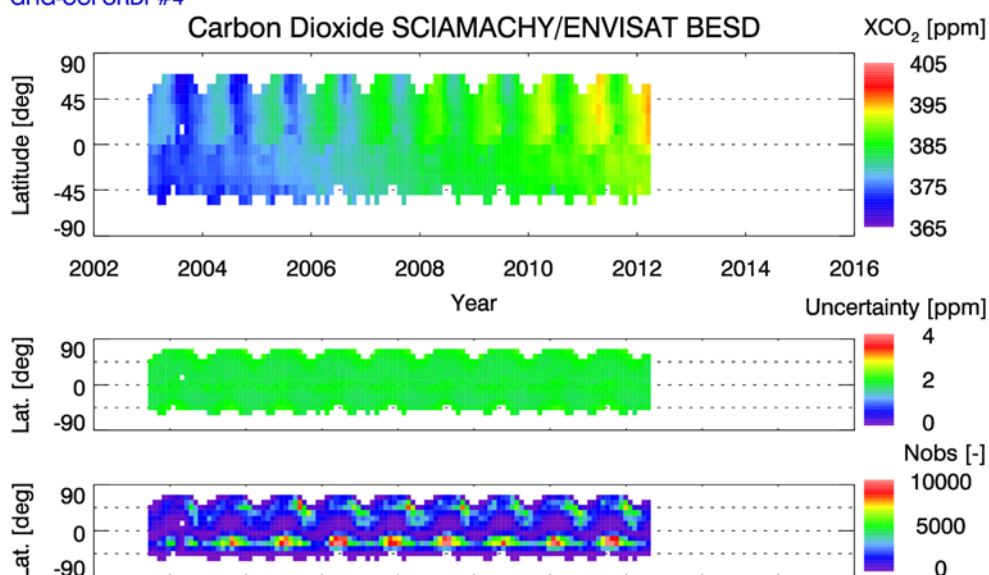


Fig. 6.4.4: As Fig. 6.4.3 but for SCIAMACHY/BESD XCO₂.



GHG-CCI CRDP#4

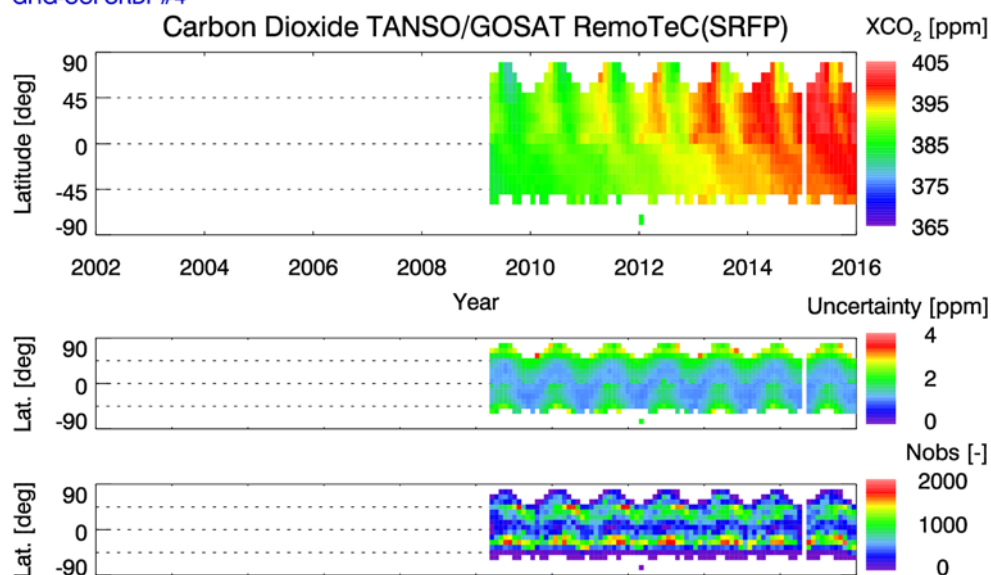


Fig. 6.4.5: As Fig. 6.4.3 but for GOSAT/SRFP XCO₂.

GHG-CCI CRDP#4

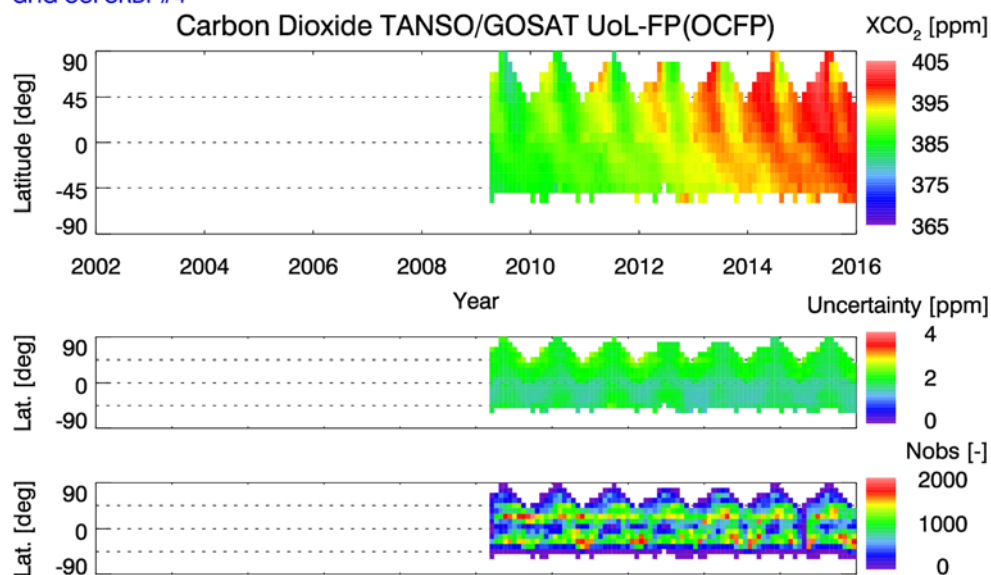


Fig. 6.4.6: As Fig. 6.4.3 but for GOSAT/OCFP XCO₂.

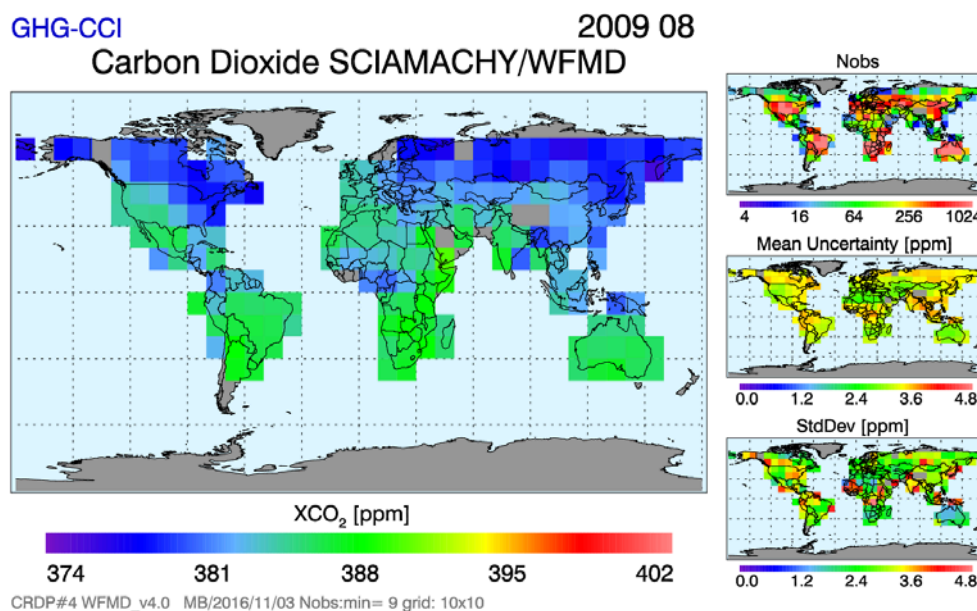


Fig. 6.4.7: Spatial maps of monthly data (here: August 2009) at 10°x10° resolution showing the SCIAMACHY/WFMD product.

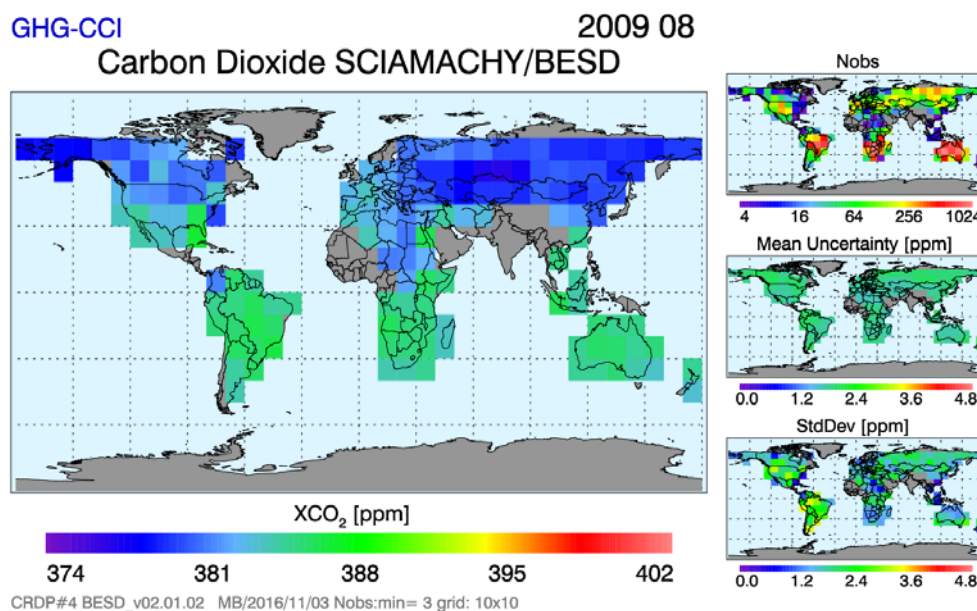


Fig. 6.4.8: As Fig. 6.4.7 but for the SCIAMACHY/BESD product.

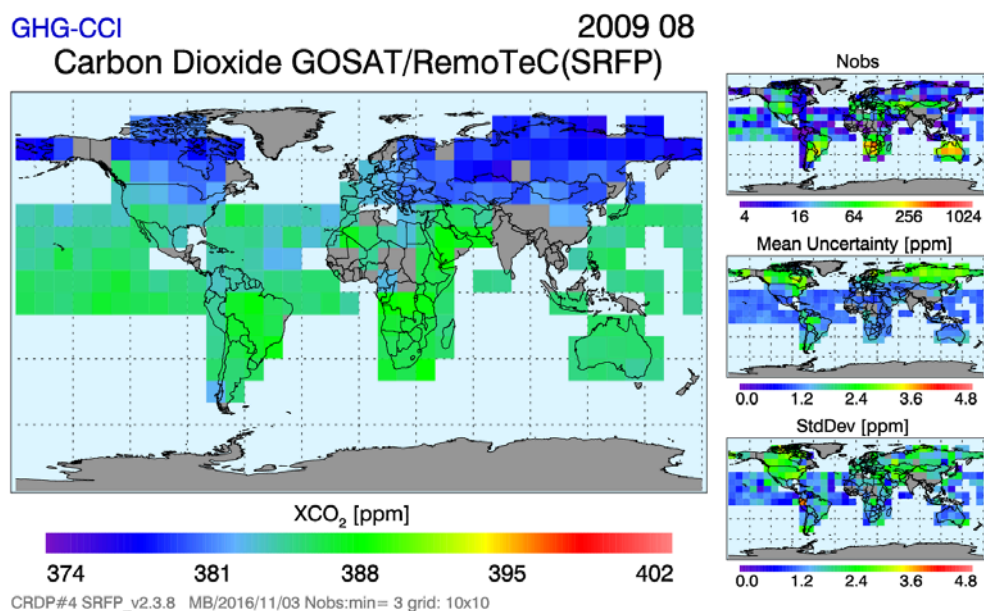


Fig. 6.4.9: As Fig. 6.4.7 but for the GOSAT/SRFP product.

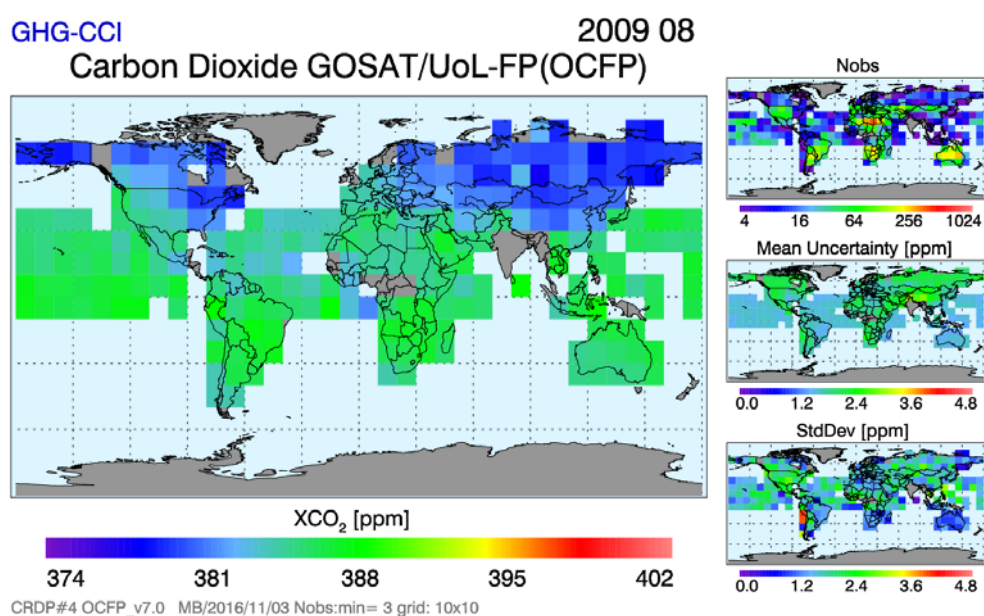


Fig. 6.4.10: As Fig. 6.4.7 but for the GOSAT/OCFP product.

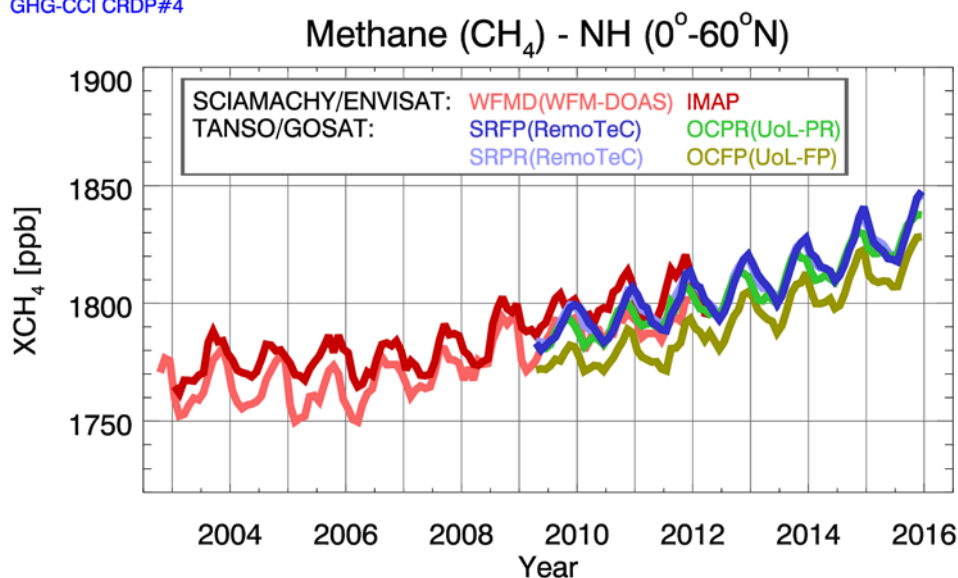
6.5 Consistency of XCH₄ data products

6.5.1 Assessment results from IUP-UB

Here similar figures are shown and discussed as presented in **Sect. 6.4** (XCO₂) but for XCH₄, i.e., we present some figures showing comparison of the various GHG-CCI XCH₄ data products. **Figure 6.5.1.1** and **6.5.1.2** show comparisons of monthly averages of northern hemispheric XCH₄ (between 0° and 60°N latitude) of the six XCH₄ products retrieved from SCIAMACHY (WFMD and IMAP) and GOSAT (baseline products SRFP and OCPR and alternative products SRPR and OCFP). As can be seen, the agreement is quite good for the GOSAT products in contrast to the SCIAMACHY products, where the differences are quite large (see below). Note that perfect agreement is not to be expected, as the data products have been used (averaged) “as is”, i.e., without any corrections for their averaging kernels and without considering their different spatio-temporal sampling within each region and month.

As can be seen, there is a bias of around 10 ppb (0.5%), depending on month and region, between the two SCIAMACHY products, with WFMD slightly higher than GOSAT and IMAP slightly lower than GOSAT (not referring to OCFP, which has a low bias relative to the other two GOSAT products).

GHG-CCI CRDP#4



Michael.Buchwitz@iup.physik.uni-bremen.de 3-Nov-2016 cmp:direct filter:all

Fig. 6.5.1.1: Comparison of monthly averages of northern hemispheric XCH₄ (0° - 60°N) between the 6 XCH₄ products retrieved from SCIAMACHY (WFMD and IMAP) and GOSAT (SRFP, SRPR and OCPR, OCFP).

GHG-CCI CRDP#4

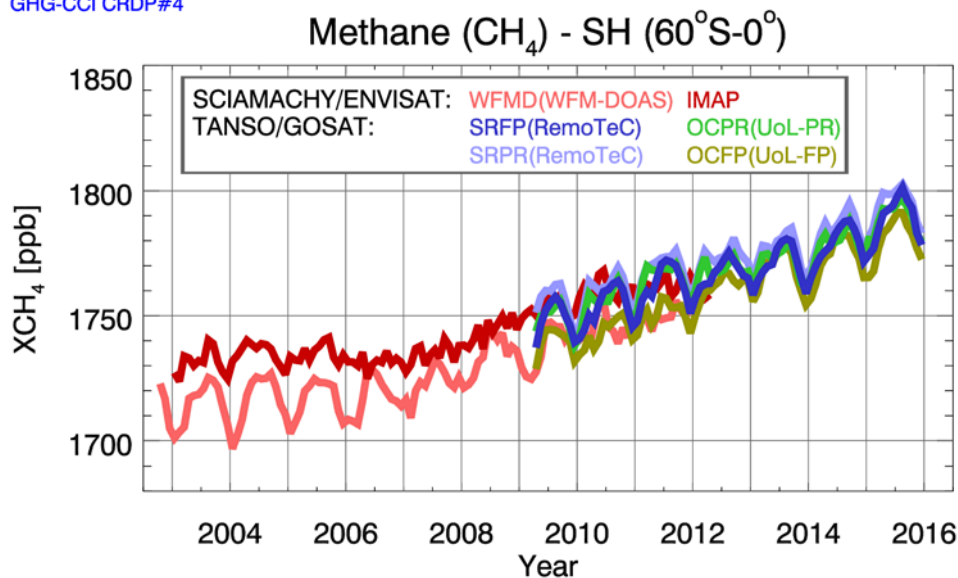


Fig. 6.5.1.2: As Fig. 6.5.1.1 but for southern hemispheric XCH₄ (0° - 60°S).

Figures 6.5.1.3 – 6.5.1.6 show latitude – time plots of the four data products. Shown is XCH₄ (top) but also the mean value of the reported uncertainty (middle) and the number of observations per grid cell (bottom; monthly and within 10° latitude bands).

As can be seen by comparing **Figs. 6.5.1.3** and **6.5.1.4.**, the two SCIAMACHY products show significant differences: the WFMD product appears to be noisier and its XCH₄ is somewhat lower compared to IMAP, in particular north of the equator up to about 40°N.

As can be seen by comparing **Figs. 6.5.1.5** and **6.5.1.6.**, the two GOSAT products agree quite well. Note the much larger number of data points for the proxy product (OCPR) compared to the full-physics product (SRFP).

Figures 6.5.1.7 – 6.5.1.8 show spatial SCIAMACHY methane maps for September 2003, i.e., in the time period before November 2005, after which the SCIAMACHY methane data suffered from detector degradation. As can be seen, the two SCIAMACHY products agree reasonably well but there are also some regional differences.

The differences between the two product can however be quite large towards the end of the SCIAMACHY mission (likely due to detector degradation, which is dealt with differently by WFMD and IMAP), e.g., in September 2011, as shown in **Figures 6.5.1.9 – 6.5.1.10.**

The differences between the GOSAT products is typically much smaller as can be seen from comparing **Figures 6.5.1.11** and **6.5.1.12.**

GHG-CCI CRDP#4

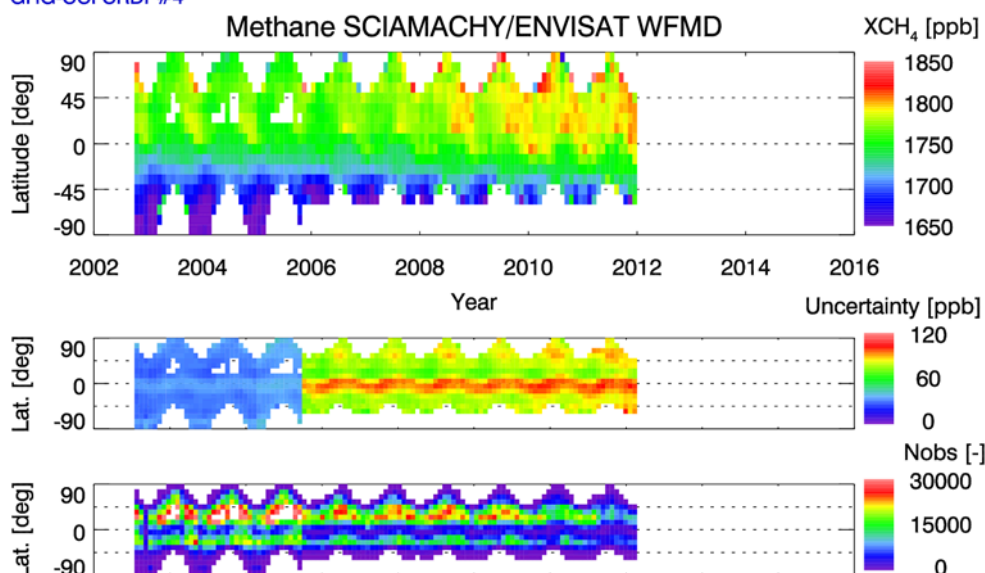


Fig. 6.5.1.3: Latitude – time plots of SCIAMACHY/WFMD XCH₄. Top: XCH₄ with spatio-temporal averaging within 10 deg latitude bands and monthly time intervals. Middle: Mean value of reported uncertainty. Bottom: Number of observations per grid cell.

GHG-CCI CRDP#4

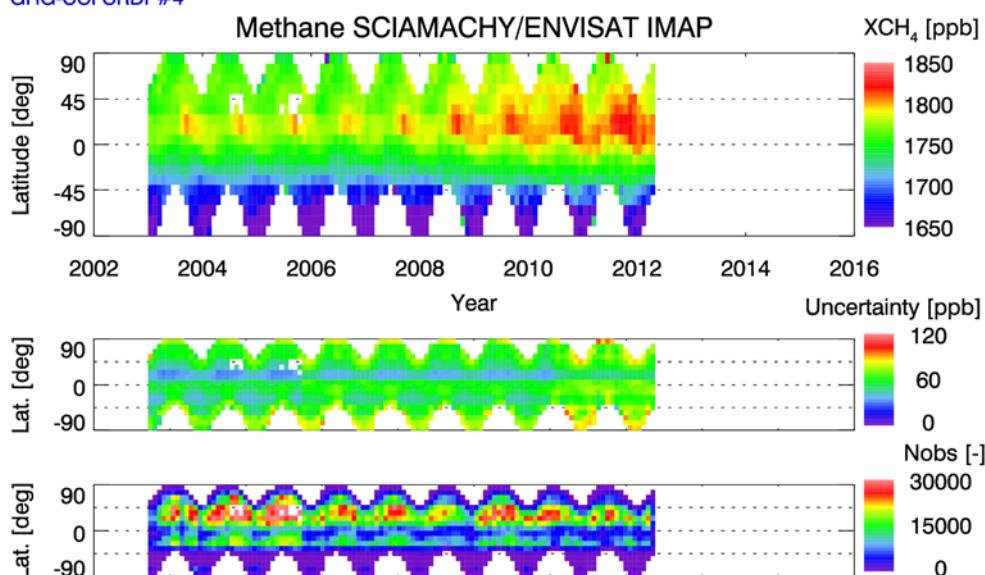


Fig. 6.5.1.4: As Fig. 6.5.1.3 but for SCIAMACHY/IMAP XCH₄.



GHG-CCI CRDP#4

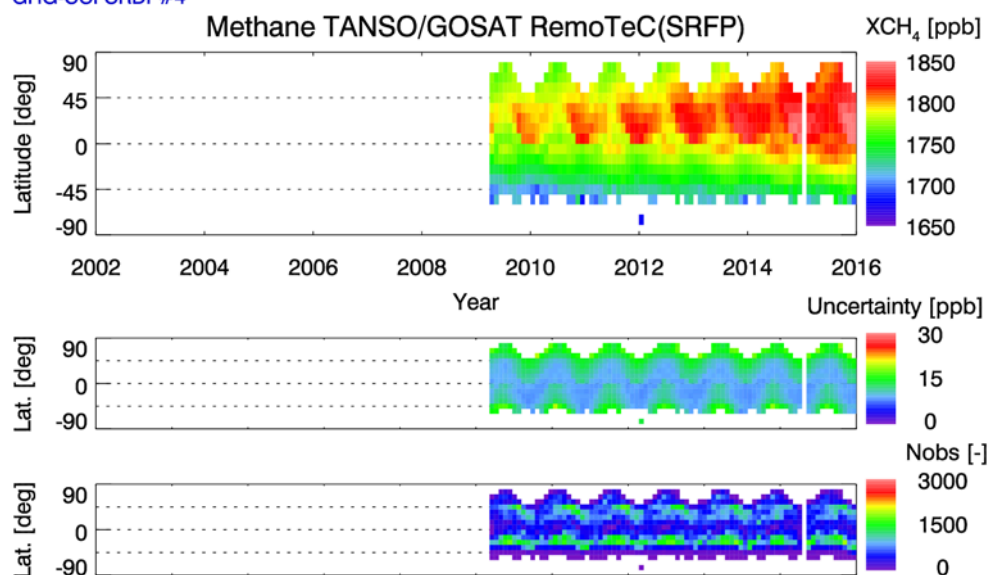


Fig. 6.5.1.5: As Fig. 6.5.1.3 but for GOSAT/SRFP XCH₄.

GHG-CCI CRDP#4

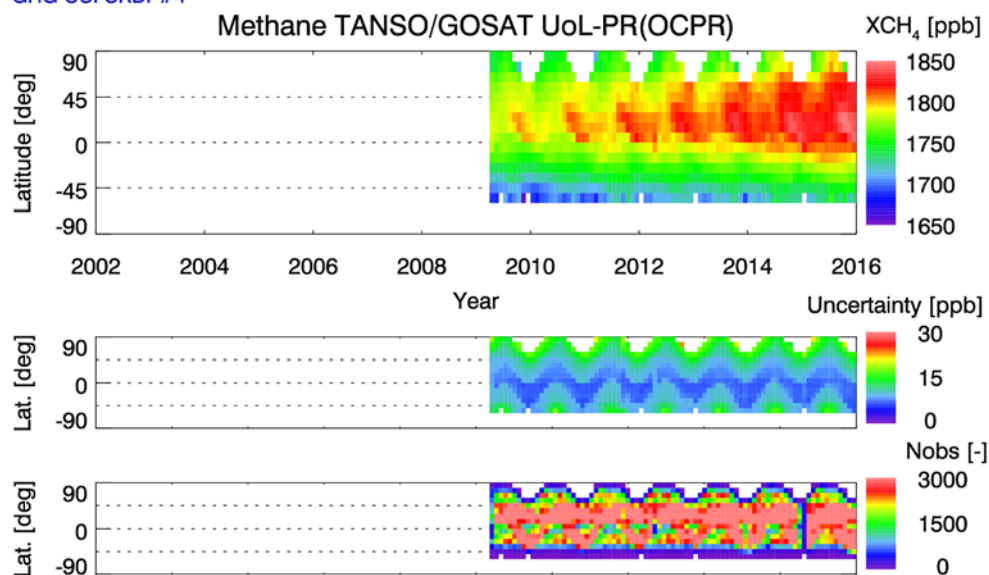


Fig. 6.5.1.6: As Fig. 6.5.1.3 but for GOSAT/OCPR XCH₄.

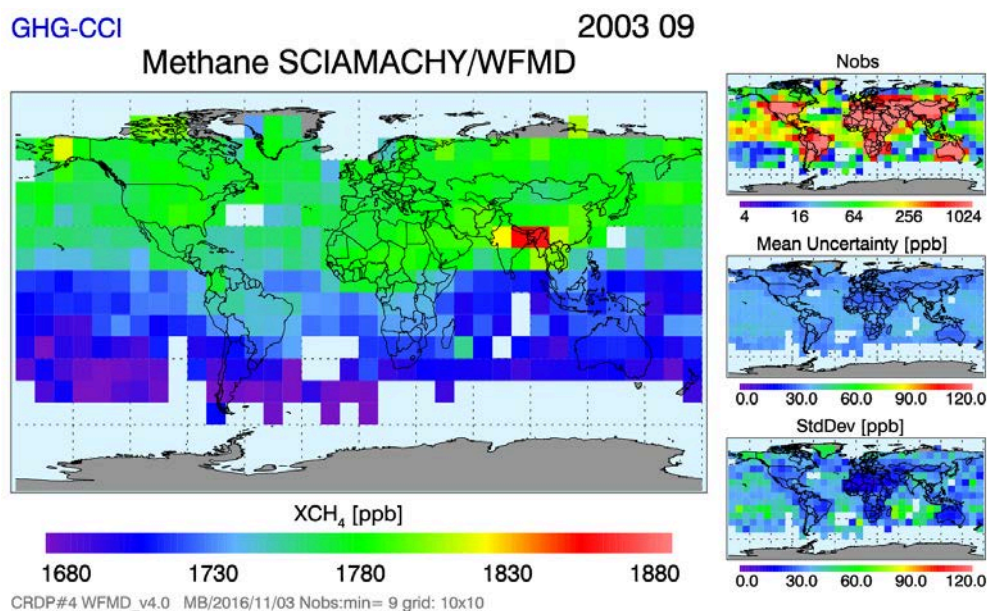


Fig. 6.5.1.7: Spatial maps of monthly data (here: September 2003) at 10°x10° resolution for the SCIAMACHY/WFMD product.

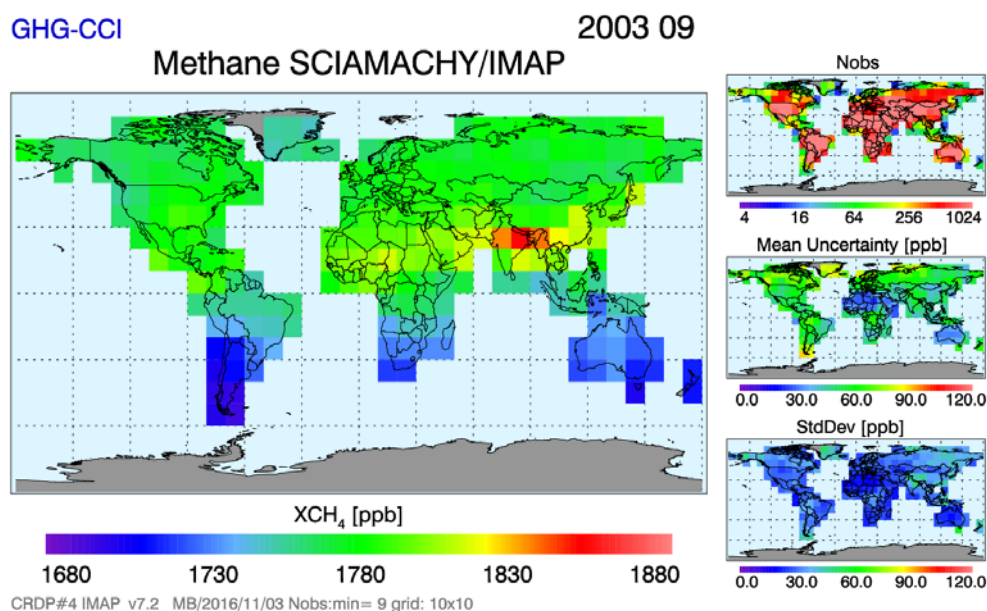


Fig. 6.5.1.8: As Fig. 6.4.1.7 but for the SCIAMACHY/IMAP product.

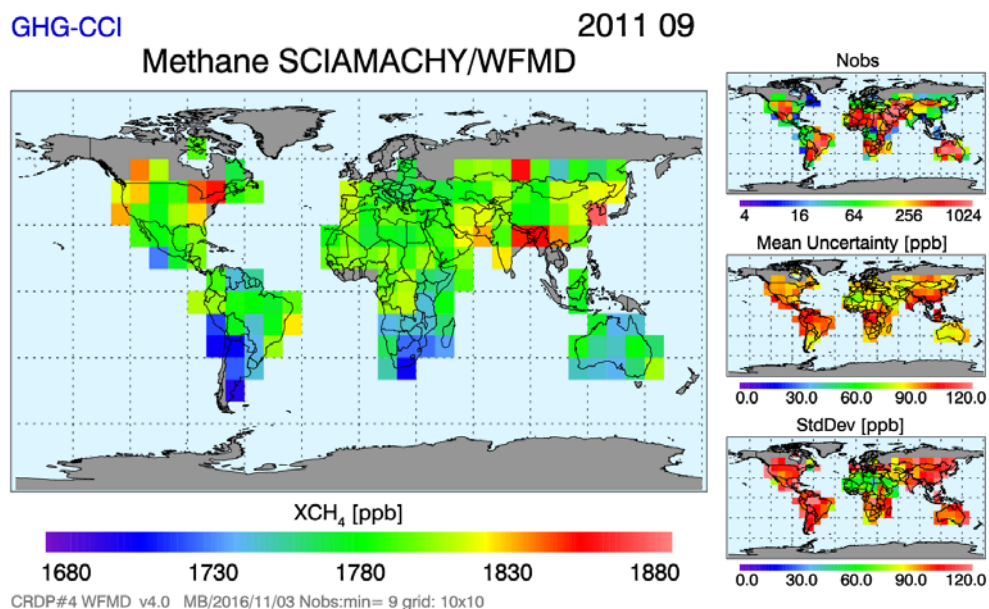


Fig. 6.5.1.9: As Fig. 6.5.1.7 but for SCIAMACHY/WFMD and September 2011.

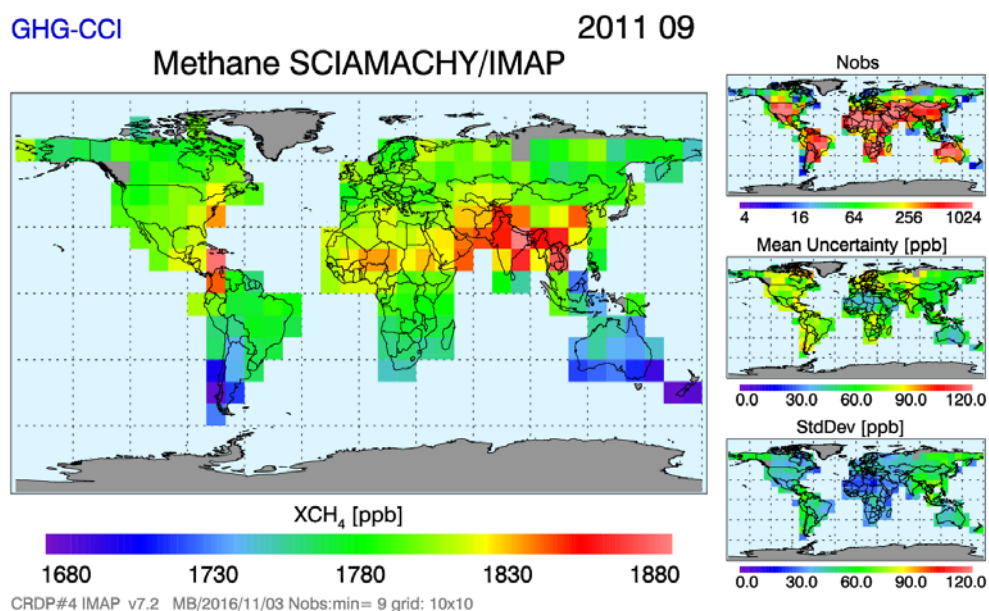


Fig. 6.5.1.10: As Fig. 6.5.1.9 but for SCIAMACHY/IMAP.

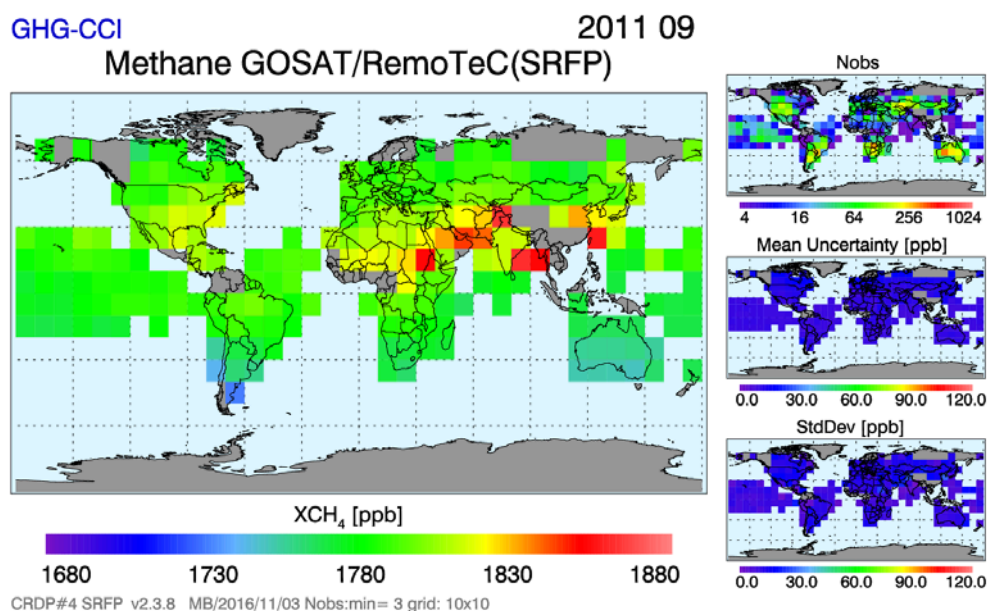


Fig. 6.5.1.11: As Fig. 6.5.1.9 but for the GOSAT/SRFP product.

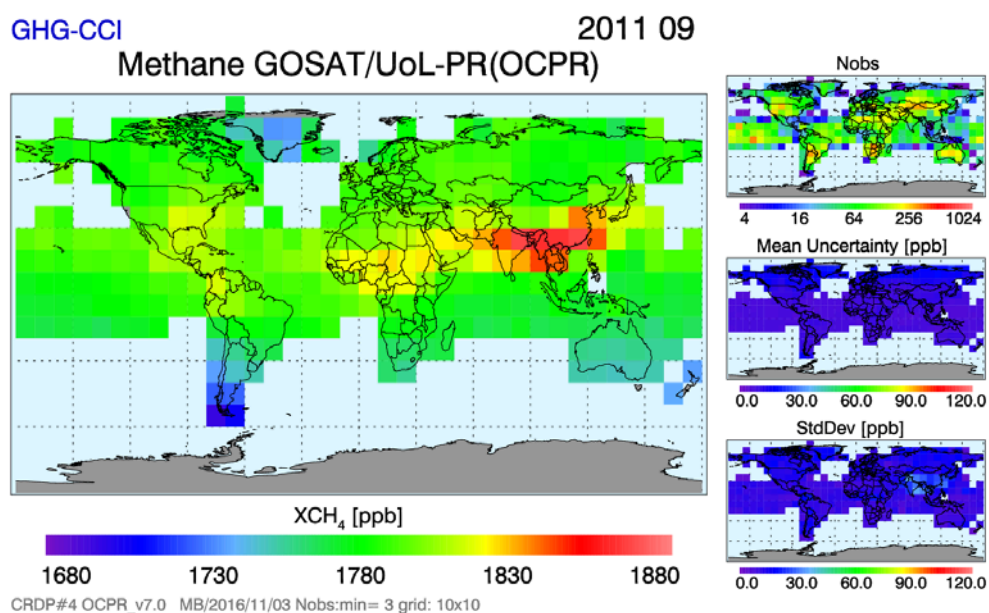



Fig. 6.5.1.12: As Fig. 6.5.1.9 but for the GOSAT/OCPR product.

	ESA Climate Change Initiative (CCI)	Page 198
	Product Validation and Intercomparison Report (PVIR)	
	for the Essential Climate Variable (ECV) Greenhouse Gases (GHG)	Version 5.0 Final
		9 Feb 2017

6.5.2 Assessment results from SRON

The consistency between SCIAMACHY XCH₄ (IMAPv7.2 and WFMDv4.0) and GOSAT XCH₄ (RemoTeC/ SRFP v2.3.8 and SRPR v2.3.8 and OCPR v7.0 and OCFP v2.02) products was investigated by comparing monthly averaged data of both satellites on a regional (see **Table 6.5.2.1**) and global scale.

The results are shown in **Figures 6.5.2.1 - 6.5.2.6**, respectively. For the global comparison, data between 60 degrees south and 60 degrees north were used to ensure a consistent comparison between the datasets.

On a global scale, we see that the differences between the two GOSAT XCH₄ PROXY datasets and the SRFP XCH₄ dataset are relatively small, on the order of 5-10 ppb at most. All three datasets show a similar seasonal pattern. The difference is largest between SRPR and SRFP during the Northern Hemisphere summer period. The OCFP product shows a larger offset compared to the other three products of approximately 15- 20 ppb. The origin of this offset is not known as of this moment.

If we look at the separate hemispheres, the differences between SRPR and SRFP disappear for the Northern hemisphere and the difference between OCPR and the SRON products is only present in summer (approx. 5-10 ppb at most). The OCFP product still shows the 15-20 ppb offset. In the Southern hemisphere the differences between SRPR and SRFP are larger, most likely due to the different sampling due to stricter filtering for the SRFP product. Interestingly the differences with the OCFP product are smaller.

At regional scales the differences are larger for regions that have fewer observations, such as the tropics and northern, boreal regions. Here differences between filter criteria are crucial due to the low number of observations in these regions.

Generally speaking however, the differences between the four GOSAT products are relatively small compared to the differences between GOSAT and SCIAMACHY and the SCIAMACHY products themselves.

Apart from an offset both SCIAMACHY datasets are in general agreement with each other until half-way 2010, although the seasonal cycle seems to be stronger for the WFMD data between 2004 and 2006, especially in the Southern hemisphere. However, from 2010 onwards there is a clear change in data quality from the SCIAMACHY data sets. The SCIAMACHY/IMAP data start to show some peculiar oscillations that unlikely are related to true methane variations. This is the same behaviour as in CRDP#3.

The SCIAMACHY WFMD also changes the expected trend but becomes more in agreement with GOSAT..

Looking at a regional scale, it can be seen that the differences between GOSAT and SCIAMACHY data sets depend significantly on the region. For example, for South Africa

GOSAT methane is very similar to the SCIAMACHY IMAP data, while for WFMD from 2010 onwards it drops significantly below the other products for South Africa.

For the other regions (i.e. Northern hemisphere) GOSAT/RemoTeC XCH₄ is lower than SCIAMACHY/IMAP for the entire period, as it is at a global scale. This is due to the ‘jump’ that occurs in the IMAP data after 2010. The outliers visible in the Northern regions in winter in the WFMD and IMAP data are most likely due to the very limited number of observations in winter at these high latitudes. Also the GOSAT SRPR and SRFP data show gaps at these high latitudes due to the solar zenith angle constraint. The OCPR product does not show these gaps, although the number of observations is also very limited, resulting in more peaked values in winter at high latitudes. This is due to the lack of a explicit solar zenith angle filter in the OCPR product.

For some regions (especially south east Eurasia and Australia) the GOSAT time series are continuing the SCIAMACHY IMAP time series well at the start of GOSAT measurements. For all regions, the differences are larger from 2010 onwards, very likely due to degraded quality of the SCIAMACHY instrument. The comparison between the two SCIAMACHY data sets depends strongly on region. North Africa shows a large offset between the two, while Southern East Eurasia shows a very similar behaviour.

REGION	Latitudes	Longitudes
Boreal North America	52 - 64 N	58 - 122 W
North America	40 - 52 N	69 - 119 W
South America	15 - 30 S	40 - 70 W
North Africa	10 – 30 N	13 W - 35 E
South Africa	10 - 30 S	13 - 50 E
Northern West Eurasia	52 - 64 N	25 - 80 E
Southern West Eurasia	40 - 52 N	25 - 80 E
Northern East Eurasia	52 - 64 N	83 - 137 E
Southern East Eurasia	40 - 52 N	83 - 137 E
Australia	12 - 30 S	113 - 151 E

Table 6.5.2.1: Definitions of the different regions used for the regional SCIAMACHY and GOSAT XCH₄ product comparisons.

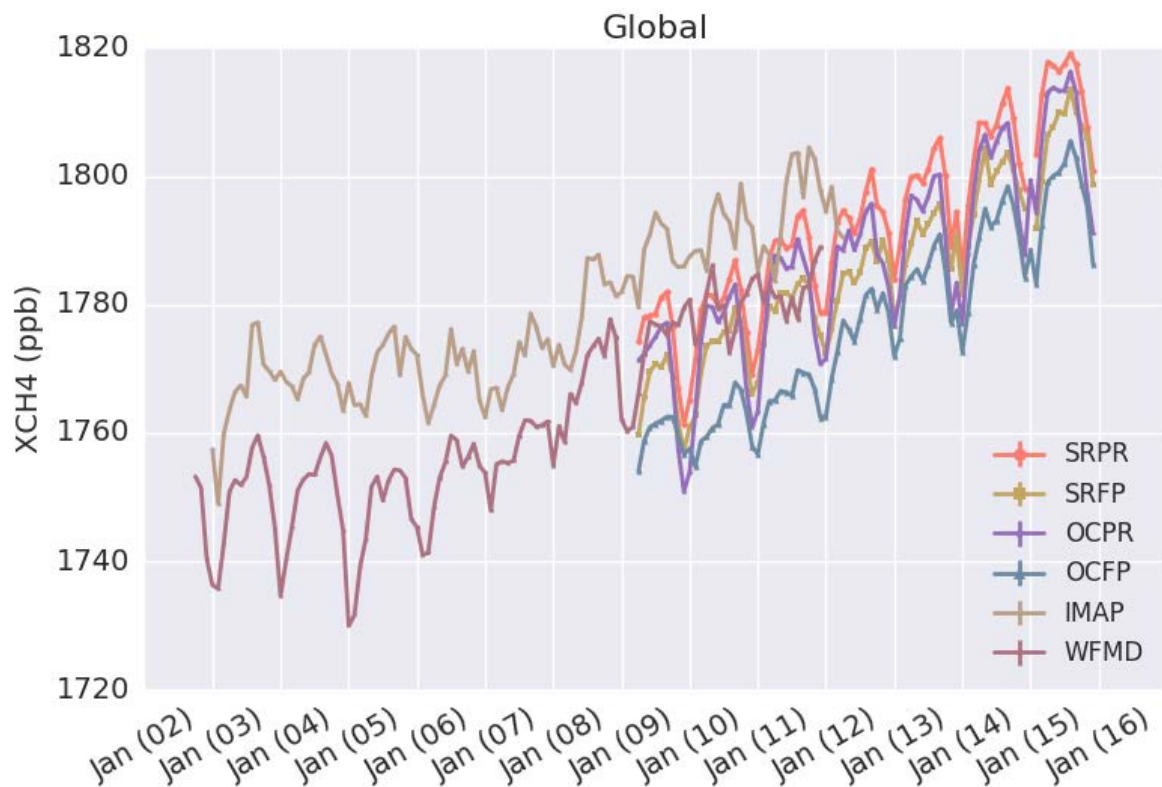


Figure 6.5.2.1: Global monthly averaged XCH_4 concentrations for SCIAMACHY (IMAPv7.2 and WFMDv4.0) and GOSAT (RemoTeC/SRFP and SRPR v2.3.8 and OCPR v7.0) data. The positive offset of the SCIAMACHY IMAP data with respect to the GOSAT data for the period 2010 – 2012 can be clearly seen.

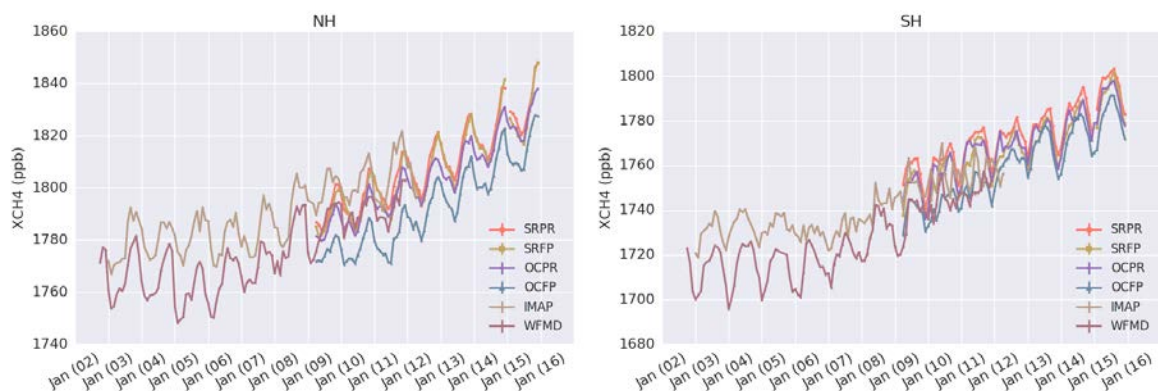


Figure 6.5.2.2: Hemisphere monthly averaged XCH_4 concentrations for SCIAMACHY (IMAPv7.2 and WFMDv4.0) and GOSAT (RemoTeC/SRFP and SRPR v2.3.8 and OCPR v7.0) data. The positive offset of the SCIAMACHY IMAP data with respect to the GOSAT data for the period 2010 – 2012 can be clearly seen in the Northern Hemisphere. For the Southern hemisphere this offset is significantly smaller.



ESA Climate Change Initiative (CCI)

Product Validation and Intercomparison Report (PVIR)

for the Essential Climate Variable (ECV)
Greenhouse Gases (GHG)

Page 201

Version 5.0
Final

9 Feb 2017

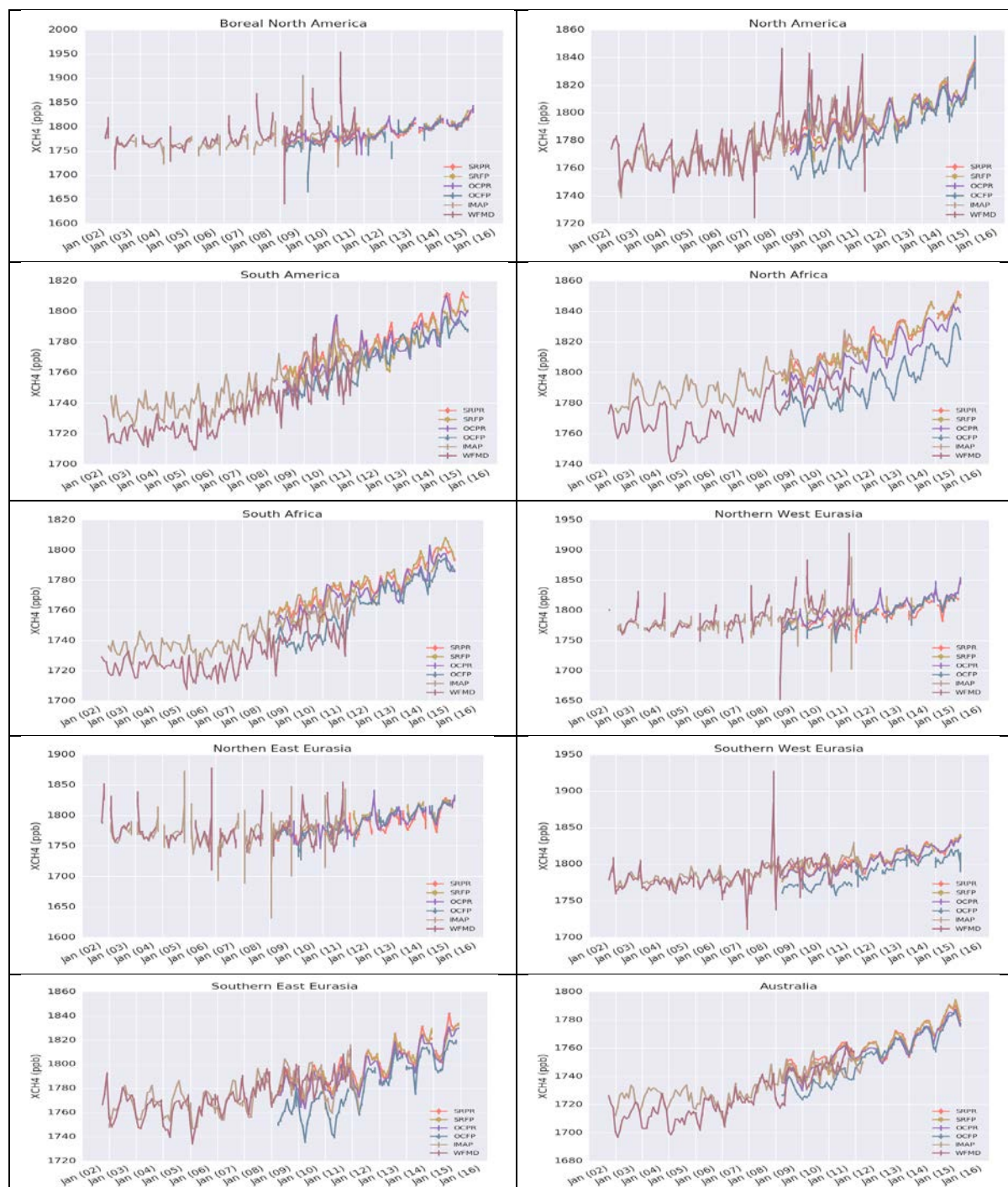


Figure 6.5.2.3: Regional monthly averaged XCH₄ concentrations for SCIAMACHY and GOSAT data.



ESA Climate Change Initiative (CCI)

**Product Validation and
Intercomparison Report (PVIR)**

for the Essential Climate Variable (ECV)
Greenhouse Gases (GHG)

Page 202

Version 5.0
Final

9 Feb 2017

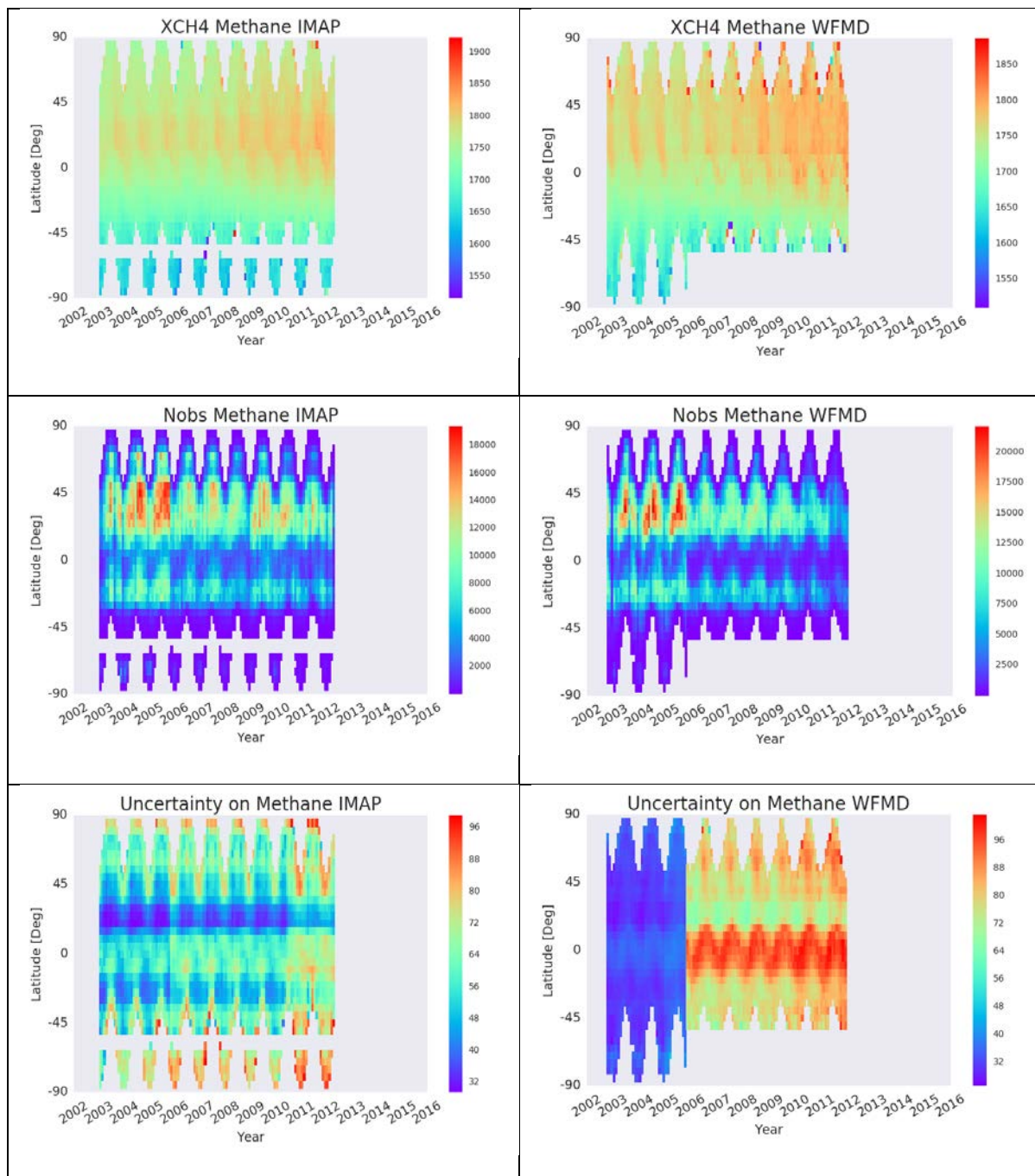


Figure 6.5.2.4: “Flying carpet” monthly averaged XCH₄ concentrations for SCIAMACHY (IMAPv7.2 and WFMDv4.0). From top to bottom: Average XCH₄ values, average uncertainty and total number of observations that passed the quality filter.



ESA Climate Change Initiative (CCI)

**Product Validation and
Intercomparison Report (PVIR)**

for the Essential Climate Variable (ECV)
Greenhouse Gases (GHG)

Page 203

Version 5.0
Final

9 Feb 2017

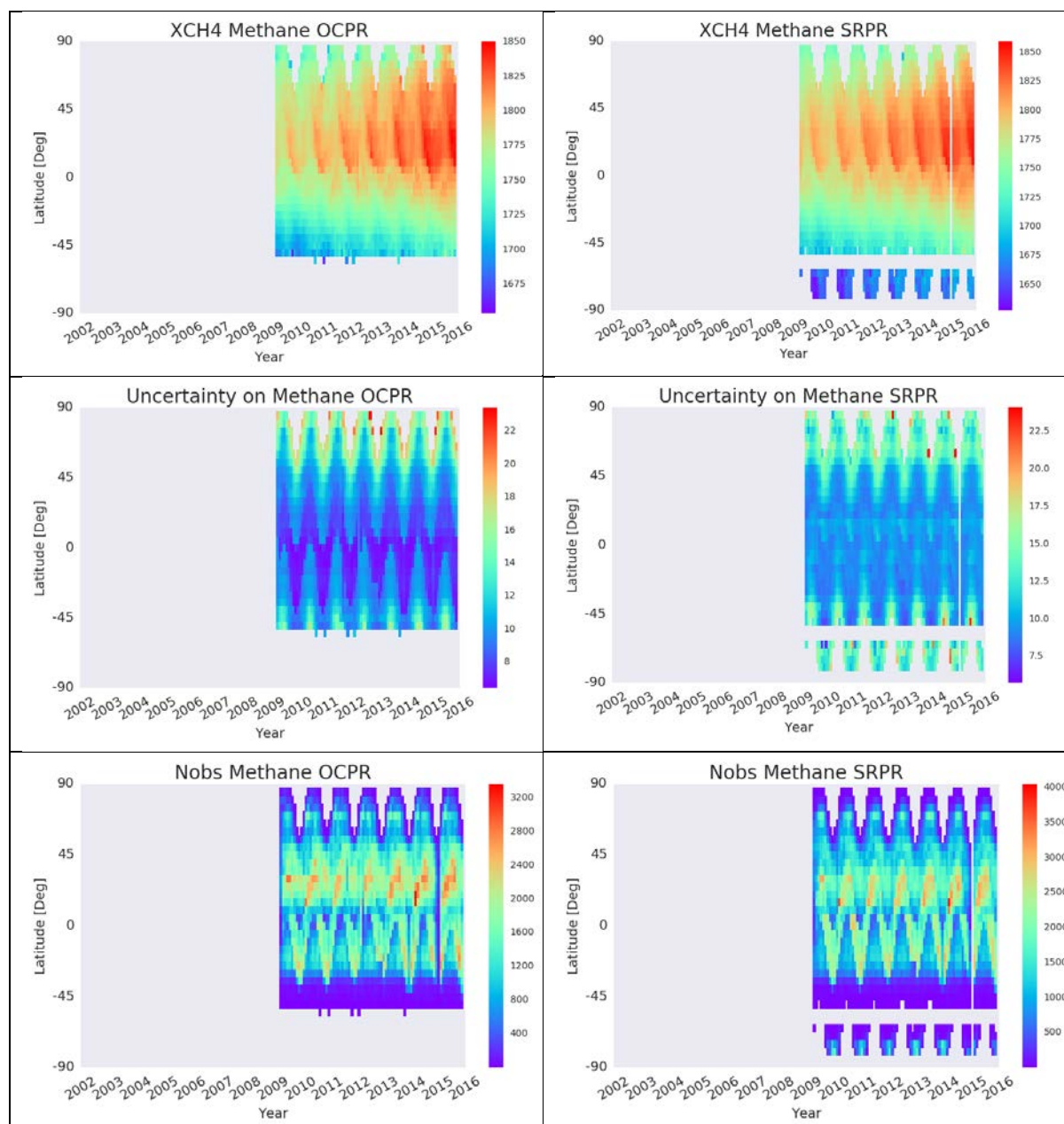


Figure 6.5.2.5: “Flying carpet” monthly averaged XCH₄ concentrations for GOSAT PROXY data (OCPR v7.0 and SRPR 2.3.8). From top to bottom: Average XCH₄ values, average uncertainty and total number of observations that passed the quality filter.



ESA Climate Change Initiative (CCI)

Product Validation and Intercomparison Report (PVIR)

for the Essential Climate Variable (ECV)
Greenhouse Gases (GHG)

Page 204

Version 5.0
Final

9 Feb 2017

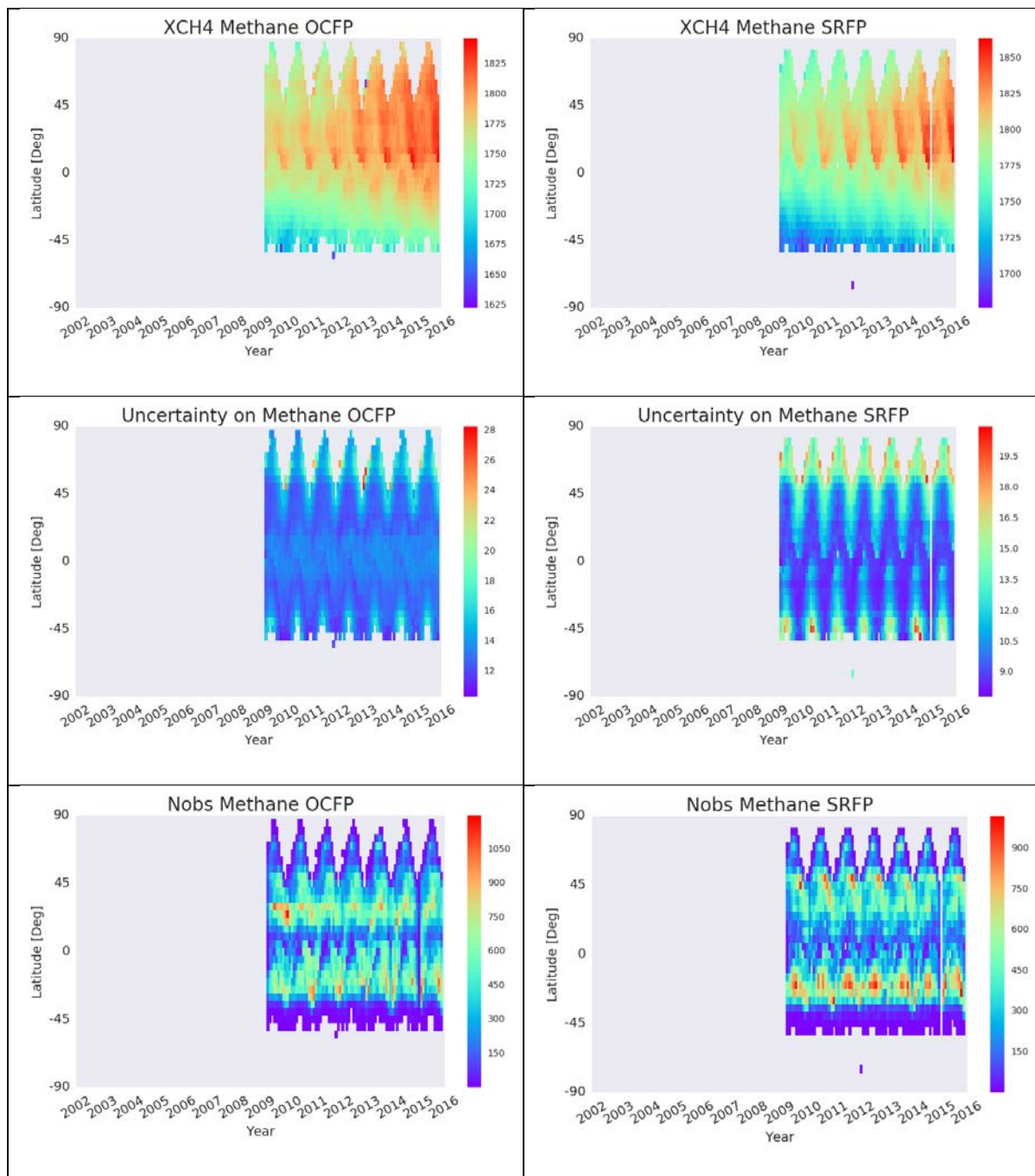



Figure 6.5.2.6: “Flying carpet” monthly averaged XCH₄ concentrations for GOSAT Full Physics data (OCFP v2.0 and SRFP 2.3.8). From top to bottom: Average XCH₄ values, average uncertainty and total number of observations that passed the quality filter.

	ESA Climate Change Initiative (CCI)	Page 205
	Product Validation and Intercomparison Report (PVIR)	
	for the Essential Climate Variable (ECV) Greenhouse Gases (GHG)	Version 5.0 Final
		9 Feb 2017

7 QA/QC: TCCON comparisons

For Quality Assurance / Quality Control (QA/QC) purposes a system has been set up which is based on a comparison of the ECA data products with corresponding TCCON products at six TCCON sites (2 in the US: Park Falls (PFA) and Lamont (LAM), 2 in Europe: Bremen (BRE) and Bialystok (BIA), 2 in the southern hemisphere: Darwin (DAR) and Wollongong (WOL)).

The main purpose is to get a reliable overview about the quality of the various data products using the same comparison method applied to all products. The results are essentially complementary to the more detailed comparison results presented in, e.g., **Sect. 3**. Note that TCCON version GGG2014 products have been used for the comparisons shown here (using TCCON data downloaded from the TCCON website on 7-Nov-2016).

For each satellite product and each of the chosen TCCON sites the following key quantities have been computed (see **Fig. 7.1** showing the analysis for product CH₄_SCI_IMAP at TCCON site Lamont):

- Bias:
 - Difference satellite – TCCON listed as mean bias +/- standard deviation (of the individual differences, i.e., using the individual (Level 2 product) satellite observations). Also listed is the “Seasonal bias”, which is the standard deviation of the biases computed for each season.
- Uncertainty:
 - Listed in **Fig. 7.1** in grey (at the top) is the mean value of the reported uncertainty (“rep.uncert.”) and the ratio (“ratio”) of the reported uncertainty to the estimated uncertainty computed as standard deviation of the difference to TCCON. This ratio should not be too far away from 1.0 if the reported uncertainty is reliable.
- Number of observations (N_{obs}):
 - This is the number of individual satellite observations used for the comparison.
- Stability:
 - Linear trend (drift) (see blue text bottom left of **Fig. 7.1**): The slope (X) and the slope error (Y, 3-sigma) of a straight line fit to the satellite – TCCON difference are listed, reported as X +/- Y.
 - Year-to-year stability (see green text bottom right of **Fig. 7.1**): In **/URD GHG-CCI v2.1/** an extended definition of “stability” has been added, not present in previous versions of the URD. To address this, annual satellite – TCCON differences have been analysed, which have been computed by averaging daily satellite – TCCON differences (black symbols in bottom panel of **Fig. 7.1**). Before this averaging the daily differences have been corrected for seasonal variations (to avoid “artificial” annual error contributions due to

different sampling of the daily data within each year) by fitting a combination of sin and cos functions to the daily differences. The results are reported as $X \pm Y$, where X is the peak-to-peak difference of the annual biases (as the URD refers to bias changes “from one year to another” and not from one year to the next) and Y is an estimate of the (3-sigma) uncertainty of X . The computed value of X is assumed to be significant (and therefore can be compared with the user requirement) if the absolute value of X is less than Y .

As can be seen from **Fig. 7.1**, the following results have been obtained for stability:

- The linear trend is -2.13 ± 1.08 ppb/yr, i.e., the obtained trend is assumed to be significant at this site (note however that the final conclusion reported later will be based on the same analysis but applied to several sites).
- The obtained value for year-to-year stability is 10.37 ± 17.92 ppb/yr, which means than a significant year-to-year instability has not been detected at this site (note however that the final conclusion reported later will be based on the same analysis but applied to several sites).

GHG-CCI

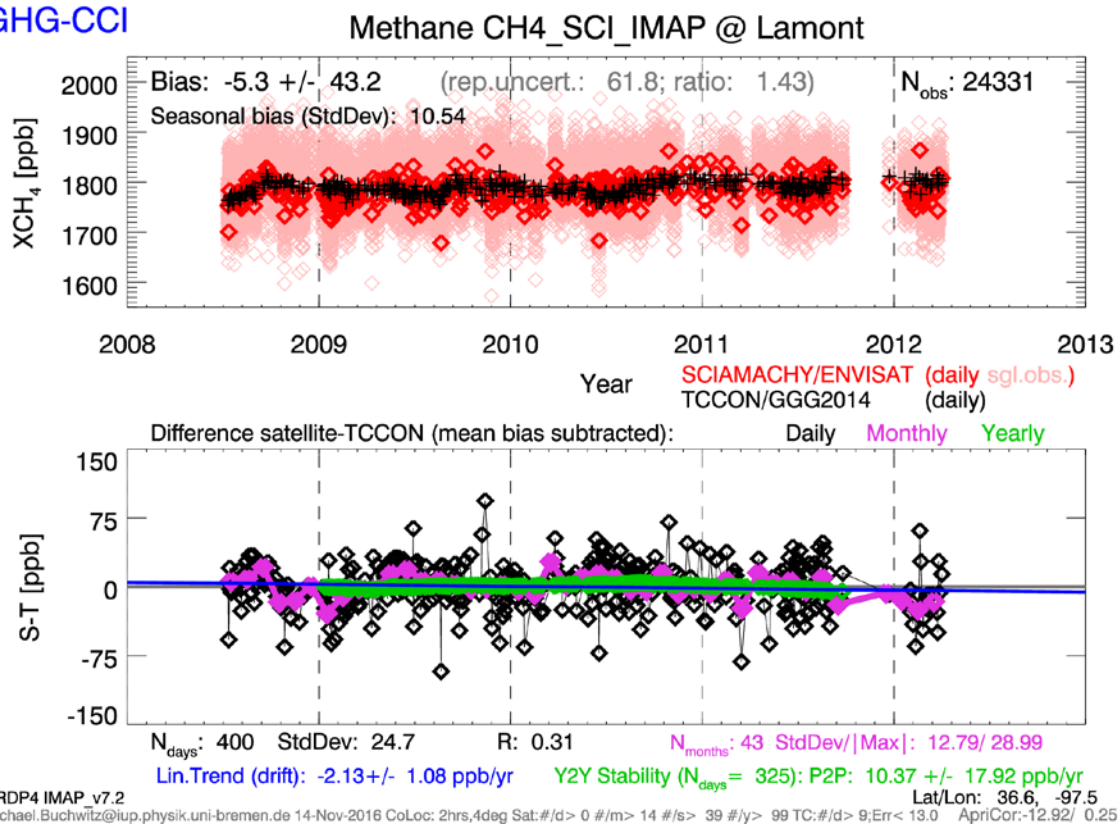


Fig. 7.1: Illustration of the QA/QC procedure and obtained results for product CH₄_SCI_IMAP at TCCON site Lamont.

Note that the extended definition of stability has been added to the URD to better consider, for example, data product „jumps“. A jump of about 20 ppb at around mid 2010 was present in the previous (CRDP#3) version of the CH₄_SCI_IMAP data product. To test the procedure it has also been applied to the CRDP#3 version (v7.1cci) of the CH₄_SCI_IMAP data product and the results for Lamont are shown in **Fig. 7.2**. As can be seen from **Fig. 7.2** the following results have been obtained for stability:

- The linear trend is 4.06 +/- 1.04 ppb/yr, i.e., the obtained trend is significant at this site.
- The obtained value for year-to-year stability is 22.47 +/- 17.45 ppb/yr, which means that there is a significant year-to-year instability at this site.

This indicates that the chosen approach to quantify year-to-year stability is reasonable (as already shown earlier, e.g., **Fig. 6.5.1.1** and **Fig. 6.5.1.2** the new IMAP product (v7.2) does not suffer from an obvious jump and is therefore of higher quality (at least for this aspect) compared to the previous version (v7.1cci).

GHG-CCI

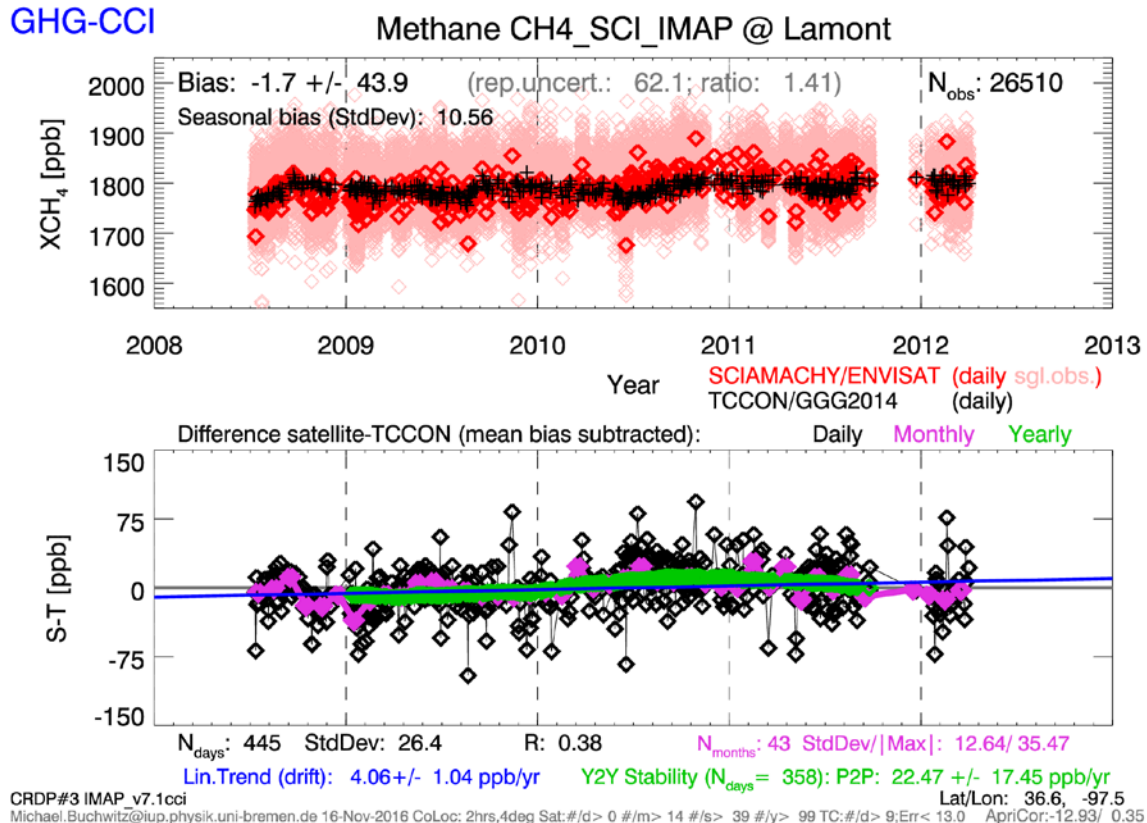


Fig. 7.2: As **Fig. 7.1** but for the previous (CRDP#3) version of the CH₄_SCI_IMAP product (v7.1cci).

The corresponding CRDP#4 results for product CH₄_SCI_WFMD are shown in **Figs. 7.3** for Lamont and **Fig. 7.4** shows a summary of the results for CH₄_SCI_WFMD at all 6 TCCON sites.

GHG-CCI

Methane CH₄_SCI_WFMD @ Lamont

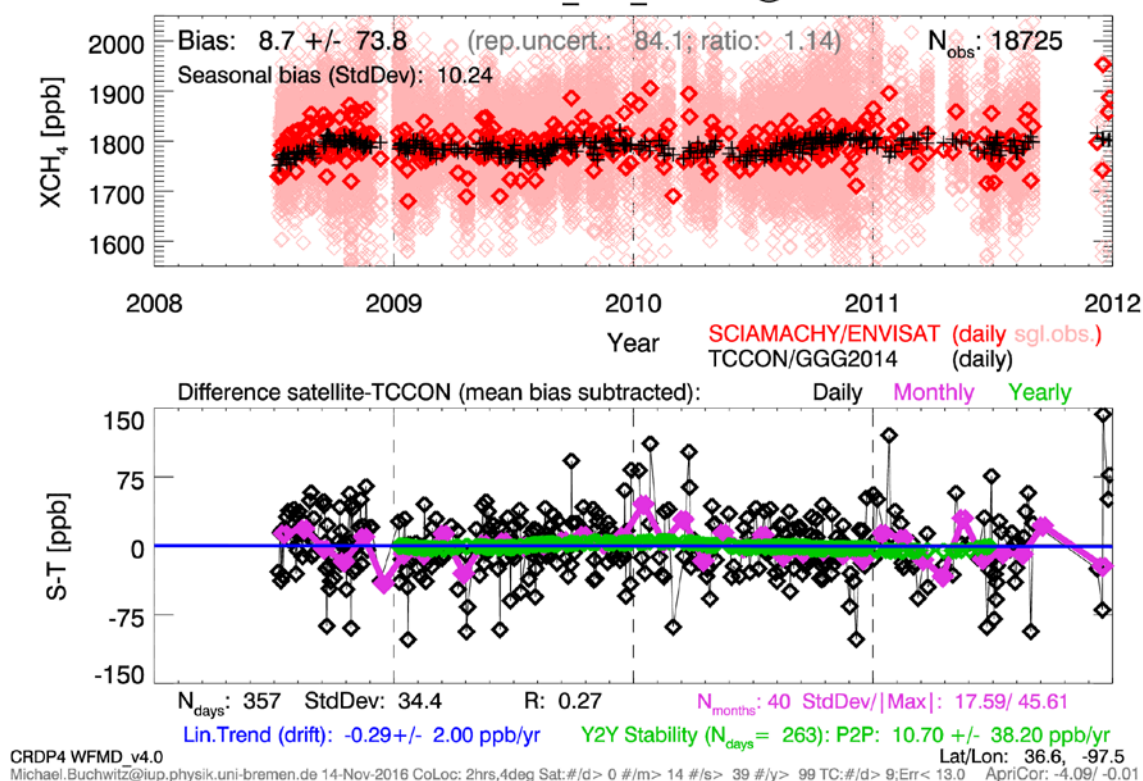


Fig. 7.3: As **Fig. 7.1** but for the CH₄_SCI_WFMD product.

GHG-CCI CRDP#4

XCH₄ product: CH4_SCI_WFMD

	N _{obs}	Bias	SeasBias	Scatter	RepUnc	UncRat	N _{years}	Trend	TrendUnc	y2ySta	y2yStaUnc
	[-]	[ppb]	[ppb]	[ppb]	[ppb]	[-]	[-]	[ppb/year]	[ppb/year]	[ppb/year]	[ppb/year]
PFA	11067	3.6	19.0	77.3	67.3	0.9	8	1.185	0.836	43.730	79.210
LAM	18725	8.7	10.2	73.8	84.1	1.1	4	-0.288	2.002	10.700	38.200
BRE	1512	2.2	18.7	91.2	85.8	0.9	5	-1.748	4.802	-	-
BIA	2230	0.5	17.8	87.3	84.2	1.0	3	5.198	7.621	-	-
DAR	10578	-15.7	15.5	66.6	82.6	1.2	7	-2.092	1.383	25.080	87.550
WOL	2831	-20.1	16.8	85.5	82.0	1.0	4	7.093	5.341	-	-
Sum	46943										
Mean		-3.5	16.3	80.3	81.0	1.0		1.558	3.664	26.503	68.320
StdDev		11.6						3.786			

Systematic error (reg.bias, 1-sigma): 11.6 ppb Seasonal: 16.3 ppb
 Uncertainty (sgl.obs., 1-sigma): 80.3 ppb
 Uncertainty ratio: 1.0
 Trend +/- uncertainty: 1.56 +/- 3.79 ppb/year
 Year2Year-Stability(p2p) +/- uncertainty: 26.50 +/- 68.32 ppb/year
 Global offset: -3.5 ppb
 N_{obs}: 46943

Michael.Buchwitz@iup.physik.uni-bremen.de 15-Nov-2016

Fig. 7.4: Summary of QA/QC assessment for WFMD XCH₄ at the chosen TCCON sites. Note that year-to-year stability (y2ySta) results are only shown for sites where enough data are available for this analysis.

Figure 7.5 shows the results for product CO2_SCI_BESD at Lamont.

An overview about the BESD XCO₂ results at all TCCON sites is shown in **Fig. 7.6**.

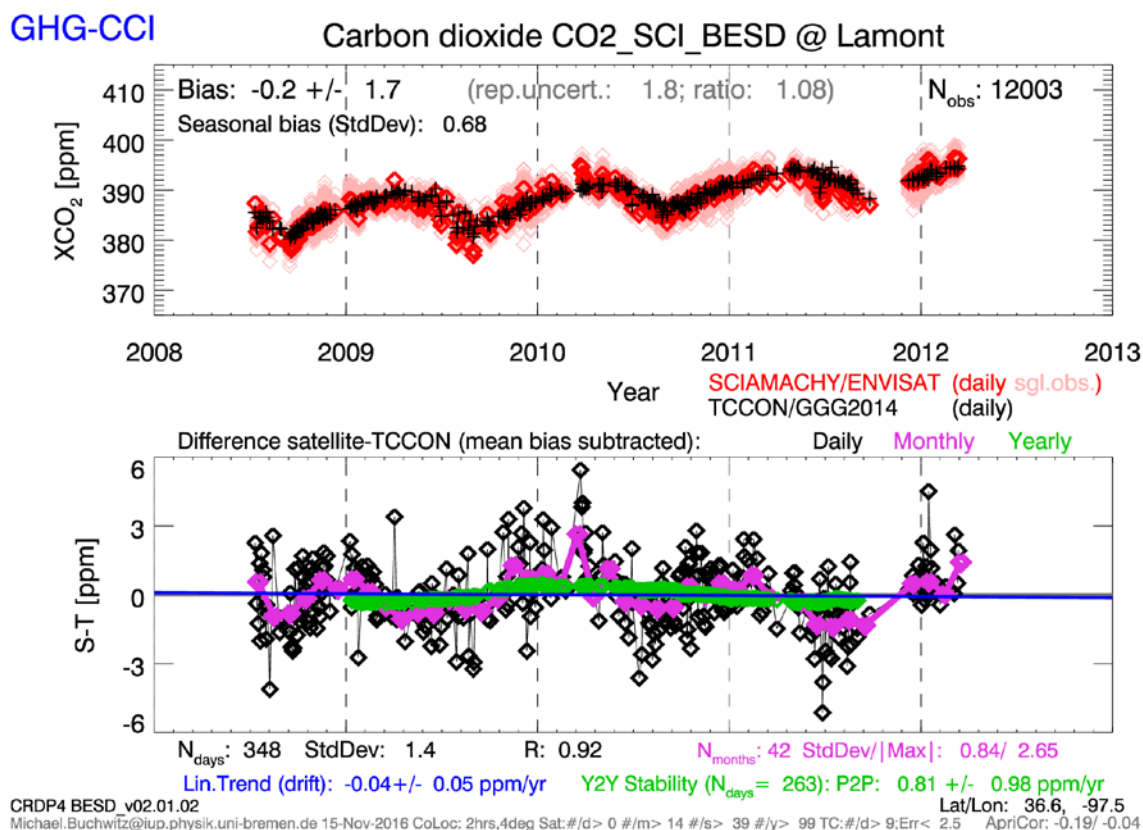


Fig. 7.5: Illustration of QA/QC assessment for BESD XCO₂ at TCCON site Lamont, USA.

GHG-CCI CRDP#4

XCO₂ product: CO2_SCI_BESD


	N _{obs}	Bias	SeasBias	Scatter	RepUnc	UncRat	N _{years}	Trend	TrendUnc	y2ySta	y2yStaUnc
	[-]	[ppm]	[ppm]	[ppm]	[ppm]	[-]	[-]	[ppm/year]	[ppm/year]	[ppm/year]	[ppm/year]
PFA	2931	-0.2	0.8	2.0	1.9	1.0	8	0.130	0.042	2.200	3.710
LAM	12003	-0.2	0.7	1.7	1.8	1.1	5	-0.042	0.046	0.810	0.980
BRE	1036	-0.4	0.8	1.8	2.0	1.1	5	-0.126	0.108	-	-
BIA	1124	-0.2	1.0	2.0	1.9	0.9	4	0.035	0.162	-	-
DAR	7323	-0.5	0.9	1.8	1.8	1.0	7	-0.061	0.042	2.020	1.400
WOL	2389	0.5	0.6	2.2	1.9	0.8	4	-0.022	0.108	-	-
Sum	26806										
Mean		-0.2	0.8	1.9	1.9	1.0		-0.014	0.085	1.677	2.030
StdDev		0.4						0.088			

Systematic error (reg.bias, 1-sigma): 0.4 ppm Seasonal: 0.8 ppm
 Uncertainty (sgl.obs., 1-sigma): 1.9 ppm
 Uncertainty ratio: 1.0
 Trend +/- uncertainty: -0.01 +/- 0.09 ppm/year
 Year2Year-Stability(p2p) +/- uncertainty: 1.68 +/- 2.03 ppm/year
 Global offset: -0.2 ppm
 N_{obs}: 26806

Michael.Buchwitz@iup.physik.uni-bremen.de 15-Nov-2016

Fig. 7.6: Summary of QA/QC assessment for BESD XCO₂ at the chosen TCCON sites. Note that year-to-year stability (y2ySta) results are only shown for sites where enough data are available for this analysis.

The results for all TCCON sites and all XCO₂ and XCH₄ products are shown in the following two sub-sections.

	ESA Climate Change Initiative (CCI)	Page 212
	Product Validation and Intercomparison Report (PVIR)	
	for the Essential Climate Variable (ECV) Greenhouse Gases (GHG)	Version 5.0 Final
		9 Feb 2017

7.1 XCO₂ QA/QC comparison results

Based on the method explained in **Sect. 7**, overall results for XCO₂ for all products have been computed. They are summarized in this section.

The overall QA/QC results for the GHG-CCI XCO₂ products BESD, WFMD, SRFP and OCFP are shown in **Tab. 7.1.1**.

Two values for the (relative) systematic error or bias are listed in column “Sys.err.”: The first value is the standard deviation of the bias at the various TCCON sites. The second value (“seasonal bias”; in brackets) is the mean value of the standard deviation of the seasonal biases at all used TCCON sites.

“Uncert.” is the mean value of the reported uncertainty and “Unc.rat.” is the ratio of the reported uncertainty to the TCCON-estimated uncertainty obtained from the standard deviation of the difference of the individual observations with TCCON. If “Unc.rat.” is “close” to 1.0 then this indicates that the reported uncertainty is (on average) realistic.

Column “Lin.Trend” lists the linear trend of the difference to TCCON and its estimated uncertainty (3 sigma). The symbol “(*)” indicates if the trend is supposed to be significant. Here a “significant trend” is an estimated trend whose absolute value is larger than its estimated uncertainty.

Column “y2yStab” lists the values obtained for “Year-to-year stability” of the annual difference to TCCON and its estimated uncertainty (3 sigma). The symbol “(#)” indicates if the obtained value for year-to-year stability is supposed to be significant. Here a “significant year-to-year instability” is indicated by a number whose absolute value is larger than its estimated uncertainty.

Column “Offset” lists the overall mean bias w.r.t. TCCON and “N_{obs}” lists the number of individual (Level 2) satellite observations used for the comparison with TCCON.

GHG-CCI CRDP#4

XCO₂ products

	Sys.err.	Uncert.	Unc.rat.	Lin.Trend	y2yStab	Offset	N _{obs}
	[ppm]	[ppm]	[-]	[ppm/year]	[ppm/year]	[ppm]	[-]
CO2_SCI_BESD	0.4 (0.8)	1.9	1.0	(*) -0.01 +/- 0.09	(#) 1.68 +/- 2.03	-0.2	26806
CO2_SCI_WFMD	0.5 (1.0)	2.7	1.2	(*) -0.04 +/- 0.10	(#) 1.86 +/- 2.41	0.1	49987
CO2_GOS_SRFP	0.4 (0.5)	1.9	1.0	(*) -0.06 +/- 0.11	(#) 1.30 +/- 2.11	0.1	8220
CO2_GOS_OCFP	0.3 (0.5)	1.7	1.0	-0.09 +/- 0.08	(#) 1.48 +/- 2.06	0.1	7474

(*): trend not significant

(#): y2y variations not significant

Tab. 7.1.1: Overall QA/QC results for the GHG-CCI XCO₂ products.

The time series of satellite – TCCON annual differences as used for the year-to-year stability assessment are shown in **Fig. 7.1.1**. As can be seen, the curves for a given product but for different TCCON sites are typically quite different, in contrast to what one would expect if there is “instability”. It is therefore concluded from visual inspection of the curves shown in **Fig. 7.1.1** that there are no clear indications for instability. This conclusion is consistent with the conclusion drawn from **Tab. 7.1.1**.

Note that from the values listed in **Tab. 7.1.1** one may conclude that product CO2_GOS_OCFP is not perfectly stable (as the trend is slightly significant according to the used interpretation, not however the year-to-year stability). As can be seen from **Fig. 7.1.1** the variation of the curves for CO2_GOS_OCFP is larger compared to the other GOSAT product, CO2_GOS_SRFP, which is not classified as having significant instability. The uncertainty of the year-to-year stability for CO2_GOS_OCFP is however only slightly larger than the computed value for year-to-year stability indicating that this product seems to be just at the edge of being unstable and this conclusion seems to be consistent with what one would conclude from the visual inspection of the curves shown in **Fig. 7.1.1**.

For stability the overall conclusions is therefore that for all four XCO₂ products no clear indications for instability have been identified. All products are therefore classified “stable”.

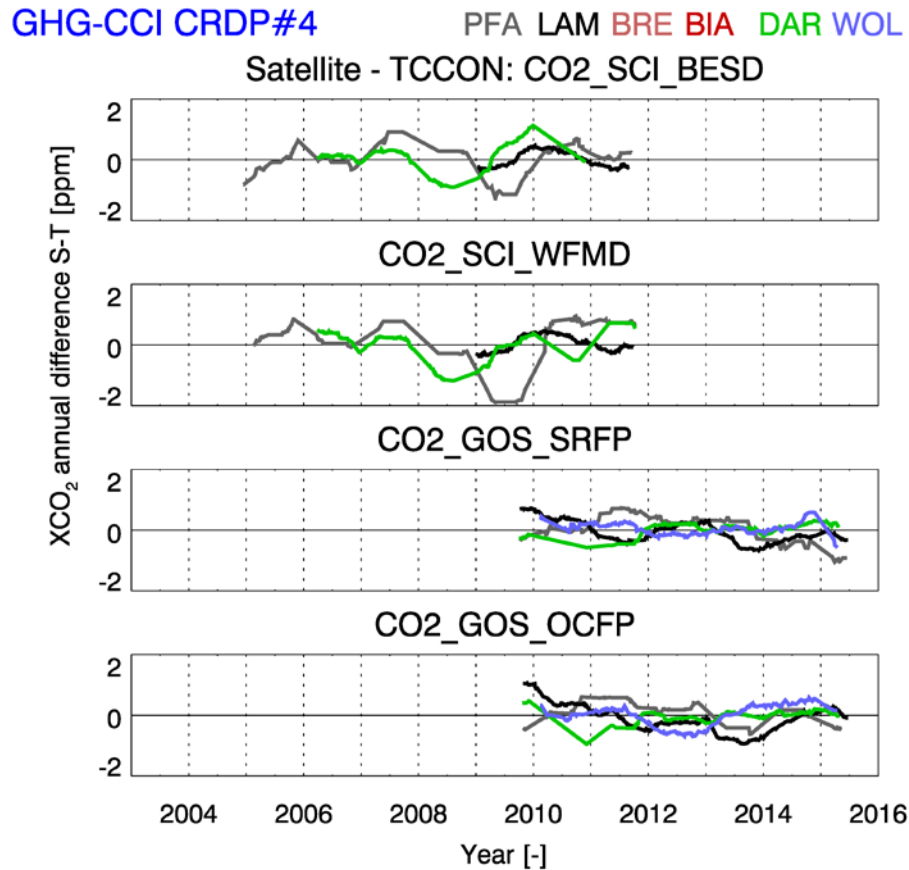



Fig. 7.1.1: Satellite – TCCON annual XCO₂ differences as used to assess year-to-year stability. If no data are shown for a certain TCCON site than this means that not enough data are available at this site to carry out the year-to-year stability assessment.

	ESA Climate Change Initiative (CCI)	Page 215
	Product Validation and Intercomparison Report (PVIR)	
	for the Essential Climate Variable (ECV) Greenhouse Gases (GHG)	Version 5.0 Final
		9 Feb 2017

7.2 XCH₄ QA/QC comparison results

Based on the method explained at the beginning of **Sect. 7**, overall QA/QC results for XCH₄ for all products have been obtained. These results are summarized in this section.

The overall QA/QC results for the six GHG-CCI XCH₄ products WFMD, IMAP, SRFP, OCPR, SRPR and OCFP are shown in **Tab. 7.2.1**.

For an explanation of this table see the description of **Tab. 7.1.1** (showing the corresponding results for XCO₂).


Concerning stability:

For product CH₄_GOS_SRPR the stability is at the edge of being significant: The trend is slightly significant (the absolute value is slightly larger than its estimated uncertainty) but the year-to-year variations are not significant. Overall it is concluded that this product is quite stable.

In contrast, product CH₄_GOS_OCFP is considered “unstable” as the obtained values for linear trend and year-to-year stability are both significant (as their uncertainties are smaller than their absolute value). This “instability” is also confirmed via the results shown in **Fig. 7.2.1**. The linear trend is however very small, only 1.2 ppb/year. This means that the linear trend meets the breakthrough user requirement of < 2 ppb/year as specified in the URD **/URD GHG-CCI v2.1/** and even nearly the goal requirement of < 1 ppb/year.

The year-to-year bias is however 15.8 ppb/year, which is larger than the threshold user requirement of 3 ppb/year. This means that this requirement is not met, if the interpretation of this user requirement is correct. Note that the value of 15.8 ppb is the peak-to-peak bias of annual errors (computed assuming error-free TCCON data and negligible contributions of other error sources such as sampling) over the entire time series of this product, which covers 6.5 years (mid 2009 to end of 2015).

Note: If one would convert the XCH₄ annual difference of 15.8 ppb to a true “per year error”, one would have to compute $15.8 \text{ ppb} / 6.5 \text{ years} = 2.4 \text{ ppb/year}$. If this interpretation is used this would mean that the < 3 ppb/year threshold requirement is met. If this interpretation is used then the number obtained to estimate “inter-annual error changes” (see **/URD GHG-CCI v2.1/**) (here: year-to-year stability or annual bias variability) can also be directly compared with the number obtained for the linear trend (which is also a true “per year error”, i.e., 1.2 ppb/year corresponds to an error of 7.8 ppb over the entire 6.5 years time period). To clarify this potential interpretation issue the authors of the URD **/URD GHG-CCI v2.1/** have been contacted. They clarified that this (alternative) interpretation is not what they had in mind when formulating the new stability requirement, i.e., the obtained value of 15.8 ppb should not be divided by the number of years. Instead, the obtained number of 15.8 ppb/year needs to be directly compared with the user requirement (of < 3 ppb/year for the threshold requirement).

	ESA Climate Change Initiative (CCI)	Page 216
	Product Validation and Intercomparison Report (PVIR)	
	for the Essential Climate Variable (ECV) Greenhouse Gases (GHG)	Version 5.0 Final
		9 Feb 2017

GHG-CCI CRDP#4

XCH₄ products

	Sys.err.	Uncert.	Unc.rat.	Lin.Trend	y2yStab	Offset	N _{obs}
	[ppb]	[ppb]	[-]	[ppb/year]	[ppb/year]	[ppb]	[-]
CH4_SCI_WFMD	11.6 (16.3)	80.3	1.0	(*) 1.56+/- 3.79	(#)26.50+/-68.32	-3.5	46943
CH4_SCI_IMAP	11.7 (11.5)	46.6	1.3	(*) 0.95+/- 2.66	(#)19.15+/-44.26	-12.5	59156
CH4_GOS_SRFPP	4.4 (3.2)	12.6	1.0	(*) -0.42+/- 1.00	(#) 8.68+/-14.67	-0.4	8244
CH4_GOS_OCPR	4.4 (3.6)	11.8	0.9	(*) -0.18+/- 0.90	(#) 7.97+/-10.75	2.0	18000
CH4_GOS_SRPR	2.3 (4.5)	12.8	0.9	-0.87+/- 0.86	(#) 8.96+/-10.62	-2.5	19195
CH4_GOS_OCFP	4.7 (4.7)	13.2	1.0	1.22+/- 0.80	15.84+/-13.67	-4.3	7320

(*): trend not significant

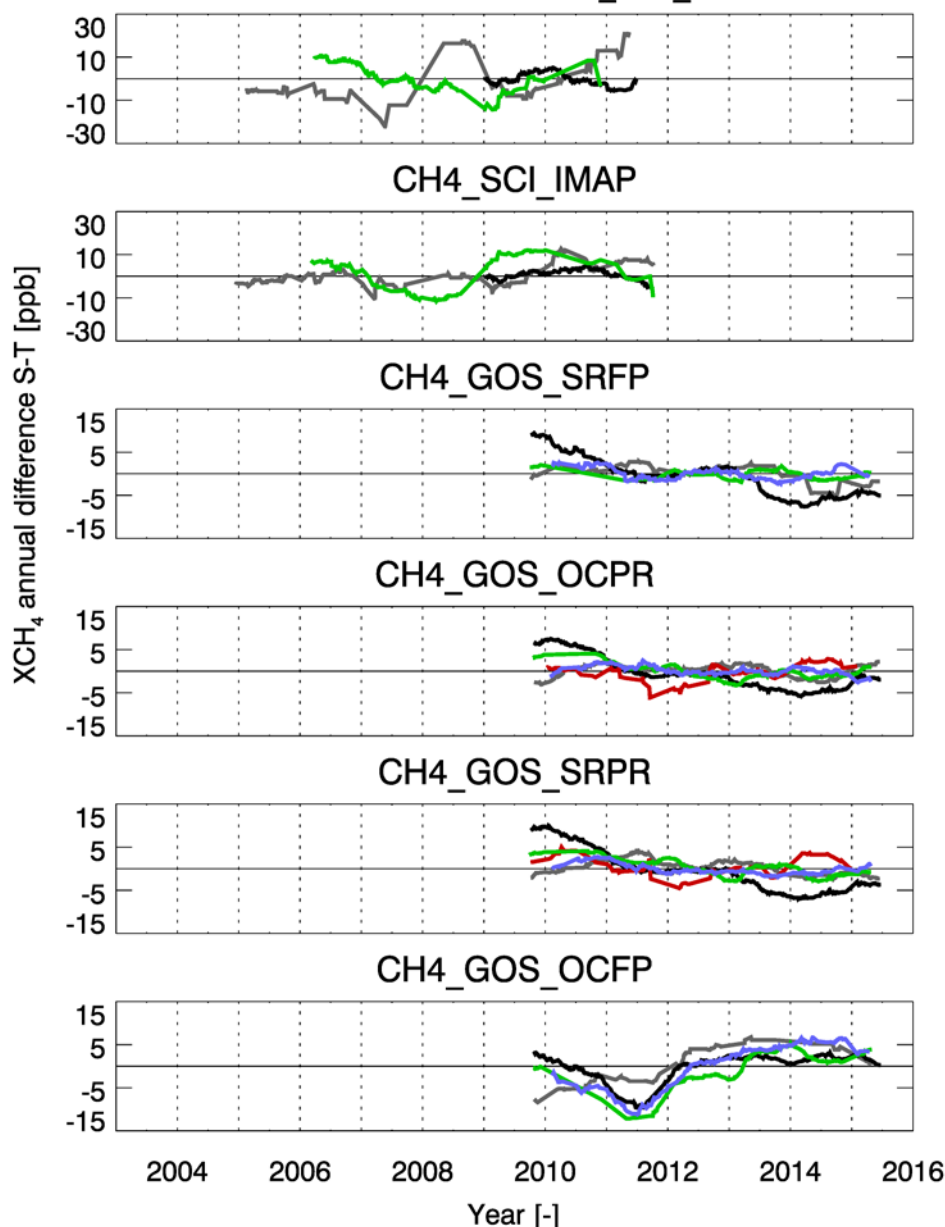
(#): y2s variations not significant

Tab. 7.2.1: Overall QA/QC results for the GHG-CCI XCH₄ products.

GHG-CCI CRDP#4

PFA LAM BRE BIA DAR WOL

Satellite - TCCON: CH₄_SCI_WFMD



CRDP4 Michael.Buchwitz@iup.physik.uni-bremen.de 15-Nov-2016

Fig. 7.2.1: Satellite – TCCON annual XCH₄ differences as used to assess year-to-year stability. If no data are shown for a certain TCCON site than this means that not enough data are available at this site to carry out the year-to-year stability assessment.

8 Assessment of aerosol induced biases

8.1 Introduction

Aerosols have been identified as an important factor causing biases in satellite GHG products (e.g. Heymann et al., 2012). Aerosols can significantly modify the length of the light path and thereby alter the apparent absorption observed by the satellite. Reliable GHG retrievals can be made only when the aerosol loading is below some threshold. Hence, to obtain accurate XCO_2 or XCH_4 observations from a satellite requires that these highly scattering scenes are correctly identified and filtered out, and that the aerosol effects for the remaining scenes are properly accounted for in the retrieval.

In this work we have investigated how well the GHG CCI CO_2 algorithms filter out the high scattering aerosol scenes and to which extent a possible bias in satellite XCO_2 can be attributed to aerosols. The XCO_2 bias (ΔXCO_2) was defined as the difference between satellite and TCCON XCO_2 . A challenge in this work was, however, that most of the TCCON stations are located in areas where the aerosol loading and the corresponding influence on the retrieval are generally quite low (Figure 8.1.1). On the other hand, TCCON provides the most accurate observations of the column-averaged dry-air mole fractions of CO_2 , and, therefore is the most useful validation data set.

To study the effect of aerosols on ΔXCO_2 , independent information on aerosols was needed. In this work the aerosol observations were obtained either from the global AERONET sunphotometer network (Holben et al., 1998), or satellite instruments dedicated to observe aerosols. The advantage of using AERONET observations is that the sunphotometers provide very accurate observations of several aerosol optical properties including aerosol optical depth (AOD). On the other hand, there are only three locations where an AERONET and a TCCON station are located next to each other. To be able to include also those TCCON stations in the analysis that don't have an AERONET station in their vicinity, GOSAT and SCIAMACHY XCO_2 observations were additionally collocated with satellite-based aerosol data. Both AERONET and satellite-based aerosol data were used to analyze the quality of the filtering for highly scattering scenes as well as the dependence of biases of the satellite XCO_2 observations (with respect to TCCON) on aerosol parameters. By using satellite-based aerosol data we were also able to carry out additional tests, e.g. to investigate how variable the aerosol conditions actually were in the surroundings of the TCCON stations.

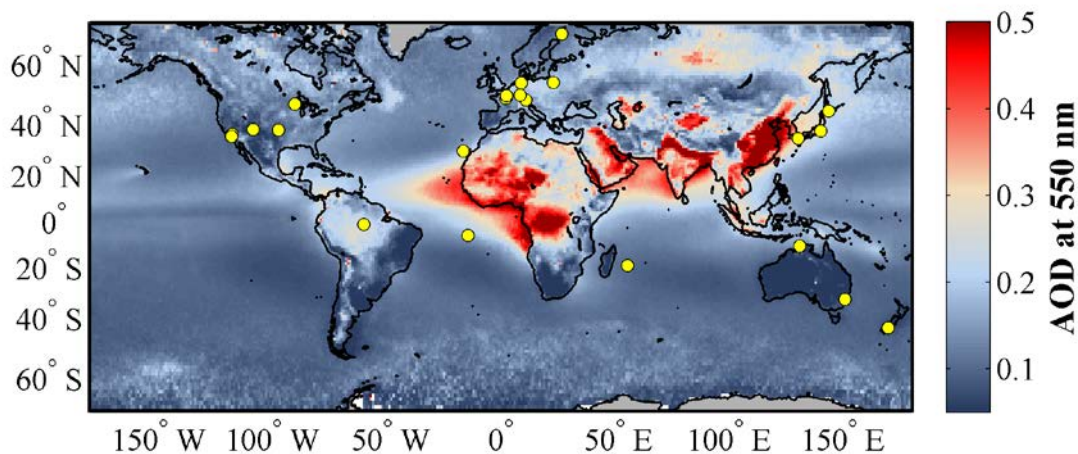


Figure 8.1.1 MODIS Aqua (Coll. 6) five year mean AOD (2009-2014) at 550 nm wavelength, and the locations of TCCON stations (yellow dots).

8.2 Data and methods

8.2.1 Data


The satellite XCO₂ data considered in this study consists of the CRDP4 datasets from the GOSAT OCFP and SRFP retrievals, as well as the SCIAMACHY BESD and WFMD retrievals. Comparisons were also made to the previous version of the satellite XCO₂ data (CRDP3). Independent XCO₂ observations were obtained from the TCCON GGG2014 dataset. All the satellite XCO₂ data used in this work were bias-corrected, unless otherwise stated, and adjusted to the TCCON a priori profile. In addition to CO₂, we have used also the TCCON H₂O observations as they may be related to hygroscopic growth and thus the optical properties of the aerosol and/or reflect the seasonal variation. The TCCON stations used in this study are listed in Table 8.2.1.1.

The independent aerosol observations were obtained either from the AERONET network or satellites. AERONET is a global sunphotometer network providing information on aerosol optical, microphysical, and radiative properties. Because the ground-based sunphotometer points directly at the sun and measurements are not significantly influenced by the surface, AERONET provides more accurate observations of the total column aerosol properties than satellites. In this work we have used Level 2.0 data (cloud-screened and quality assured) of Aerosol optical depths (AODs), and data from Spectral Deconvolution Algorithm (SDA) retrievals (Fine and coarse mode AOD, Fine mode fraction FMF, Angström coefficient AE, and derivative of Angström coefficient AE'; O'Neill et al. 2003). There are only three TCCON

stations, Lamont, Darwin, and Pasadena/JPL that have or had an AERONET-station in the immediate vicinity. In addition, data from five different AERONET stations located in Asia were used to test how efficiently the high aerosol scattering scenes were identified in environments where the aerosol loading is generally higher than at the TCCON stations. The AERONET stations used in this work are shown in Table 8.2.1.1.

TCCON station	Abbreviation	TCCON Data availability	AERONET station	AERONET Data availability
Lamont	LA	07/2008→	Cart Site	01/1998→
Park Falls	PF	06/2004→	-	-
Pasadena	PA	09/2012→	CalTech	04/2010→
JPL	JPL	07/2007-06/2008	-	-
		05/2011-07/2013	CalTech	04/2010→
Darwin	DA	05/2008→	Darwin	04/2004-08/2010
			ARMDarwin	08/2010-12/2014
Wollongong	WO	06/2008→	-	-
Bialystok	BI	03/2009→	-	-
Orleans	OR	08/2009→	-	-
-	-	-	Kanpur	01/2001-11/2015
-	-	-	Dhaka Univ.	06/2012-07/2015
-	-	-	Karachi	08/2006-09/2014
-	-	-	Beijing	01/2002→
-	-	-	XiangHe	09/2004-08/2015

Table 8.2.1.1: The TCCON and AERONET stations used in this study. For AERONET stations the data availability are shown for periods when lev. 2.0 data was available. At Cart Site the

	ESA Climate Change Initiative (CCI)	Page 221
	Product Validation and Intercomparison Report (PVIR)	
	for the Essential Climate Variable (ECV) Greenhouse Gases (GHG)	Version 5.0 Final
		9 Feb 2017

measurements started already in 1994, but before 1998 the measurements were made only for single months.

The satellite-based aerosol observations were obtained from the Advanced Along Track Scanning Radiometer (AATSR) or MODerate Imaging Spectroradiometer (MODIS). The aerosol observations from the AATSR instrument onboard ESA's ENVISAT satellite are available via the Aerosol-CCI project. The primary Aerosol-CCI products include AATSR Level 2 daily aerosol observations from three different algorithms at 10x10 km² spatial resolution (Holzer-Popp et al., 2013, de Leeuw et al., 2015). Available products are the Swansea University AATSR retrieval (SU), the FMI AATSR retrieval (ADV/ASV), and the Oxford RAL Aerosol and Cloud retrieval (ORAC). In this work we have only used the AATSR SU L2 v.4.21 data, which was collocated with the data from the two SCIAMACHY XCO₂ algorithms.

The Moderate Resolution Spectroradiometer (MODIS) onboard the NASA Aqua satellite is a member of NASA's A-Train constellation and has been providing observations on aerosols and clouds since 2002. In this work we have used the MODIS Aqua Level 2 Collection 6.0 aerosol data at 10 km x 10 km spatial resolution (Levy et al., 2013). The MODIS aerosol observations were collocated with both GOSAT OCFP and SRFP high-gain XCO₂ data.

8.2.2 Collocation of the data

The satellite XCO₂ data were collocated with TCCON stations by defining a spatial average of all good quality XCO₂ pixels falling within $\pm 5^\circ$ area around the TCCON station. The corresponding TCCON data were temporally averaged over a time interval of ± 1 hours of the satellite overpass. AERONET observations were averaged ± 1 hours of the satellite overpass in the same way as TCCON. For two specific tests, more stringent spatial collocation criteria were applied. For investigating the quality of the filtering for highly scattering scenes, satellite XCO₂ data were collocated with AERONET stations with a spatial criterion of $\pm 0.15^\circ$. In addition, to obtain aerosol information at all TCCON stations included in the study, MODIS and AATSR pixels were collocated with TCCON within $\pm 0.1^\circ$.

Since the SCIAMACHY and AATSR instruments were onboard the same ENVISAT satellite, the XCO₂ and aerosol observations could be obtained simultaneously from the two instruments. However, due to the narrower swath of the AATSR instrument (512 km), the SCIAMACHY 960 km swath was not completely covered. For each good quality SCIAMACHY XCO₂ 30 km x 60 km pixel, the aerosol data from all matching 10 km x 10 km AATSR pixels with their center point located within the 30 x 60 km² SCIAMACHY pixel were averaged. The spatial mean around a TCCON was calculated using only those SCIAMACHY XCO₂ pixels where at least one matching AATSR observation was found, and similarly, the AATSR spatial



average included only those pixels having a matching good quality XCO₂. Figures 8.2.2.1 and 8.2.2.2 show the distributions of ΔXCO_2 (satellite XCO₂-TCCON XCO₂) for the SCIAMACHY BESD and WFMD products collocated in this way.

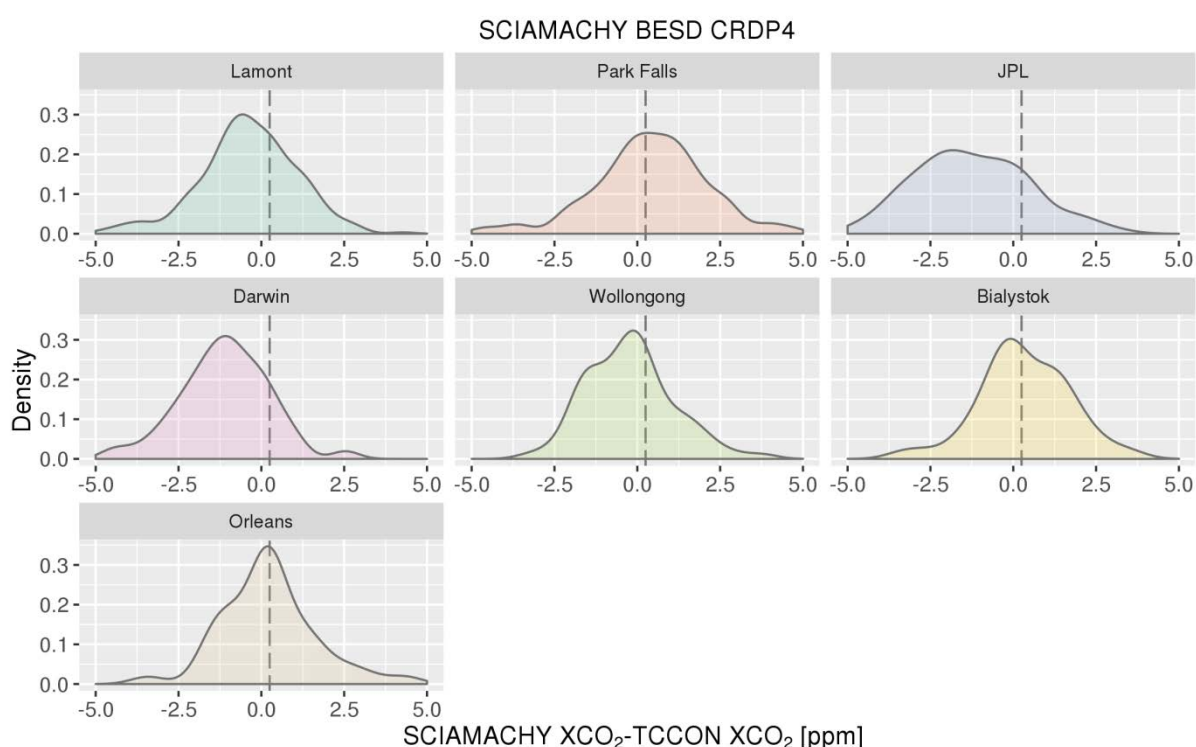


Figure 8.2.2.1: Frequency distributions of the XCO₂ bias for collocated SCIAMACHY BESD and AATSR data of the years 2004-2012. The SCIAMACHY XCO₂ spatial means have been defined only for those pixels where matching AATSR observations were found.

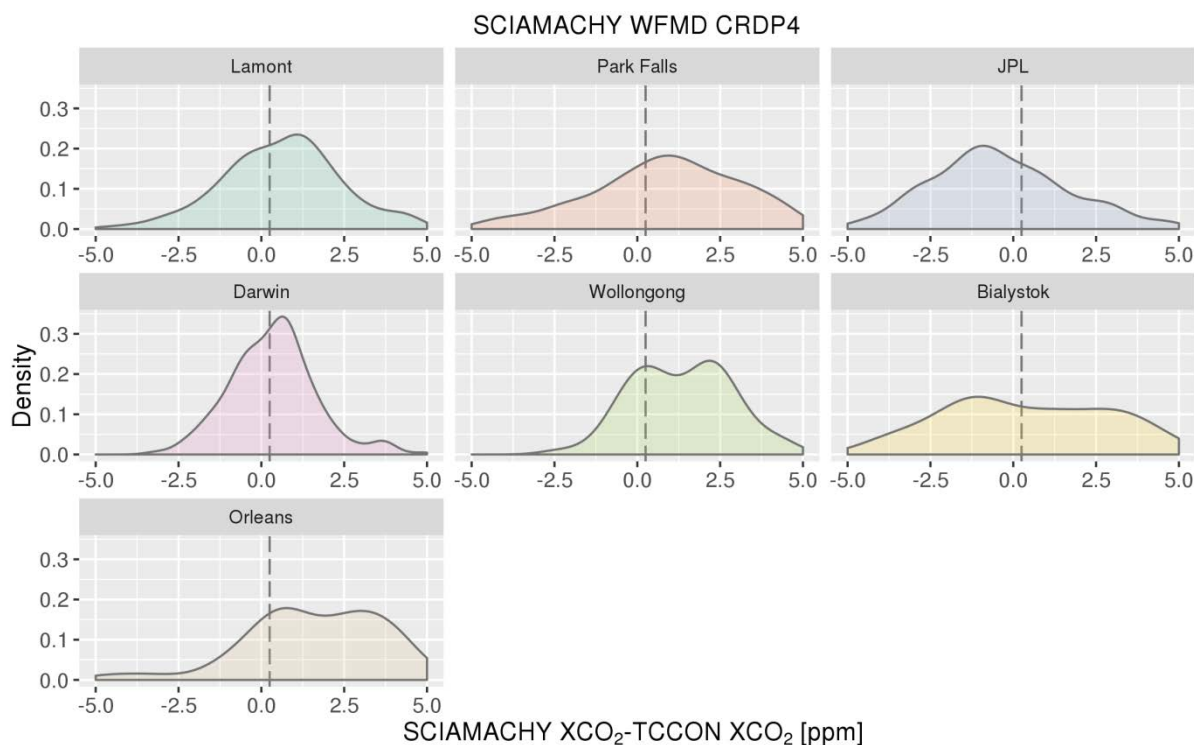


Figure 8.2.2.2: Same as Fig 8.2.2.1, but for collocated SCIAMACHY WFMD and AATSR data.

For GOSAT, collocated aerosol observations from the Moderate Resolution Spectroradiometer (MODIS) onboard the Aqua satellite were used. MODIS Aqua crosses the equator at about 13:30 local time (ascending node), GOSAT at about 13:00 (descending node). The aerosol-XCO₂ observations are thus about 30 minutes apart. Furthermore, the tracks of the satellites are not exactly the same. In this study we used the MODIS aerosol observations at 10x10 km² spatial resolution. A match between MODIS and GOSAT was considered if the center point of the MODIS pixel was within the GOSAT XCO₂ pixel. Spatial averaging at TCCON sites was done in the same way as for the pair SCIAMACHY and AATSR. Figures 8.2.2.3 and 8.2.2.4 show the distributions of ΔXCO_2 for the collocated GOSAT SRFP and OCFP and MODIS data.

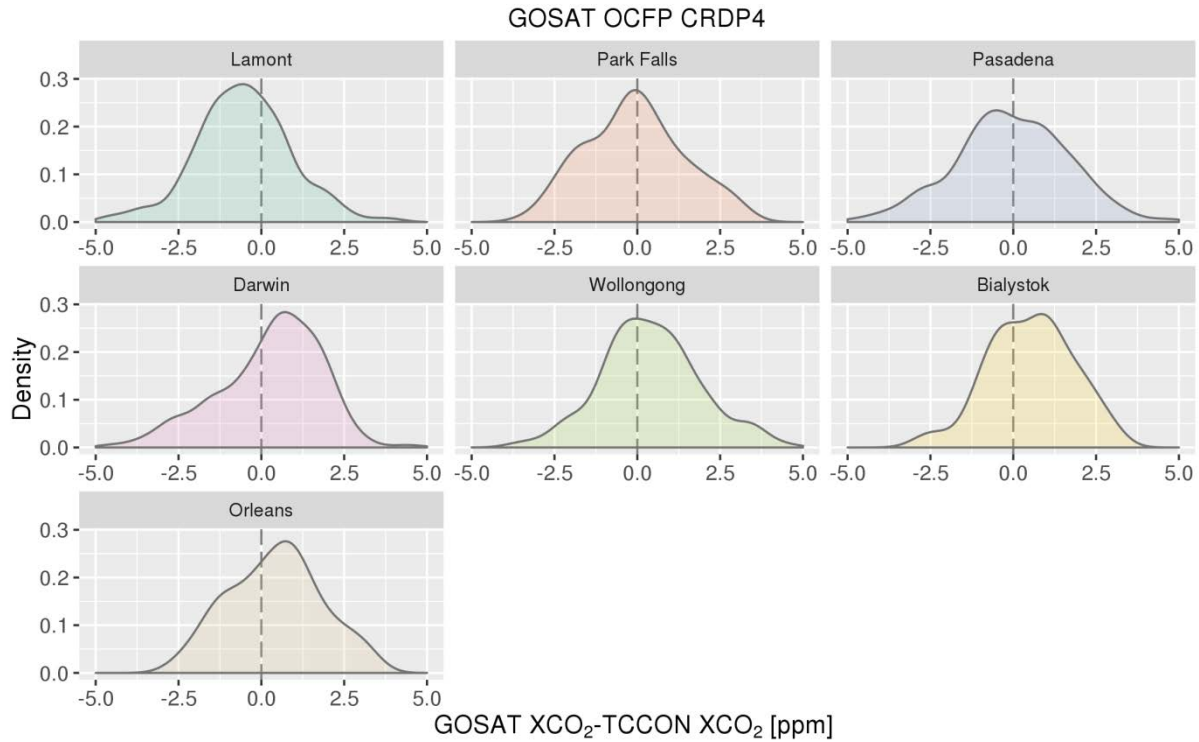


Figure 8.2.2.3: Frequency distributions of the XCO₂ bias for collocated GOSAT OCFP XCO₂ and MODIS aerosol data of the years 2009-2015. The GOSAT XCO₂ spatial means have been defined only for those pixels where matching MODIS observations were found.

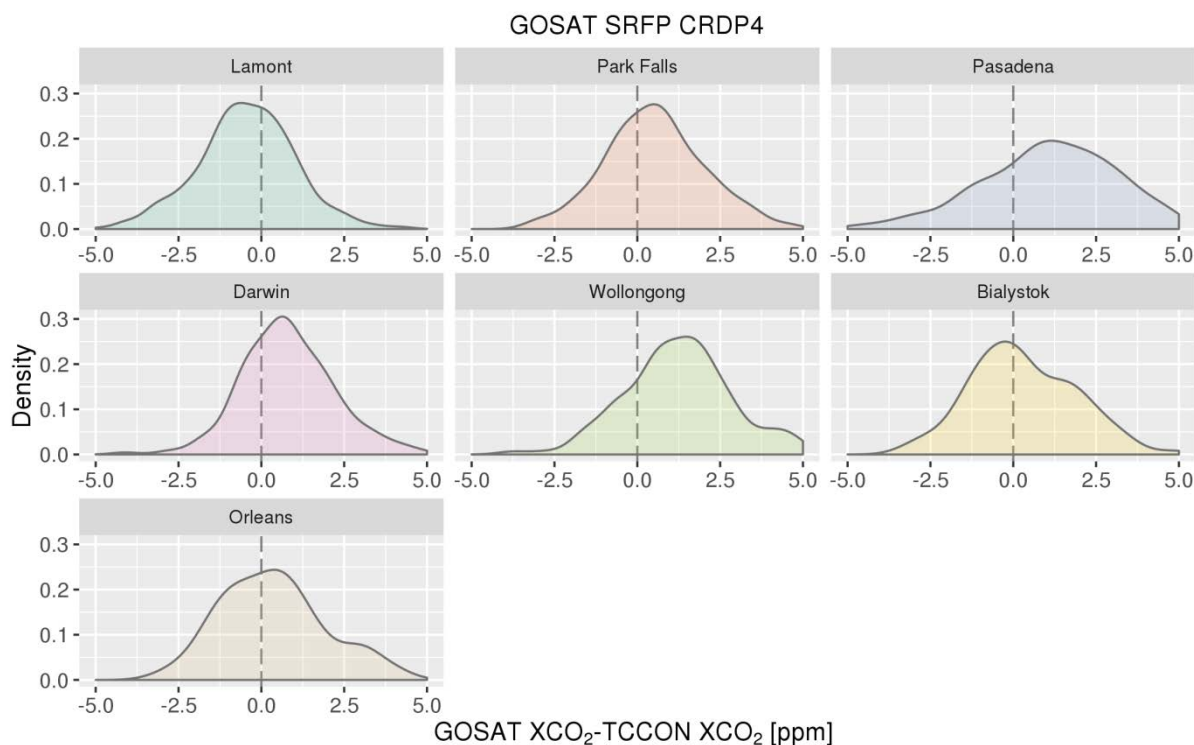


Figure 8.2.2.4: Same as Fig 8.2.2.3, but for collocated GOSAT SRFP and MODIS data.

Due to the spatial averaging, the ΔXCO_2 values do not reflect the uncertainty of a single pixel but usually of a mean of several pixels. For GOSAT SRFP, in 70-76% of the cases the spatial mean of XCO_2 was made up of more than two observations when collocated with AERONET. For GOSAT OCFP only at Darwin more than 70% of the means were defined by more than two observations, while at Lamont and Pasadena the corresponding percentages were 67% and 55%, respectively. For both SCIAMACHY algorithms more than 85% of the spatial means were defined by at least three pixels.

The situation was different for the satellite XCO_2 data collocated with satellite-based aerosol observations. For all four XCO_2 algorithms, the fraction of the cases where the satellite XCO_2 mean was made up by at least three observations decreased. From Fig. 8.2.2.5 it can be seen that for GOSAT the number of cases where the mean is made up by more than two pixels are always lower than for SCIAMACHY. This is due to the sparser sampling of GOSAT XCO_2 and that MODIS and TANSO FTS aren't onboard the same satellite, and hence spatial and temporal differences exist.

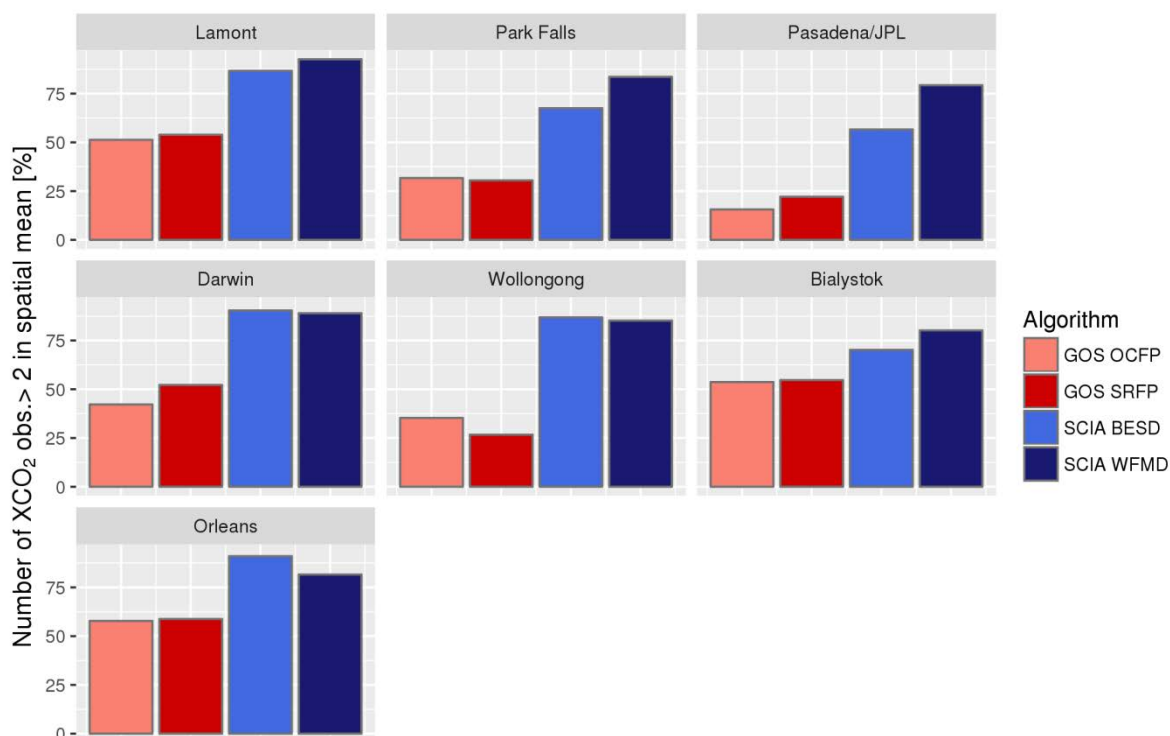



Figure 8.2.2.5: The percentage of cases where the number of satellite pixels included in the spatial XCO₂ mean is three or more, after the satellite XCO₂ has been collocated with satellite-based aerosol data.

8.2.3 Multiple linear regression model

A multiple linear regression model was employed to investigate if biases between satellite and TCCON XCO₂ were correlated with aerosol parameters. The multiple linear regression models were built by using aerosol observations from either AERONET or one of the two satellites, AATSR and MODIS, as explanatory variables. In both cases, the dependent variable in the regression model was the XCO₂ bias (ΔXCO_2), defined as the difference between satellite and TCCON XCO₂. When using data from AERONET, the explanatory were selected from the following six parameters: AERONET AOD (at 675 nm wavelength), Angström coefficient (ANG), derivative of Angström coefficient (dANG), Fine Mode Fraction (FMF), TCCON XH₂O, and solar zenith angle (SZA). AOD characterizes the amount of aerosols in the total atmospheric column responsible for the scattering of radiation at a given wavelength. AERONET does not provide observations at 765 nm wavelength, and therefore we choose to


	ESA Climate Change Initiative (CCI)	Page 227
	Product Validation and Intercomparison Report (PVIR)	
	for the Essential Climate Variable (ECV) Greenhouse Gases (GHG)	Version 5.0 Final
		9 Feb 2017

use the AOD at 670 nm. The Angström coefficient describes the spectral dependence of AOD and indicates whether the aerosol size distribution is dominated by coarse or small particles. FMF provides qualitative information about the aerosol size distribution and describes the ratio of fine mode AOD to the total AOD. The parameter dANG describes the spectral dependence of the Angström coefficient and can be used as an indication of different aerosol types. Additional explanatory variables were TCCON XH₂O as a rough measure of the influence of humidity on hygroscopic growth of the aerosols, and SZA (SCIAMACHY or GOSAT) since aerosol-related retrieval biases may depend on SZA. Both of these parameters could also reflect the seasonal variation of XCO₂ bias.

The AATSR and MODIS L2 data include somewhat different sets of aerosol-related parameters. In order to make the results comparable, only variables available from, or computable for, both instruments were used. For both SCIAMACHY XCO₂ algorithms the explanatory parameters from the AATSR were AOD and surface reflectance at 670 nm, as well as Angström coefficient (ANG). Surface reflectance is a parameter available from both AATSR and MODIS that adds an interesting dimension to the analysis that is not available when using AERONET data. Surface reflectance often has the most significant effect on the radiance observed at the top of the atmosphere even in the presence of aerosol scattering (e.g. Zhang et al., 2016). The TCCON XH₂O and SZA from SCIAMACHY were also included as explanatory variables.

For GOSAT explanatory parameters from MODIS were AOD and surface reflectance at 660 nm. Due to accuracy issues related to the MODIS Angström coefficient over land (Mielonen et al., 2011), the Angström coefficient is not included in the latest MODIS collection 6 L2 aerosol data used in this work (Levy et al., 2013). For this study, however, we derived the Angström coefficient from the MODIS AODs at 660 and 2130 nm. The Angström coefficient (especially over land) from satellite measurements include large uncertainties, and are less accurate as well as less validated than the satellite-based AOD (e.g. Russel et al., 2007), which should be kept in mind when interpreting the results. The TCCON XH₂O and SZA from GOSAT were also in this case included as explanatory parameters.

To obtain an optimal set of explanatory parameters, the variables were ranked according to their potential influence on the bias. This was done by a recursive algorithm suggested by Mäder et al. (2007). At the start, the regression model was overfitted by including all six (AERONET) or five (AATSR, MODIS) explanatory parameters. Then, the parameter with the largest p-value, i.e. the least significant parameter, was removed from the model and the regression model was fitted again with one parameter less. This was repeated until all parameters were removed. The removed parameters were ranked from one to six or five. Number one was the last (most significant) and number six / five the first (least significant) parameter removed. The optimal model was selected so that all the explanatory parameters were statistically significant, i.e. for each parameter $p \leq 0.05$.

	ESA Climate Change Initiative (CCI)	Page 228
	Product Validation and Intercomparison Report (PVIR)	
	for the Essential Climate Variable (ECV) Greenhouse Gases (GHG)	Version 5.0 Final
		9 Feb 2017

8.3 Results

8.3.1 Quality of the filtering for highly scattering aerosol scenes

An important step in the satellite XCO₂ retrieval is to identify and filter out scenes having a high aerosol loading. Each of the GHG CCI algorithms has its own approach to perform this filtering. For GOSAT SRFP one of the criteria for excluding a pixel is when the GOSAT AOD at 765 nm > 0.3 (Detmers and Hasekamp, 2015). In GOSAT OCFP algorithm the same criterion is applied but together with other aerosol related thresholds (Hewson, 2016). The common feature for all CO₂ algorithms is that for all those pixels where the quality flag is “good”, the aerosol loading in the retrieval has been defined to be below the “critical” level.

Figure 8.3.1.1 shows the frequency distributions of MODIS and AATSR AODs collocated with good quality GOSAT and SCIAMACHY XCO₂. The distributions consist only of observations collected within $\pm 5.0^\circ$ from the TCCON stations considered in this study. Since neither MODIS nor AATSR observe the AOD at 765 nm, the AOD at 765 nm has been interpolated, for MODIS from AOD observations made at 660 nm and 2130 nm channels, and for AASTR using the AATSR Angström coefficient and AOD at 550 nm.

For all four algorithms, in the majority of the cases the satellite-based AOD values were below 0.2. The main difference between the two GOSAT and SCIAMACHY algorithms was the “tail” of MODIS AODs towards rather large values well above the critical threshold of 0.3, which was not observed with SCIAMACHY and AATSR. Further inspection showed that for both GOSAT algorithms the majority of MODIS AODs > 0.3 were observed at Pasadena. It is noteworthy, that the results for GOSAT at Pasadena differed this much from the results obtained at other stations or from the results for SCIAMACHY. This indicates that at Pasadena the GOSAT AOD and MODIS AOD have major differences. On the other hand, based on these results it is not clear whether MODIS AODs were biased high or the GOSAT AODs biased low. This specific issue was further investigated in the supplementary material which indicated that the AOD differences between MODIS and GOSAT were partly related to the close presence of clouds.

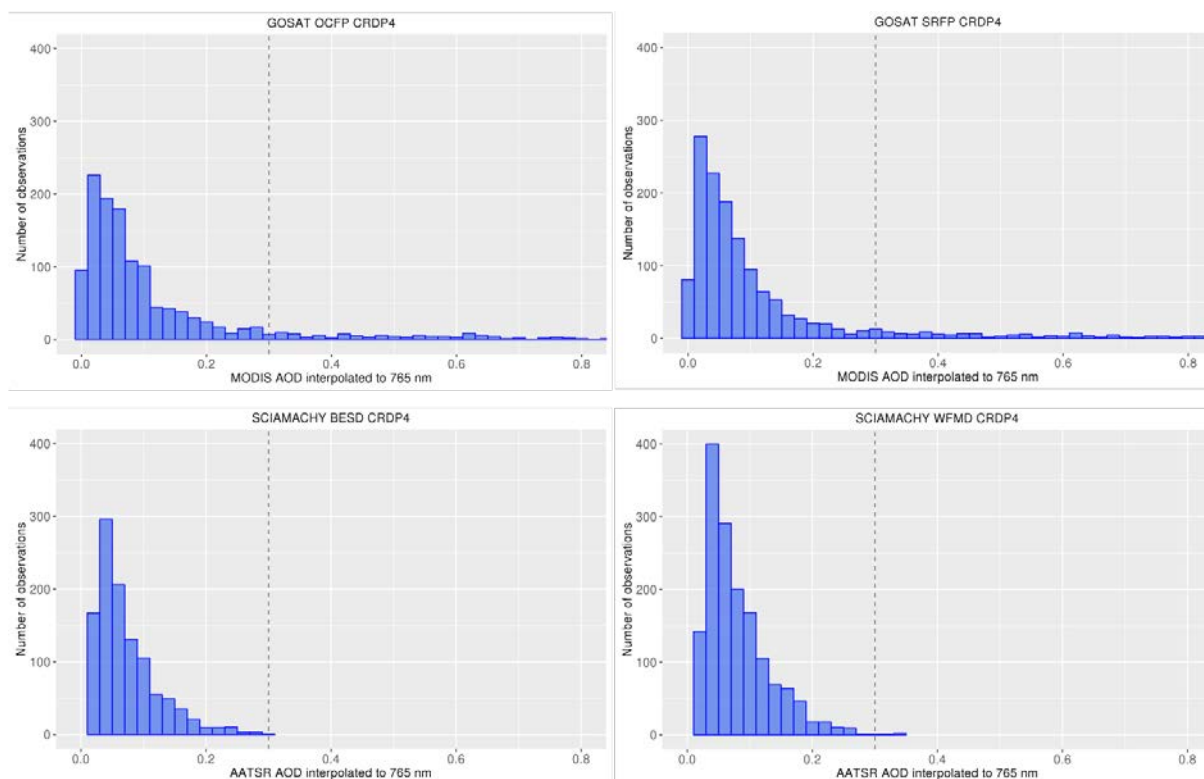


Figure 8.3.1.1: Satellite-based AOD distributions for collocated GOSAT (upper row) and SCIAMACHY (lower row) XCO₂ observations. The data consist of only those observations that were within $\pm 5^\circ$ from the TCCON stations considered in this study and the quality of the corresponding XCO₂ pixels were labelled as “good”. The vertical dashed line is the critical AOD of 0.3 usually applied to filter out highly scattering scenes.

As shown in Fig. 8.1.1, the TCCON stations are located over areas where the aerosol loading is generally rather low. To further examine the efficiency of the filtering algorithms, an additional analysis was carried out using AERONET observations in highly polluted regions in Asia. The SCIAMACHY XCO₂ data were collocated with the AERONET stations Beijing, XiangHe and Kanpur and GOSAT with the stations Beijing, Dhaka University and Karachi. As suggested by Fig. 8.3.1.2, scenes with high AODs were less successfully filtered out by GOSAT SRFP and SCIAMACHY WFMD algorithms than by those of GOSAT OCFP and SCIAMACHY BESD. For GOSAT SRFP and SCIAMACHY WFMD 36% of the collocated XCO₂ observations were associated with AOD > 0.3, whereas for GOSAT OCFP the corresponding percentage was 17%, and for SCIAMACHY BESD 9%.

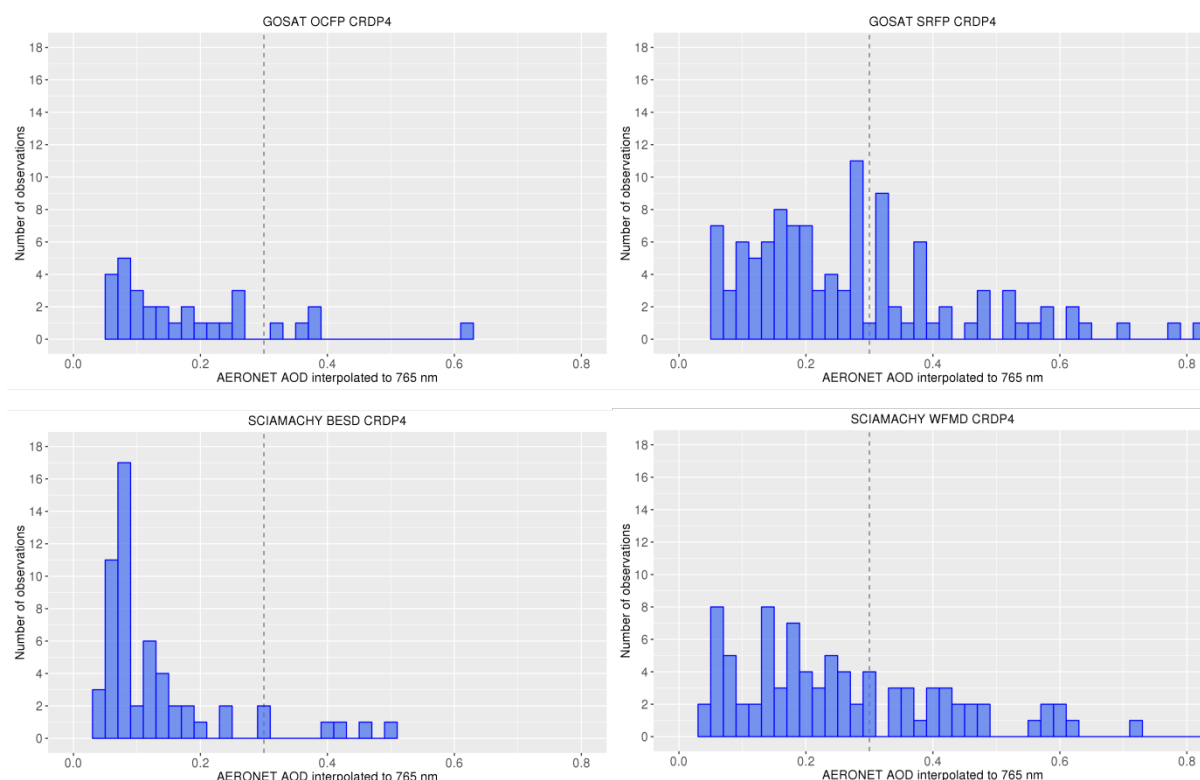



Figure 8.3.1.2: AERONET AOD distributions obtained for collocated good quality satellite XCO₂ values. The collocated GOSAT data includes observations from Beijing, Dhaka University and Karachi AERONET stations and the SCIAMACHY data from Beijing, XiangHe and Kanpur. The portion of observations with AODs > 0.3 (vertical dashed line) has erroneously been flagged as "good" by the algorithms.

8.3.2 Regression of XCO₂ bias against AERONET aerosol observations

The multiple linear regression model was applied for GOSAT OCFP and SRFP as well as SCIAMACHY WFMD at the three TCCON stations Lamont, Pasadena/JPL, and Darwin. For SCIAMACHY BESD the model was applied only at Lamont and Darwin, because the number of collocated observations at JPL was too small (14).

The best regression model for each station and algorithm was obtained using the backward selection as described in Sect 8.2.3. As shown by Figure 8.3.2.1, the selected models vary by algorithm and station, and in the majority of the cases most of the observed ΔXCO_2 variability remains unexplained by the model. This is not surprising given the fact that a major fraction of the total variance of about 2 to 4 ppm² is determined by the single pixel precision,

	ESA Climate Change Initiative (CCI)	Page 231
	Product Validation and Intercomparison Report (PVIR)	
	for the Essential Climate Variable (ECV) Greenhouse Gases (GHG)	Version 5.0 Final
		9 Feb 2017

which is of the order of 2 ppm, i.e., a variance of about 4 ppm² (Buchwitz et al., 2016). For both GOSAT algorithms the lowest R^2_{adj} values, 4.2% (OCFP), and 3.1% (SRFP), were obtained at Lamont. For OCFP the model could explain only 0.09 ppm² of the variance of 2.04 ppm², and for SRFP only 0.06 ppm² of the variance of 2.1 ppm². For OCFP the R^2_{adj} values obtained at Pasadena and Darwin were significantly higher than at Lamont. At Pasadena the selected model explained 0.53 ppm² (17.2%) of the 3.1 ppm² ΔXCO_2 variance, and at Darwin 0.38 ppm² (17.3%) of the 2.22 ppm² variance. For SRFP the highest R^2_{adj} was obtained at Pasadena, where the selected model explained 0.45 ppm² (11.7%) of the 3.87 ppm² ΔXCO_2 variance, and at Darwin the selected model explained 0.1 ppm² (4.9%) of the 1.94 ppm² ΔXCO_2 variance.

For both SCIAMACHY algorithms, higher R^2_{adj} were obtained than for GOSAT, especially at Lamont. For BESD the selected model explained 0.75 ppm² (30%) of the 2.49 ppm² variance, and for WFMD 1.94 ppm² (41.2%) of the 4.69 ppm² variance. It is also noted that at Lamont WFMD had almost twice as high variance as BESD. At Darwin the differences in variance were significantly smaller. For BESD, the selected model at Darwin explained 0.43 ppm² (27.7%) of the 1.54 ppm² variance, and for WFMD 0.44 ppm² (24.4%) of the 1.79 ppm² variance. The only significant parameter at JPL for WFMD was FMF, which explained 0.92 ppm² (15.2%) of the high total variance of 6.0 ppm².

Despite the fact that the selected models vary by station and algorithm, some similarities could be found. For both GOSAT algorithms AOD was selected as the most significant parameter at Pasadena, with sensitivities of -1.55 ppm (OCFP) and -1.28 ppm (SRFP) per 0.1 change in AOD. In all algorithms, AOD was also selected at Darwin as one of the two most significant parameters. In contrast to Pasadena, however, the sensitivity for AOD was positive in all four cases with values of: 0.88 ppm (OCFP), 0.43 ppm (SRFP), 0.75 ppm (BESD), and 0.5 ppm (WFMD) per 0.1 change in AOD. Overall, the contribution of other aerosol related parameters remained very small in the selected models, except for SCIAMACHY WFMD, where ANG and FMF were selected among the three most significant parameters at Lamont, and FMF as the most significant parameter at JPL. The sensitivities for ANG and FMF at Lamont were -0.10 ppm and -0.19 ppm per 0.1 unit change, respectively. At JPL the sensitivity for FMF was -0.50 ppm per 0.1 unit change.



ESA Climate Change Initiative (CCI)

**Product Validation and
Intercomparison Report (PVIR)**

for the Essential Climate Variable (ECV)
Greenhouse Gases (GHG)

Page 232

Version 5.0
Final

9 Feb 2017

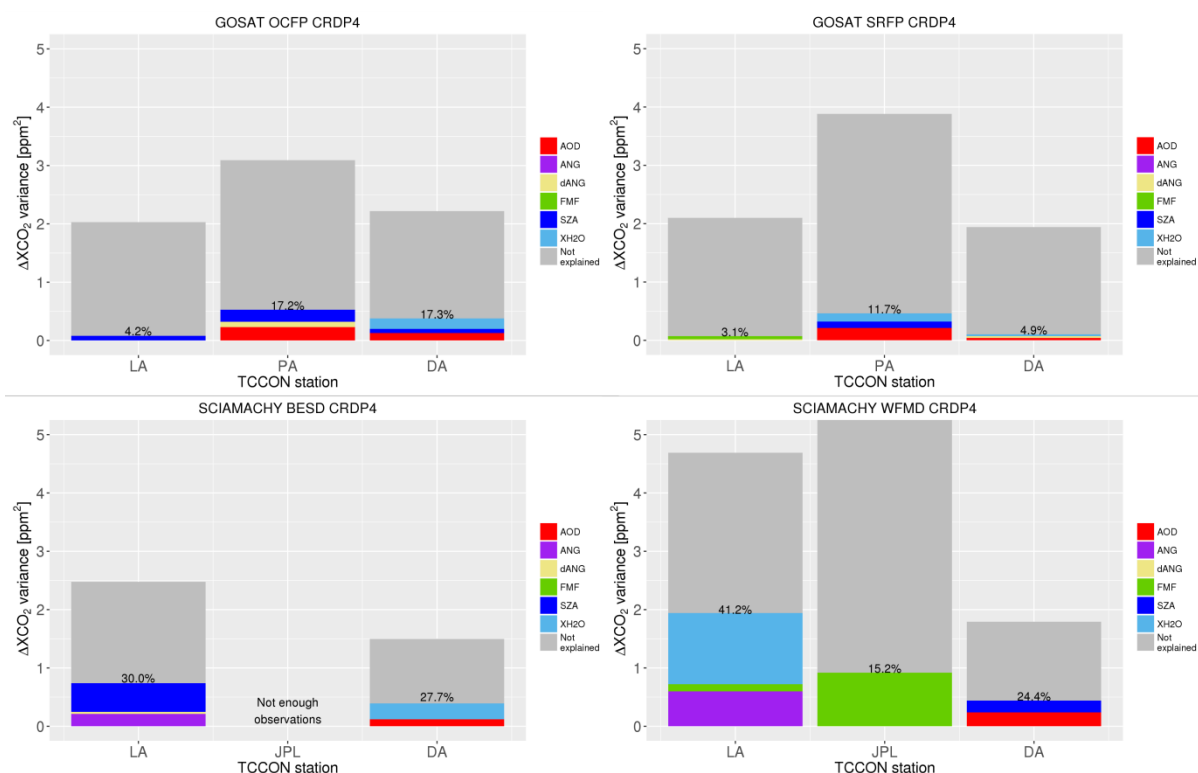



Figure 8.3.2.1: ΔXCO_2 variances explained by the selected linear regression model for CRDP4 data, when using AERONET-based aerosol data. In each column the grey part represents the unexplained part of ΔXCO_2 variances whereas the colored part represents the best model selected for the station and algorithm. For each model also the R^2_{adj} is shown (in percentages). Each color denotes a specific explanatory variable.

Comparison of the results with the previous version of the data (CRDP3) shows that for both GOSAT algorithms the clearest differences were observed at Pasadena, where the R^2_{adj} values were almost twice as high for CRDP3 than for CRDP4. On the other hand, even though at Pasadena for both GOSAT algorithms the ranking of the explanatory variables changed between CRDP3 and CRDP4, AOD and SZA remained among the most significant parameters in both cases. At Lamont, a decrease of R^2_{adj} from 11% (CRDP3) to 3% (CRDP4) was observed for SRFP. Also the ranking of the parameters changed. For CRDP3 the selected model included only SZA whereas for CRDP4 the selected parameters were FMF and dANG. On the other hand, for SCIAMACHY WFMD an increase of R^2_{adj} from 29.3% (CRDP3) to 41.2% (CRDP4) was observed at Lamont. For other stations the results didn't change notably for the GOSAT and SCIAMACHY algorithms when upgrading from the CRDP3 to the CRDP4 data. The small differences were mainly related to the ranking of the parameters.

	ESA Climate Change Initiative (CCI)	Page 233
	Product Validation and Intercomparison Report (PVIR)	
	for the Essential Climate Variable (ECV) Greenhouse Gases (GHG)	Version 5.0 Final
		9 Feb 2017

8.3.3 AOD differences between the TCCON and satellite XCO₂ pixel locations

When the AERONET –based aerosol parameters were used as the explanatory variables in the regression model, it was assumed that the aerosol conditions didn't differ significantly between the TCCON/AERONET station and the location of the actual satellite XCO₂ pixels. To test how valid this assumption actually was, MODIS and GOSAT data were used. For SCIAMACHY significantly lower number of simultaneous AATSR observations at TCCON and the location of SCIAMACHY XCO₂ were obtained.

Figure 8.3.3.1 shows the distribution of the MODIS AOD difference (Δ AOD) at the satellite XCO₂ pixel location and TCCON for the example of GOSAT OCFP. For SRFP the observed distributions are similar. At most of the TCCON stations the difference Δ AOD varied between -0.2 and 0.2, and the median of the Δ AOD was located close to zero. Deviations from this general behavior were observed, however, at Darwin and Pasadena. In 60% of the cases at Darwin, the MODIS AOD values were at least 0.05 higher at the TCCON station than at the GOSAT XCO₂ pixel. On the other hand in 65% (OCFP) and 59% (SRFP) of the cases at Pasadena the AOD at the GOSAT XCO₂ pixel was at least 0.05 larger than at the TCCON station. In 24% (OCFP and SRFP) of the cases the MODIS AOD was even more than 0.25 larger at the GOSAT pixel than at the TCCON station. The site Darwin thus seems to be somewhat more polluted than its surroundings within the collocation distance of $\pm 5^\circ$, whereas the opposite is true for the site Pasadena. Using a large collocation distance could be more problematic at these sites compared to the other TCCON sites.

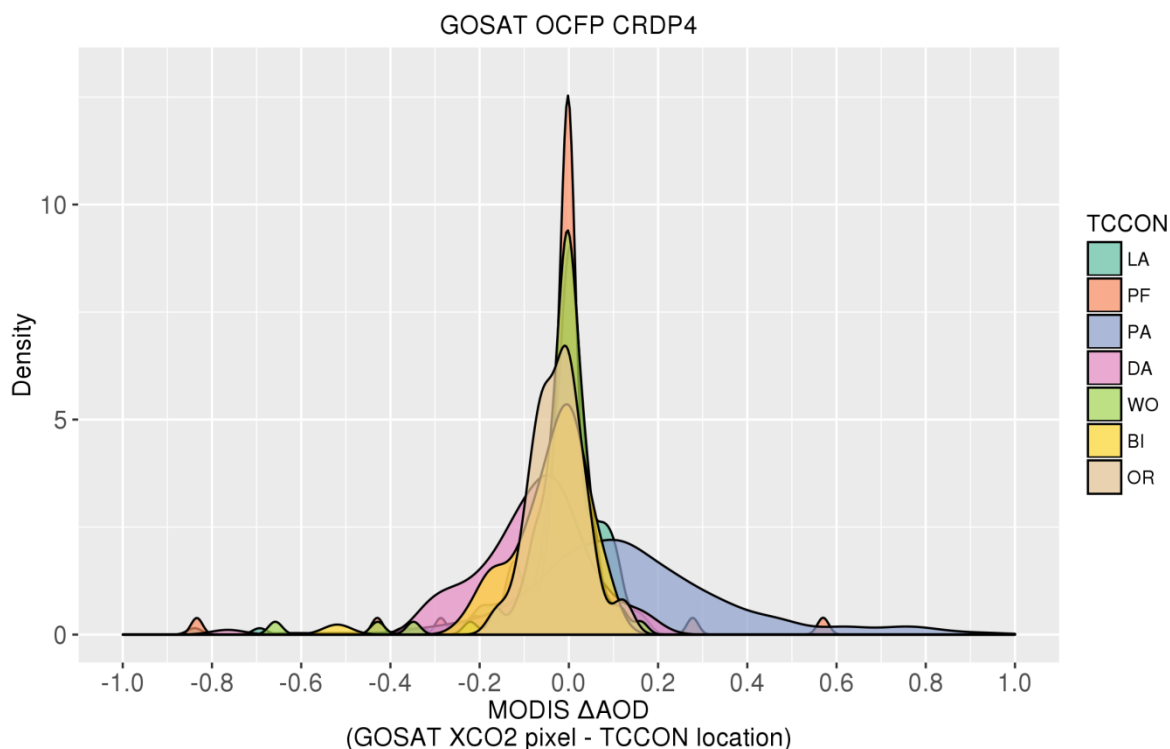


Figure 8.3.3.1: Distributions of the MODIS AOD differences at the TCCON and GOSAT XCO₂ pixel locations. Colors indicate different TCCON stations (abbreviations for the stations are listed in Table 8.2.1.1.).

An important question is whether the bias ΔXCO_2 is directly related to the mean differences in AOD at a given TCCON station and the corresponding satellite XCO₂ pixel locations, as this may indicate that the bias is simply a result of true spatial gradients in XCO₂ within the collocation region rather than a retrieval issue. Figure 8.3.3.2 shows box-plots of the biases ΔXCO_2 for different bins of the difference in MODIS AOD between satellite XCO₂ pixel location and TCCON location at the stations Darwin and Pasadena for both GOSAT algorithms. Even at these two locations with the largest ΔAOD values the connection is not very clear. At Pasadena there is possibly a weak increasing tendency of ΔXCO_2 with increasing ΔAOD , which could be an indication of the presence of common sources of aerosols and CO₂.

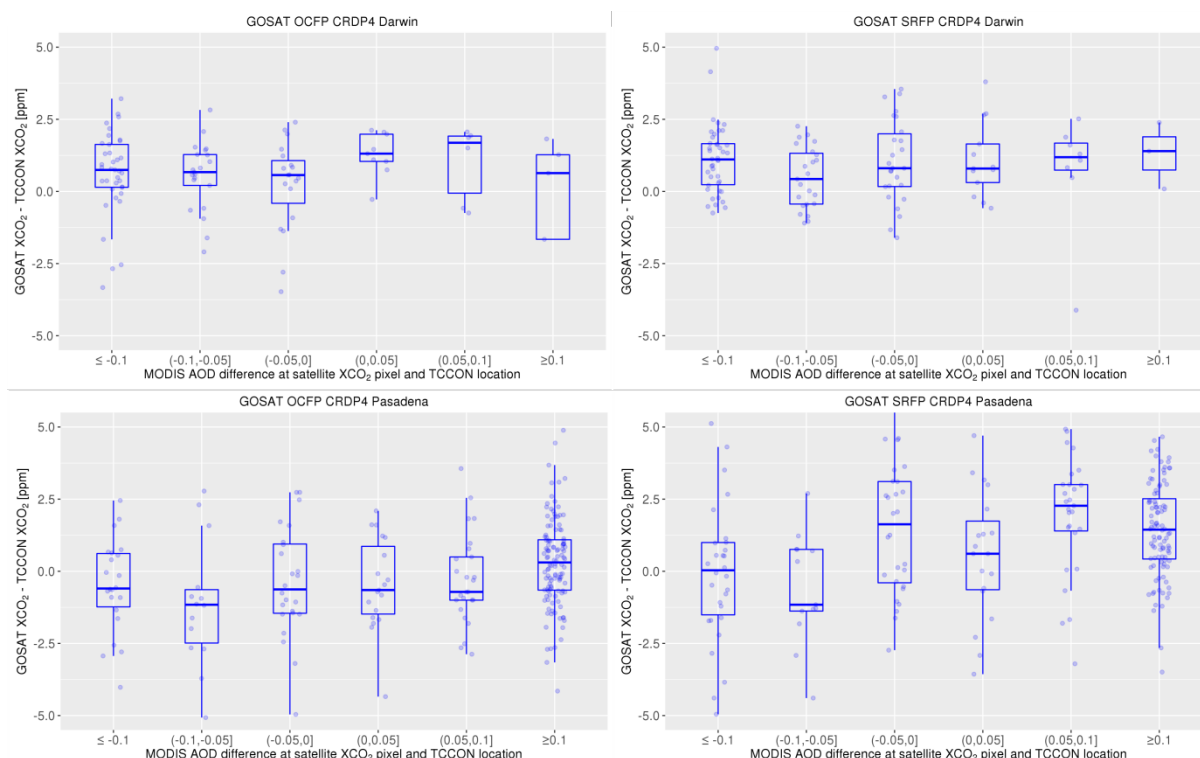


Figure 8.3.3.2: An example of the relation between the MODIS AOD difference (satellite XCO₂ pixel location – TCCON) and XCO₂ bias at Darwin (upper row) and Pasadena (lower row).

8.3.4 Regression of XCO₂ bias against satellite aerosol observations

The analysis of possible aerosol induced biases in the satellite XCO₂ data could be extended to all seven TCCON stations when using satellite-based aerosol data as explanatory variables in the multiple linear regression. While the uncertainties for the satellite-based aerosol data are larger than for AERONET, the advantage of the satellite AOD data is that they can be obtained for the exact location of the satellite XCO₂ and may thus be more representative for the conditions at the location of the satellite XCO₂ pixels as shown in Sect 8.3.3. In this approach also surface reflectance is considered as one possible explanatory variable in the regression model.

As explained in Sect 8.2.2, the GOSAT XCO₂ data were collocated with MODIS Aqua aerosol observations whereas the SCIAMACHY XCO₂ data were collocated with the AATSR observations. MODIS and AATSR provide observations at slightly different wavelengths (660 and 670 nm), but the difference is too small to significantly affect. In this case, the AODs were



not interpolated to 765nm to avoid uncertainties related to the interpolation and/or Angström coefficient.

As Figures 8.3.4.1-8.3.4.4 show, also in this approach the selected models tend to vary by station and algorithm, and in the majority of the cases most of the ΔXCO_2 variance remains unexplained. For GOSAT OCFP, the R^2_{adj} values remain below 10% except at Darwin, where the model explains 21.6% of the ΔXCO_2 variance, which is higher than what was obtained in Sect. 8.3.2 with the AERONET data. The other difference to the AERONET-based results for OCFP at Darwin was that while H_2O were in both cases selected among the two most significant parameters in the model, with MODIS-based aerosol data the surface reflectance was ranked as the second most important parameter and AOD as the least significant. For OCFP an interesting feature in the sensitivity of ΔXCO_2 to AOD was seen at Pasadena between the AERONET and satellite-based data. With the AERONET data the sensitivity to AOD was negative (-0.15ppm/0.1 change in AOD), but with the MODIS data the sensitivity changed to positive, 0.18 ppm/0.1 change in AOD. When these MODIS-based results were compared to those obtained for OCFP CRDP3, it was seen that overall the R^2_{adj} values have decreased for CRDP4, especially at Pasadena where the R^2_{adj} decreased from 34% (CRDP3) to 8.6% (CRDP4). The other difference between OCFP CRDP3 and CRDP4 data was that the contribution of SZA in the regression models has been decreased. On the other hand, somewhat larger contribution of surface reflectance was seen for CRDP4 than for CRDP3.

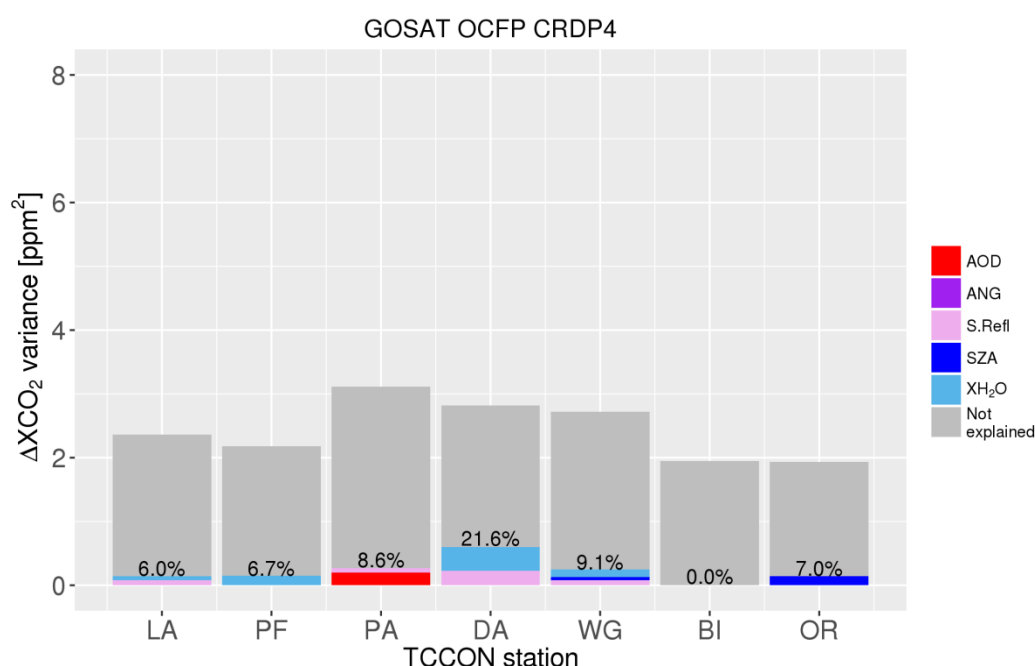


Figure 8.3.4.1: ΔXCO_2 variances explained by the selected linear regression model for GOSAT OCFP CRDP4 data, when collocated with MODIS-based aerosol data. In each

column the grey part represents the unexplained part of ΔXCO_2 variances whereas the colored part represents the best model selected for the station. For each model also the R^2_{adj} is shown (in percentages). Each color denotes a specific explanatory variable.

For GOSAT SRFP at Lamont, Bialystok, and Orleans none of the explanatory variables were statistically significant, and hence a linear regression model could not be established at these locations. For SRFP the highest R^2_{adj} of 13% was obtained at Pasadena, surface reflectance being the most important, and AOD the second most important parameter in the selected model. Also at Darwin the best model consisted of surface reflectance and AOD, but in this case AOD was the most important parameter. When comparing these results at Pasadena and Darwin to those obtained with the AERONET data, it can be seen that while at Darwin the sensitivity of ΔXCO_2 to AOD was more or less the same (AERONET; 0.43 ppm/0.1 AOD change, MODIS; 0.35 ppm / 0.1 AOD change), at Pasadena the sensitivity changed from -1.28 ppm/0.1 AOD change (AERONET) to 0.17 ppm/0.1 AOD change (MODIS). Similar feature was observed with OCFP. The results also showed that for SRFP the sensitivity of ΔXCO_2 to surface reflectance was different at Darwin and Pasadena, -3.1 ppm and 0.84 ppm per 0.1 surface refl. change, respectively. When the CRDP4 results were compared with those obtained with CRDP3 data, also for SRFP decreases in R^2_{adj} values were observed. The change was significant especially at Bialystok and Orleans, where the R^2_{adj} values for CRDP3 were, 20.1% and 19.6% respectively, and for CRDP4 0.0%.

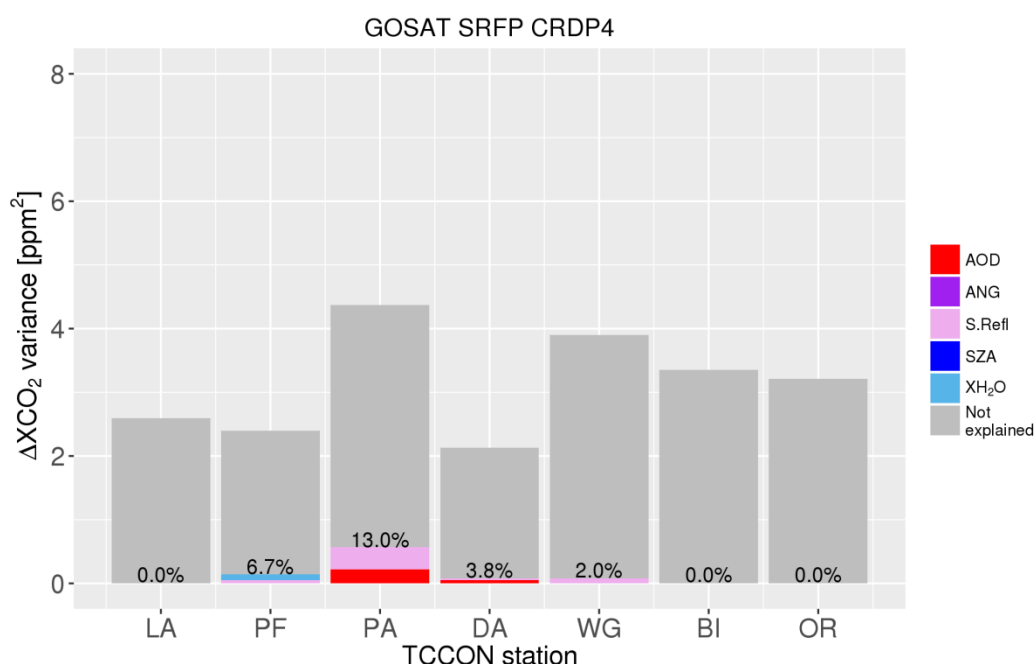


Fig 8.3.4.2: The same as Fig. 8.3.4.1, but for GOSAT SRFP.

Overall, for both SCIAMACHY algorithms higher R^2_{adj} values were obtained than for GOSAT when using the satellite-based aerosol data. In contrast to the GOSAT algorithms a slight increase of R^2_{adj} values was found for the CRDP4 data sets as compared to CRDP3. For SCIAMACHY BESD the highest R^2_{adj} of 24.3% and 22.0% were obtained at Lamont and Bialystok. Another difference to GOSAT results is that for SCIAMACHY BESD the Angström coefficient was selected as significant parameter at two locations (Wollongong and Bialystok), while for GOSAT the Angström coefficient was never selected. For BESD the sensitivities to the Angström coefficient were -0.6 ppm (Bialystok) and -0.4 ppm (Wollongong) per 0.1 change in ANG. At JPL, none of the parameters was statistically significant and so no model could be established at this site. This contrasts with the two GOSAT algorithms, for which one of the highest R^2_{adj} were obtained specifically at Pasadena.

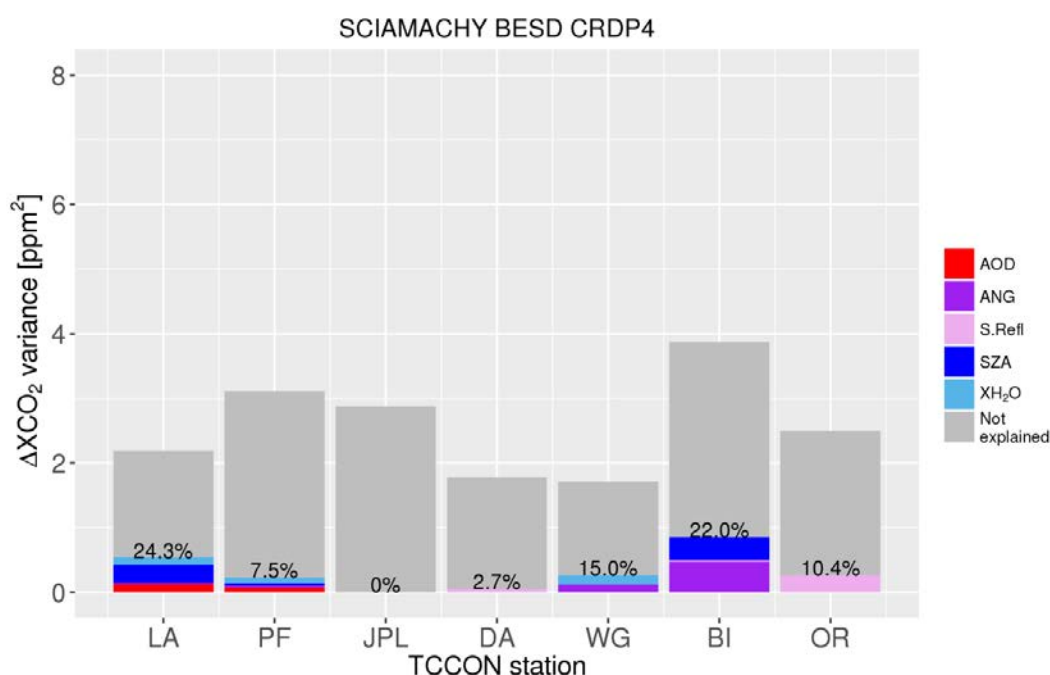


Fig 8.3.4.3: ΔXCO_2 variances explained by the selected linear regression model for SCIAMACHY BESD CRDP4 data, when collocated with AATSR-based aerosol data. In each column the grey part represents the unexplained part of ΔXCO_2 variances whereas the colored part represents the best model selected for the station. For each model also the R^2_{adj} is shown (in percentages). Each color denotes a specific explanatory variable.

For SCIAMACHY WFMD the XCO_2 variance was systematically higher than for other algorithms, and also the R^2_{adj} values obtained from the regression model were higher. At Bialystok, the selected model for WFMD could explain 53.6% (4.17 ppm²) of the 7.79 ppm² XCO_2 variance, the TCCON XH_2O having a significant contribution to the R^2_{adj} . This was the only case where the obtained R^2_{adj} value was above 50%. At Lamont the selected parameters for the WFMD were the same as for BESD, but the R^2_{adj} was much higher. On the other hand, at JPL the selected model for WFMD could explain 29.7% (1.81 ppm²) of the XCO_2 variance, whereas for BESD no regression model could be established. For WFMD, AOD was selected to the model in five cases out of seven. The sensitivities of ΔXCO_2 to AOD varied by station: at Lamont, Park Falls, and Bialystok the sensitivities were between -1.1 ppm and -1.4 ppm per 0.1 AOD change, respectively, whereas at JPL and Darwin the sensitivities were 2.2 ppm and 0.5 ppm per 0.1 AOD change, respectively. When comparing the results to CRDP3, a slight increase in the R^2_{adj} values was observed for WFMD.

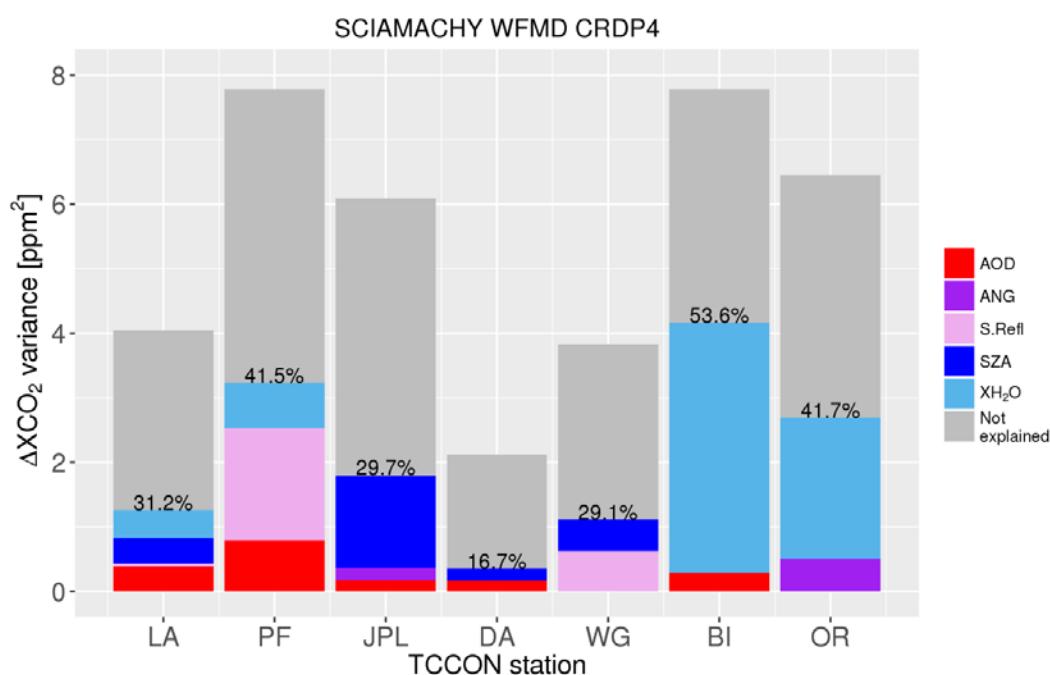


Fig 8.3.4.4: The same as Fig. 8.3.4.3, but for SCIAMACHY WFMD.

One likely explanation for the higher R^2_{adj} values obtained in the multiple linear regression for SCIAMACHY WFMD, and also in some cases for BESD, is that biases exhibit a significant seasonal variation. As a consequence, the two variables with the largest seasonal component, i.e., TCCON H_2O and satellite SZA were selected by the regression model as the most significant explanatory variables.



This is further illustrated by Figure 8.3.4.5 which shows the seasonal variation in XCO₂ biases. As can be seen, for WFMD the seasonal variation is different from the three other algorithms. Because such a seasonal dependence may be caused by factors not related to aerosols, the regression model was also applied to seasonally adjusted time series in the previous CAR report for the CRPD3 data from SCIAMACHY BESD and WFMD. The results showed that after adjustment the R^2_{adj} tended to decrease. Unfortunately, such a seasonal adjustment could not be applied reliably to the GOSAT data due to the sparsity of the collocated observations.

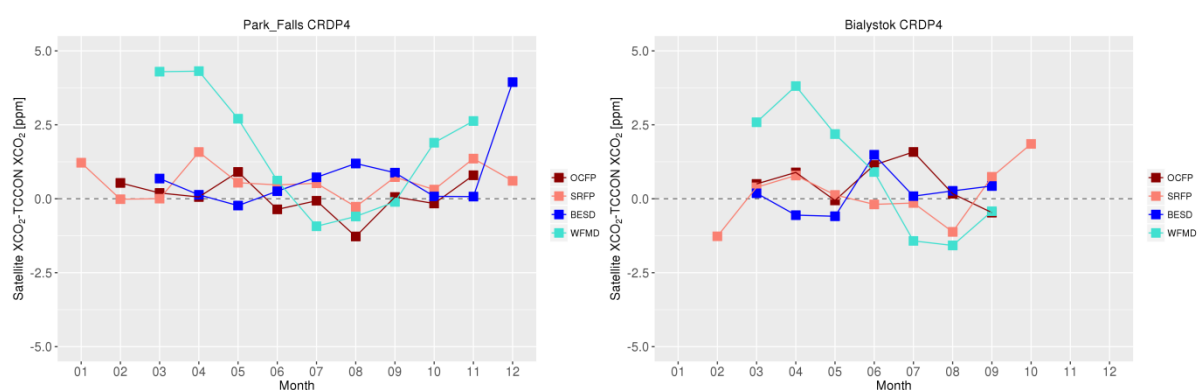



Fig 8.3.4.5: Seasonal variation of XCO₂ bias for all four algorithms at Park Falls and Bialystok. The monthly means have been calculated using XCO₂ data that has been collocated with satellite-based aerosol data.

8.4 Summary

Aerosols can cause large biases in satellite XCO₂ observations if they are not properly accounted for. There are two important steps in the satellite XCO₂ retrieval where the aerosol scattering needs to be taken into account. First, highly scattering scenes must be correctly identified and filtered out. Second, the remaining pixels need to be corrected for the effects of aerosol scattering on the photon paths in order to retrieve correct XCO₂ values. In this work both of these topics were addressed. The independent information on aerosols was obtained either from AERONET, the global network of ground-based sun-photometers or from MODIS and AATSR satellite instruments. AERONET observations are more accurate than the satellite-based aerosol data, but the number of sites collocated with TCCON observations is very limited. Satellite-based aerosol data are less accurate but have the advantage of being available at all TCCON stations. Furthermore, the satellite data can be used to assess spatial

	ESA Climate Change Initiative (CCI)	Page 241
	Product Validation and Intercomparison Report (PVIR)	
	for the Essential Climate Variable (ECV) Greenhouse Gases (GHG)	Version 5.0 Final
		9 Feb 2017


gradients in aerosol concentrations in the surroundings of a TCCON site that may affect the biases between satellite and TCCON XCO₂ observations.

In general, the algorithms efficiently filtered out scenes with high AOD loading. In the GOSAT retrievals at Pasadena, however, rather high fraction (SRFP 51%, OCFP 48%) of good quality XCO₂ pixels coincided with high MODIS AOD values above the retrieval thresholds. This could indicate that highly scattering scenes have not been identified correctly, but also that the MODIS AOD were biased high. An additional analysis using AERONET data in more polluted regions over Asia revealed that good quality XCO₂ values were more often (in relative terms) associated with high AODs in the GOSAT SRFP and SCIAMACHY WFMD retrievals than in the other two products. Based on these results it can be concluded that highly scattering aerosol scenes are not a significant problem in the vicinity of the existing TCCON stations, but that the algorithms may still benefit from improved filtering over areas with high aerosol loading.

A multiple linear regression model was used to investigate to which extent differences between SCIAMACHY and GOSAT XCO₂ and TCCON XCO₂ (Δ XCO₂) could be attributed to aerosols. The linear regression models were used either AERONET or satellite-based aerosol data as explanatory variables, as well as TCCON XH₂O and satellite SZA. For each station and algorithm an optimal set of explanatory variables was obtained by a backward selection method. The selected variables differed strongly between sites and algorithms and in most cases the regression model could explain less than 20% of the Δ XCO₂ variance. This indicates that the effects of aerosols are relatively small in comparison to the single measurement precision and show little systematic behavior. The latter may be related to the fact that the analyzed data products have already been corrected for biases with respect to TCCON observations and that this correction already accounts for biases related to AOD (modeled or as retrieved by the XCO₂ satellite).

When using AERONET data, the R^2_{adj} values of the selected regression models varied between 4% and 17% for GOSAT OCFP, and between 3% and 11% for SRFP. For the two SCIAMACHY products the R^2_{adj} values were higher, between 27% and 30% for BESD, and between 15% and 41% for WFMD. Even though the major part of the Δ XCO₂ variance remained unexplained, the selected models included at least one aerosol related parameter, with the exception of the model for GOSAT OCFP at Lamont where only SZA was a statistically significant variable. On average the AERONET aerosol contribution could explain at most 0.3 ppm² of the variance in XCO₂ biases for the two GOSAT algorithms and SCIAMACHY BESD, and about 0.6 ppm² for the SCIAMACHY WFMD algorithm.


When interpreting these results, it should be kept in mind that the AERONET observations are made next to the TCCON stations, whereas the coincident satellite XCO₂ pixels can be located hundreds of kilometers away. If both aerosol and CO₂ concentrations show significant gradients in the vicinity of a TCCON site, any correlation between AERONET aerosol parameters and XCO₂ biases could simply be a result of the correlations in these gradients

	ESA Climate Change Initiative (CCI)	Page 242
	Product Validation and Intercomparison Report (PVIR)	
	for the Essential Climate Variable (ECV) Greenhouse Gases (GHG)	Version 5.0 Final
		9 Feb 2017

rather than a true retrieval issue. This possibility was further investigated using satellite-based aerosol observations, which showed that at most of the TCCON stations the aerosol conditions do not vary systematically within the $\pm 5^\circ$ collocation area. The only exceptions were Pasadena and Darwin where the average AOD was somewhat lower and higher at the station than at surrounding area, respectively. At these sites the contribution of AOD in the multiple linear regression may thus be partly related to true gradients in aerosol and CO₂ concentrations rather than to retrieval errors, although a clear connection between ΔXCO_2 and AOD differences could not be found.

When using satellite-based aerosol data in the multiple linear regression, any possible aerosol variations within the $\pm 5^\circ$ area could be taken into account. On the other hand, the additional requirement for collocation with a satellite aerosol observation decreased the fraction of cases where the XCO₂ spatial mean was defined from multiple pixels, especially for GOSAT. For both GOSAT algorithms as well as for SCIAMACHY BESD the R^2_{adj} values obtained from the linear regression remained mainly below 10%, and the aerosol contribution to the XCO₂ bias variance below 0.2 ppm². Significantly higher R^2_{adj} values were obtained for WFMD, which could be partly explained by the pronounced seasonal variation of the XCO₂ bias in this product.

Based on the results obtained in this study, both with AERONET and satellite-based data, it can be concluded that aerosols have only a minor effect on the XCO₂ bias at the existing TCCON stations. However, it would be desirable to have TCCON observations also at locations with higher aerosol loading, so that any aerosol effects could be investigated more rigorously.

	ESA Climate Change Initiative (CCI)	Page 243
	Product Validation and Intercomparison Report (PVIR)	
	for the Essential Climate Variable (ECV) Greenhouse Gases (GHG)	Version 5.0 Final
		9 Feb 2017

9 References

References Sect. 1-7:

/Bergamaschi et al., 2009/ Bergamaschi, P., Frankenberg, C., Meirink, J. F., Krol, M., Villani, M. G., Houweling, S., Dentener, F., Dlugokencky, E. J., Miller, J. B., Gatti, L. V., Engel, A., and Levin, I.: Inverse modeling of global and regional CH₄ emissions using SCIAMACHY satellite retrievals, *J. Geophys. Res.*, 114, D22301, doi:10.1029/2009JD012287, 2009.

/Bergamaschi et al., 2010/ Bergamaschi, P., Krol, M., Meirink, J. F., Dentener, F., Segers, A., van Aardenne, J., Monni, S., Vermeulen, A., Schmidt, M., Ramonet, M., Yver, C., Meinhardt, F., Nisbet, E. G., Fisher, R., O'Doherty, S., and Dlugokencky, E. J.: Inverse modeling of european CH₄ emissions 2001-2006, *J. Geophys. Res.*, 115, D22309, doi:10.1029/2010JD014180, 2010.

/Buchwitz et al., 2013/ Buchwitz, M., M. Reuter, O. Schneising, H. Boesch, S. Guerlet, B. Dils, I. Aben, R. Armante, P. Bergamaschi, T. Blumenstock, H. Bovensmann, D. Brunner, B. Buchmann, J. P. Burrows, A. Butz, A. Chédin, F. Chevallier, C. D. Crevoisier, N. M. Deutscher, C. Frankenberg, F. Hase, O. P. Hasekamp, J. Heymann, T. Kaminski, A. Laeng, G. Lichtenberg, M. De Mazière, S. Noël, J. Notholt, J. Orphal, C. Popp, R. Parker, M. Scholze, R. Sussmann, G. P. Stiller, T. Warneke, C. Zehner, A. Bril, D. Crisp, D. W. T. Griffith, A. Kuze, C. O'Dell, S. Oshchepkov, V. Sherlock, H. Suto, P. Wennberg, D. Wunch, T. Yokota, Y. Yoshida, The Greenhouse Gas Climate Change Initiative (GHG-CCI): comparison and quality assessment of near-surface-sensitive satellite-derived CO₂ and CH₄ global data sets, *Remote Sensing of Environment*, doi:10.1016/j.rse.2013.04.024, in press (<http://authors.elsevier.com/sd/article/S0034425713003520>), 2013.


/Butz et al., 2010/ Butz, A., Hasekamp, O. P., Frankenberg, C., Vidot, J., and Aben, I., CH₄ retrievals from space-based solar backscatter measurements: Performance evaluation against simulated aerosol and cirrus loaded scenes, *J. Geophys. Res.*, Volume 115, Issue D24, 27, DOI: 10.1029/2010JD014514, 2010.

/Butz et al., 2011/ Butz, A., Guerlet, S., Hasekamp, O., et al., Toward accurate CO₂ and CH₄ observations from GOSAT, *Geophys. Res. Lett.*, doi:10.1029/2011GL047888, 2011.

/Cogan et al., 2011/ Cogan, A. J., Boesch, H., Parker, R. J., et al., Atmospheric carbon dioxide retrieved from the Greenhouse gases Observing SATellite (GOSAT): Comparison with ground-based TCCON observations and GEOS-Chem model calculations, *J. Geophys. Res.*, 117, D21301, doi:10.1029/2012JD018087, 2012.

/Crevoisier et al., 2004/ Crevoisier C., Heilliette S., Chédin A., et al., Midtropospheric CO₂ concentration retrieval from AIRS observations in the tropics, *Geophys. Res. Lett.*, 31, L17106, 2004.

/Crevoisier et al., 2009/ Crevoisier, C., Chédin, A., Matsueda, H., et al., First year of upper tropospheric integrated content of CO₂ from IASI hyperspectral infrared observations, *Atmos. Chem. Phys.*, 9, 4797-4810, 2009.

	ESA Climate Change Initiative (CCI)	Page 244
	Product Validation and Intercomparison Report (PVIR)	
	for the Essential Climate Variable (ECV) Greenhouse Gases (GHG)	Version 5.0 Final
		9 Feb 2017

/Crevoisier et al., 2013/ Crevoisier, C., Nobileau, D., Armante, R., et al., The 2007–2011 evolution of tropical methane in the mid-troposphere as seen from space by MetOp-A/IASI, *Atmos. Chem. Phys.*, 13, 4279–4289, 2013.

/Dils et al., 2014/ B. Dils, M. Buchwitz, M. Reuter, O. Schneising, H. Boesch, R. Parker, S. Guerlet, I. Aben, T. Blumenstock, J. P. Burrows, A. Butz, N. M. Deutscher, C. Frankenberg, F. Hase, O. P. Hasekamp, J. Heymann, M. De Mazière, J. Notholt, R. Sussmann, T. Warneke, D. Griffith, V. Sherlock, D. Wunch :The Greenhouse Gas Climate Change Initiative (GHG-CCI): Comparative validation of GHG-CCI SCIAMACHY/ENVISAT and TANSO-FTS/GOSAT CO₂ and CH₄ retrieval algorithm products with measurements from the TCCON network, *Atmos. Meas. Tech.*, 7, 1723–1744, 2014.

/Dlugokencky et al., 2009/ Dlugokencky, E. J., Bruhwiler, L., White, J. W. C., Emmons, L. K., Novelli, P. C., Montzka, S. A., Masarie, K. A., Lang, P. M., Crotwell, A. M., Miller, J. B., Gatti, L. V., Observational constraints on recent increases in the atmospheric CH₄ burden, *Geophys. Res. Lett.*, 36, L18803, doi:10.1029/2009GL039780, 2009.

/Durry et al., 2010/ Durry, G., J. Li, I. Vinogradov, A. Titov, A.V. Kalyuzhny, L. Joly, J. Cousin, T. Decarpenterie, N. Amarouche, M. Liu, B. Parvitte, O. Korablev, M. Gerasimov and V. Zeninari, "Near infrared diode laser spectroscopy of C₂H₂, H₂O, CO₂ and their isotopologues and application to TDLAS, a tunable diode laser spectrometer for the Martian PHOBOS-Grunt space mission", *Applied Physics B*, Vol. 99, pp339–351, 2010.


/Foucher et al., 2009/ Foucher, P. Y., Chédin, A., Dufour, G., Capelle, V., Boone, C. D., and Bernath, P.: Technical Note: Feasibility of CO₂ profile retrieval from limb viewing solar occultation made by the ACE-FTS instrument, *Atmos. Chem. Phys.*, 9, 2873–2890, doi:10.5194/acp-9-2873-2009, <http://www.atmos-chem-phys.net/9/2873/2009/>, 2009.

/Foucher et al., 2011/ Foucher, P. Y., Chédin, A., Armante, R., Boone, C., Crevoisier, C., and Bernath, P.: Carbon dioxide atmospheric vertical profiles retrieved from space observation using ACE-FTS solar occultation instrument, *Atmos. Chem. Phys.*, 11, 2455–2470, doi:10.5194/acp-11-2455-2011, <http://www.atmos-chem-phys.net/11/2455/2011/>, 2011.

/Frankenberg et al., 2011/ Frankenberg, C., Aben, I., Bergamaschi, P., et al., Global column-averaged methane mixing ratios from 2003 to 2009 as derived from SCIAMACHY: Trends and variability, *J. Geophys. Res.*, doi:10.1029/2010JD014849, 2011.

/GCOS-107/ Global Climate Observing System (GCOS), SYSTEMATIC OBSERVATION REQUIREMENTS FOR SATELLITE-BASED PRODUCTS FOR CLIMATE, Supplemental details to the satellite-based component of the "Implementation Plan for the Global Observing System for Climate in Support of the UNFCCC", Prepared by World Meteorological Organization (WMO), Intergovernmental Oceanographic Commission, United Nations Environment Programme (UNEP), International Council for Science, Doc.: GCOS 107 (WMO/TD No. 1338), Sept 2006, 2006.

/GCOS-154/ Global Climate Observing System (GCOS), SYSTEMATIC OBSERVATION REQUIREMENTS FOR SATELLITE-BASED PRODUCTS FOR CLIMATE, Supplemental details to the satellite-based component of the "Implementation Plan for the Global Observing System for Climate in Support of the UNFCCC (2010 update)", Prepared by World Meteorological Organization (WMO), Intergovernmental Oceanographic Commission,

	ESA Climate Change Initiative (CCI)	Page 245
	Product Validation and Intercomparison Report (PVIR)	
	for the Essential Climate Variable (ECV) Greenhouse Gases (GHG)	Version 5.0 Final
		9 Feb 2017

United Nations Environment Programme (UNEP), International Council for Science, Doc.: GCOS 154, 2010.

/GCOS-200/ The Global Observing System for Climate: Implementation Needs, World Meteorological Organization (WMO), GCOS-200 (GOOS-214), pp. 325, http://unfccc.int/files/science/workstreams/systematic_observation/application/pdf/gcos_ip_1_Ooct2016.pdf, 2016.

/Karion et al., 2010/ Karion, A., Sweeney, C., Tans, P., and Newberger, T., AirCore: An Innovative Atmospheric Sampling System, *Journal of Atmospheric and Oceanic Technology*, Nov. 2010, doi: 10.1175/2010JTECHA1448.1.

/Keppel-Aleks et al., 2010/ Keppel-Aleks, G., Wennberg, P. O., and Schneider, T.: Sources of variations in total column carbon dioxide, *Atmos. Chem. Phys.*, 11, 3581-3593, doi:10.5194/acp-11-3581-2011, 2011.

/Laeng et al., 2015/ Laeng, A., J. Plieninger, T. von Clarmann, U. Grabowski, G. Stiller, E. Eckert, N. Glatthor, F. Haenel, S. Kellmann, M. Kiefer, A. Linden, S. Lossow, L. Deaver, A. Engel, M. Hervig, I. Levin, M. McHugh, S. Noël, G. Toon, and K. Walker, Validation of MIPAS IMK/IAA methane profiles, *Atmos. Meas. Tech.*, 8, 5251-5261, 2015.

/Noël et al., 2011/ Noël, S., Bramstedt, K., Rozanov, A., et al., Stratospheric methane profiles from SCIAMACHY solar occultation measurements derived with onion peeling DOAS, *Atmos. Meas. Tech.*, 4, 2567-2577, 2011.

/Noël et al., 2016/ Noël, S., K. Bramstedt, M. Hilker, P. Liebing, J. Plieninger, M. Reuter, A. Rozanov, C. E. Sioris, H. Bovensmann and J. P. Burrows, Stratospheric CH₄ and CO₂ profiles derived from SCIAMACHY solar occultation measurements, *Atmos. Meas. Tech.*, 9(4), 1485-1503, doi: 10.5194/amt-9-1485-2016, 2016.
URL <http://www.atmos-meas-tech.net/9/1485/2016/>

/Notholt et al., 2012/ Notholt, J., Blumenstock, T., Brunner, D., Buchmann, B., Dils, B., De Mazière, M., Popp, C., Sussmann, R., Product Validation and Algorithm Selection Report (PVASR) for the Essential Climate Variable (ECV) Greenhouse Gases (GHG), Aug. 2012, available from GHG-CCI website: <http://www.esa-ghg-cci.org> (end of August 2012), 2012.


/Oliphant T.E. 2006/, "A Bayesian perspective on estimating mean, variance, and standard-deviation from data", All Faculty Publications. 278, 2006.

URL <http://scholarsarchive.byu.edu/facpub/278>

/Parker et al., 2011/ Parker, R., Boesch, H., Cogan, A., et al., Methane Observations from the Greenhouse gases Observing SATellite: Comparison to ground-based TCCON data and Model Calculations, *Geophys. Res. Lett.*, doi:10.1029/2011GL047871, 2011.

/Peters et al., 2007/ Peters, W., Jacobson, A. R., Sweeney, C., Andrews, A. E., Conway, T. J., Masarie, K., Miller, J. B., Bruhwiler, L. M. P., Pétron, G., Hirsch, A. I., Worthy, D. E. J., van der Werf, G. R., Randerson, J. T., Wennberg, P. O., Krol, M. C., and Tans, P. P.: An atmospheric perspective on North American carbon dioxide exchange: CarbonTracker, *Proceedings of the National Academy of Sciences (PNAS) of the United States of America*, November 27, 2007, 104, 18 925–18 930, doi:10.1073/pnas.0708986104.

/Plieninger et al., 2015/ Plieninger, J., von Clarmann, T., Stiller, G. P., Grabowski, U., Glatthor, N., Kellmann, S., Linden, A., Haenel, F., Kiefer, M., Höpfner, M., Laeng, A., and

	ESA Climate Change Initiative (CCI)	Page 246
	Product Validation and Intercomparison Report (PVIR)	
	for the Essential Climate Variable (ECV) Greenhouse Gases (GHG)	Version 5.0 Final
		9 Feb 2017

Lossow, S.: Methane and nitrous oxide retrievals from MIPAS-ENVISAT, *Atmos. Meas. Tech.*, 8, 4657-4670, doi:10.5194/amt-8-4657-2015, 2015.. Link: <http://www.atmos-meas-tech.net/8/4657/2015/amt-8-4657-2015.html>

/Plieninger et al., 2016/ Plieninger, J., Laeng, A., Lossow, S., von Clarmann, T., Stiller, G. P., Kellmann, S., Linden, A., Kiefer, M., Walker, K. A., Noël, S., Hervig, M., McHugh, M., Lambert, A., Urban, J., Elkins, J. W., and Murtagh, D.: Validation of revised methane and nitrous oxide profiles from MIPAS-ENVISAT, *Atmos. Meas. Tech.*, 9, 765-779, 2016. doi:10.5194/amt-8-12105-2015, 2015. Link: <http://www.atmos-meas-tech-discuss.net/amt-2015-335/>

/PVIRv2 CRDP#1/ Product Validation and Intercomparison Report (PVIR), Notholt et al., version 2 (4. Nov. 2013), PVIR for GHG-CCI Climate Research Data Package No. 1 (CRDP#1), available from http://www.esa-ghg-cci.org/index.php?q=webfm_send/152, 2013.

/Reuter et al. 2011/ Reuter, M., Bovensmann, H., Buchwitz, M., Burrows, J. P., Connor, B. J., Deutscher, N. M., Griffith, D.W. T., Heymann, J., Keppel-Aleks, G., Messerschmidt, J., and et al.: Retrieval of atmospheric CO₂ with enhanced accuracy and precision from SCIAMACHY: Validation with FTS measurements and comparison with model results., *Journal of Geophysical Research*, 116, doi:10.1029/2010JD015047, URL <http://dx.doi.org/10.1029/2010JD015047>, 2011

/Reuter et al., 2013/ Reuter, M. H. Bösch, H. Bovensmann, A. Bril, M. Buchwitz, A. Butz, J. P. Burrows, C. W. O'Dell, S. Guerlet, O. Hasekamp, J. Heymann, N. Kikuchi, S. Oshchepkov, R. Parker, S. Pfeifer, O. Schneising, T. Yokota, and Y. Yoshida, A joint effort to deliver satellite retrieved atmospheric CO₂ concentrations for surface flux inversions: The ensemble median algorithm EMMA, *Atmos. Chem. Phys.*, 13, 1771-1780, 2013.


/Rigby et al., 2008/ Rigby, M., Prinn, R. G., Fraser, P. J., Simmonds, P. G., Langenfelds, R. L., Huang, J., Cunnold, D. M., Steele, L. P., Krummel, P. B., Weiss, R. F., O'Doherty, S., Salameh, P. K., Wang, H. J., Harth, C. M., Mühle, J., Porter, L. W., Renewed growth of atmospheric methane, *Geophys. Res. Lett.*, 35, L22805, doi:10.1029/2008GL036037, 2008.

/Rodgers, 2000/ Rodgers C. D.: *Inverse Methods for Atmospheric Sounding: Theory and Practice*, World Scientific Publishing, 2000

/Schneising et al., 2011/ Schneising, O., Buchwitz, M., Reuter, M., et al., Long-term analysis of carbon dioxide and methane column-averaged mole fractions retrieved from SCIAMACHY, *Atmos. Chem. Phys.*, 11, 2881-2892, 2011.

/Schneising et al., 2014a/ Schneising, O., Reuter, M., Buchwitz, M., Heymann, J., Bovensmann, H., and Burrows, J. P., Terrestrial carbon sink observed from space: variation of growth rates and seasonal cycle amplitudes in response to interannual surface temperature variability, *Atmos. Chem. Phys.*, 14, 133-141, 2014.

/Schneising et al., 2014b/ Schneising, O., Burrows, J. P., Dickerson, R. R., Buchwitz, M., Reuter, M., Bovensmann, H., Remote sensing of fugitive methane emissions from oil and gas production in North American tight geologic formations, *Earth's Future*, 2, DOI: 10.1002/2014EF000265, pp. 11, 2014.

	ESA Climate Change Initiative (CCI)	Page 247
	Product Validation and Intercomparison Report (PVIR)	
	for the Essential Climate Variable (ECV) Greenhouse Gases (GHG)	Version 5.0 Final
		9 Feb 2017

/Thoning et al., 1985/ Thoning, K.W., P.P. Tans, and W.D. Komhyr, 1989, Atmospheric carbon dioxide at Mauna Loa Observatory, 2. Analysis of the NOAA/GMCC data, 1974 1985., J. Geophys. Res. ,94, 8549 8565.

/URD GHG-CCI v1/User Requirements Document (URD), ESA Climate Change Initiative (CCI) GHG-CCI project, Version1, 3 Feb 2011, available from: http://www.esa-ghg-cci.org/sites/default/files/documents/public/documents/URDv1_GHG-CCI_final.pdf, 2011.

/URD GHG-CCI v2/ User Requirements Document (URD), ESA Climate Change Initiative (CCI) GHG-CCI project, Version 2, 28 Aug 2014, available from: http://www.esa-ghg-cci.org/?q=webfm_send/173 , 2014.

/URD GHG-CCI v2.1/ User Requirements Document (URD), ESA Climate Change Initiative (CCI) GHG-CCI project, Version 2.1, 19 Oct 2016, available from: http://www.esa-ghg-cci.org/?q=webfm_send/344 2016.


/Wofsy et al., 2012/ Wofsy, S. C., B. C. Daube, R. Jimenez, E. Kort, J. V. Pittman, S. Park, R. Commane, B. Xiang, G. Santoni, D. Jacob, J. Fisher, C. Pickett-Heaps, H. Wang, K. Wecht, Q.-Q. Wang, B. B. Stephens, S. Shertz, A.S. Watt, P. Romashkin, T. Campos, J. Haggerty, W. A. Cooper, D. Rogers, S. Beaton, R. Hendershot, J. W. Elkins, D. W. Fahey, R. S. Gao, F. Moore, S. A. Montzka, J. P. Schwarz, A. E. Perring, D. Hurst, B. R. Miller, C. Sweeney, S. Oltmans, D. Nance, E. Hints, G. Dutton, L. A. Watts, J. R. Spackman, K. H. Rosenlof, E. A. Ray, B. Hall, M. A. Zondlo, M. Diao, R. Keeling, J. Bent, E. L. Atlas, R. Lueb, M. J. Mahoney. 2012. HIPPO Merged 10-second Meteorology, Atmospheric Chemistry, Aerosol Data (R_20121129). Carbon Dioxide Information Analysis Center, Oak Ridge National Laboratory, Oak Ridge, Tennessee, U.S.A.
http://dx.doi.org/10.3334/CDIAC/hippo_010 (Release 20121129)

/Wunch et al. 2011/ Wunch, D., Toon, G. C., Blavier, J.-F. L., Washenfelder, R. A., Notholt, J., Connor, B. J., Griffith, D. W. T., Sherlock, V., and Wennberg, P. O.: The Total Carbon Column Observing Network (TCCON), Philosophical Transactions of the Royal Society of London, Series A: Mathematical, Physical and Engineering Sciences, 369, 2087–2112, doi:10.1098/rsta.2010.0240, 2011.

/Wunch et al. 2010/ Wunch, D., Toon, G. C., Wennberg, P. O., Wofsy, S. C., Stephens, B. B., Fischer, M. L., Uchino, O., Abshire, J. B., Bernath, P., Biraud, S. C., Blavier, J.-F. L., Boone, C., Bowman, K. P., Browell, E. V., Campos, T., Connor, B. J., Daube, B. C., Deutscher, N. M., Diao, M., Elkins, J. W., Gerbig, C., Gottlieb, E., Griffith, D. W. T., Hurst, D. F., Jiménez, R., Keppel-Aleks, G., Kort, E. A., Macatangay, R., Machida, T., Matsueda, H., Moore, F., Morino, I., Park, S., Robinson, J., Roehl, C. M., Sawa, Y., Sherlock, V., Sweeney, C., Tanaka, T., and Zondlo, M. A.: Calibration of the Total Carbon Column Observing Network using aircraft profile data, Atmospheric Measurement Techniques, 3, 1351–1362, doi:10.5194/amt-3-1351-2010, URL <http://www.atmos-meas-tech.net/3/1351/2010/>, 2010.

References Sect. 8 (Aerosol induced biases):

Buchwitz, M., Dils, B., Boesch, H., Crevoisier, C., Detmers, R., Frankenberg, C., Hasekamp, O., Hewson, W., Laeng, A., Noel, S., Notholt, J., Parker, R., Reuter, M., and Schneising, O.: PVIRv4, Product Validation and Intercomparison Report for the Essential Climate Variable

	ESA Climate Change Initiative (CCI)	Page 248
	Product Validation and Intercomparison Report (PVIR)	
	for the Essential Climate Variable (ECV) Greenhouse Gases (GHG)	Version 5.0 Final
		9 Feb 2017

(ECV) Greenhouse Gases (GHG) for data set Climate Research Data Package No. 3 (CRDP#3), 2016.

De Leeuw, G., Holzer-Popp, T., Bevan, S., Davies, W., Descloitres, J., Grainger, R. G., Griesfeller, J., Heckel, A., Kinne, S., Klüser, L., Kolmonen, P., Litvinov, P., Martynenko, D., North, P., Ovigneur, B., Pascal, N., Poulsen, C. A., Ramon, D., Schulz, M., Siddans, R., Sogacheva, L., Tanre, D., Thomas, G.E., Virtanen, T.H., von Hoyningen-Hüne, W., Vountas, M., and S. Pinnock: Evaluation of seven European aerosol optical depth retrieval algorithms for climate analysis, *Remote Sens. Env.*, 162, 295–315, 2015.

Detmers, R., and Hasekamp, O.: Product User Guide (PUG) for the RemoTeC XCO₂ Full Physics GOSAT Data Product, Version 3.0, 2015.

Heymann, J. and Bovensmann, H. and Buchwitz, M. and Burrows, J. P. and Deutscher, N. M. and Notholt, J. and Rettinger, M. and Reuter, M. and Schneising, O. and Sussmann, R. and Warneke, T.: SCIAMACHY WFM-DOAS XCO₂: reduction of scattering related errors, *Atmos. Meas. Tech.*, 5, 2375-2390, doi:10.5194/amt-5-2375-2012, 2012.


Hewson, W.: Product User Guide University of Leicester full physics XCO₂ retrieval algorithm for CRDP3 OCFP v 6.0, version 3, 2016.

Holben, B., Eck, T. F., Slutsker, I., Tanre, D., Buis, J. P., Setzer, A., Vermote, E., Reagan, J. A., Kaufman, Y. J., Nakajima, T., Lavenue, F., Jankowiak, I., and Smirnov, A.: AERONET – A Federated Instrument Network and Data Archive for Aerosol Characterization, *Remote Sens. Environ.*, 66, 1–16, 1998.

Holzer-Popp, T., de Leeuw, G., Griesfeller, J., Martynenko, D., Klüser, L., Bevan, S., Davies, W., Ducos, F., Deuzé, J. L., Grainger, R. G., Heckel, A., von Hoyningen-Hüne, W., Kolmonen, P., Litvinov, P., North, P., Poulsen, C. A., Ramon, D., Siddans, R., Sogacheva, L., Tanre, D., Thomas, G.E., Vountas, M., Descloitres, J., Griesfeller, J., Kinne, S., Schulz, M., and S. Pinnock: Aerosol retrieval experiments in the ESA Aerosol cci project, *Atmos. Meas. Tech.*, 6, 1919–1957, doi:10.5194/amt-6-1919-2013, 2013.

Levy, R.C., Mattoo, S., Munchak, L.A., Remer, L.A., Sayer, A.M., Patadia, F., and N.C. Hsu: The Collection 6 MODIS aerosol products over land and ocean, *Atmos. Meas. Tech.*, 6, 2989–3034, doi:10.5194/amt-6-2989-2013, 2013.

Mielonen, T., Levy, R.C., Aaltonen, V., Komppula, M., de Leeuw, G., Huttunen, J., Lihavainen, H., Kolmonen, P., Lehtinen, K.E.J., and A. Arola: Evaluating the assumptions of surface reflectance and aerosol type selection within the MODIS aerosol retrieval over land: the problem of dust type selection. *Atmos. Meas. Tech.*, 4, 201–214, doi:10.5194/amt-4-201-2011, 2011.

	ESA Climate Change Initiative (CCI)	Page 249
	Product Validation and Intercomparison Report (PVIR)	
	for the Essential Climate Variable (ECV) Greenhouse Gases (GHG)	Version 5.0 Final
		9 Feb 2017

Mäder, J. A., J. Staehelin, D. Brunner, W. A. Stahel, I. Wohltmann, and T. Peter: Statistical modeling of total ozone: Selection of appropriate explanatory variables, J. Geophys. Res., 112, D11108, doi:10.1029/2006JD007694, 2007.

O'Neill, N. T., T. F., Eck, A. Smirnov, B. N. Holben, S. Thulasiraman, Spectral discrimination of coarse and fine mode optical depth, J. Geophys. Res., 108, D17, 4559-4573, doi:10.1029/2002JD002975, 2003.

Russell, P. B. , Livingston, J. M. , Redemann, J., Schmid, B., Ramirez, S. A., Eilers, J., Kahn, R., Chu, D. A., Remer, L. , Quinn, P. K., Rood, M. J. and Wang, W.: Multi-grid-cell validation of satellite aerosol property retrievals in INTEX/ITCT/ICARTT 2004, J. Geophys. Res., 112, D12, doi:10.1029/2006JD007606, 2007.

Zhang, Q., R.-L. Shia, S. P. Sander, and Y. L. Yung (2016), XCO₂ retrieval error over deserts near critical surface albedo, Earth and Space Science, 3, 36–45, doi:10.1002/2015EA000143, 2016.



10 Acronyms and Abbreviations

Abbreviations	Meaning
ACE-FTS	Atmospheric Chemistry Experiment-Fourier Transform Spectrometer
ACA	Additional Constraints Algorithm
ACOS	Atmospheric CO ₂ Observations from Space
ATBD	Algorithm Theoretical Basis Document
BESD	Bremen optimal ESTimation DOAS
CCI	Climate Change Initiative
CDR	Climate Data Record
CMUG	Climate Modelling User Group (of ESA's CCI)
CRDP	Climate Research Data Package
CRG	Climate Research Group
DOAS	Differential Optical Absorption Spectroscopy
DP	Data Provider
ECA	ECV Core Algorithm
ECMWF	European Centre for Medium Range Weather Forecasting
ECV	Essential Climate Variable
EMMA	Ensemble Median Algorithm
EO	Earth Observation
EOST	Earth Observation Science Team
ESA	European Space Agency
FCDR	Fundamental Climate Data Record
FP	Full Physics
FTIR	Fourier Transform InfraRed
FTS	Fourier Transform Spectrometer
GCOS	Global Climate Observing System
GHG	GreenHouse Gas
GMES	Global Monitoring for Environment and Security



ESA Climate Change Initiative (CCI)

**Product Validation and
Intercomparison Report (PVIR)**


for the Essential Climate Variable (ECV)
Greenhouse Gases (GHG)

Page 251


Version 5.0
Final

9 Feb 2017

GOSAT	Greenhouse Gases Observing Satellite
IASI	Infrared Atmospheric Sounding Interferometer
IMAP-DOAS	Iterative Maximum A posteriori DOAS
IMLM	Iterative Maximum Likelihood Method
IPCC	International Panel in Climate Change
IUP	Institute of Environmental Physics (IUP) of the University of Bremen, Germany
JAXA	Japan Aerospace Exploration Agency
LMD	Laboratoire de Météorologie Dynamique
LUT	Look-up table
MACC	Monitoring Atmospheric Composition and Climate, EU GMES project
MIPAS	Michelson Interferometer for Passive Atmospheric Sounding
MODIS	Moderate Resolution Imaging Spectrometer
NA	Not applicable
NDACC	Network for the Detection of Atmospheric Composition Change
NASA	National Aeronautics and Space Administration
NIES	National Institute for Environmental Studies
NOAA	National Oceanic and Atmospheric Administration
OCO	Orbiting Carbon Observatory
OE	Optimal Estimation
PBL	Planetary Boundary Layer
PPDF	Photon path length Probability Density Function
PVP	Product Validation Plan
PVR	Product Validation Report
QA	Quality Assurance
QC	Quality Control
RMS	Root-Mean-Square
RTM	Radiative transfer model
SCIATRAN	RTM for SCIAMACHY

	ESA Climate Change Initiative (CCI)	Page 252
	Product Validation and Intercomparison Report (PVIR)	
	for the Essential Climate Variable (ECV) Greenhouse Gases (GHG)	Version 5.0 Final
		9 Feb 2017

SCIAMACHY	SCanning Imaging Absorption spectroMeter for Atmospheric ChartographY
TANSO	Thermal And Near infrared Sensor for carbon Observation
TBC	To be confirmed
TBD	To be defined / to be determined
TCCON	Total Carbon Column Observing Network
VAL	Validation
VALT	Validation Team
WFM-DOAS (or WFMD)	Weighting Function Modified DOAS

	ESA Climate Change Initiative (CCI)	Page 253
	Product Validation and Intercomparison Report (PVIR)	
	for the Essential Climate Variable (ECV) Greenhouse Gases (GHG)	Version 5.0 Final
		9 Feb 2017

11 Acknowledgements

The work presented in the document has been funded by ESA / ESRIN via ESA's Climate Change Initiative (CCI, <http://www.esa-cci.org/>) via the GHG-CCI project led by University of Bremen (<http://www.esa-ghg-cci.org/>).

We highly appreciate the availability of GOSAT Level 1 data products generated in Japan by JAXA and made available by NIES (<http://www.gosat.nies.go.jp/>).

JAXA/NIES GOSAT Level 1 data have also been obtained from the ESA Third Party Mission GOSAT data archive. The availability of this service by ESA is also highly appreciated.

We also highly appreciate the availability of validation reference data from the Total Carbon Column Observing Network (TCCON), which have been obtained from <http://www.tccon.caltech.edu/>.

We also very much acknowledge the NASA/ACOS team and in particular Dr. Chris O'Dell, Colorado State University, USA, for making GOSAT ACOS XCO₂ retrievals available, which have been used for the EMMA product and related assessments and NIES, Japan, for making available GOSAT Level 2 XCO₂ data products (operational and PPDF products), which have also been used in the framework of the EMMA activities.

We also highly appreciate the availability of CarbonTracker data from NOAA, which have been obtained from <http://www.esrl.noaa.gov/gmd/ccgg/carbontracker/>.

End of document